ICLPR - ST

3rd International Conference on Laser, Plasma and Radiation – Science and Technology

29 June – 3 July 2026
Poiana Brasov

BOOK OF ABSTRACTS

iclpr-st.inflpr.ro

3rd International Conference on Laser, Plasma, and Radiation – Science and Technology 2026

BOOK OF ABSTRACTS

Poiana Brasov, Romania
29 June – 3 July, 2026

Organized by:

National Institute for Laser, Plasma and Radiation Physics
in partnership with
Laser, Plasma and Radiation – Science and Technology Association

Editors:
Bogdana MITU, Valentin CRACIUN,
Nicolaie PAVEL, Nicu SCARISOREANU

Assistant editors:
Cristina-Petruta GHEORGHE, Cristina-Mihaela POPESCU

On behalf of the **National Institute for Laser, Plasma and Radiation Physics** (**INFLPR**), with the support of the **Association Laser, Plasma and Radiation - Science and Technology** (**LPR-ST**), we are pleased to welcome you to the **3rd International Conference on Laser, Plasma and Radiation - Science and Technology** (**ICLPR-ST**), during **29 June - 3 July, 2026** in Poiana Brasov, Brasov county, Romania in Alpin Resort Hotel, in the heart of the Carpathian Mountains.

Following the previous editions, **ICLPR-ST** continues to develop as an international forum dedicated to scientific exchange, collaboration, and the presentation of recent advances in laser science, plasma physics, radiation technologies, and related interdisciplinary areas. This **third edition** reflects our continued commitment to building a lasting scientific tradition around these fields and to bringing together researchers, academics, and industry experts working on both fundamental and applied aspects of laser, plasma, and radiation science.

The scientific programme reflects the broad scope and rapid development of laser, plasma, photonic, and radiation-based sciences, bringing together fundamental studies, advanced diagnostics and modelling, optical and photonic concepts, and technologies based on photonic and plasma processes. It also highlights the growing relevance of these fields for major societal challenges, including life sciences, energy production and storage, and environmental protection through pollutant monitoring, detection, and mitigation.

Through plenary lectures, invited talks, oral presentations, and poster sessions, the conference offers an opportunity to discuss recent results, exchange ideas, and explore new perspectives across complementary research areas. Particular attention is given to the connection between fundamental mechanisms and technological applications, highlighting the role of laser, plasma, and radiation-based methods in addressing current scientific and societal challenges.

We hope that the 3rd ICLPR-ST will provide a stimulating scientific environment, encourage fruitful discussions, and support the development of new collaborations within the international community, in the pleasant and inspiring atmosphere of Poiana Brasov.

Bogdana MITU, Valentin CRACIUN, Nicolaie PAVEL, Nicu SCARISOREANU

Number of pages:194
ISSN: 2821-7101
ISSN-L: 2821-7101
2026-INFLPR

COMMITTEES

Chairs

Bogdana MITU, Valentin CRACIUN, Nicolaie PAVEL, Nicu SCARISOREANU

Honorary Chairs

Maria DINESCU, Ion N. MIHAILESCU

International Scientific Committee

- Peter BRUGGEMAN - USA
- Nadezhda M. BULGAKOVA - Czech Republic
- Douglas B. CHRISEY - USA
- Adrian DINESCU - Romania
- Gheorghe DINESCU - Romania
- Lucian-Marian GHEORGHE - Romania
- Camelia GHIMBEU - France
- Achim Walter HASSEL - Austria
- Dunpin HONG - France
- Yongfeng LU - USA
- Selma MEDEDOVIC THAGARD - USA
- Andrea MURARI - Italy
- Alexandra PALLA PAPAVLU - Romania
- Adrian PETRIS - Romania
- Fabio DI PIETRANTONIO - Italy
- Angela STAICU - Romania
- Razvan STOIAN - France
- Emmanuel STRATAKIS - Greece
- Hendrik SWART - South Africa
- Daniel VIZMAN - Romania
- Andrea ZILLE - Portugal

Executive Committee

Nicolae-Cristian MIHAILESCU, Felix SIMA, Gabriel SOCOL

Local Organizing Committee

- Alexandru ACHIM
- Gabriel CRISTEA
- Gabriela DORCIOMAN
- Cristina-Petruta GHEORGHE
- Aurelian MARCU
- Natalia MIHAILESCU
- Catalin PATRU
- Cristina POPESCU
- Carmen RISTOSCU
- Laurentiu RUSEN
- Ionut UNGUREANU
- Iuliana URZICA

Contact: https://iclpr-st.inflpr.ro/

CONFERENCE SPONSORS

We would like to thank the sponsors for their generous support.

PROFESSIONAL ASSOCIATIONS SUPPORTING THE CONFERENCE

INTERNATIONAL SOCIETY OF ELECTROCHEMISTRY

LPR-ST
Laser, Plasmă, Radiație - Știință și Tehnologie

Elite Sponsor
BCR

Silver Sponsor
APEL
lighting the future

Bronze Sponsor
PHANOS

SocialEvents Sponsor
infosec center

SocialEvents Sponsor
HISTERESIS
TECHNOLOGY FOR THE FUTURE

SocialEvents Sponsor
AntiFocal

SocialEvents Sponsor
SPECSGROUP

BlueSpace TECHNOLOGY

INNO robotics
innovation has no limit

Kurt J. Lesker Company

SHIMADZU
Excellence in Science

CONFERENCE TOPICS

Topic 1. Fundamentals, Diagnostics and Modelling in Laser, Plasma and Radiation Physics

Topic 2. Advances in Optics, Laser and Photonics

Topic 3. Environmental Protection and Pollutants Monitoring

Topis 4. Devices Based on Photonic and Plasma Technologies

Topic 5. Energy Production and Storage

Topis 6. Life Sciences Applications

TABLE OF CONTENTS

Plenary

Invited Lectures

Oral Presentation

Poster Presentations

Topic 1. Fundamentals, Diagnostics and Modelling in Laser, Plasma and Radiation Physics

Topic 2. Advances in Optics, Laser and Photonic

Topic 3. Environmental Protection and Pollutants Monitoring

Topic 4. Devices Based on Photonic and Plasma Technologies

Topic 5. Energy Production and Storage

Topic 6. Life Sciences Applications

PLENARY LECTURES

Scale-Bridging Multi-Modal Analytics in Energy Research: Harnessing Data Correlation and Machine Learning for Enhanced Materials and Device Optimization

Silke CHRISTIANSEN[1,2,3], George SARAU[1], Andre BORCHERS[1], Berik UZAKBAIULY[1], Gihoon CHA[1], Hyoungwon PARK[1], Daniel AUGSBURGER[1], Dennis POSSART[1], Rajkumar REDDY KOLAN[1,2], Peter SUTER[4], Tor HILDEBRAND[4]

[1]*Fraunhofer Institute for Ceramic Technology and Systems - IKTS, Forchheim 91301, Germany*
[2]*Institute of Nanotechnology and Correlative Microscopy - INAM, Forchheim 91301, Germany*
[3]*Free University Berlin, Physics Department, Berlin 14195, Germany*
[4]*Lucid Concepts AG, Zürich 8005, Switzerland*
Corresponding author: *silke.christiansen@ikts.fraunhofer.de*

The dynamic field of battery technology necessitates sophisticated analytical methodologies to advance device performance and promote sustainability. Our team employs a groundbreaking scale-bridging, multi-modal analytical framework to examine the intricate interactions within battery materials with unprecedented precision, spanning from macro to nano scales.

Our methodology integrates various microscopy techniques - including electron, ion, optical, probe, and X-ray microscopy - alongside advanced spectroscopic methods such as Raman, IR, and mass spectroscopy. These techniques are further refined through the use of nanoGPS technology, enabling accurate correlations across different imaging modalities [1].

Our analytical approach focuses on true multi-modal data correlation across various scales, which is crucial for identifying material defects and device imperfections that could compromise device performance.

We incorporate operando techniques, such as the latest Carl Zeiss microscopy developments, which allow for the observation of cycling devices within an electron microscope. This capability is pivotal for enhancing the longevity and performance of solid-state battery materials and device architectures.

Our commitment to artifact-free analytical data is ensured by maintaining fully inert workflows, including glovebox operations (e.g. an atomic force microscope installed in a glovebox) and the use of transfer holders from sample preparation through to analysis.

Through the application of statistical techniques and machine learning algorithms, we analyze complex, heterogeneous data sets, significantly enhancing the material and device optimization processes.

Our presentation will explore the integration of these multi-modal analytics within a unified workflow facilitated by the 'Correlyze' data platform [2]. This platform not only supports the assessment and quantification of data but also bolsters the predictive capabilities vital for the advancement of battery technologies. We anticipate that our approach will substantially influence battery development, fostering innovations that align with rigorous standards of quality and environmental sustainability.

[1] https://www.horiba.com/int/scientific/products/detail/action/show/Product/nanogps-navyx-4959/
[2] https://correlyze.org

The Promises and Challenges of Plasma Medicine and Oncology

Sander BEKESCHUS[1,2]

[1]*ZIK Plasmatis, Leibniz Institute for Plasma Science and Technology (INP Greifswald), Greifswald 17489, Germany*
[2]*Department for Dermatology, Rostock University Medical Center, Rostock 18057, Germany*
Corresponding author: *sander.bekeschus@inp-greifswald.de*

In plasma medicine, partially ionized gases are employed for biomedical therapy [1]. Despite more than a decade of clinical experience in plasma wound healing, the identification of key plasma effectors and molecular mechanisms of action remain to be unraveled [2]. Moreover, routine clinical applications of plasma cancer treatment have not come into fruition, partially due to the lack of clinical studies, but also due to an overarching science-driven framework putting plasma treatment within the regular oncology therapy schemes and defining its added value [3]. This plenary talk will draw major lines in the development of the field of plasma medicine, with a particular focus on its reactive species production and mechanisms of actions [4], along with current paths such as the multidisciplinary TARGET-H consortium aiming to enable plasma skin cancer treatment in the near future (Fig. 1).

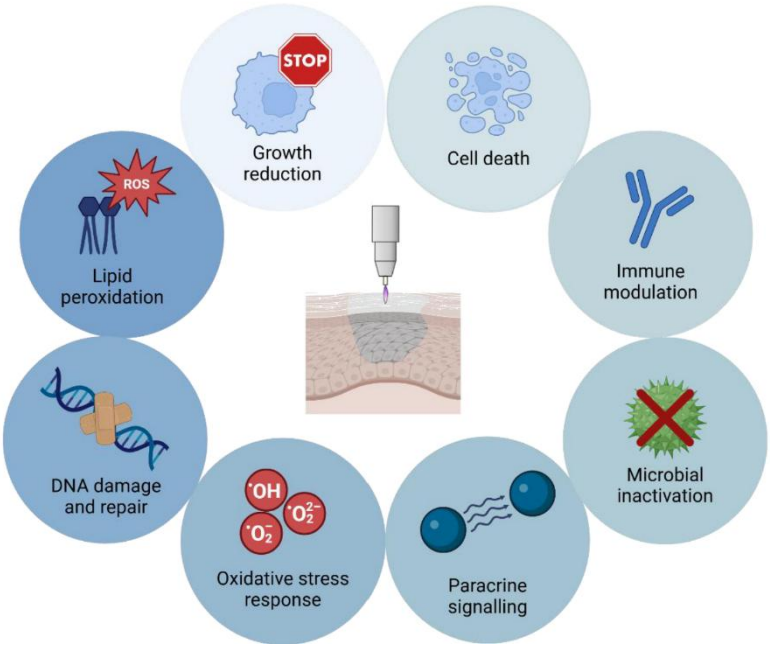

Fig. 1. Potential mechanisms of action of medical gas plasma therapy (image from [5]).

Acknowledgements: *This review was written with the support of the project TARGET-H in the framework (grant number EXF-25-1043-P3) of the State-Excellence-Initiative funded by the European Fund of Regional Development (EFRE) and the Ministry of Science, Culture, Federal and European Affairs of Mecklenburg-Western-Pommerania (Germany).*

[1] M. Laroussi, S. Bekeschus, M. Keidar, A. Bogaerts**,** A. Fridman, X. Lu, K. Ostrikov, M. Hori, K. Stapelmann, V. Miller, S. Reuter, C. Laux, A. Mesbah, J. Walsh, C. Jiang, S. M. Thagard, H. Tanaka, D. Liu, D. Yan, and M. Yusupov, "Low-Temperature Plasma for Biology, Hygiene, and Medicine: Perspective and Roadmap," IEEE Trans. Radiat. Plasma Med. Sci. **6**(2), 127-157 (2022).

[2] S. Bekeschus, T. von Woedtke, S. Emmert, A. Schmidt, "Medical gas plasma-stimulated wound healing: Evidence and mechanisms," Redox Biol. **46**, 102116 (2021).

[3] S. Bekeschus, "Medical gas plasma technology: Roadmap on cancer treatment and immunotherapy," Redox Biol. **65**, 102798 (2023).

[4] S. Bekeschus, "Gas plasmas technology: from biomolecule redox research to medical therapy," Biochem. Soc. Trans. **51**(6), 2071-2083 (2023).

[5] L. McKeever, L. Boeckmann, A. Bogaerts, S. Emmert, A. Privat-Maldonado, E. Robert, D. Singer, E. Smits, A. Stancampiano, A. Sobota, T. von Woedtke, K.-D. Weltmann, K. Wende, S. Bekeschus, "Advancing Dermatological Care: Potential of Gas Plasma Technology for Actinic Keratosis Treatment," IEEE Trans. Radiat. Plasma Med. Sci. **xx**, 11278788 (2026). Online publication: https://doi.org/10.1109/trpms.2025.3639175

Programmable Laser Nanostructuring

Razvan STOIAN

Laboratoire Hubert Curien, UMR 5516, CNRS, Université Jean Monnet, Saint Etienne, France
Corresponding author: *razvan.stoian@univ-st-etienne.fr*

The advances in ultrafast laser deep nanoscale structuring, aiming for characteristic dimensions well-below 100 nm, rely essentially on localized material reactions and on the generation of near fields [1,2]. These fields, self-triggered, permit extreme energy confinement and nanoablation events, being controllable by the vectorial characteristics of the beam. The design of polarization becomes key in controlling features sizes and patterns. We show that automated time-design of polarization can trigger new patterns, assisting a complex self-organization process, and generate extreme nanostructuring scales, well beyond the optical resolution. Such energy confinement challenges conventional views on ultrafast laser ablation mechanisms. New physical insights on the correlation of electromagnetic fields and material evolution as well as ablative processes at the nanoscale will be discussed.

Acknowledgements: The support of the Banque Publique D'Investissement France (iDEMO grant Glacier) and the French National Research Agency (grant ANR-21-CE08-0005) is gratefully acknowledged.

[1] R. Stoian and J. Bonse Eds. Ultrafast Laser Nanostructuring. The Pursuit of Extreme Scales, Springer Series in Optical Sciences 239 (2023).
[2] G. Zhang, A. Rudenko, R. Stoian and G. Cheng, "Ultrafast laser high-aspect-ratio extreme nanostructuring of glass beyond lambda/100," Ultrafast Sci. **5**, 0103 (2025).

INVITED LECTURES

Advances in Scattering-Type Scanning Near-Field Optical Microscopy: From Quantitative and Correlative Nanoscale Characterization to AI-Enhanced Imaging

Stefan G. STANCIU[1,2], Denis E. TRANCA[1,2], Radu HRISTU[1,2], Stefan-Razvan ANTON[1,2], Gabriella CINCOTTI[3], Zeev ZALEVSKY[4], Avi KARSENTY[5], George A. STANCIU[2]

[1]*Photon-X Spectrum Lab, CAMPUS Research Institute, National University of Science and Technology POLITEHNICA Bucharest, 313 Splaiul Independentei, Bucharest 060042, Romania*
[2]*Center for Microscopy-Microanalysis and Information Processing, National University of Science and Technology POLITEHNICA Bucharest, 313 Splaiul Independentei, Bucharest 060042, Romania*
[3]*Department of Civil, Computer and Aeronautical Engineering, University Roma Tre, via Vito Volterra 62, I-00146 Rome, Italy* [4]*Faculty of Engineering, Bar-Ilan University, Ramat Gan 52900, Israel*
[5]*Nanotechnology Center for Research and Education and the Applied Physics/Electro-Optics Engineering Department, Jerusalem College of Technology (JCT), Jerusalem 9116001, Israel*
Corresponding author: *stefan.g.stanciu@upb.ro*

Scattering-type scanning near-field optical microscopy (s-SNOM) has become a powerful platform for nanoscale optical characterization, enabling access to local electromagnetic properties beyond the diffraction limit [1]. In this invited talk, I will present recent advances in s-SNOM that extend its capabilities from qualitative imaging toward quantitative, correlative, and data-driven nanoscopy. First, I will present working principles, typical experimental configurations, and popular applications of s-SNOM. Examples will be given for nanostructured materials and hybrid systems, highlighting applications such as the characterization of polymer-coated metallic nanoparticles [2] and other heterogeneous nanoscale architectures. In this part of the presentation, I will also emphasize on approaches for extracting local optical properties, including the complex permittivity [3], from near-field signals. Next, I will introduce correlative imaging strategies that combine s-SNOM with complementary modalities such as confocal laser scanning microscopy [4], or non-linear optical microscopy [5]. These approaches enable the multimodal investigation of biological tissues and advanced materials, providing both nanoscale optical contrast and larger-scale structural and functional context. Recent developments in tip engineering and signal interpretation will also be addressed [6], including perspectives for improving spatial resolution and reducing imaging artifacts. Finally, I will discuss recent efforts toward integrating artificial intelligence and machine learning into near-field microscopy workflows. These include hybrid machine learning approaches for accelerating near-field spectroscopy, s-SNOM data modelling and data-driven inference of s-SNOM signals from complementary measurements. I will also outline in this context on the importance of curated datasets [7] for benchmarking and training. Overall, this talk will highlight how the convergence of quantitative analysis, correlative imaging, and AI-enhanced methodologies is driving the development of more robust, scalable, and accessible near-field optical nanoscopy, with applications spanning nanophotonics, materials science, and biomedicine.

Acknowledgements: Stefan G Stanciu acknowledges the financial support of UEFISCDI Grants: PN-IV-P7-7.1-PED-2024-2374 (POLYNANO); PN-IV-PCB-RO-MD-2024-0541 (OPTOCARSEMO); PN-IV-P8-8.3-PM-RO-TR-2024-0068 (CONAGAI).

[1] R. Hillenbrand, Y. Abate, M. Liu, X. Chen, and D.N. Basov, "Visible-to-THz near-field nanoscopy," Nat. Rev. Mater. **10**(4), 285-310 (2025).
[2] S.G. Stanciu, D.E. Tranca, G. Zampini, R. Hristu, G.A. Stanciu, X. Chen, M. Liu, H.A. Stenmark, L. Latterini, "Scattering-type scanning near-field optical microscopy of polymer-coated gold nanoparticles," ACS Omega **7**(13), 11353-11362 (2022).
[3] S.G. Stanciu, D.E. Tranca, G. Zampini, R. Hristu, G.A. Stanciu, X. Chen, M. Liu, H.A. Stenmark, L. Latterini, "Characterization of nanomaterials by locally determining their complex permittivity with scattering-type scanning near-field optical microscopy," ACS Appl. Nano Mater. **3**(2), 1250-1262 (2020).
[4] S.G. Stanciu, D.E. Tranca, R. Hristu, G.A. Stanciu, "Correlative imaging of biological tissues with apertureless scanning near-field optical microscopy and confocal laser scanning microscopy," Biomed. Opt. Express **8**(12), 5374-5383 (2017).
[5] R. Hristu, D.E. Tranca, S.G. Stanciu, L.G. Eftimie, and G.A. Stanciu, "Quantitative imaging of collagen fibrils via correlated far-field and near-field optical techniques," ACS Materials Lett. **7**(11) 3642-3651 (2025).
[6] J. Belhassen, S. Glass, E. Teblum, G.A. Stanciu, D.E. Tranca, Z. Zalevsky, S.G. Stanciu, A. Karsenty, "Toward augmenting tip-enhanced nanoscopy with optically resolved scanning probe tips," Adv. Photon. Nexus **2**(2), 026002 (2023).
[7] M. Lucidi, D.E Tranca, L. Nichele, D. Ünay, G.A Stanciu, P. Visca, A.M. Holban, R. Hristu, G. Cincotti, S.G Stanciu, "SSNOMBACTER: A collection of scattering-type scanning near-field optical microscopy and atomic force microscopy images of bacterial cells," GigaScience **9**(11), giaa129 (2020).

Ultrahigh-Speed, Ultrahigh-Aspect-Ratio Glass Through-Hole Drilling using a Single Ultrafast Bessel Pulse in GHz Burst Mode

Koji SUGIOKA[1], Shuntaro TANI[1], Yuhei MIYAHARA[2],
Ryosuke YAGINUMA[2], Toshinori OKADA[2]

[1]*RIKEN Center for Advanced Photonics, Wako, Saitama 351-0198, Japan*
[2]*Enplas Laboratories, 1-19-57 Kamiaoki, Kawaguchi City, Saitama 333-0844 Japan*
Corresponding author: ksugioka@riken.jp

Through-glass via (TGV) formation technology is a key enabler for next-generation semiconductor devices, particularly in advanced packaging and heterogeneous integration. High-aspect-ratio, high-quality via formation in glass substrates offers superior electrical performance, thermal stability, and design flexibility compared to conventional silicon-based interposers. Therefore, the development of innovative and reliable TGV manufacturing technologies is essential for future high-performance, energy-efficient semiconductor systems.

Laser processing is considered one of the most promising approaches for TGV fabrication. We applied ultrafast laser induced selective etching technique combined with Bessel beam for rapid fabrication of glass though holes [1]. A single shot of a Bessel pulse, followed by chemical etching using NaOH, can create a through-hole with a diameter of 8 μm in 50 μm-thick borosilicate glass (aspect ratio: 6.25). By scanning the laser beam, an array of through-holes can be formed at a rate of 3,000 holes/s (Fig. 1a). Meanwhile, Guilberteau et al. demonstrated that a single shot of an ultrafast Bessel pulse in GHz burst mode can create a through-hole with a diameter of 4 μm and an aspect ratio of 182 in glass without chemical etching [2]. However, cracks were generated around the periphery of the processed region along the fabricated holes, which is unacceptable for TGV applications.

In this paper, we further advance this technology by optimizing fabrication conditions for next-generation semiconductor device manufacturing. By optimizing the irradiation conditions, a GHz burst-mode ultrafast laser successfully created an array of through-holes with a diameter of 1.1 μm in a 1.1 mm-thick borosilicate glass substrate (aspect ratio: ~1000) without crack formation (Fig. 1b). The fabrication speed reached 3000 holes/s and can be scaled up to over 10.000 holes/s. Importantly, the diameter of the through-holes can be precisely controlled by post-processing chemical etching using NaOH.

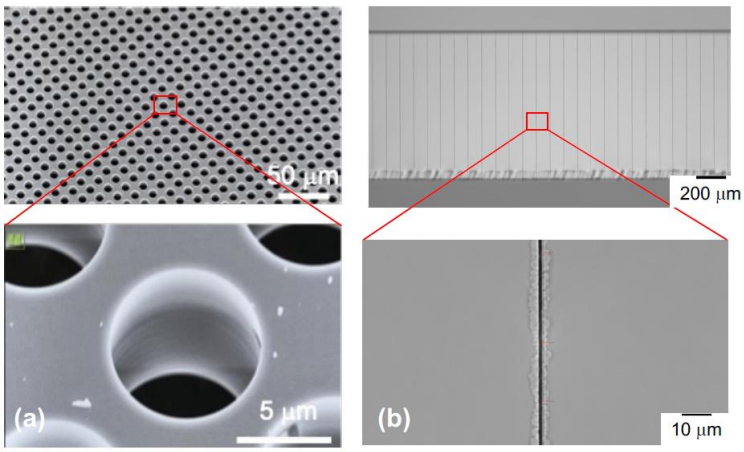

Fig. 1. Fast fabrication of an array of through holes in borosilicate glass by **(a)** ultrafast laser induced selective etching technique combined with Bessel beam and **(b)** GHz burst-mode ultrafast Bessel laser pulses

[1] J. Zhang, K. Obata, K. Ozasa, T. Uzawa, Y. Ito, K. Sugioka, "Rapid Manufacturing of Glass-Based Digital Nucleic Acid Amplification Chips by Ultrafast Bessel Pulses," Small Sci. **4**(2), 2300166 (2024).
[2] T. Guilberteau, P. Balage, M. Lafargue, J. Lopez, Laura Gemini, I. Manek-Hönninger, "Bessel Beam Femtosecond Laser Interaction with Fused Silica Before and After Chemical Etching: Comparison of Single Pulse, MHz-Burst, and GHz- Burst," Micromachines **15**(11), 1313 (2024).

Three Decades of Innovation in Femtosecond Laser Functionalization of Glass Substrates: From Pioneer Works Reaching Industrial Maturity to Challenges and Opportunities

Yves BELLOUARD

Galatea Lab, Institute of Electricity and Micro-engineering (IEM), Faculty of Engineering, Ecole Polytechnique Fédérale de Lausanne (EPFL), Switzerland
Corresponding author: yves.bellouard@epfl.ch

Femtosecond laser offers a means to confine energy beyond the diffraction limit. Triggered by pioneer works performed at the turn of the millennia, the use of femtosecond lasers to induce non-ablative transformation of transparent materials have emerged as a key technology for functional devices impacting numerous fields, from integrated photonics to complex micro-parts processing fluids or fulfilling mechanical functions (including actuators), and from high-density optical memories to solving complex packaging issues.

The core of all these technological developments is the ability of ultrafast lasers, thanks to non-linear absorption processes and strong field interaction with high energy confinement, to tailor the intimate structure of the matter and inducing a variety of localized structural modifications, including densification, nano-crystallization, or phase separation.

Here, we will propose an overview on how this peculiar laser-matter interaction provides a means for tuning a variety of interesting physical properties in materials, ranging from the etching selectivity to the change of density, and from heat conductivity, thermal expansion, Young's modulus to electrical conductivity. Specifically, we will show how these structural modifications can be related to functional properties and be leveraged to create novel types of 'direct-write' composite materials.

Finally, as exciting developments in this blooming research field, we will discuss our recent results related to femtosecond laser-induced modifications crystallization and how it differs from classical, long-pulse and continuous-wave laser annealing processes as well as novel observations related to femtosecond laser-matter interaction in the UV regime.

Recent publications from our group on this specific topic

[1] G. Torun, Y. Bellouard, "Femtosecond laser interaction with ULE® glass," Acta Mater. **314**, 122355 (2026).
[2] E. Gribaudo and Y. Bellouard, "UV femtosecond laser induced self-organisation of micro-structures in the bulk of fused silica," Opt. Express **34**(7), 12822-12840 (2026).
[3] E. Gribaudo, M. Deckart, P. Vlugter, and Y. Bellouard, "Sub-wavelength femtosecond laser based nanostructuring of complex patterns in the bulk of fused silica," Opt. Express **33**(5), 11529-11540 (2025).
[4] L. Ackermann, B. Hermann, D. Echarri, E. Gribaudo, and Y. Bellouard, "High-speed femtosecond UV laser writing of low-loss waveguides in fused silica," Opt. Lett. **50**(8), 2506-2509 (2025).
[5] G. Torun, A. Romashkina, T. Kishi, and Y. Bellouard, "Femtosecond-laser direct-write photoconductive patterns on tellurite glass," Phys. Rev. Appl. **21**, 014008 (2024).
[6] R. Ricca, V. Boureau, and Y. Bellouard, "Influence of ionization and cumulative effects on laser-induced crystallization in multilayer dielectrics," Phys. Rev. Mater. **8**, 063402 (2024).
[7] S. Lee, T. Kishi, and Y. Bellouard, "Wide-Field Polarimetric Second-Harmonic Imaging for Rapid and Nondestructive Investigation of Laser-Induced Crystallization Phenomena," ACS Nano **18**(36), 24929-24940 (2024).
[8] R. Ricca and Y. Bellouard, "Single-Layer Subwavelength Femtosecond-Laser-Induced Confined Nanocrystallization in Multistack Dielectrics," Phys. Rev. Appl. **19**, 044035 (2023).
[9] G. Torun, T. Kishi, D. Pugliese, D. Milanese, and Y. Bellouard, "Formation Mechanism of Elemental Te Produced in Tellurite Glass Systems by Femtosecond Laser Irradiation," Adv. Mater. **35**(20), 2210446 (2023).

In-operando Sub-picosecond X-ray Diagnostics for High-Resolution Material Analysis and Imaging

Raphael CLADY[1], Krishna KHAKUREL[2], Amelie FERRÉ[1], Olivier PEYRUSSE[1], Adrien STOLIDI[3], Victor BUSSY[3], Marc SENTIS[1], Olivier UTÉZA[1]

[1]*Aix-Marseille Université, CNRS, LP3 UMR 7341, 13288, Marseille, France*
[2]*ELI Beamlines Facility, The Extreme Light Infrastructure ERIC Za Radnicí 835, Dolní Břežany 25241, Czech Republic*
[3]*Université Paris-Saclay, CEA, List F-91120, Palaiseau, France*
Corresponding author: olivier.uteza@univ-amu.fr

Ultrashort pulsed lasers are pivotal to engineer materials because of their capability to induce controlled changes in a small volume and with high selectivity and resolution [1,2]. To understand and to guide those transformations, in-operando diagnostics are helpful, enabling fully-resolved analytics of the interaction and of its outcomes. Ideally, they encompass short-pulse duration optical and X-ray probes to uncover the details of laser energy coupling to the electron sub-system of the material and the subsequent changes incurred by the lattice atoms upon relaxation of the absorbed energy. In this context, table-top multi-beamline ultrafast (fs) laser facilities of moderate energy (10's TW class) and repetition rate (100's Hz) are of high interest due to their ability to propose performant multimodal pump-probe arrangements in a flexible and versatile laboratory environment [3,4]. This perspective motivated the development of the ASUR (*Applications des Sources Ultra-Rapides*) platform in LP3 laboratory for more than 10 years. As it will be presented in this paper, our efforts result in the successful demonstration of hard energetic jitter-free point-like pulsed X-ray K□ sources (Mo@17.48 keV and Cu@8.04 keV), synchronized with laser optical probe and pump, suitable for deep and detailed material analysis, possibly under laser excitation [5] (Fig. 1-left). To illustrate the analytic capability of ASUR platform, we will present X-ray diffraction measurements. A first measurement demonstrates elongation of GaS unit cell along the c-axis through accumulation of laser-induced thermomechanical stress [6] and a second one measures time-resolved coherent phonon oscillations in gold excited by 400-nm femtosecond laser pulses (Fig. 1-right, [5]), as well as its recrystallization dynamics and characteristics. To highlight the relevance of the platform for imaging, a 3D X-ray tomography of a calibration object will also be presented where dedicated strategies for both acquisitions and reconstruction algorithms have been investigated. These achievements open up avenues to access detailed knowledge at the atomic scale in material science and to develop smart laser engineering of materials, as well as to promote novel X-ray imaging protocols that can find applicative opportunities in biology, medicine or non-destructive testing.

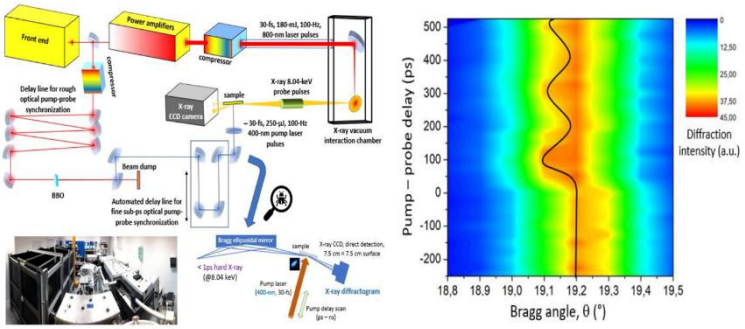

Fig. 1. Left: ASUR pump-probe X-ray platform. Right: Time-resolved coherent phonon oscillations in gold excited by 400-nm femtosecond laser pulses [5].

[1] Z. Lin and M. Hong, "Femtosecond Laser Precision Engineering: From Micron, Submicron, to Nanoscale," Ultrafast Sci. **2021**, 9783514 (2021).
[2] R. Stoian and J.-Ph. Colombier, "Advances in ultrafast laser structuring of materials at the nanoscale," Nanophotonics **9**(16), 4665-4688 (2020).
[3] M. Hada, J. Matsuo, "Ultrafast X-ray sources for time-resolved measurements," X-Ray Spectrom. **41**(4), 188-194 (2012).
[4] K. Sokolowski-Tinten, C. Blome, C. Dietrich, et al., "Femtosecond X-Ray Measurement of Ultrafast Melting and Large Acoustic Transients," Phys. Rev. Lett. **87**(22), 225701 (2001).
[5] O. Utéza, R. Clady, Y. Azamoum, et al., "High flux sub-picosecond laser-based x-ray platform for advanced material analysis and imaging," Rev. Sci. Instrum. **97**(1), 013006 (2026).
[6] K. Khakurel, R. Clady, S. Espinoza, et al., "Engineering GaS Crystal Anisotropy via Ultrafast Laser Excitation," Opt. Mat. Express **15**(10), 2534-2544 (2025).

Chromogenic Coatings for Energy Efficient Windows

Sergiu VATAVU[1], Gheorghe GHILETCHII[1], Alexandru VARZARI[1],
Oleg SHAPOVAL[1], Alexandr BELENCHUK[1], Petronela GAROI[2], Valentin CRACIUN[2],
Stefan-Andrei IRIMICIUC[2,3]

[1]*Physics of Semiconductors and Devices Laboratory, Faculty of Physics and Engineering, Moldova State University, 60 A. Mateevici str., Chişinău, MD-2009, Moldova*
[2]*National Institute for Laser, Plasma and Radiation Physics, Magurele 077125, Romania*
[3]*Institute of Physics of Czech Academy of Sciences, Prague 186 00, Czechia*
Corresponding author: *sergiu.vatavu@usm.md*

Chromatic smart systems are of particular interest due to their ability to reversibly modulate their spectral response to external stimuli [1]. Chromic transition metal oxide systems are actively investigated for applications in smart windows, building-integrated thermal-management coatings, optical and gas-sensing systems, visual indicators, adaptive camouflage, information-storage and display concepts, and other thin-film optoelectronic devices [2]. The chromic optical response in transition metal oxides is assigned mainly to two classes of mechanisms: phase transitions and small-polaron injection.

This work integrates coating technology, thin films characterization, and theoretical calculations, and is focused on developing a coating that combines thermochromic and electrochromic materials.

The experimental set-up and the technology which implies the co-assembly approach to prepare multilayered devices, integrating both thermochromic and electrochromic thin film materials, namely Metalorganic Aerosol Deposition (MAD), was developed [3]. Nanolayers of VO_2 by use of both $V(acac)_3$ and $VO(acac)_2$ precursors were prepared onto SiO_x/Si(111) and a-cut Al_2O_3 substrates. The same substrate types were used for undoped and NiO:(Cu, Ag, Na, Ga, V, La, In) nanolayers preparation by MAD using a single liquid solution containing all necessary precursors at substrate temperature in the range of 450-650°C.

Complementary NiO and VO_2, 150 nm thin films were deposited by pulsed laser deposition (PLD, 266 and 248 nm, 2 J/cm^2) on a wide range of transparent substrates (fused Si, MgO, Al_2O_3) at various temperatures characteristic for each material 500-700 for NiO and 450-650°C for VO_2. Additionally, the VO_2 samples were doped by simultaneous addition of TiO_2 by colliding plasma approach. This new deposition strategy focuses on the angular and kinetic dependence of the oxidation state of metallic species in the plasma and allows fine control off doping in a single deposition process. The in-situ monitoring reveals a stronger relationship between the thermochromic phases and the growth thermodynamics rather than plasma phase reactions.

Structural properties, morphology, composition, and oxidation states of thin oxide films were studied using X-ray diffraction accompanied by Rietveld refinement and Williamson-Hall plot analysis, Atomic Force Microscopy, Scanning Electron Microscopy, Energy-Dispersive X-Ray Spectroscopy, and X-ray photoelectron spectroscopy. Optical properties in the range of 230-2000 nm were characterized by ellipsometry.

Theoretical calculations, in the framework of the Green's function method applied to the extended Hubbard-Holstein model, the complex dielectric function of VO_2 as well as the spectra of the refractive index n(ω) and of the extinction coefficient k(ω) were numerically calculated and compared with ellipsometry data.

Acknowledgements: CNCS-UEFISCDI, project number 18ROMD/20.05.2024, the NATO grant SPS MYP G6153 and MEC subprogram 011207.

[1] C. Ahn, A. Cavalleri, A. Georges, S. Ismail-Beigi, A. J. Millis, J.-M. Triscone, "Designing and Controlling the Properties of Transition Metal Oxide Quantum Materials," Nat. Mater. **20**, 1462-1468 (2021).
[2] A. Cannavale, U. Ayr, F. Fiorito, F. Martellotta, "Smart Electrochromic Windows to Enhance Building Energy Efficiency and Visual Comfort," Energies **13**(6), 1449 (2020).
[3] A. Belenchuk, O. Shapoval, V. Roddatis, K. Stroh, S. Vatavu, J. Wawra, and V. Moshnyaga, "Spinodal decomposition introduces strain-enhanced thermochromism in polycrystalline $V_{1-x}Ti_xO_2$ thin films," Nanoscale **15**(27), 11592-11602 (2023).

Advanced Functional Materials for Hydrogen Storage and Piezomagnetic Transduction

Fabio DI PIETRANTONIO

Institute for Microelectronics and Microsystems - CNR, Rome 00133, Italy
Corresponding author: *fabio.dipietrantonio@cnr.it*

The development of advanced functional materials is playing a central role in addressing some of the most pressing technological challenges related to sustainable energy and next-generation devices. In this invited contribution, a review of two highly promising classes of materials will be presented: materials for hydrogen storage and materials exhibiting piezomagnetic behaviour for magneto-mechanical transduction. The first research area is closely linked to the growing demand for efficient, safe, and scalable solutions for hydrogen-based energy systems, where the design of nanostructured and surface-engineered materials is opening new opportunities for improving storage capacity and release dynamics. The second concerns piezomagnetic materials, whose coupling between mechanical excitation and magnetic response makes them attractive for innovative transducers, sensors, and mechanical antennas. Although these topics belong to different application domains, they share a common scientific vision based on the engineering of material properties to obtain targeted multifunctional performance. The presentation will provide an overview of the main material strategies, the governing physical mechanisms, and the current limitations that still hinder broader technological deployment. By bridging energy-related materials and magneto-mechanical concepts, this review aims to highlight emerging perspectives, unresolved challenges, and future directions for industrially relevant and interdisciplinary research.

Correlative Spectroscopy and Microscopy Analysis of Micro- and Nanoplastics and Their Effects on Cells and Tissues

George SARAU, Silke CHRISTIANSEN

Fraunhofer Institute for Ceramic Technologies and Systems IKTS, Äußere Nürnberger Str. 62, 91301 Forchheim, Germany
Corresponding author: george.sarau@ikts.fraunhofer.de

Current human risk assessment for micro- and nanoplastics (MNPs) particles requires comprehensive data on the relevant physio-chemical properties of MNPs that lead to ingestion and inhalation toxicity. To correlate particle properties with toxicity assays, we established measurement protocols for the visualization, characterization, and quantification of MNPs both separately and within complex biological matrices. These workflows involved correlative spectroscopy, microscopy, and biomedical investigations, including Raman, optical, fluorescence, and electron techniques, among others. Representative MNP materials, such as PS, PVC, LDPE, PET, and TPU, were used to assess the toxicity effects on human Calu-3 lung cells, podocytes (kidney cells), as well as on organ tissues from mice and zebrafishes exposed to MNPs. Raman spectroscopy (spontaneous and stimulated) was applied to unambiguously distinguish between MNP particles and the biological background of cells and tissues based on their specific chemical fingerprint. The Raman results were complemented by high-resolution imaging using scanning electron microscopy (SEM) and fluorescence for stained MNPs, mostly combined at the same regions of interest employing precise and automatic relocalization technologies from Horiba, such as Nano-Global Positioning System (nanoGPS) and Particle Finder [1]. In addition to the chemical composition, our correlative experimental approach supported by customized machine learning algorithms, enabled us to automatically determine the number, shape, size, morphology, and clustering of particles inside and on top of the cells and tissues in a statistically relevant manner. The MNP descriptors mentioned above, along with other descriptors like surface charge and reactivity, phospholipid interaction, dissolution rate, molecular weight, molecular mobility, and crystallinity, were correlated to various biomedical tests including cytotoxicity, interleukin-8 levels, inflammatory and macrophage responses, and gut microbiome alterations. It was found that MNPs can increase proinflammatory cytokines and disrupt the gut microbiome, reducing microbial diversity and shifting bacterial populations towards pro-inflammatory and potentially pathogenic species [2].

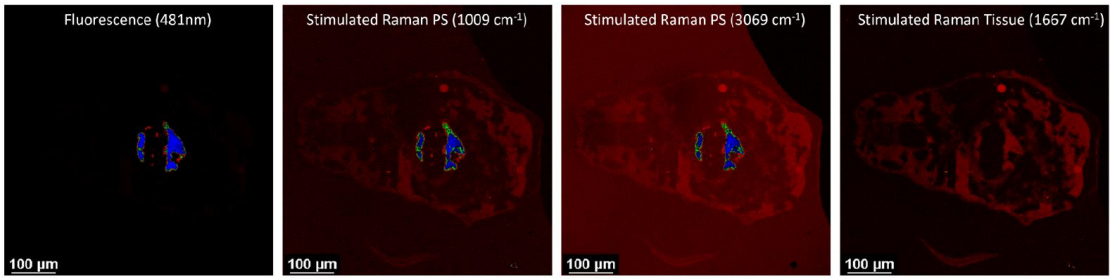

Fig. 1. Correlative fluorescence and Raman measurements on a zebrafish sample with 50 nm PS particles in blue.

[1] G. Sarau, M. Yarbakht, B. Oßmann, L. Kling, J. Ast, F. Vollnhals, J. Mueller-Deile, M. Schiffer, S. Christiansen, "Context Microscopy and Fingerprinting Spectroscopy of Micro- and Nanoplastics and Their Effects on Human Kidney Cells Using NanoGPS and Particle Finder," Horiba Readout **54**, 23-32 (2020).

[2] V. Kopatz, U. Resch, K. Draganic, et al., "Polystyrene micro- and nanoplastics aggravates colitis in a mouse model – effects on biodistribution, macrophage polarization, and gut microbiome," Micropl.&Nanopl. **6**, 9 (2026).

Thin Film Batteries Prepared by Physical Vapour Deposition (PVD) Methods

Thomas LIPPERT[1,2,3]

[1]*PSI Center for Neutron and Muon Sciences, Paul Scherrer Institute, 5232 Villigen, Switzerland*
[2]*Laboratory of Inorganic Chemistry, Department of Chemistry and Applied Biosciences, ETH Zürich, 8093 Zürich, Switzerland*
[3]*International Institute for Carbon-Neutral Energy Research (WPI-I2CNER), Kyushu University, 744 Motooka, Nishi-ku, Fukuoka 819-0395, Japan*
Corresponding author: *thomas.lippert@psi.ch*

Thin film solid-state Li-ion batteries (TFSSBs) represent a promising advancement for next-generation energy storage devices. Their reduced dimensions, higher power density, and rapid charge/discharge rates make them attractive [1]. A critical component of TFSSBs is the solid electrolyte (SE). Currently, LiPON is a popular choice as thin film SE due to its wide electrochemical window, high electronic resistivity together with sufficiently high ionic conductivity. Conversely, its amorphous character inhibits high-temperature fabrication of TFSSBs heterostructures due to the risk of LiPON crystallization, thus limiting the material range of potential electrode-electrolyte parings.

In this study, we evaluate the applicability of lithium germanium phosphate ($Li_{4-x}Ge_{1-x}P_xO_4$, LGPO) as a thin film Li-ion conductor fabricated by pulsed laser deposition (PLD) for use as a SE. LGPO films demonstrate acceptable ionic conductivity (~10^{-6} S/cm), comparable to the LGPO bulk and also amorphous LiPON films [2]. Notably, the conductivity of LGPO films remains consistent across various deposition temperatures, providing a wide deposition temperature range suitable for the fabrication of the device [2]. We have investigated the conductivity of LGPO films using in situ impedance spectroscopy, allowing us to study the films immediately after growth inside the vacuum chamber in a controlled atmosphere of our interest (Ar, N_2, and O_2) without air exposure. Furthermore, we have investigated the structural, morphological, and electrochemical properties of $Li_4Ti_5O_{12}$ (LTO) and $LiMn_2O_4$ (LMO) as anode and cathode, respectively, grown on Nb-doped $SrTiO_3$ substrates buffered with a thin conducting layer as a current collector to provide an improved matching of the lattice parameters and thereby reduce interfacial strain.

Our investigation of crystalline LGPO thin films grown at 550 ºC as solid-state oxide electrolytes has demonstrated a high ionic conductivity (up to 10^{-5} S/cm) at room temperature (RT), showing their applicability in TFSSBs. In addition, we have observed an acceptable ionic conductivity (up to 10^{-7} S/cm) for amorphous LGPO thin films grown at RT. The LTO and LMO electrode layers are shown to grow epitaxially and can be cycled in liquid cells at high C rates (100C for LMO and 400C for LTO) with impressive cyclability (5000 cycles at 50C) due to the strain engineering with the thin interlayer. First examples of thin film batteries will also be shown.

Acknowledgements: The authors acknowledge financial support from the Paul Scherrer Institute and the Swiss National Science Foundation (SNSF) through the project scheme (204103) and Ambizione scheme (216196).

[1] K. V. Kravchyk, F. Okur, M. V. Kovalenko, "Break-Even Analysis of All-Solid-State Batteries with Li-Garnet Solid Electrolytes," ACS Energy Lett. **6**(6), 2202-2207 (2021).
[2] S. D. Lacey, E. Gilardi, E. Müller, C. Merckling, G. Saint-Girons, C. Botella, R. Bachelet, D. Pergolesi, M. El Kazzi, "Integration of $Li_4Ti_5O_{12}$ Crystalline Films on Silicon Toward High-Rate Performance Lithionic Devices,". ACS Appl. Mater. Interfaces, **15**(1), 1535-1544 (2023).

Anodic Memristors: A New Generation of Nanoscale Devices for Memory and Artificial Synapse Applications

Andrei Ionut MARDARE[1,2], Elena ATANASOVA[1], Achim Walter HASSEL[1,3]

[1]*Institute of Chemical Technology of Inorganic Materials, Johannes Kepler University Linz, 4040 Linz, AUSTRIA*
[2]*National Institute for Lasers, Plasma and Radiation Physics, 077125 Magurele, ROMANIA*
[3]*Faculty of Medicine and Dentistry, Danube Private University, 3500 Krems an der Donau, AUSTRIA*
Corresponding author: andrei.mardare@jku.at

Valve metals will always be in the focus of electrochemical community due their anodization particularities at the nm scale. Their anodic oxides have shown promising qualities as memristive elements, in which the resistance state of a device can be switched between two or more levels by externally applied electrical fields. This impacts the conductive pathways formation, which is mediated by oxygen vacancies and/or cations, and their field-activated movement inside the oxide. Oxides of Hf, Nb, Ta, Ti and W are most relevant for such applications and are easily produced anodically lowering the device cost [1, 2]. The conductive pathway can be a direct one, as in filamentary switching of hafnia, or an interfacial type mediated by crystalline inclusions in oxides such as titania [3,4]. Figure 1 shows examples from both. Memristor fabrication by anodization is an underestimated topic with great industrial implementation potential.

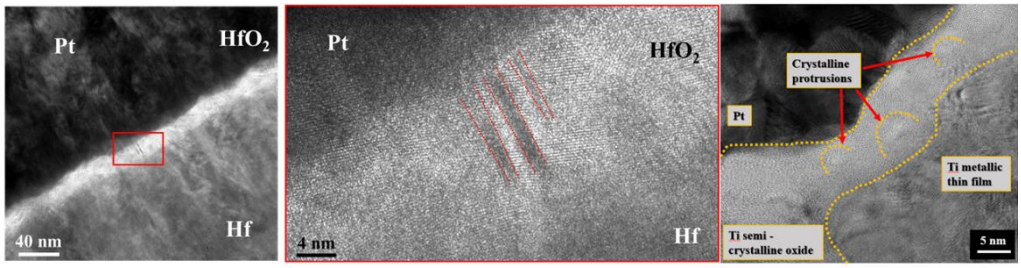

Fig. 1 Filamentary and interfacial memristive switching features in anodic oxides.

A combinatorial route is applied for obtaining new memristive materials. Atomic mixture deposition (by co-sputtering) and wedge-type thickness gradient deposition (by sequential sputtering) are used for obtaining binary metallic material libraries. Upon anodization, mixed oxide combinatorial libraries are obtained. Enhanced memristive properties are reported when the material contains regions with different oxidation states. The applied anodic oxidation route directly results in a vertical compositional gradient, no additional processing step being necessary. Metal-insulator-metal structures are systematically screened as a function of their composition. Memristive electrical testing in a high throughput approach reveals the best mixture of oxides for improved devices.

Acknowledgements: This research was funded in whole or in part by the State of Upper Austria through the Linz Institute of Technology (project COMSENS, LIT-2023-12-SEE-111).

[1] I. Zrinski, C. C. Mardare, L.-I. Jinga et al., "Electrolyte-Dependent Modification of Resistive Switching in Anodic Hafnia," Nanomaterials **11**(3), 666 (2021).
[2] I. Zrinski, C. C. Mardare, L.-I. Jinga et al., "Phosphate incorporation in anodic hafnium oxide memristors," Appl. Surf. Sci. **548**, 149093 (2021).
[3] E. Atanasova, A. Greul, A. W. Hassel, M. Santamaria and A. I. Mardare "A brief overview of anodic memristors: fundamentals, classification and properties," Mat. Adv. **7**(3), 1357-1377 (2026).
[4] E. Atanasova, A. Greul, I. M. Ghitiu, N. Scarisoreanu, A. W. Hassel, A. I. Mardare, "Combinatorial Screening for Europium Induced Defect Engineering in Titania Anodic Memristors," Adv. Mater. Interfaces **13**(3), e00883 (2026).

Advanced Monitoring of Air Non-Thermal Plasma Sources: Key Applications

Beatrice SPINU[1], Ioana Cristina GERBER[2], Ilarion MIHAILA[2], Valentin POHOATA[1], Ionut TOPALA[1]

[1]*Iasi Plasma Advanced Research Center (IPARC), Faculty of Physics, Alexandru Ioan Cuza University of Iasi, Carol I, No. 11, 700506, Iasi, ROMANIA*
[2]*Integrated Center of Environmental Science Studies in the North-Eastern Development Region (CERNESIM), Alexandru Ioan Cuza University of Iasi, Carol I, No. 11, 700506, Iasi, ROMANIA*
Corresponding author: *ionut.topala@uaic.ro*

Atmospheric pressure plasma sources are widely studied in laboratories and applied in industry across materials science, life sciences, and environmental science [1-6]. Overall, atmospheric pressure plasma (APP) sources offer key technological advantages, such as their versatility in integrating with complex devices, compatibility with standard or non-standard electrical excitation methods, and effective operation at atmospheric or sub-atmospheric pressures. Additional benefits include the absence of ion etching processes, high collisionality paired with a low Debye length, low ionization degrees, and gas temperatures close to room temperature. Furthermore, APPs enable pulsed chemistry while generating a high density of reactive species per unit volume.

In many studies, plasma diagnostic setups monitor electrical, optical, or spectroscopic data from the plasma source. For instance, applied voltage and discharge current reveals the plasma's operating regime, while emission or absorption spectroscopy identifies excited atomic and molecular species within the plasma volume and can be used to estimate specific plasma temperatures. Advanced techniques like mass spectrometry or high-speed imaging provide supplementary insights into gas-phase composition or propagation dynamics, over short periods of time. Nevertheless, multi-technique diagnostics of atmospheric pressure plasma sources over multiple operation cycles and the impact of discharge variability on effects in materials, life, and environmental sciences remain rarely discussed.

In this paper, we describe and discuss a novel approach for advanced monitoring of air non-thermal plasma sources interacting with liquids. This involves collecting large amount of electrical, optical, and temperature data over extended operation times, combined with gas-phase diagnostics and liquid analysis. All data are used to assess discharge variability and identify operational windows that ensure consistent effects across many plasma source operation cycles. By adjusting high-voltage excitation parameters, along with gas feed, liquid target or geometric features, the characteristics of atmospheric pressure plasma sources can be precisely controlled to meet the growing demands of applications in materials science, life sciences, and environmental science.

[1] J. Winter, R. Brandenburg, and K.-D. Weltmann, "Atmospheric pressure plasma jets: an overview of devices and new directions," Plasma Sources Sci. Technol. **24**(6), 064001 (2015).
[2] H. Kakiuchi, H. Ohmi, and K. Yasutake, "Atmospheric-pressure low-temperature plasma processes for thin film deposition," J. Vac. Sci. Technol. A **32**(3), 030801 (2014).
[3] G. Y. Park, S. J. Park, M. Y. Choi, et al., "Atmospheric-pressure plasma sources for biomedical applications," Plasma Sources Sci. Technol. **21**(4), 043001 (2012).
[4] F. Bilea, M. Garcia-Vaquero, M. Magureanu, et al., "Non-thermal plasma as environmentally-friendly technology for agriculture: A review and roadmap," Crit. Rev. Plant Sci. **43**(6), 428-486 (2024).
[5] L. I. Leti, I. C. Gerber, I. Mihaila et al., "The modulatory effects of non-thermal plasma on seed's morphology, germination and genetics - A review," Plants **11**(16), 2181 (2022).
[6] R. Brandenburg, H. Barankova, L. Bardos et al., "Plasma-based depollution of exhausts: principles, state of the art and future prospects," in Monitoring, Control and Effects of Air Pollution, ed. A. G. Chmielewski, InTech Open Book, 229-254 (2011).
[7] I. C. Gerber, I. Mihaila, D. Hein et al., "Time behaviour of helium atmospheric pressure plasma jet electrical and optical parameters," Appl. Sci. **7**(8), 812 (2017).
[8] B. Tatarcan, V. Pohoata, I. C. Gerber et al., "Effects of long-duration non-thermal plasma treatment on quinoa seeds: surface chemistry, mesoscale morphology and germination under optimal and saline conditions," Food Biosci. **68**, 106709 (2025).
[9] C. Lazarou, C. Anastassiou, I. Topala, A. S. Chiper, I. Mihaila, V. Pohoata and G. E. Georghiou, "Numerical simulation of capillary helium and helium-oxygen atmospheric pressure plasma jets: propagation dynamics and interaction with dielectric," Plasma Sources Sci. Technol. **27**(10), 105007 (2018).
[10] A. Nastuta, I. Topala, V. Pohoata, I. Mihaila, C. Agheorghiesei, N. Dumitrascu, "Atmospheric pressure plasma jets in inert gases: Electrical, optical and mass spectrometry diagnosis," Rom. Rep. Phys. **69**(1), 407 (2017).

Tailoring Optical Properties in Fluoride Crystals via Tb and Tm Incorporation

Marius STEF[1], Gabriel BUSE[2], Philippe VEBER[1], Daniel VIZMAN[1]

[1]*West University of Timisoara, Faculty ov Physics, Bd. V.Parvan 4, Timisoara*
[2]*West University of Timisoara, ICAM, Bd. V.Parvan 4, Timisoara*
Corresponding author: *daniel.vizman@e-uvt.ro*

Rare-earth-doped materials are key enabling materials for a wide range of photonic applications, including solid-state lasers, wavelength converters, magneto-optical components, scintillators and luminescent phosphors. In particular, fluorite-type hosts such as CaF_2 and BaF_2 have attracted sustained interest for visible and near-infrared photonics, due to their low multiphonon relaxation rates and high optical quality, which enable efficient emission and amplification processes, or magneto-optical properties. Tm^{3+} is a very interesting doping cation because of its electronic configuration, which allows several optical emissions at 1.5 μm, 1.9 μm and 2.3 μm. Hence, Tm^{3+}-doped fluoride single crystals are promising for the realization of eye-safe laser, remote sensing of atmospheric species such as CH_4, infrared counter-measurements or for medicine purposes.

Tb^{3+}-doped single crystals are attractive materials for green photonic applications due to their low phonon energy, high optical transparency, and efficient Tb^{3+} emission.

CaF_2 and BaF_2 single crystals doped with different TbF_3 concentrations (1, 5, and 10 mol%) and different TmF_3 content (0.1, 1 and 5 mol%) were grown by Bridgman technique [1-3] and systematically investigated in order to clarify the concentration-dependent spectroscopic behaviour of rare earth ions in a fluorite host. We focused on the influence of dopant concentration on optical absorption and UV-VIS luminescence behavior.

Effective partitions coefficients of rare earth dopant in CaF_2 and BaF_2, which are of high importance for adjusting initial dopant content in the growth load in order to obtain as much as possible the final content of dopant in as-grown crystal, were calculated by two methods: ICP-MS coupled with LIBS and by optical absorption spectroscopy.

Chemical characterization has shown that single crystals exhibit a highly homogenous [Tm] content distribution throughout the whole boule volume, but optical absorption measurements have displayed the presence of both Tm^{3+} and Tm^{2+} cations. The simultaneous presence of these cations is assumed to be likely due to the carbon environment and synproportionation partial reaction of TmF_3 which leads to Tm-mixed-valency-doped CaF_2 single crystals since Tm^{2+} can enter easily in the CaF_2 matrix because no charge compensation is needed.

The results provide a consistent and detailed picture of the radiative behaviour of Tb and Tm ions in a fluorite-type host in the visible spectral range and clarify the role of concentration-dependent effects on their optical performance.

Acknowledgements: This work was supported by a grant of the Ministry of Education and Research, Romania, CCCDI - UEFISCDI, project number PN-IV-P6-6.1-CoEx-2024-0154, within PNCDI IV.

[1] I. Bodea, C. Schornig, G. Buse, P. Veber, D. Vizman, "Spectroscopic Properties of Tb^{3+} Ions in TbF_3-Doped CaF_2 Crystals," Materials **19**(4), 801 (2026).

[2] M. Stef, C. Schornig, G. Buse, M. Poienar, P Veber, D. Vizman, "Spectroscopic analysis and Judd-Ofelt modelling of Tm^{3+}-doped BaF_2 crystals," Opt. Mater. **169**, 117689 (2026).

[3] G. Buse, C. Schornig, M. Stef, M. Poienar, D. Tatomirescu, A. Popescu, J. Debray, V. Motto-Ros, F. Pelascini, D. Vizman, P. Veber, "Single crystal growth by the Bridgman-Stockbarger technique of CaF_2-rich - TmF_3 solid solutions: Evidence of mixed valence Tm^{2+} and Tm^{3+} cations," J. Alloys Compd. **1010**, 177784 (2025).

Packaging Technologies for Robust, Hybrid Laser Systems

Erik BECKERT

Fraunhofer-Institute for Applied Optics and Precision Engineering (IOF), Albert-Einstein-Strasse 7, 07745 Jena, Germany
Corresponding author*:* erik.beckert@iof.fraunhofer.de

The transition of hybrid laser setups from a functional demonstration in the laboratory towards a stable deployment in various fields of applications result in stringent engineering challenges. For example, the use of lasers in space and aviation requires stability vs. thermal vacuum, mechanical vibration, and radiation loads, resulting in significant engineering effort to maintain the laser-optical functionality over the anticipated time of service.

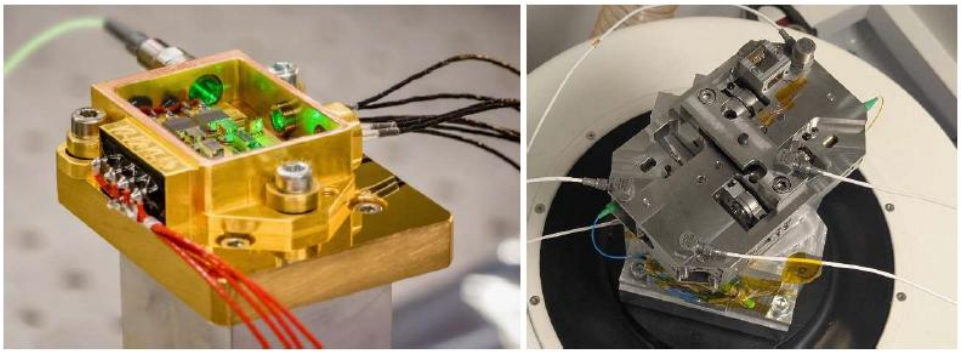

Fig. 1. (left) Narrow-band 532 nm, 100 mW laser for the Raman instrument of EXOMARS; **(right)** GHz entangled photon source for satellite-based quantum communication.

Potential approaches, such as reducing the degrees and ranges for the alignment of discrete components, stable and durable bonding technologies, and/ or full or partial monolithic integration have to be considered and are illustrated in the contribution based on two space application examples. The first one is the miniaturized 532 nm, 100 mW (in fiber) narrow-band laser for the laser induced breakdown Raman spectroscopy instrument of the EXOMARS mission that aims to find traces of life on the surface of plant Mars, and that poses the additional requirements of polymer-free devices and systems for planetary protection. Second example is a high-performant entangled photon source, that emits entangled photons in the C-band, and in a GHz regime for an efficient link with >200 bit final secure key rate per pass of a LEO satellite quantum key distribution mission. Both hybrid laser-optical sources were realized as either flight models (FM) or Engineering Qualification Models (EQM), surpassing stringent qualification during environmental testing.

Acknowledgements: The EXOMARS laser was funded by Spanish space agency INTA, the GHz entangled photon source was developed within the QUDICE "Quantum devices and subsystems for communications in space" project that has received funding from the European Union's Horizon Europe research and innovation programme under grant agreement No 101082596.

[1] P. Ribes-Pleguezuelo, D. Guilhot, M. Gilaberte Basset, E. Beckert, R. Eberhardt and A. Tünnermann, "Insights of the qualified ExoMars laser and mechanical considerations of its assembly process," Instruments **3**(2), 25 (2019).

[2] E. Beckert, C.-A. Melo Luna, N. Pavlovic, F. Kraze, T. Dietrich, and R. Sebak, "Ultracompact, space-suitable, and hybrid entangled photon source for satellite-based QKD," Proc. SPIE **13919**, Quantum Computing, Communication, and Simulation VI, 139190I (5 March 2026).

Plasma-Activated Liquids: From Fundamental Science to Biomedical Applications

Hiromasa TANAKA, Camelia MIRON, Masaaki MIZINO, Kenji ISHIKAWA, Shinya TOYOKUNI, Hiroaki KAJIYAMA, Masaru HORI

Center for Low-temperature Plasma Sciences, Nagoya University, Furo-cho, Chikusa-ku, Nagoya 464-8603, Japan
Corresponding author: tanaka.hiromasa.g1@f.mail.nagoya-u.ac.jp

Low-temperature plasma has evolved from a tool in materials processing to a versatile platform enabling complex interactions with liquids and biological systems. In particular, plasma-liquid systems provide a unique environment where nonequilibrium chemistry drives the formation of chemically rich solutions with emerging biological functionalities.

At the Center for Low-Temperature Plasma Sciences, Nagoya University, we have been developing an interdisciplinary framework that connects plasma physics, solution chemistry, and life science. Plasma irradiation of biologically relevant liquids induces not only reactive oxygen and nitrogen species but also complex reaction pathways involving organic molecules, leading to the formation of previously uncharacterized compounds. These plasma-driven chemical transformations are closely linked to selective biological effects, particularly in cancer cells.

To elucidate the underlying mechanisms, we have combined advanced analytical techniques with systems-level biological analyses, revealing how plasma-induced chemical complexity can influence intracellular signalling pathways and metabolic regulation.

In parallel, recent work at our Center has expanded the scope of plasma applications to soft materials, particularly plasma-treated polymers such as chitosan. Plasma processing enables modification of polymer structures and crosslinking behavior, leading to the formation of functional hydrogels with tunable physicochemical properties. These developments highlight the versatility of plasma-driven chemistry not only in liquid systems but also in polymeric materials, opening new possibilities for biomedical and bioengineering applications.

By integrating plasma science across liquids, polymers, and biological systems, we are beginning to establish a unified understanding of how plasma-induced reactions can be harnessed to design functional materials and control biological responses.

In parallel with these fundamental investigations, translational research toward clinical applications has progressed, including preclinical validation and early-stage human studies. These efforts demonstrate the feasibility of plasma-activated solutions as a novel class of therapeutic agents.

A major challenge moving forward is to achieve predictive control over plasma-induced reactions across different states of matter-liquids and polymers-by linking microscopic reaction pathways to macroscopic functionality. Establishing such design principles will enable the rational development of plasma-based systems tailored to specific biomedical and agricultural applications. This approach may ultimately establish plasma-enabled life science as a new interdisciplinary frontier.

Acknowledgements: This work was partly supported by a Grant-in-Aid for Scientific Research (A) (No. 24H00202) from the Ministry of Education, Culture, Sports, Science and Technology of Japan, as well as the joint usage / research program of the Center for Low-Temperature Plasma Science, Nagoya University, and the Plasma-Bio Consortium.

Plasma-Activated Colloids for Bioapplications: Characteristics of a Surface-Wave Microwave Discharge and Design of Laser Ablation in Liquid System

Kinga KUTASI[1], Péter HARTMANN[1], Zsolt TÓTH[2], Cédric NÖEL[3]

[1]*HUN-REN Wigner Research Centre for Physics, H-1121 Budapest, Hungary*
[2]*Department of Medical Physics and Informatics, University of Szeged, H-6720, Szeged, Hungary*
[3]*University of Lorraine, CNRS, IJL, 54000 Nancy, France*
Corresponding author: *kutasi.kinga@wigner.hun-ren.hu*

The plasma-treated, i.e. reactive oxygen and nitrogen species (RONS) enriched liquids, hydrosols and hydrogels have been long tested in several applications in the field of medicine (wound healing/disinfection or cancer therapy) and agriculture (seed priming, decontamination, fertilizer). Combining RONS with nanoparticles (NPs) it is expected to enhance the efficiency of plasma-treated liquid based methods.

Plasma-activated NP colloids can be achieved through two different approaches: (*i*) plasma treatment of NP colloid [1] and (*ii*) laser ablation in plasma-treated liquid [2]. By using the plasma-treated liquid for laser ablation different ionic environments [3] can be provided for the NP formation, which influences the particle formation and their morphological and optical properties. The presentation focuses on two main topics: (*i*) the characteristics of an atmospheric pressure surface-wave microwave discharge used for plasma treatment of liquids [4,5] and (*ii*) the design of a laser ablation in liquid system allowing efficient NP production [2].

The surface-wave microwave discharge is generated with the help of a surfatron wave launcher in a few mm diameter dielectric tube and is sustained by the surface-wave travelling on the dielectric and plasma column boundary. At atmospheric pressure, where the plasma plume exits into the free air, the boundary conditions become variable. The surfatron is designed to launch the wave in the (0,0) mode, which results in a plasma column filling the central part of the discharge tube. However, during operation the filamentation of the discharge can occur. The random appearance, the moving and collapsing of the filaments can be observed at μs scale. The presentation will discuss (*i*) the influence of the variable boundary conditions on the discharge characteristics, such as temperature and electron density, (*ii*) the effect of the operation conditions on the stability of the plasma column and the filamentation of the discharge, and (*iii*) the interaction of the plasma plume with the liquid surface and the deposition of reactive species into the batch and flowing liquids.

The NP colloids are prepared by laser ablation of solid surfaces in liquid, i.e. by laser ablation in liquid (LAL) method. The method relies on a high intensity pulsed laser, in the present case a ns 1064 nm Nd:YAG laser. Several system geometries, which favour the energy deposition and allows the guiding of laser beam through or outside of ablated material can be designed. The presentation will discuss the design of a system, which makes possible a very efficient NP production, i.e. high concentration in very short ablation time, in the case of metals with different structural and physical properties.

[1] K. Kutasi, N. Krstulović, A. Jurov, K. Salamon, D. Popović and S. Milošević, "Controlling: the composition of plasma-activated water by Cu ions," Plasma Sources Sci. Technol. **30**(4), 045015 (2021).
[2] K Kutasi, L. Péter and Z. Tóth, "Plasma-deposited reactive species assisted synthesis of colloidal zinc-oxide nanostructures," J. Phys. D-Appl. Phys. **57**(31), 315201 (2024).
[3] K. Kutasi, L. Bencs, Z. Tóth, S. Milošević, "The role of metals in the deposition of long-lived reactive oxygen and nitrogen species into the plasma activated liquids," Plasma Process. Polym. **20**(3), 2200143 (2023).
[4] K Kutasi, D. Popović, N. Krstulović and S. Milošević, "Tuning the composition of plasma-activated water by a surface-wave microwave discharge and a kHz plasma jet," Plasma Sources Sci. Technol. **28**(9), 095010 (2019).
[5] K Kutasi, C. Nöel, T. Belmonte and P. Hartmann, "Low-power atmospheric-pressure surface-wave microwave discharge in contact with batch and flowing liquids," J. Phys. D-Appl. Phys. **59**(1), 015208 (2026).

Pulsed Laser Ablation in Liquids of MnZn Ferrites:From Green Synthesis to Sustainable Nanomagnetic Devices

Catalin-Daniel CONSTANTINESCU[1], Raphael COQUARD[1], Alaa ALASADI[1,2,3], Nicola A. MORLEY[3], Maria-Catalina PETRESCU[1,4], Anne-Patricia ALLONCLE[1], Romain SCARABELLI[1], Ahmed AL-KATTAN[1], Lucian-Gabriel PETRESCU[1,4]

[1]*Aix-Marseille Université, CNRS, LP3 UMR 7341, Marseille, France*
[2]*Technical Institute of Karbala, Department of Computer Systems, Al-Furat Al-Awsat Technical University, Iraq*
[3]*School of Chemical, Materials and Biological Engineering, University of Sheffield, Sheffield S1 3JD, United Kingdom*
[4]*UNSTPB - National University of Science and Technology POLITEHNICA Bucharest, Bucharest 060042, Romania*
Corresponding author: catalin.constantinescu@cnrs.fr

Rethinking the design and fabrication of magnetic materials is essential for enabling sustainable technologies. Manganese–Zinc (MnZn) ferrites are key candidates for high frequency, energy-efficient devices, yet challenges remain in reconciling performance, scalability, and sustainability. Here, we propose a unified, laser-driven approach to MnZn ferrites across multiple length scales, from bulk to thin films and nanoparticles, where laser matter interaction serves as a central enabling tool.

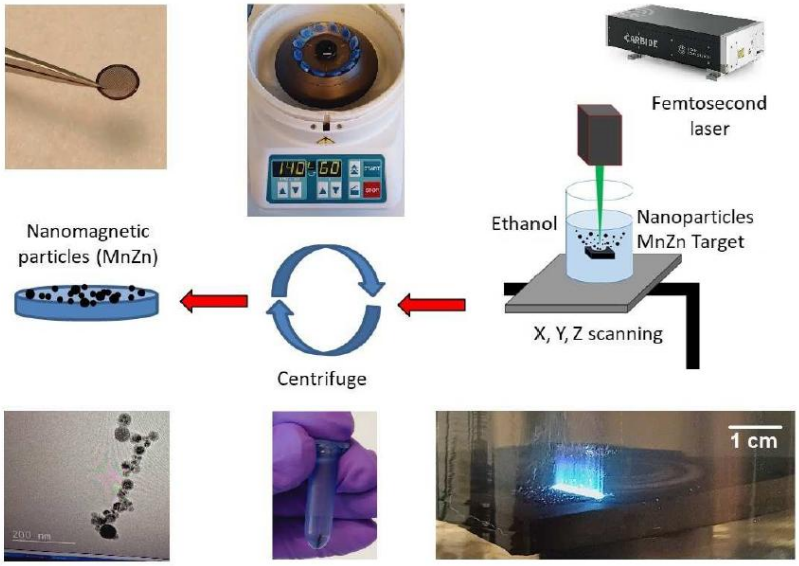

Fig. 1. Schematic diagram of the pulsed laser ablation in liquids (PLAL) technique, and real images of the experimental process.

We first revisit bulk $Mn_{0.75}Zn_{0.25}Fe_2O_4$ as a reference system, establishing controlled relationships between composition, microstructure, and magnetic behaviour. This framework is extended to thin films, where laser-based processing enables tailored crystallographic orientation and anisotropy through controlled growth conditions. At the nanoscale, pulsed laser ablation in liquids (PLAL) emerges as a green, single-step synthesis route for high-purity, surfactant-free nanoparticles with tunable size and magnetic properties, as shown in Fig. 1. By bridging bulk, thin films, and nanoparticles within a single laser-enabled strategy, this work outlines a coherent pathway for designing nanomagnetic materials. It highlights a vision in which fabrication, functionality, and sustainability are intrinsically linked, opening routes toward energy-efficient electronics and advanced magnetic devices.

Acknowledgements: The authors gratefully acknowledge: (i) the mobility funding provided by the EUROPHOTONICS Erasmus Mundus Joint Master Programme at Aix-Marseille Université, which supported the visit of Prof. Lucian Petrescu to LP3; (ii) the financial support awarded to Prof. Alaa Alasadi for his fellowship at LP3 by the French Embassy in Iraq and Campus France, within the framework of the strategic partnership between France and Iraq; and (iii) the funding provided by the Institut Marseille Imaging to Raphaël Coquard for his master internship at LP3.

Advancing Spherical Torus Proton–Boron Fusion: Physics, Technology, and AI-Enabled Control

Dani GALLART and the ENN Energy Research Team

ENN Science and Technology Development Co., Ltd. Langfang 065001, People's Republic of China
Corresponding author: daniegalla@enn.cn

The development of commercially viable fusion energy is entering a new phase, driven by the convergence of advanced plasma concepts, enabling technologies, and private-sector investment. This talk presents the strategy and recent progress of ENN Group toward realizing compact, cost-effective fusion based on proton–boron (p–^{11}B) reactions. Unlike conventional deuterium–tritium approaches, p–^{11}B fusion offers the prospect of aneutronic operation, reduced radioactive burden, and direct energy conversion, but requires significantly higher plasma performance.

ENN's approach combines spherical torus configurations with innovative heating and fueling schemes to enhance reactivity and confinement. Experimental results from the EXL-50 and EXL-50U devices demonstrate megampere-class discharges, high-temperature hydrogen–boron plasmas, and non-inductive current drive, providing a strong foundation for next-generation devices [1]. The upcoming EHL-2 experiment is designed to access regimes relevant for p–^{11}B burn [2].

A key element of this program is the integration of artificial intelligence for real-time plasma control and operation, enabling rapid optimization and improved stability. Together, these advances define a roadmap toward a compact fusion demonstration and potential commercialization in the next decade.

[1] Y. Shi, Y. Wang, B. Liu, X. Song, S. Song, X. Jiang, D. Guo, D. Luo, X. Gu, T. Sun, X. Huang, Z. Li, L. Dong, X. Wang, G. Yin, M. Wang, W. Liu, H. Zhao, H. Xie, L. Yong, D. Qi, B. Xing, J. Ding, C. Wu, L. Li, H. Zhang, Y. Yang, X. Zhao, E. Yang, W. Luo, P. Zhou, L. Han, Q. Zhou, H. Wang, J. Dong, B. Yuan, Y.-K. M. Peng, M. Liu and the EXL-50 team, "Overview of EXL-50 research progress," Nucl. Fusion **65**(9), 092004 (2025).

[2] Y. Liang, H. Xie, Y. Shi, X. Gu, X. Jiang, L. Dong, X. Wang, D. Yang, W. Liu, T. Sun, Y. Wang, Z. Li, J. Cai, X. Song, M. Tan, G. Yang, H. Zhao, J. Dong, Y.-K. M. Peng, S. Song, Z. Chen, Y. Li, B. Liu, D. Luo, Y. Yang, M. Liu and the EHL-2 Team, "Overview of the physics design of the EHL-2 spherical torus," Plasma Sci. Technol. **27**(2), 024001 (2025).

Laser Scanning for Optimizing Optical Coherence Tomography-Based Imaging

Virgil-Florin DUMA

3OM Optomechatronics Group, Department of Measurements and Electro-Optics, Faculty of Electronics, Telecommunications, and Information Technology, Polytechnic University of Timisoara, 2 Vasile Parvan Ave., 300223 Timisoara, Romania
Corresponding author: virgil.duma@upt.ro

Laser scanning is one of the key techniques for a range of imaging applications that include confocal microscopy (CM) and optical coherence tomography (OCT) [1]. This presentation focuses on our contributions and on-going work on galvanometer- and MEMS-based scanning for OCT. Thus, for galvanometer scanners (GSs) [2], the following aspects are discussed: **(i)** *The three most common scanning regimes* (sinusoidal, sawtooth and triangular) were studied experimentally with regard to their parameters (theoretical duty cycle, scan frequency and amplitude); the triangular function was demonstrated to be the best in providing artefact-free images in OCT [3]; **(ii)** *A mathematical model for sawtooth and triangular scanning* was obtained, demonstrating for the first time the GS saturation with the theoretical duty cycle, validating the results through OCT imaging, and extracting rules-of-thumb to properly exploit GSs for OCT [4]; **(iii)** *The optimal function of GSs* (to provide the highest duty cycle) was demonstrated to be linear plus parabolic [5], not linear plus sinusoidal, as previously considered in the literature [6].

For MEMS, the above results in GSs have been exploited in achieving *the first distortion-free real-time OCT imaging (without post-processing) with a MEMS-based probe, with pre-shaped input signals,* demonstrated for GD-OCM [7]. It must be pointed out that previous work on MEMS-based scanning probes (light weight, with lower cost than commercial ones) have required post-processing of images that made real-time OCT impossible [8]. Further on, 2D GSs and MEMS have been studied and optimized raster scanning algorithms were developed [9]. Finally, perspectives of the field in terms of other scanning systems and modalities are discussed.

Acknowledgements: *This work is supported by the European Union - NextGenerationEU, through the National Recovery and Resilience Plan (PNRR) of Romania, Component 9, Investment 4, under the Important Project of Common European Interest (IPCEI ME/CT), project ASSET-IxC - UPT (Contract No. 5.PI/I4/C9), implemented by the Polytechnic University of Timisoara in collaboration with Aumovio Technologies Romania (formerly Continental Automotive Romania). The content of this material does not necessarily represent the official position of the European Union or of the Government of Romania.*

[1] W. Drexler, M. Liu, A. Kumar, T. Kamali, A. Unterhuber, et al. "Optical coherence tomography today: speed, contrast, and multimodality," J. Biomed. Opt. **19**(7), 071412 (2014).
[2] G.F. Marshall, G.E. Stutz, Eds., Handbook of Optical and Laser Scanning, CRC Press, London (2011).
[3] V.-F. Duma, K.-S. Lee, P. Meemon, J.P. Rolland, "Experimental investigations of the scanning functions of galvanometer-based scanners with applications in OCT," Appl. Opt. **50**(29), 5735-5749 (2011).
[4] V.-F. Duma, P. Tankam, J. Huang, J.J. Won, J.P. Rolland, "Optimization of galvanometer scanning for Optical Coherence Tomography," Appl. Opt. **54**(17), 5495-5507 (2015).
[5] V.-F. Duma, "Optimal scanning function of a galvanometer scanner for an increased duty cycle," Opt. Eng. **49**(10), 103001 (2010).
[6] J. Montagu, Scanners - Galvanometric and Resonant, Encyclopedia of Optical Engineering (2003), 2465-2487.
[7] A. Cogliati, C. Canavesi, A. Hayes, P. Tankam, V.-F. Duma, A. Santhanam, K. P. Thompson, and J. P. Rolland, "MEMS-based handheld scanning probe with pre-shaped input signals for distortion-free images in Gabor-Domain Optical Coherence Microscopy," Opt. Express **24**(12), 13365-13374 (2016).
[8] C. D. Lu, M. F. Kraus, B. Potsaid, J. J. Liu, W. Choi, V. Jayaraman, A. E. Cable, J. Hornegger, J. S. Duker, and J. G. Fujimoto, "Handheld ultrahigh speed swept source optical coherence tomography instrument using a MEMS scanning mirror," Biomed. Opt. Express **5**(1), 293-311 (2014).
[9] V.-F. Duma, "Laser scanners with oscillatory elements: Design and optimization of 1D and 2D scanning functions," Appl. Math. Model. **67**, 456-476 (2019).

Ultrafast Laser for Biomimetic Surfaces and Their Applications

Xxx SEDAO

University of Lyon, Jean Monnet University, UMR 5516 CNRS, Laboratory Hubert Curien
F-42000 Saint-Etienne, France
Corresponding author: *xxx.sedao@univ-st-etienne.fr*

Nature has evolved highly efficient strategies over millions of years to optimize functional performance, inspiring the development of artificial materials and surfaces designed to achieve specific properties for practical applications. Ultrafast laser is one of the potent tools used to create bio-inspired, biomimetic as well as bio-sourced surfaces for targeted applications: i.e. liquid transport [1], optics [2,3], biomedical [4] and vision correction [5] are discussed as examples of functions and applications. Appropriate choice of laser parameter and processing conditions, such as laser pulse duration, wavelength, polarization, burst etc, is key to biomimicry.

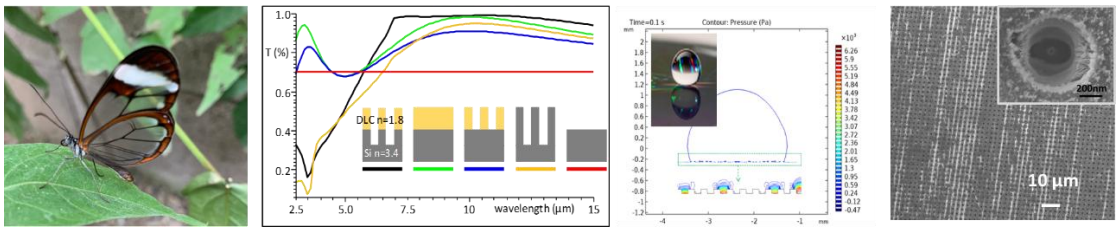

Fig. 1. Nature-inspired multi-function surface: anti-reflection (left), and water repellent (right).

As a first example, Greta oto (a dragonfly species from Central/South America) is presented as a model for biomimetic surface design, inspiring the development of optical windows with antireflective and self-cleaning properties [6]. Such functionalities are achieved through densely packed micro/nanostructures, which can be fabricated using ultrafast laser patterning, as shown in Fig.1. The text emphasizes the broad applicability of these techniques in biomedical and ophthalmological fields, where ultrafast lasers enable both research and clinical innovations. It also highlights the importance of process scalability and automation -through technologies such as beam shaping, fast optics, and robotics - to translate laboratory results into economically viable industrial applications [7,8].

Acknowledgements: *This work was mainly supported by the French National Research Agency (ANR) under the project Last-Flow (ANR-22-CE24-0026-01). Part of the work was also financed by French National Research Agency (ANR) under the "France 2030" investment plan, with reference EUR MANUTECH SLEIGHT-ANR-17-EURE-0026, by Agence de la Biomédecine, Appel d'Offre Recherche et Greffe 2022, and by Fondation des Aveugles de Guerre. At last but not at least, some of the research was funded by the European Union's Horizon 2020 research and innovation programme LaserImplant, under Grant Agreement Number: 951730.*

[1] Y. Lyu, C. Li, X. Sedao, H. Yuan, J. Zhao, "Laser-fabricated bionic surface microstructures inspired by shark and sailfish for drag reduction," Opt. & Laser Techn. **200**, 115189 (2026).
[2] J. Prada-Rodrigo, Y. Di Maio, N. Faure, E. Kachan, J. P. Colombier, X. Sedao, "Influence of the wavelength on femtosecond laser ablation thresholds and incubation coefficients of silicon and germanium," J. Laser Micro Nanoeng. **19**(3), 179-184 (2024).
[3] I. S. Omeje, J. Prada-Rodrigo, E. Gamet, Y. Di Maio, J. P. Colombier, T. Itina, X. Sedao, "Prediction of Wetting Behaviors of fs Laser Texturized Surfaces," J. Laser Micro Nanoeng. **20**(1), 49-56 (2025).
[4] S. Papa, M. Maalouf, P. Claudel, X. Sedao, Y. Di Maio, H. Hamzeh-Cognasse, M. Thomas, A. Guignandon, V.Dumas, "Key topographic parameters driving surface adhesion of Porphyromonas gingivalis," Sci. Rep. **13**(1), 15893 (2023).
[5] I. Aouimeur, L. Coulomb, S. Fraine, Z. He, G. Bonnet, T. Sagnial, G. Travers, X. Sédao, C. Mauclair, A. Moisan, P. Gain, G. Thuret, C. Maurin, "Tissue-Engineered Endothelial Keratoplasty with Controlled Cell Density: Toward Super TEEKs," Tissue Eng. Part A (2025); early access: DOI 10.1177/19373341251381346.
[6] T. Kämpfe, L. Dubost, X. Sedao, Optical Device, US 20220373718A1 patent.
[7] M. Maalouf, Y. Di Maio, S. Papa, D. Pallares-Aldeiturriaga, X. Sedao, L. Hivert, S. Papa, E. Dalix, M. Thomas, A. Guignandon, V. Dumas, "Femtosecond laser upscaling strategy and biological validation for dental screws with improved osteogenic performance," Surf. Interfaces **66**, 106546 (2025).
[8] Di Maio Y. *et al.*, "Ultrafast Laser Micro and Nanoprocessing of Cylindrical Objects," book chapter from Scaling of Laser Processing, Springer (2026).

Biomedical Optical Imaging for Translational Diagnostics and Treatment: From 3D Optical Biopsies to Pixel-precision Laser Theranostics

Daniel L. FARKAS

Department of Biomedical Engineering, University of Southern California, Los Angeles, CA 90089, USA
Corresponding author: DLFarkas@gmail.com

One of the best uses of advanced technologies is improving human health. For helping the bench-to-bedside dream of *translational* healing (by moving lab advances into the clinic) become a reality, we develop biophotonic approaches that, while technologically sophisticated, allow deployment into a clinical setting [1]. Our focus area is where light, an exceptional investigative tool [2] and patient meet [3], and improvements that yield better outcomes by addressing obstacles preventing the timely clinical adoption of laboratory-based advances, not the least of which is the difficulty of studying very small entities (molecules, organelles, cells) *within* the human body, especially quantitatively, dynamically, and preferably intrinsically (without contrast agents). *How and where we look* becomes critically important, especially if one targets - as one should - early diagnosis; for this, new tools and strategies are needed. The fact that today we can image dust on Mars better than we can image inside a human patient in our best hospitals should provide a lot of motivation, for both technologists and physicians.

We proposed and implemented a multimode [4, 5], mesoscopic [6] approach to biomedical optical imaging at all levels of biological organization, featuring lasers and hyperspectral imaging originally developed for satellite reconnaissance, and optimized for earlier, more quantitative and reproducible detection of abnormalities. Our work on cancer [7] (especially skin cancers [8, 9]) focused on generating maps of lesions within the body (3-D optical biopsy by inferential topology), while in neuro [10] we focused on primary events by high-speed imaging [11], and on the very early detection of Alzheimer's Disease [12] using the eye (retina) as a window to the brain. A tighter spatio-temporal coupling between optical diagnosis and intervention (*theranostics*) is a desirable goal [13] that we achieved by hyperspectral imaging leading to interpreted maps of *in vivo* tissue guiding pixel-specific *laser* surgery [14]. Addressing major areas of unmet need in the clinic with these new approaches could yield important improvements in disease management, and illustrative applications were chosen to emphasize the new technologies and strategies needed to achieve the desired imaging performance, and their physics/engineering underpinnings. Thoughts [15] about better ways for academia, the clinical and the corporate world to work together for innovative light-based solutions and their addressing major disease [16] will be outlined, highlighting the role of international collaborations.

Acknowledgements: The work reviewed was supported by the US National Science Foundation, National Institutes of Health and DoD, as well as by foundations and other private sources.

[1] P. Frykman et al. "Spectral imaging for precise surgical intervention in Hirschsprung's disease" J. Biophotonics **1**, 97-103, (2008).
[2] J. Fujimoto, and D.L. Farkas (editors) "Biomedical Optical Imaging", Oxford Univ. Press (2009).
[3] D. L. Farkas "Molecular biology in surgical oncology: the role of molecular imaging" in Principles and Practice of Surgical Oncology, Lippincott, Williams and Wilkins pp. 18-28, (2009).
[4] D. L. Farkas "Multimode light microscopy and the dynamics of molecules, cells and tissues," Ann. Rev. Physiol. **55**, 785-817, (1993).
[5] J. Y. Hwang et al. "A Multimode Optical Imaging System for Preclinical Applications In Vivo: Technology Development, Multi-scale Imaging and Chemotherapy Assessment," Molec. Imaging & Biology, **14**, 431-442 (2011).
[6] J. Y. Hwang "Multimodality imaging in vivo for preclinical assessment of tumor-targeted doxorubicin nanoparticles," PLoS One, **7**, e34463, (2012).
[7] X. Yuan et al. "Isolation of cancer stem cells from adult glioblastoma multiforme," Oncogene**, 23,** 9392-9400 (2006).
[8] F. Vasefi et al. "Polarization-sensitive hyperspectral imaging in vivo: A multimode dermoscope for skin analysis," Scientific Reports (a Nature journal), **4,** 4924.1-10 (2014).
[9] F. Vasefi et al. "Separating melanin from hemodynamics in nevi using multimode hyperspectral dermoscopy and spatial frequency domain spectroscopy" J. Biomed. Opt. **21**(11):114001 (2016).
[10] F. Vasefi et al. "Review of the potential of optical technologies for cancer diagnosis in neurosurgery: a step toward intra-operative Neurophotonics", Neurophotonics. **4**(1), 011010 (2017).
[11] E. Wachman et al. "Variability in the spatial distribution of presynaptic calcium entry during single action potentials," J. Neurosci. **24**, 2877-2885 (2004).
[12] M. Koronyo-Hamaoui et al. Identification of amyloid plaques in retinas from Alzheimer's patients and noninvasive in vivo optical imaging of retinal plaques in a mouse model," NeuroImage, **54 Supl. 1**, S204-17 (2011).
[13] H. Agadjanian et al. "Tumor detection & elimination by a targeted gallium corrole" Proc. Natl. Acad. Sci. USA, **106**, 6105-10 (2009).
[14] G. E. Carver et al. "High-speed multispectral confocal imaging," J. Biomed. Opt. **19**, 36016 (2013).
[15] D. L. Farkas, "Invention and commercialization in optical bioimaging," Nature Biotechnol. **21**(11), 1269-1271 (2003).
[16] D. L. Farkas, "Biomedical Applications of Translational Optical Imaging: From Molecules to Humans," Molecules **26**(21), 6651 (2021).

Metal-Doped Functional Nanoprobes for Multimodal Imaging-Guided Synergistic Tumor Theranostics

Fang YANG

Ningbo Institute of Materials Technology & Engineering, Chinese Academy of Sciences, Ningbo 315201, China
Corresponding author: yangf@nimte.ac.cn

Precise control of nanoparticle properties is key for tumor theranostics. We propose a metal-doping strategy to build multifunctional nanoprobes with programmable imaging and therapy (Fig. 1). Using $Zn_xFe_{3-x}O_4$, we show that low Zn content ($Zn_{0.2}Fe_{2.8}O_4$) enhances magnetic response, while higher doping broadens optical absorption [1,2]. $Zn_{0.2}Fe_{2.8}O_4$ combines nanoscale stiffness and magnetic responsiveness, promoting cellular uptake and force transmission under rotating fields; stiffer probes induce greater cytoskeletal remodeling, making mechanical stiffness critical for magneto-mechanical therapy. Its broadband absorption enables dual-mode MRI/PAI: T_2-weighted MRI and PA imaging at 808 nm, plus deep-tissue photothermal ablation at 1064 nm [3].

This platform achieves magneto-mechanical/photothermal synergy against triple-negative breast cancer. Photothermal therapy damages primary tumors, while magneto-mechanical stimulation disrupts cytoskeleton and suppresses metastasis via EMT reversal [3,4]. In xenografts, combined treatment yields near-complete regression, reduced lung metastasis, and prolonged survival [4]. Extending this strategy, Ga-rich Prussian blue nanoparticles disrupt iron homeostasis and mTOR/MAPK pathways for tumor suppression with multimodal imaging [5]; Yb-doped Prussian blue reprograms metabolism via mTOR inhibition and AMPK activation [6]. Thus, metal doping broadly enables nanomedicines that modulate oncogenic metabolic pathways.

Overall, this work links composition, structure-property, imaging, and synergistic therapy into a coherent framework, highlighting single-component nanoplatforms for precision cancer theranostics.

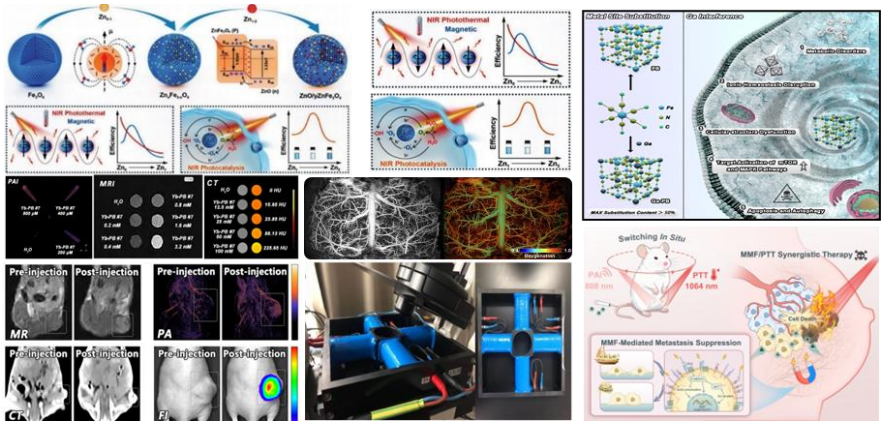

Fig. 1. Metal-doped functional nanoprobes for multimodal diagnosis and therapeutic application.

[1] Y. Ma, J. Xia, C. Yao, F. Yang, S. G. Stanciu, P. Li, Y. Jin, T. Chen, J. Zheng, G. Chen, H. Yang, L. Luo, A. Wu, "Precisely Tuning the Contrast Properties of $Zn_xFe_{3-x}O_4$ Nanoparticles in Magnetic Resonance Imaging by Controlling Their Doping Content and Size," Chem. Mater. **31**(18), 7255-7264 (2019).

[2] H. Du, F. Yang, C. Yao, Z. Zong, P. Jiang, S. G. Stanciu, H. Peng, J. Hu, B. Jiang, Z. Li, W. Lv, F. Zheng, H. A. Stenmark, A. Wu, "Multifunctional Modulation of High-Performance $Zn_xFe_{3-x}O_4$ Nanoparticles by Precisely Tuning the Zinc Doping Content," Small **18**(42), 2201669 (2022).

[3] H. Du, F. Yang, C. Yao, W. Lv, H. Peng, S. G. Stanciu, H. A. Stenmark, Y. M. Song, B. Jiang, A. Wu, A., (2022). "Double-punch" strategy against triple-negative breast cancer via a synergistic therapy of magneto-mechanical force enhancing NIR-II hypothermal ablation," Biomater. **291**, 121868 (2022).

[4] C. Yao, F. Yang, L. Sun, Y. Ma, S. G. Stanciu, Z. Li, O. U. Akakuru, L. Xu, N. Hampp, H. Lu, A. Wu, "Magnetically switchable mechano-chemotherapy for enhancing the death of tumour cells by overcoming drug-resistance," Nano Today **35**, 100967 (2020).

[5] J. Yao, Y. Qiu, J. Xing, Z. Li, A. Zhang, K. Tu, M. Peng, X. Wu, F. Yang, A. Wu, "Highly-Efficient Gallium-Interference Tumor Therapy Mediated by Gallium-Enriched Prussian Blue Nanomedicine," ACS Nano **18**(7), 5556-5570 (2024).

[6] J. Yao, J. Xing, Y. Yao, X. Wu, Y. Qiu, Z. Li, S. Xiong, H. Peng, F. Yang, A. Wu, "Ytterbium Doping-Retooled Prussian Blue for Tumor Metabolism Interference Therapy," ACS Nano **18**(52), 35758-35770 (2024).

Advancing Atmospheric Pressure Plasma Surface Engineering for Environmental and Catalytic Applications

Fiorenza FANELLI

National Research Council (CNR), Institute of Chemistry of Organometallic Compounds (ICCOM), Bari Unit, via Orabona 4, 70126 Bari, Italy
Corresponding author: *fiorenza.fanelli@cnr.it*

In recent years, low-temperature atmospheric pressure plasmas (APPs) have attracted growing attention in surface engineering [1-3]. Their unique features have enabled the development of a broad range of processes that can significantly advance the rational design of emerging functional materials, opening new prospects in environmental protection and remediation, as well as in a wide variety of catalytic applications.

In this contribution, an overview of our recent progress in surface engineering using low-temperature APPs will be presented with special focus on materials for environmental applications and catalysis. The developed plasma processes will be classified into two main research directions: one addressing the modulation of surface wettability, and the other focusing on the preparation of supported catalysts.

First, we will discuss the preparation of superhydrophobic/superoleophilic open-cell polyurethane (PU) foams that can be used as selective absorbents for oil/water separation [4]. The proposed APP process involves the etching/nanotexturing of the foam surfaces and the subsequent overcoating with a low-surface energy hydrocarbon thin film, which ultimately leads to simultaneous superhydrophobic and superoleophilic wetting properties. The plasma-treated foams exhibit promising performances in terms of oil absorption capacity, separation selectivity and recyclability. We will then present our latest results on the design of surfaces for water condensation applications. In particular, it will be shown that APP deposition allows the preparation of hydrophobic and superhydrophobic thin films on metal surfaces, promoting different water condensation regimes, such as dropwise condensation and jumping-droplet condensation, which are of interest for many environmental and energy-related applications.

Second, we will present the aerosol-assisted APP deposition of TiO_2-containing nanocomposite thin films [3,5]. This approach enables the immobilization of photocatalytic TiO_2 nanoparticles (NPs) onto macroporous supports for potential applications in water treatment [5]. Finally, we will report our recent results on the plasma-driven exsolution of Ni nanoparticles from a perovskite oxide [6]. Plasma exsolution is carried out in less than 15 min at room temperature and atmospheric pressure, using both inert gases and hydrogen-containing mixtures. Plasma-exsolved NPs show competitive performance in various catalytic processes of environmental and energy relevance.

Acknowledgements: This research was funded by the Italian Ministry for University and Research (MUR) under grant ARS01_00849. Support from the National Research Council National of Italy (2020 STM program) and the Royal Society (IES\R2\212049) is also gratefully acknowledged.

[1] F. Fanelli and F. Fracassi, "Atmospheric pressure non-equilibrium plasma jet technology: general features, specificities and applications in surface processing of materials," Surf. Coat. Technol. **322**, 174-201 (2017).
[2] F. Fanelli, P. Bosso, A.M. Mastrangelo and F. Fracassi, "Thin film deposition at atmospheric pressure using dielectric barrier discharges: advances on three-dimensional porous substrates and functional coatings," Jpn. J. Appl. Phys. **55**(7S2), 07LA01 (2016).
[3] A. Uricchio and F. Fanelli, "Low-temperature atmospheric pressure plasma processes for the deposition of nanocomposite coatings," Processes **9**(11), 2069 (2021).
[4] A. Uricchio, T. Lasalandra, E.R.G. Tamborra, G. Caputo, R.P. Mota and F. Fanelli, "Atmospheric pressure plasma-treated polyurethane foam as reusable absorbent for removal of oils and organic solvents from water," Materials **15**(22), 7948 (2022).
[5] A. Uricchio, E. Nadal, B. Plujat, G. Plantard, F. Massines and F. Fanelli, "Low-temperature atmospheric pressure plasma deposition of TiO2-based nanocomposite coatings on open-cell polymer foams for photocatalytic water treatment," Appl. Surf. Sci. 561, 150014 (2021).
[6] A. ul Haq, F. Fanelli, L. Bekris, A. Martinez Martin, S. Lee, H. Khalid, C.D. Savaniu, K. Kousi, I.S. Metcalfe, J.T.S. Irvine, P. Maguire, E.I. Papaioannou and D. Mariotti, "Dielectric barrier plasma discharge exsolution of nanoparticles at room temperature and atmospheric pressure," Adv. Sci. **11**(34), 2402235 (2024).

Catalytic Plasma Coatings for Remediation Challenges within the Planetary Boundaries Framework

Paula NAVASCUÉS, Dirk HEGEMANN

Laboratory for Advanced Fibers, Empa, Lerchenfeldstrasse 5, 9014, St. Gallen, Switzerland
Corresponding author: *paula.denavascues@empa.ch*

The latest Planetary Health Check indicates that seven out of nine Planetary Boundaries have been breached [1]. This raises serious concerns about Earth's safe operating space and motivates us to approach integral challenges rather than separate issues. In this regard, for example, antimicrobial resistance (AMR) should also be considered a key indicator of ecological stress, and not only through a self-limited clinical conceptualization [2]. Moreover, water scarcity and pollution are urgent concerns that further destabilize coupled Earth systems. Within this context, reactive oxygen species (ROS) provide a sustainable radical-chemistry route for remediation strategies. They can be generated solely from water and oxygen molecules by catalytic materials without the use of harsh reagents. Advances in nanotechnology are enabling ROS-based approaches for environmentally aligned antimicrobial [3] and water treatment applications [4].

Thin film systems combining catalytic metal oxides and plasma polymers offer a flexible strategy for controlled production and release of ROS. Low-pressure plasma deposition techniques such as magnetron sputtering are green approaches for efficiently fabricate these catalytically active systems. The appropriate coupling of semiconductors enables activation by visible light and reduces charge-carrier recombination, allowing catalytic ROS generation from water and oxygen molecules even in the absence of illumination. Plasma polymerization of organosilicon monomers is then applied to introduce ultrathin, nanoporous plasma-polymer coatings that impart additional functionality. Functionalizing catalytic plasma coatings with ultrathin plasma polymer films enables accurate control over ROS delivery. By tuning the thickness of the nanoporous functional layers, it is possible to regulate the dose of released ROS and selectively influence the conversion of superoxide into singlet oxygen. ROS production is evaluated using fluorescence spectroscopy with complementary analytical methods [5].

Although metal-oxide catalysts initially show strong performance, their activity diminishes during use and storage. Plasma surface treatment, both at low and atmospheric pressure, provides an effective method to recover high catalytic activity: species generated in the plasma reestablish the appropriate surface oxidation states and reopen porous nanostructures, thereby regenerating active sites for ROS formation. These catalytic systems are assessed for different challenges such as antiviral and antibacterial applications as well as degradation of emerging contaminants in water.

Acknowledgements: This work was financed by Swiss National Science Foundation (SNSF) Grants (i) COST 2022 (No. 213368) and (ii) Ambizione 2024 (No. 233133).

[1] Planetary Health Check - Our planet's vital signs are flashing red, (n.d.). https://www.planetaryhealthcheck.org/#reports-section (accessed March 31, 2026).
[2] C. Kirchhelle and A.P. Roberts, "Beyond breakpoint – reconceptualising AMR as a symptom of planetary stress", NPJ Antimicrobials and Resistance **3**(1), 47 (2025).
[3] G. Reina, D. Panáček, K. Rathammer, S. Altenried, P. Meier, P. Navascués, Z. Baďura, P. Bürgisser, V. Kissling, Q. Ren, R. Zbořil, P. Wick, "Light Irradiation of N-Doped Graphene Acid: Metal-Free Strategy Toward Antibacterial and Antiviral Coatings with Dual Modes of Action," Ecomat. **7**(4), e70009 (2025).
[4] A. Veciana, S. Steiner, Q. Tang, V. Pustovalov, J. Llacer-Wintle, J. Wu, X.-Z. Chen, T. Manyiwa, V. U. Ultra Jr., B. Garcia-Cirera, J. Puigmartí-Luis, C. Franco, D. J. Janssen, L. Nyström, S. Boulos, S. Pané, "Breaking the Perfluorooctane Sulfonate Chain: Piezocatalytic Decomposition of PFOS Using $BaTiO_3$ Nanoparticles," Small Sci. **4**(12), 2400337 (2024).
[5] P. Navascués, F. Kalemi, F. Zuber, P. Meier, L. M. Epasto, M. Góra, B. Hanselmann, S. Kucher, E. Bordignon, Q. Ren, G. Reina, D. Hegemann, "Plasma Functionalization Enables Diffusion Control of Reactive Oxygen Species," Small **21**(35), 2502311 (2025).

Process Characterization of High-Entropy Transition Metal Disulphides Deposited by R-HiPIMS in H_2S Atmosphere

Ivana VENKRBCOVÁ[1,2], Yue WANG[3], Hana KRÝSOVÁ[1,4], Zdeněk HUBIČKA[1], Tomáš POLCAR[3], Martin ČADA[1]

[1]*Institute of Physics of the Czech Academy of Sciences, Na Slovance 2, 182 00 Prague 8, Czech Republic*
[2]*Palacký University in Olomouc, Faculty of Science, Joint Laboratory of Optics of Palacký University and Institute of Physics of the Czech Academy of Sciences, 17. listopadu 12, 779 00 Olomouc, Czech Republic*
[3]*Czech Technical University in Prague, Faculty of Electrical Engineering, Karlovo náměstí 13, 120 00 Prague 2, Czech Republic*
[4]*J. Heyrovsky Institute of Physical Chemistry of the Czech Academy of Sciences, Dolejškova 3, 182 00 Prague 8, Czech Republic*
Corresponding author: cada@fzu.cz

High-entropy alloys (HEAs) are renowned for their superior mechanical properties, which outperform those of traditional transition metal alloys. HEA disulfides form a 2D graphene-like material that exists in the form of the *2H* hexagonal polymorph, which is a semiconductor with promising electrocatalytic activity [1]. We demonstrate that reactive HiPIMS is an attractive technique for growing VNbMoTaW disulfide at temperatures not exceeding 500°C. In our work, thin films were deposited under an argon mass flow rate of 20 sccm, together with a mass flow rate of H_2S ranging from 0 sccm to 20 sccm. The equimolar composition of V, Nb, Mo, Ta and W was used as a sputtering source with an unbalanced magnetron of diameter 2“. HiPIMS pulse frequency varied in range 150-350 Hz keeping the average power 200 W. The pulse-on time was set on 100 µs. The working pressure varied between 1.3-2.1 Pa depending on the mass flow rate of H_2S. The time-resolved ion flux on the substrate during the deposition process was measured by the Sobolewski probe. The thin films prepared for H_2S mass flow rate higher than 10 sccm demonstrated a crystalline phase of $2H$-MoS_2 with corresponding peaks at $2\theta = 14°$, 33° and 58° that can be attributed to the (002), (100), and (110) planes. The Raman spectra showed the broad peaks around 180 cm^{-1} and 270 cm^{-1} corresponding to vibrational and out-ofplane modes of the disulphide of individual metals. The nanocrystalline morphology of the deposited films was confirmed by SEM photographs. In addition, EDAX demonstrated that a H_2S mass flow rate of at least 5 sccm is sufficient for the correct HEAS composition to be produced. Depending on the H_2S mass flow rate, the ion flux on the substrate either peaks immediately after the HiPIMS pulse (pure Ar gas), or a secondary peak appears near the beginning of the pulse when the H_2S mass flow rate is nonzero (see Fig. 1).

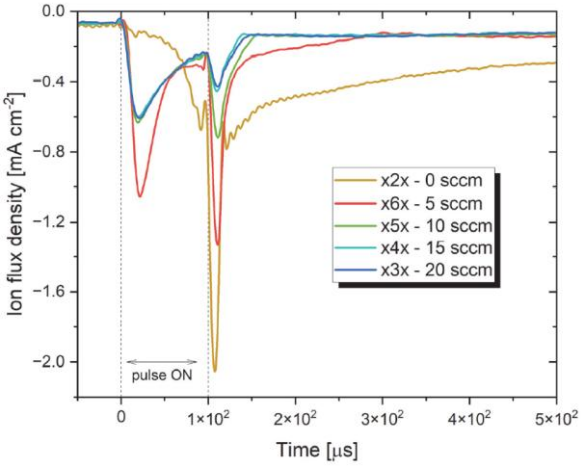

Fig. 1. Time-resolved ion flux on the substrate for different mass flow rates of H_2S.

Acknowledgements: The authors would like to thank the Czech Science Foundation (project 25-17542S).

[1] J. Qu, A. Elgendy, R. Cai, M. A. Buckingham, A. A. Papaderakis, H. de Latour, K. Hazeldine, G. F. S. Whitehead, F. Alam, C. T. Smith, D. J. Binks, A. Walton, J. M Skelton, R. A. W. Dryfe, S. J. Haigh, and D. J. Lewis, “A Low-Temperature Synthetic Route Toward a High-Entropy 2D Hexernary Transition Metal Dichalcogenide for Hydrogen Evolution Electrocatalysis,” Adv. Sci. 1**0**(14), 2204488 (2023).

Low-Temperature Plasma Engineering of Advanced 2D and 3D Carbon-Based Architectures: from Fundamental Plasma-Surface Interactions to Functional Applications

Eva KOVACEVIC

CNRS &Univeristé d'Orleans, GREMI UMR 7344, France
Corresponding author: *eva.kovacevic@gmail.com*

Low-temperature plasmas offer unique opportunities for the sustainable synthesis, modification, and functionalization of advanced materials through highly non-equilibrium plasma chemistry and precise plasma–surface interactions. Our research focuses on the plasma-assisted growth, doping, and surface engineering of a wide range of carbon-based nanostructures, including nanoparticles, mesoporous carbons, 2D/3D hybrid architectures.

A central aspect of this work is the understanding and control of plasma–surface interactions governing nucleation, growth, etching, doping, and long-term material stability. Through advanced in situ and operando diagnostics combined with ex situ structural, chemical, and electrical characterization, correlations are established between plasma parameters, material evolution, and device performance. Particular attention is devoted to the role of reactive species, ion bombardment, energetic pathways, and interface formation in determining the properties of nanostructured materials.

The developed plasma-engineered materials are investigated for a broad range of applications, including energy storage and conversion devices such as supercapacitors, metal-ion batteries, and microgenerators, as well as sensing platforms, functional coatings, and emerging technologies related to extreme environments and astrophysical processes.

ORAL PRESENTATIONS

Software-in-the-Loop Simulation of an Adaptive-Optics Control Loop for a Multi-kW Laser Beam Delivery System

Alexandru CRACIUN[1], Petru-Vlad TOMA[2], Oana-Valeria GRIGORE[1], Răzvan UNGUREANU[2], Traian DASCALU[3]

[1]*National Institute for Laser, Plasma and Radiation Physics, Laboratory of Solid-State Quantum Electronics, Magurele 077125, Romania*
[2]*National Institute for Laser, Plasma and Radiation Physics, Center for Advanced Laser Technology CETAL, Magurele 077125, Romania*
[3]*National Institute for Laser, Plasma and Radiation Physics, Magurele 077125, Romania*
Corresponding author: *alexandru.craciun@inflpr.ro*

Delivering a multi-kW laser beam over ranges from hundreds of meters to one kilometer onto a moving target requires real-time closed-loop control [1] of wavefront distortions and beam pointing. In this work, we present a software-in-the-loop [2] simulation framework for the adaptive-optics [3] control loop. Such an environment allows us to validate the control software code and tune the control parameters and also evaluate design choices for both the adaptive-optics system and the beam-delivery system.

The beam-delivery system uses a reflective telescope composed of two off-axis parabolic mirrors, where the focal distance is adjusted by a small axial displacement of the exit mirror along the common axis of the paraboloids. The control system uses sensor data to generate commands for the fast-steering mirror and the deformable mirror, placed along the beam path to correct pointing error and pre-compensate aberrations induced by atmospheric turbulence, as well as for the translation stage that moves the exit parabolic mirror. The adaptive-optics system relies on the wavefront-sensor measurements of a return beacon from the target. The sent beacon beam propagates toward the target coaxial to the main beam but is considerably larger in diameter, ensuring that part of it is diffusely reflected by the target even when the system line of sight is not perfectly aligned with the target direction.

We derive a first-order analytical model of the receiving path using an augmented ray-transfer matrix formalism [4], extending the standard ABCD approach to account for off-axis propagation. We then use this model to fit the optical design realized using OpticStudio [5]. The resulting parametrization can be used in the simulation as a mathematical function that relates the parameters of the beam in the wavefront-sensor pupil to the parameters of the beam entering the system. Propagation through the atmosphere toward and from the target is modeled using a split-step Fourier beam propagation method [6].

We present the first results obtained with the software-in-the-loop simulation, such as evaluating the sensitivity of system performance (energy delivered on target/Strehl ratio) to the quality of the exit-pupil – deformable mirror – wavefront sensor relay conjugation, the ratio of beam size to deformable-mirror active-aperture size, the modal reconstruction and calibration choices, data-acquisition delay, atmospheric turbulence and thermal blooming effects, and the fast-steering-mirror control law. These results are intended to guide both optical systems design improvements and control software optimization.

Acknowledgements: This work was funded from the project "Technological platform for the production of high-power lasers and laser processing equipment (LASER FO)" Contract no. 390058/16.09.2025, SMIS Code 329264, funded by the European Regional Development Fund under the Operational Program for Smart Growth, Digitization and Financial Instruments (POCIDIF), Priority 1 – Supporting and promoting an attractive and competitive CDI system in Romania and by the Ministry of Education and Research, Romania, program NUCLEU-LAPLAS VII 30N/2023.

[1] P.H. Merritt and J.R. Albertine, "Beam control for high-energy laser devices," Opt. Eng. **52**(2), 021005 (2013).
[2] J. Kiesbye, D. Messmann, M. Preisinger, G. Reina, D. Nagy, F. Schummer, M. Mostad, T. Kale, and M. Langer, "Hardware-In-The-Loop and Software-In-The-Loop Testing of the MOVE-II CubeSat," Aerospace **6**(12), 130 (2019).
[3] R.B. Holmes, "Adaptive Optics for Directed Energy: Fundamentals and Methodology," AIAA J. **60**(10), 5633-5644 (2022).
[4] A.E. Siegman, Lasers (University Science Books, Mill Valley, CA, 1986), Chap. 15, Sec. 15.4.
[5] Ansys Zemax Optic Studio, Release 2025 R1, optical design software (Ansys Zemax, Canonsburg, PA, 2025).
[6] M. Mansuripur, E.M. Wright, and M. Fallahi, "The Beam Propagation Method," Opt. Photonics News **11**(7), 42-45 (2000).

Large-Area Pulsed Laser Deposition Growth of Transparent Conductive Al-Doped ZnO Thin Films

Elena Isabela BANCU[1,2], Valentin ION[1], Mihai Adrian SOPRONYI[1], Alexandru DAN[1], Florin ANDREI[1], Ioan-Mihail GHITIU[1,2], Stefan ANTOHE[2,3] and Nicu Doinel SCARISOREANU[1]

[1]*National Institute for Laser, Plasma and Radiation Physics, Magurele 077125, Romania*
[2]*Faculty of Physics, University of Bucharest, 405 Atomistilor Street, Magurele 077125, Romania*
[3]*Academy of Romanian Scientists, Ilfov St 3, Bucharest 050045, Romania*
Corresponding author: *elena.bancu@inflpr.ro*

This study focuses on the development of indium-free transparent conductive oxides (TCOs) based on aluminum-doped zinc oxide (AZO) on large-area (4-inch) silicon (Si) wafer using an industrial-scale pulsed laser deposition (PLD) system at a substrate temperature of 330 °C. The purpose of the study was to obtain AZO layers over a large area with low electrical resistivity and high optical transmission across the visible (VIS) spectrum by varying the substrate temperature and deposition pressure. The morphological and structural properties of the AZO layers were obtained by using different characterization methods such as SEM, AFM, XRD and HR-TEM. Moreover, the electrical properties were analyzed using Hall measurements, showing a low electrical resistivity of 3.98 x 10^{-4} Ω cm, a high carrier concentration (n) of 1.05 x 10^{21} cm^{-3}, and a charge carrier mobility of 17.9 cm^2/V s, at room temperature. Additionally, optical characterization conducted through spectroscopic ellipsometry (SE) measurements showed that the large-area AZO sample exhibits an increased optical transparency in the VIS range with a near-zero extinction coefficient (k) and a wide bandgap of 3.75 eV. Therefore, AZO thin films prepared on large-area Si wafer fulfill the requirements for use as transparent conductive electrodes.

Acknowledgements: This work was supported by a grant from the Ministry of Education and Research, Romania, CCCDI-UEFISCDI, project number PN-IV-P7-7.1-PED-2024-2303, within PNCDI IV. Part of this work was performed using C400 PHOTOPLASMAT facilities acquired within the POC153/2016 IN2-FOTOPLASMAT project.

3D Printed Carbon Materials: Fabrication Challenges and Applications

Jérémy DRUON[1,2,3], Quentin BAUERLIN[1,2], Arnaud SPANGENBERG[1,2], Camélia GHIMBEU[1,2,3]

[1]*Institut de Science des Matériaux de Mulhouse, UMR 7361 CNRS-Université de Haute Alsace, Mulhouse, FRANCE,*
[2]*Université de Strasbourg, France*
[3]*Réseau sur le Stockage Electrochimique de l'Energie (RS2E), CNRS FR3459, Amiens Cedex, France*
Corresponding author: *camelia.ghimbeu@uha.fr*

Carbon materials are undoubtedly the most versatile materials owing to their tuneable properties and large pallet of possible applications. Their morphology, porosity, structure, and surface functionalities can be adjusted to satisfy applications including air cleaning, sensors, catalysis and energy storage. In most applications, carbon cannot be integrated as a powder and often requires customized shaping, either by the fabrication of monoliths (limited to specific precursors) or by employing polymeric binders. However, the use of binders generally leads to 2D shaped materials, can block porosity and contribute as dead-mass that decrease the material's performance. To solve these issues, 3D printing techniques emerged in the recent years as attractive methods to obtain various shapes of carbon materials [1]. Light assisted 3D printing approaches such as DLP (digital light processing) allow to obtain carbon structures using layer-by-layer printing of polymeric photoresist, followed by pyrolysis in inert atmosphere. Yet, most of commercial resins are derived from petrochemical sources, and the resulting carbon objects lack of structural resolution and mechanical stability. To address this inconvenient, a bio-sourced resin was developed in this work, which afforded to increase the C-yield after pyrolysis and to obtain robust carbon objects (Fig. 1) with tuned graphitisation degree, suitable for battery applications [2]. The integration of different templates in this resin induced the formation of hierarchical materials, with various ratios of micro/meso/macro pores. These materials were shaped in electrode form and evaluated as electrodes in supercapacitors. The results highlighted that specific capacitance and retention strongly correlate to the porous features and electronic conductivity properties. Nevertheless, we proposed a novel and complementary printing technique to DLP, i.e., volumetric additive manufacturing (VAM) to reduce significantly the fabrication time and defects in the materials. The combination of VAM technique with specific stabilization protocols and fast pyrolysis allowed to obtain in a very short time carbon materials with complex design.

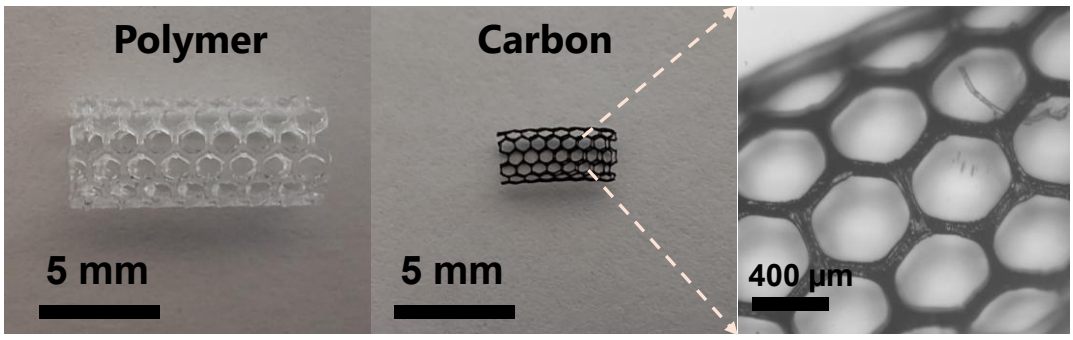

Fig. 1. 3D printed polymer (left) and carbon (middle) structures, along with numeric microscopic zoom on carbon (right).

Acknowledgements: We acknowledge the financial support of this work by Université de Haute-Alsace (UHA) and Réseau sur le Stockage Electrochimique de l'Energie (RS2E) network (ANR-10-LABX-76-01), and technical support through France 2030 program (Mat-Light 4.0 – ANR-21-EXES-0012) and IS2M platforms.

[1] P. Blyweert, V. Nicolas, V. Fierro, A. Celzard, "3D printing of carbon-based materials: A review," Carbon **183** (15), 449-485 (2021)
[2] Q. Bauerlin, A Spangenberg, C Matei Ghimbeu, Mélange pour l'impression 3D de matériaux carbonés, FR2507005, 25/06/2025

Semi-Industrial Level Manufacturing Process of Chemoresistive Gas Sensing Devices

Andrei-Silviu ZANCU, Maria-Luiza STINGESCU, Mihai-Adrian SOPRONYI, Mihai-Robert ZAMFIR, Nicu Doinel SCARISOREANU

National Institute for Laser, Plasma and Radiation Physics, C400 Department, Magurele 077125, Romania
Corresponding author: *mihai.zamfir@inflpr.ro*

The Internet of Things (IoT) is a relatively young concept and has emerged as a response to the continuous increase in demand for automation and efficiency of certain technologies [1]. Living in our present society, it is easy to notice that almost every electronic device, but not limited to, can be connected to a network, based on the type of communication technology, and have remote control capability. This has enabled the emergence of concepts like Smart Cities, Smart Agriculture, Smart Healthcare and others. At the core of all these concepts relies the integration of sensors for detection and monitoring, depending on the field of applications, and the facile transmission and interpretation of information. Therefore, there's a continuous increase in demand for devices with better performance and capabilities, while decreasing weight and dimensions with an emphasis on also reducing the cost. In that regard we present here a complete technological process of manufacturing sensing devices, developed on the facilities of C400 Fotoplasmat INFLPR. The steps involve processing of simple oxides such as ZnO, CeO_2, TiO_2, on large area substrates (from 4" to 8") and integration through optical lithography and E-beam evaporation, resulting in fabrication of tens up to few hundreds of devices, depending on the architecture. The optimization and reproducibility of the process are refined through various types of analysis, and the device performances are validated through detection measurements of various types of gases in terms of time of response and recovery time, which are better or comparable with previous reports based on similar materials. Furthermore, these devices are easily integrated in a complete and/or autonomous gas sensor in collaboration with our economical partners.

Acknowledgements: This work was financed by project Platformă Națională pentru Tehnologiile Semiconductorilor (PNTS) SMIS 304244, program NUCLEU-LAPLAS VII 30N/2023, Ministry of Education and Research, Romania, and was performed using the facilities of C400 – FOTOPLASMAT INFLPR.

[1] S. Jeddou, L. Diez, A. Baina, N. Abdellah, R. Agüero, "A Review of the Internet of Things (IoT) Landscape: Technologies, Applications, and Open Challenges," J. Electr. Comput. Eng. **1**, 6657578 (2026).

Application of Plasma Chill Spray Technology for Inactivation of *Escherichia Coli* Biofilms on Stainless Steel Surfaces

Negar RAVASH[1], Xianqin YANG[2], M. S. ROOPESH[1]

[1]*Department of Agricultural, Food and Nutritional Science, University of Alberta, Edmonton, AB T6G 2P5, Canada*
[2]*Lacombe Research and Development Centre, Agriculture and Agri-Food Canada, Lacombe, Alberta, Canada*
Corresponding author email: roopeshms@ualberta.ca

Conventional chemical sanitizers are commonly used but may leave harmful residues, raise environmental concerns, and contribute to antimicrobial resistance [1]. Plasma-activated water (PAW) has emerged as a non-thermal alternative capable of disrupting biofilms through reactive oxygen and nitrogen species (RONS) that penetrate the extracellular polymeric substances matrix, thereby reducing microbial viability [2]. This study hypothesized that a high-pressure plasma chill spray generated from PAW would enhance biofilm inactivation through combined oxidative, cold, and mechanical stresses. The objective was to evaluate its efficacy against *Escherichia coli* biofilms on stainless steel surfaces.

Biofilms of *E. coli* AW1.7 and *E. coli* 8-77 were developed on stainless steel surfaces. PAW was generated by treating 150 mL of distilled water for 20 minutes using a bubble spark discharge plasma reactor integrated with a vortex tube cooling system and spray nozzle. Air or CO_2 was used as the plasma-forming gas at a flow rate of 2 litres per minute. Biofilm-coated surfaces were subjected to sequential treatments combining plasma chill spray and distilled water spray at different temperatures. PAW and spray characteristics, including pH, oxidation–reduction potential (ORP), electrical conductivity, and RONS concentrations, were measured along with antimicrobial efficacy.

Lower PAW generation temperatures enhanced the stability and accumulation of RONS, including H_2O_2, O_3, and NO_3^-. The resulting PAW and plasma sprays exhibited low pH, high ORP, and increased conductivity, indicating strong antimicrobial potential. Plasma chill spray treatments reduced *E. coli* biofilms to below detection limits (>6.12 log CFU/cm²), likely due to the combined effects of oxidative, cold, and mechanical stresses. Air, as the plasma-producing gas, showed higher antimicrobial efficacy than CO_2. Additionally, higher RONS yields were achieved at lower temperatures with reduced energy input, highlighting the importance of temperature in optimizing plasma efficiency.

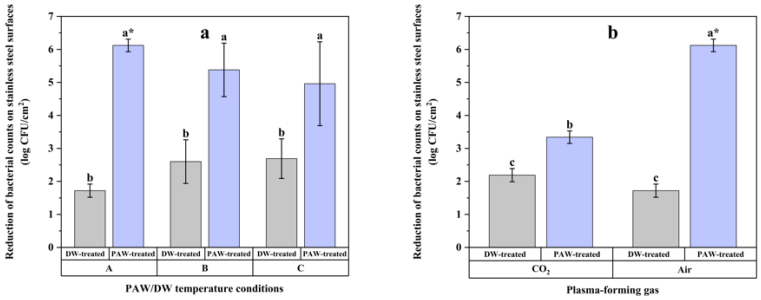

Figure 1. Antimicrobial efficacy of plasma chill spray treatments.
a-c indicate statistically significant differences among treatments ($p < 0.05$).
A: Utilizing ice inside the water container and covering the container with an ice-water mixture during PAW generation;
B: Covering the water container with an ice-water mixture during PAW generation; C: PAW generation under ambient conditions.

Plasma chill spray treatments demonstrate strong potential as a sustainable, residue-free alternative for decontaminating food-contact surfaces. Further research is needed to validate its performance under industrial conditions.

Acknowledgements: This work was supported by the Beef Cattle Research Council (BCRC), Natural Sciences and Engineering Research Council of Canada (NSERC), and Agriculture and Agri-Food Canada.

[1] R. Charron, M. Boulanger, R. Briandet, and A. Bridier. "Biofilms as protective cocoons against biocides: from bacterial adaptation to One Health issues," Microbiol. **169**(6), 001340 (2023).
[2] A. Mai-Prochnow, R. Zhou, T. Zhang, K. Ostrikov, S. Mugunthan, S. A. Rice, and P. J. Cullen, "Interactions of plasma-activated water with biofilms: inactivation, dispersal effects and mechanisms of action," npj Biofilms Microbiomes **7**(1), 00180 (2021).

$La_xNd_yGd_zY_wSc_{4-x-y-z-w}(BO_3)_4$-LGYSB:Nd, a New High-Performance Near-Infrared Laser Crystal

Lucian GHEORGHE, Alin BROASCA, Madalin GRECULEASA, Flavius VOICU,
Stefania HAU, Cristina GHEORGHE, Gabriela CROITORU

National Institute for Laser, Plasma and Radiation Physics, Laboratory of Solid-State Quantum Electronics, Magurele, 077125, Romania
Corresponding author: lucian.gheorghe@inflpr.ro

Incongruent melting $La_xNd_yGd_zY_wSc_{4-x-y-z-w}(BO_3)_4$ - LGYSB:Nd crystals with different Y concentrations (w = 0.15, 0.05, and 0.025) have been grown for the first time by the Czochralski method. For all crystals, the Nd^{3+} doping concentration in the starting melt composition was chosen to be 5 at.% (y = 0.05). Due to the peritectic nature of $La_xNd_yGd_zY_wSc_{4-x-y-z-w}(BO_3)_4$ compounds, which follow the stoichiometric composition (x + y + z + w = 1), a scandium deficiency (Sc < 3) is required in the starting melt composition to facilitate Czochralski growth of trigonal (space group *R32*) LGYSB:Nd-type crystals. To fulfill this requirement, the scandium content in the starting compositions was set to 2.75 (4 - x - y - z -w = 2.75). Considering the growth of $La_xNd_yGd_zSc_{4-x-y-z}(BO_3)_4$ - LGSB:Nd type crystals [1], the optimal content of La in the starting melts was also fixed to x = 0.628. Consequently, the starting melt compositions were established as $La_{0.628}Gd_{0.422}Y_{0.15}Nd_{0.05}Sc_{2.75}(BO_3)_4$ - LGYSB:Nd_1, $La_{0.628}Gd_{0.522}Y_{0.05}Nd_{0.05}Sc_{2.75}(BO_3)_4$ - LGYSB:Nd_2, and $La_{0.628}Gd_{0.547}Y_{0.025}Nd_{0.05}Sc_{2.75}(BO_3)_4$ - LGYSB:Nd_3, respectively. The grown crystals shared the same optimal growth parameters, namely a pulling rate of 2 mm/h and a rotation rate of 8 rpm. In these conditions, the LGYSB:Nd_3 crystal exhibits superior optical quality in terms of the number of visible defects. The LGYSB:Nd_3 laser operated at the emission wavelength of 1062 nm with very high slope efficiencies of η_{sa} = 0.74 (Fig. 1a) and η_{sa} = 0.64 (Fig. 1b) in quasi-CW and CW regimes, respectively, thus demonstrating its outstanding properties to generate efficient laser emission in the NIR range.

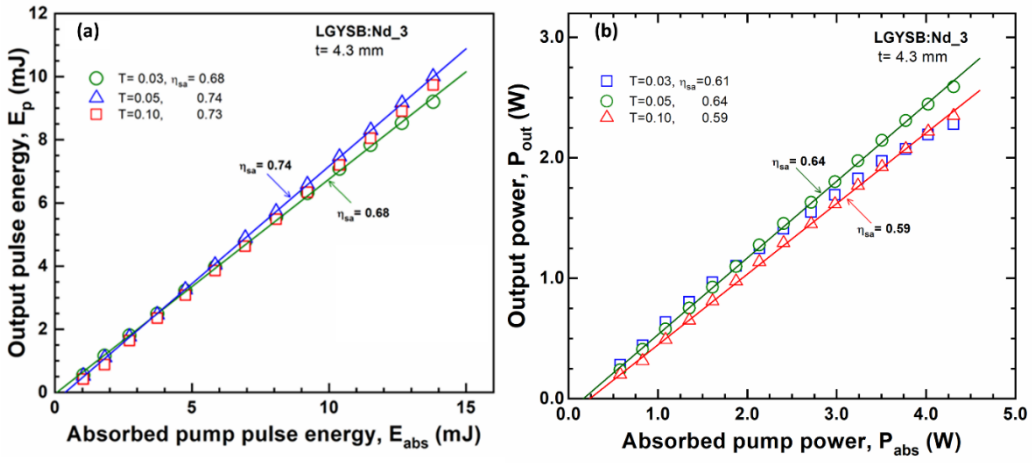

Fig. 1. Laser pulse energy, E_p versus absorbed energy of the pump pulse, E_{abs} **(a)**, and output power, P_{out} versus absorbed pump power, P_{abs} **(b)** for LGYSB:Nd_3 crystal. T = transmission of output coupling mirrors and t = thickness of laser active medium.

Acknowledgements: This work was supported by the Ministry of Education and Research, Romania, CCCDI – UEFISCDI, project number PN-IV-P6-6.1-CoEx-2024-0154, within PNCDI IV and program NUCLEU-LAPLAS VII 30N/2023.

[1] M. Greculeasa, A. Broasca, F. Flavius, S. Hau, G. Croitoru, G. Stanciu, C. Gheorghe, N. Pavel, L. Gheorghe, "Bifunctional $La_xNd_yGd_zSc_{4-x-y-z}(BO_3)_4$ crystal: Czochralski growth, linear and nonlinear optical properties, and near-infrared laser emission performances," Opt. Laser Technol. **131**, 106433(2020).

Growth and Characterization of Bifunctional Nd:LGSB Crystals

Madalin GRECULEASA, Alin BROASCA, Flavius VOICU, Cristina GHEORGHE,
Stefania HAU, Catalina-Alice SUSALA, Nicolaie PAVEL, Lucian GHEORGHE

National Institute for Laser, Plasma and Radiation Physics, Laboratory of Solid-State Quantum Electronics, Magurele 077125, Romania
Corresponding author: madalin.greculeasa@inflpr.ro

Currently, lasers find extensive applications in various fields, so extensive research has been conducted on the development of new laser crystals. Many researches are focused on the development of new bifunctional laser and nonlinear optical (NLO) crystals or on improving existing ones based on new concepts. Very recently, our group has developed Czochralski-grown $La_xGd_yNd_zSc_{4-x-y-z}(BO_3)_4$ (Nd:LGSB) bifunctional crystals [1], as very promising active media for the construction of highly efficient lasers in the near-infrared (NIR) domain, as well as compact visible (VIS) lasers based on self-frequency doubling (SFD) processes. Bifunctional Nd:LGSB crystals with incongruent melting and different concentrations of Nd^{3+} dopant ions were grown by the Czochralski method. The as-grown crystals have excellent quality, characterized by high transparency and the absence of visible defects. All the grown crystals present a hexagonal transversal section characteristic of ***c***-axis grown huntite-type crystals and are shown in Fig. 1.

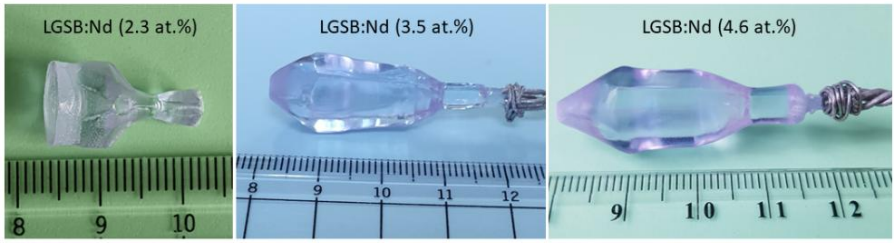

Fig. 1. The Photos of Czochralski-grown Nd:LGSB-type crystals.

The spectroscopic investigations of the Nd:LGSB crystals revealed that Nd^{3+} ions substitute only La^{3+} cations in the LGSB crystal matrix, as well as their high potential to generate efficient laser emission in the NIR domain at ~1.06 μm. The laser emission performances in the CW regime at 1062 nm were evaluated for each Nd-doping concentration using uncoated crystal samples with different crystallographic orientations, such as *a*-cut, *c*-cut, and *SFD*-cut. In terms of slope efficiency, the c-cut 4.6 at.% Nd:LGSB has permitted to obtain the highest value of η_{sa}= 0.68, while the optical-to-optical efficiency reached η_{oa}= 0.63 at high absorbed pump power, P_{abs}=2.14 W. The NIR emission of the **c**-cut Nd:LGSB crystal was randomly polarized, while the *a*-cut 4.6 at% Nd:LGSB crystal delivered a linearly polarized output beam with the highest laser slope efficiency of η_{sa}= 0.63. In the case of *SFD*-cut 3.5 at % Nd:LGSB crystal sample, slightly lower slope and optical-to-optical efficiencies (η_{sa}= 0.56 and η_{oa}= 0.52) were reached, and increased output powers of ~2 W were obtained. The laser emission performances at ~531 nm in SFD configuration under CW regime of both 2.3 at.% and 3.5 at.% Nd:LGSB crystals were also investigated. The diode-to-green conversion efficiency improved significantly from 0.17% in the case of 2.3 at.% Nd:LGSB crystal to 1.44% (of about 8.5 times increase) in the case of 3.5 at.% Nd:LGSB crystal, highlighting the importance of optimizing Nd doping concentration and crystal length for enhanced SFD performance.

Acknowledgements: This work was supported by a grant of the Ministry of Education and Research, Romania, CCCDI - UEFISCDI, project number PN-IV-P6-6.1-CoEx-2024-0154, within PNCDI IV, and program NUCLEU-LAPLAS VII 30N/2023.

[1] A. Broasca, M. Greculeasa, F. Voicu, C. Gheorghe, S. Hau, C.A. Susala and L Gheorghe, "Bifunctional Nd-doped LGSB crystals: a roadmap for crystal growth and improved laser emission performance in the NIR and green domains," Materials **18**(5), 964 (2025).

On the Stability of Passive Films on Dental Titanium Under Harsh Chemical and Physical Conditions

Achim Walter HASSEL[1,2], Andreas GREUL[1], Manuel HOFINGER[1], Vasilios ALEVIZAKOS[2], Constantin von SEE[2], Christoph KLEBER[2]

[1]*Institute of Chemical Technology of Inorganic Materials, Johannes Kepler University Linz, Altenberger Strasse 69, 4040 Linz Austria*
[2]*Danube Private University Krems, Steiner Landstrasse 124, Krems, Austria*
Corresponding author*:* achimwalter.hassel@jku.at

Titanium is the gold standard for implant materials in dental applications. Its passive film protects the material against aggressive intra oral environments including salts, acidic conditions, elevated temperature and even hydrogen peroxide produced from inflammatory processes. This study explores the stability of the passive film on Ti under two different special conditions. The 1st is the use of mouth rinsing solutions MRS. The 2nd is more extreme; it investi-gates the behavior when a new explantation technique is applied using a a high frequency voltage to loosen a defective implant prior to removal.

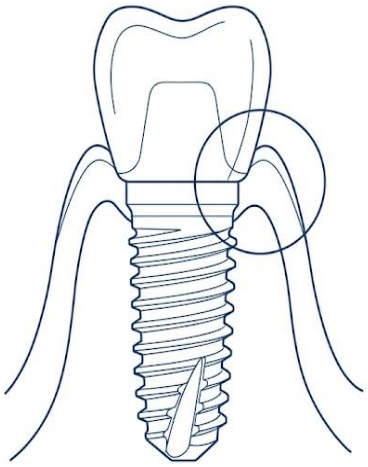

Fig.1 Schematic Drawing of a titanium implant with zirconia crown and fitting gingiva. (generated image)

In part one of the study various MRS were used as electrolytes and were compared to an artificial saliva the so-called Fusayama-Meyer solution with different pH. MRS often make use of hypochloric acid and this is in principal an aggressive agent. A novel electrochemical cell was designed to mimic the oral environment including a temperature control to 33 °C simulating the conditions at the entrance of the body that is the mouth. Standard procedures for corrosion testing were employed using open circuit potential measurements, electrochemical impedance spectro-scopy, cyclic voltammetry to determine corrosion potential and corrosion current. Moreover, electro-chemical noise measurements were performed to characterize this passive material. In the second part of the study the Ti implant screws were treated by an electrotome i.e. a high frequency voltage generator. The potential drop at the highest resistance in the metal-oxide-bone system causes a significant heating at the surface of the implant. For both parts inductively coupled plasma optical emission spectroscopy (ICP-OES) was used as an additional way to quantify dissolution rate Ti.

A dental Ti implant is intended to be a once in a life time solution which sets the requirements for its performance very high. The quantification of the chemical dissolution of Ti was performed under harsh conditions. It is evident that all tested samples display an elevated Ti content after the treatment, with results ranging from 4.9 to 5.4 µg L^{-1}. While the Ti levels are clearly raised these results still suggest a minor Ti exposure during the treatment. The concentrations found are on the lower end of Ti concentrations typically found in drinking water and are below the latest WHO report concerned with Ti exposure declares no adverse effects up to exposures of 1 g kg^{-1} body weight per day. Furthermore, the estimated Ti exposure by commonly administered medications in humans was found to be 1.71 mg per day.

Acknowledgements: This work was supported by the Austrian Research Promotion Agency (FFG) within the COMET Project "PI-SENS" (Project No. 915477) as well as by the Federal Provinces of Lower Austria and Tirol.

[1] A. Greul, V. Alevizakos, M. Hofinger, C. von See, C. Kleber, A. W. Hassel, "Quantification of the Titanium Dissolution of Dental Implants during a new Explantation Technique," Phys. Status Solidi A Appl. Mater. Sci. **223**, e202500341 (2026).

Gyrokinetic Validation Framework for Statistical Test-Particle Transport Models

Ligia-Maria POMARJANSCHI[1,2], Dragoş Iustin PALADE[1]

[1]*National Institute for Laser, Plasma and Radiation Physics, Lab. 220, Plasma Theory Group, Magurele 077125, Romania*
[2] *Doctoral School of Physics of the University of Bucharest, Magurele 077125, Romania*
Corresponding author: *ligia.pomarjanschi@inflpr.ro*

Turbulent transport in magnetized fusion plasmas is often modeled using reduced statistical approaches, such as test-particle methods, which trade physical detail for computational speed. However, the assumptions underlying these models (spectral representations, homogeneity, stationarity, and mixing) have rarely been tested against first-principles simulations.

We present a gyrokinetic validation framework built around the GENE code [1,2] to assess the T3ST statistical test-particle model [3]. The workflow covers simulation setup across relevant parameter regimes, convergence checks, and extraction of turbulence diagnostics, such as spectra, transport fluxes, and spatiotemporal correlations, in forms directly comparable to reduced model outputs. This enables both quantitative benchmarking of transport predictions and systematic testing of the statistical assumptions underlying T3ST.

Acknowledgements: This work has been carried out within the framework of the EUROfusion Consortium, funded by the European Union via the Euratom Research and Training Programme (Grant Agreement No 101052200 - EUROfusion). Views and opinions expressed are however those of the author(s) only and do not necessarily reflect those of the European Union or the European Commission. Neither the European Union nor the European Commission can be held responsible for them. This work was also supported by a grant of the Ministry of Education and Research, Romania, CNCS - UEFISCDI, project number PN-IV-P2-2.1-TE-2023-1102, within PNCDI IV and by the Romanian National Core Program LAPLAS VIIcontract no. 30N/2023.

[1] F. Jenko, W. Dorland, M. Kotschenreuther, and B. N. Rogers, "Electron temperature gradient driven turbulence," Phys. Plasmas 7**(5)**, 1904-1910 (2000).
[2] T. Goerler, X. Lapillonne, S. Brunner, T. Dannert, F. Jenko, F. Merz, and D. Told, "The global version of the gyrokinetic turbulence code GENE," J. Comput. Phys. **230**(18), 7053-7071 (2011).
[3] D.I. Palade, and L.M. Pomârjanschi, "T3ST code: turbulent transport in tokamaks via stochastic trajectories," Nucl. Fusion **65**(8), 086007 (2025).

A Low-Cost, Open-Source Single-Photon Detection System

Irina BRADU[1], Radu IONICIOIU[2]

[1]*National University of Science and Technology POLITEHNICA Bucharest, Faculty of Applied Sciences, 060042 București, Romania*
[2]*Horia Hulubei National Institute of Physics and Nuclear Engineering, Department of Theoretical Physics, 077125 Magurele, Romania*
Corresponding author: *irina.bradu@upb.ro*

The ability to detect single photons is essential for both quantum optics and quantum technologies. The rapid development of quantum communications and photonic computing has increased the demand for low-cost, reliable single-photon detectors [1]. However, commercially-available detectors are expensive (in excess of €4000) and without integrated coincidence logic. This bottleneck limits the widespread adoption of useful technologies, such as quantum cryptography, quantum imaging and quantum sensing.

Here we describe a low-cost, single-photon detection architecture based on off-the-shelf components. The system uses a Geiger-mode avalanche photodiode (APD) biased by a compact, high-voltage boost converter (12V DC to 130V DC) and stabilised through passive filtering to mitigate switching noise. We develop a custom active-quenching circuit controlled by a low-cost ARM-based microcontroller. Using the Programmable Input/Output (PIO) of the microcontroller we implement photon counting and coincidence detection without expensive FPGA-based hardware.

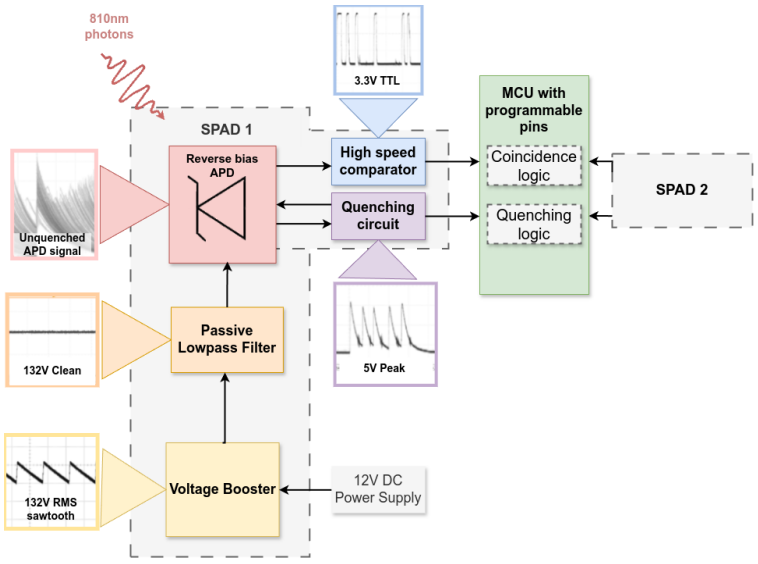

Fig.1. Single-Photon Avalanche Detector (SPAD) and coincidence logic pipeline with corresponding waveform.

Our open-source design [2] integrates photon detection and coincidence logic into a single unit (Fig.1). The prototype costs less than €100. We analyse the impact of power-supply noise on detector performance and show that appropriate filtering enables stable operation despite the use of low-cost components.

The initial results demonstrate that cost-effective implementations provide a viable alternative for accessible quantum optics experiments and educational quantum communication demonstrators. Future work will include a complete characterisation of detection efficiency, timing jitter and long-term stability.

[1] M. D. Eisaman, J. Fan, A. Migdall, and S. V. Polyakov, "Invited review article: Single-photon sources and detectors", Rev. Sci. Instrum. **82** (7), 071101 (2011).
[2] Custom SPAD, GitHub repository, https://github.com/irina-b-dev/custom_spad, accessed April 2026.

Near-Infrared Optical Limiting in the Novel Nonlinear Optical Compound DNA-Biopolymer – Spirulina Natural Dye

Petronela GHEORGHE, Adrian PETRIS

National Institute for Laser, Plasma and Radiation Physics, Department of Lasers, Magurele 077125, Romania
Corresponding author: *adrian.petris@inflpr.ro*

The passive optical limiting is a nonlinear optical process in which the optical transmission of a material decreases when the incident laser intensity is higher than a threshold value [1-5]. It is used to protect the eyes and sensitive optical and optoelectronic devices from laser-induced damage. The optical limiting is of considerable importance with the continuous development of increasingly powerful lasers.

We present our recent results of an experimental study on absorptive nonlinear optical properties of deoxyribonucleic acid (DNA) biopolymer functionalized with spirulina natural dye, as solutions in butanol, and, for comparison, on the same properties of similar solutions with spirulina only. The linear absorbance spectra of the investigated samples have been recorded by Ultraviolet–Visible-Near-Infrared (UV-VIS-NIR) spectroscopy.

Their optical limiting functionality is experimentally demonstrated by the Intensity-scan method at the wavelength of 1550 nm using ultrashort (~120 fs) laser pulses. Important parameters of the optical limiting, as the nonlinear absorption coefficient β and the saturation intensity, I_{sat}, are determined in the investigated materials by processing the experimental curves of the nonlinear absorbance. The results of our experimental investigation reveal a significant absorptive nonlinear optical response of spirulina and its potential for optical limiting. The beneficial effect of the DNA biopolymer on the nonlinear absorption in the investigated compounds, resulting in the enhancement of their optical limiting potential, is demonstrated.

Our study shows that the DNA-CTMA-spirulina compound is a promising material for passive optical limiting in the near-infrared domain.

Acknowledgements: This research was supported by the National Authority for Research in the framework of the program NUCLEU-LAPLAS VII 30N/2023, Ministry of Education and Research, Romania.

[1] Z. Liu, B. Zhang, Y. Chen, "Recent Progress in Two-Dimensional Nanomaterials for Laser Protection," Chemistry **1**, 17-43 (2019).
[2] H. Lundén, E. Glimsdal, M. Lindgren, C. Lopesa, "How to assess good candidate molecules for self-activated optical power limiting," Opt. Eng. **57**, 030802 (2018).
[3] D. Dini, M.J.F. Calvete, M. Hanack, "Nonlinear Optical Materials for the Smart Filtering of Optical Radiation," Chem. Rev. **116**, 13043-13233 (2016).
[4] P. Gheorghe, A. Petris, A.M. Anton, "Optical limiting properties of DNA biopolymer doped with natural dyes," Polymers **16**, 96 (2024).
[5] L. Liang, Y. Fu, D. Wang, Y. Wei, N. Kobayashi, T. Minari, "DNA as Functional Material in Organic-Based Electronics," Appl. Sci. **8**, 90 (2018).

Efficient Diode-Pumped Laser Operation in Nd-Doped LYSB Nonlinear Optical Crystal

Alin BROASCA, Madalin GRECULEASA, Flavius VOICU, Cristina GHEORGHE, Stefania HAU, Gabriela CROITORU, Lucian GHEORGHE

National Institute for Laser, Plasma and Radiation Physics, Laboratory of Solid-State Quantum Electronics, Magurele 077125, Romania
Corresponding author: *alin.broasca@inflpr.ro*

Incongruent melting Nd-doped $La_xY_ySc_{4-x-y}(BO_3)_4$ crystals were grown for the first time by the Czochralski method. The starting melt composition was optimized to reduce the defects in the grown crystal. The composition of the best-quality grown crystal was measured to be $La_{0.7830}Nd_{0.0398}Y_{0.3533}Sc_{2.8239}(BO_3)_4$. The Powder X-ray Diffraction revealed a trigonal single phase (space group *R32*). The spectroscopic properties of Nd^{3+} ions were investigated at room temperature and at 10 K. Laser experiments demonstrate multi-wavelength emission at 0.9 µm, 1.06 µm, and 1.3 µm in Nd:LYSB crystal, with slope efficiencies comparable to Nd:YAG and vanadate lasers, while offering the additional advantage of intrinsic nonlinear optical properties for second- and third-harmonic generation. The laser emission performance in the free generation regime at λ_{em} = 1.06 µm is presented in Fig. 1 under laser diode pumping at 808 and 880 nm, respectively.

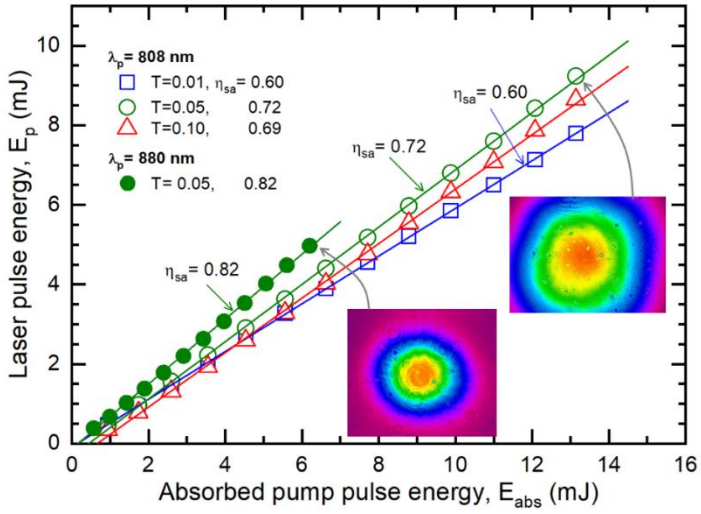

Fig. 1. Laser pulse energy (E_p) at 1.06 µm obtained from the Nd:LYSB crystal under pumping at 808 nm and 880 nm. Insets show the near-field beam profiles (2D intensity maps) at the indicated operating points. T denotes the output coupler mirror (OCM) transmission at 1.06 µm. Solid lines represent fits to the experimental data.

Laser pulses with a maximum energy of 9.2 mJ were obtained under 808 nm pumping using an output coupler mirror (OCM) with 5% transmission. The optical-to-optical efficiency and the slope efficiency, defined with respect to the absorbed pump pulse energy (E_{abs}), were determined to be η_{oa} = 0.70 and η_{sa} = 0.72, respectively. Under 880 nm pumping, the slope efficiency increased to η_{sa} = 0.82, approaching the theoretical limit due to the reduced quantum defect.

Acknowledgements: This work was supported by the Ministry of Education and Research, Romania, CCCDI – UEFISCDI, project number PN-IV-P6-6.1-CoEx-2024-0154, within PNCDI IV and program NUCLEU-LAPLAS VII 30N/2023.

Two Photon Polymerization of 3D Porous Structures for Evaluation of X-Ray Radiation Effect on Cancer Cells

Alexandra BRAN[1,2], Daniel AVRAM[1], Florin JIPA[1], Anca BONCIU[1], Cosmin DOBREA[1], Elena STANCU[1], Stefana OROBETI[1,3], Emanuel AXENTE[1], Livia E. SIMA[3], Ion TISEANU[1], Koji SUGIOKA[4], Felix SIMA[1,4]

[1]*National Institute for Laser, Plasma and Radiation Physics, CETAL Department, Magurele 077125, Romania*
[2]*Photon-X Spectrum Lab, CAMPUS Research Institute, National University of Science and Technology POLITEHNICA Bucharest, Bucharest 060042, Romania*
[3]*Institute of Biochemistry of the Romanian Academy, Bucharest 060031 Romania*
[4]*RIKEN Center for Advanced Photonics, Wako 351-0198, Japan*
Corresponding authors: *alexandra.bran@inflpr.ro, felix.sima@inflpr.ro*

Metastatic cancer cells are suffering extreme cytoskeleton morphological deformations during migration through confined spaces. We herein propose the fabrication of 3D artificial pore networks in polymeric materials to mimic the native *in vivo* constrictive environment cancer cells interact with. By applying two photon polymerization (TPP) we were able to generate multi-layered, woodpile-like, scaffolds made of parallel and perpendicular lines with tunable inter-lines dimensions (Fig. 1(a)) to further develop pore networks with controlled dimensions. A Nanoscribe Photonic Professional system equipped with a near-infrared laser beam of pulse duration of 100 fs and repetition rate of 80MHz was used to induce polymerization in SU8, a biocompatible negative photoresist. The scaffolds were then used to evaluate the invasive capacity of melanoma cancer cells by immunofluorescence microscopy (Fig. 1(b)). An extended area of penetrating filopodia inside the scaffolds was observed with the increase of pore dimensions from 0.7 to 1.6 µm. Further, focal adhesion points were found denser when collagen was applied, but much stronger in the absence of the coating. A larger spreading area and a higher mean migration velocity were found for melanoma cells grown on collagen-coated scaffolds, corresponding to a more aggressive cell invasive behavior [1].

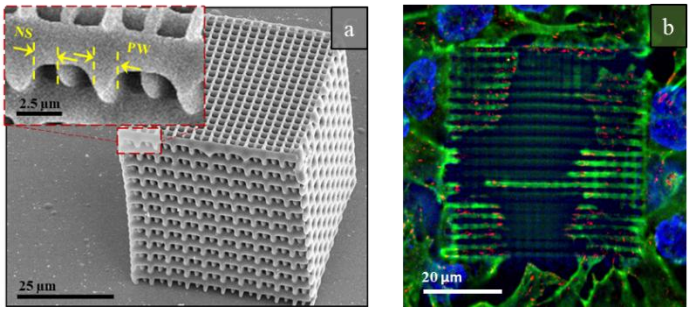

Fig. 1. (a) 3D scaffolds with tunable pore dimensions (NS) made by two photon polymerization are used to evaluate (**b**) the behavior of melanoma cancer cells when interacting with micrometer-sized constrictive spaces

The scaffolds the quantification immunoassaying protocols were further applied to evaluate the behavior of melanoma cancer cells at interaction with porous structures. After exposure to either continuous or pulsed X-ray radiation, melanoma cancer cells invasive capacity inside porous scaffolds was found decreasing with irradiation dose. In addition, spreading area was found more compact for cells exposed to continuous X-rays radiation as compared with pulsed X-ray for the same cumulative dose.

Acknowledgements: *This research was supported by Institute of Atomic Physics through the ELI-RO_2024_10 Project, No. 10/2024; We acknowledge the support of National Interest Infrastructure facility IOSIN – CETAL at INFLPR.*

[1] A. Bran, S. Orobeti, F. Jipa, A. Bonciu, E. Axente, L.E. Sima, F. Sima, K. Sugioka, "Tissue-Like Scaffolds Created by Two-Photon Polymerization for Testing Cancer Cell Behavior in Confined Environments," ACS Appl. Bio Mater. **8** (8), 7344-7356 (2025).

In Situ Optical Monitoring of UV-Crosslinked Hydrogels for the Controlled Delivery of Motexafin Lutetium in Breast Cancer Phototheranostics

Tatiana TOZAR[1,2], Alexia TANASE[3], Angela STAICU[1], Mihaela BALAS[4], Mihai BONI[1]

[1]*National Institute for Laser, Plasma and Radiation Physics, Lasers Department, Magurele 077125, Romania*
[2]*"Horia Hulubei" National Institute for R&D in Physics and Nuclear Engineering, Extreme Light Infrastructure - Nuclear Physics, Magurele 077125, Romania*
[3]*National University of Science and Technology Politehnica Bucharest, Faculty of Medical Engineering, Bucharest 060042, Romania*
[4]*Faculty of Biology, Department of Biochemistry and Molecular Biology, University of Bucharest, Bucharest, Romania*
Corresponding author: *tatiana.alexandru@inflpr.ro*

The systemic administration of photosensitizers presents limitations regarding biodistribution and cutaneous photosensitivity. Targeted delivery *via* crosslinked hydrogels offers a mechanism to localize photosensitizing agents within the tumour microenvironment. This work details the synthesis and real-time monitoring of hydrogel matrices loaded with motexafin lutetium (MLu), a texaphyrin-based near-infrared photosensitizer, for localized photodynamic therapy (PDT) in breast cancer models.

Hydrogels containing gelatin methacrylate (GelMa), poly(ethylene glycol) diacrylate (PEGDa), GelMa-PEGDa hybrids, and polycaprolactone-PEGDa (PCL-PEGDa) were synthesized. Photopolymerization was initiated using a 355 nm Nd:YAG pulsed laser and the photoinitiator Irgacure 2959. Crosslinking kinetics were monitored in real-time through transmitted energy measurements and laser-induced fluorescence (LIF), utilizing specific emission peaks to quantify compound consumption and matrix gelation. The photophysical properties of MLu were evaluated under near-infrared excitation. Singlet oxygen generation was quantified *via* direct 1270 nm phosphorescence detection, establishing the singlet oxygen quantum yield against a Rose Bengal reference standard. Hydrogel properties were characterized through swelling thermodynamics, Attenuated Total Reflection Fourier Transform Infrared (ATR-FTIR) spectroscopy, and *in vitro* MLu release kinetics in phosphate-buffered saline.

The singlet oxygen quantum yield of MLu was measured at 0.65, demonstrating conversion efficiency via a Type II photodynamic mechanism. Real-time LIF monitoring indicated that the fluorescence intensity of the Irgacure peak decreased continuously within the crosslinking matrices, corresponding to photoinitiator consumption during network propagation. Transmitted energy measurements confirmed micro-scale phase separation and structural changes, identifying the gelation threshold. ATR-FTIR spectroscopy verified the positional stability of specific amide bands, indicating that MLu integration maintained the crosslinking density of the networks. Physical characterization demonstrated that PEGDa networks exhibited the highest swelling ratios, while GelMa exhibited the lowest. The hybrid GelMa (5%) + PEGDa (5%) formulation demonstrated the highest diffusion-controlled release of MLu, whereas the PCL-PEGDa (10%) copolymer restricted water penetration, yielding the lowest release rate.

The implementation of real-time LIF and transmitted energy diagnostics facilitated the controlled synthesis of photosensitizer-loaded hydrogels. Based on structural stability, swelling thermodynamics, and defined MLu release profiles, three formulations-GelMa (10%), PEGDa (10%), and the hybrid GelMa (5%)-PEGDa (5%)-were selected as delivery platforms for subsequent in vitro evaluation in targeted breast cancer therapy.

Acknowledgements: This work was supported by a grant of the Ministry of Education and Research, Romania, CNCS - UEFISCDI, project number PN-IV-P2-2.1-TE-2023-1059, within PNCDI IV.

Nanostructured Sensing Platforms for Trace Element Analysis via Laser-Induced Breakdown Spectroscopy (LIBS)

Rosalba GAUDIUSO[1], Milica VINIĆ[1], Caterina GAUDIUSO[2], Antonio SANTAGATA[3], Lucrezia CATANZARO[4], Giuseppe R. COMPAGNINI[4], Alessandro DE GIACOMO[1,2]

[1]*University of Bari "A. Moro", via Orabona 4, Bari, 70125, Italy*
[2]*Institute for photonics and nanotechnology – CNR, via Amendola 173, 70125, Bari, Italy*
[3] *Institute of Structure of Matter – CNR, Zona Industriale Tito Scalo 85050 Tito Scalo (PZ), Italy*
4University of Catania, viale Doria 6, 95125, Catania, Italy
Corresponding author: Rosalba.gaudiuso@uniba.it

Despite its practical advantages as a portable, fast technique for elemental analysis of a variety of matrices, Laser-Induced Breakdown Spectroscopy (LIBS) still suffers from relatively low sensitivity, limiting its usefulness to concentrations in the order of parts per million. Several signal-intensification methods have been proposed, involving multiple laser pulses, additional electrical discharges, and various sample preparation and preprocessing strategies [1,2]. While providing good performance in laboratory settings, these can be challenging in the field. Acting on the laser-substrate coupling, on the other hand, has the potential to be a highly efficient field-compatible strategy. To this end, we present two substrate-modification methods for the fabrication of sensing platforms either functionalized or texturized with nanostructures, and their effect on the intensification of LIBS signals of deposited fluids. The first is based on the generation of Laser-Induced Periodic Surface Structures (LIPSS), the second involves the functionalization of substrates with noble-metal nanoparticles. We will discuss the results that we obtained with liquid matrices relevant to biomedical analysis (biological fluids from patients and healthy controls) and environmental monitoring (aqueous solutions of heavy metals) for the signal intensification of several metallic traces. As an example, calibration lines of $PbCl_2$ obtained with glass slides functionalized with Ag nanoplates are reported in Figure 1, and show a decrease of almost one order of magnitude of the limit of detection (LOD) of the analyte of interest, thus confirming the remarkable potential of this experimental approach for trace element analysis.

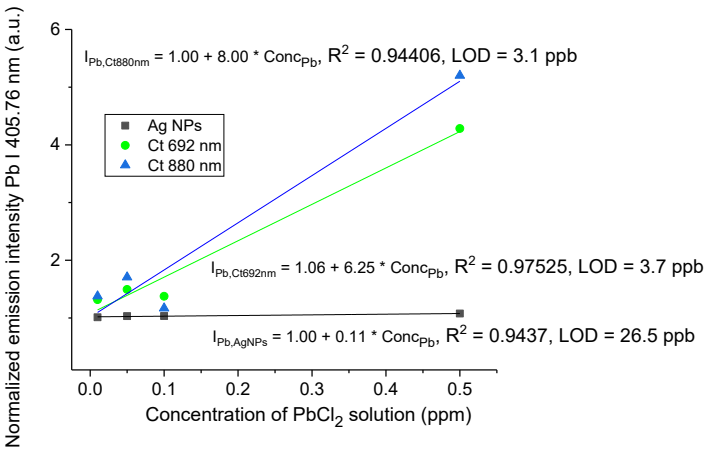

Fig. 1. Pb calibration lines and corresponding limit of detection (LOD) with classical drop-cast NELIBS (black line and squares) and substrates functionalized with Ag nanoplates (Ag-NPTs) having plasmon resonance wavelength maxima at 692 nm (green line and circles) and at 880 nm (blue line and triangles).

[1] G. Galbács, "A critical review of recent progress in analytical laser-induced breakdown spectroscopy," Anal. Bioanal. Chem. **407**, 7537 (2015).
[2] S. C. Jantzi, V. Motto-Ros, F. Trichard, Y. Markushin, N. Melikechi, A. De Giacomo, "Sample treatment and preparation for laser-induced breakdown spectroscopy," Spectrochim. Acta B **115**, 52 (2016).

ZnO Nanowire on Thick Targets in Laser Particle Acceleration

Maria BALAN[1,2], Constantin DIPLASU[1], Razvan UNGUREANU[1], Mihai SERBANESCU[1], Razvan MIHALCEA[1] Ana TIULEANU[1,3], Youmali SANWOGOU[4], Mihai STAFE[2], Ioana DINCA[1], Cornel STAICU[1], Dorina TICOS[1], Adrian SCURTU[1], Georgiana GIUBEGA[1], Gabriel COJOCARU[1], Beatrice PARASCHIV[1], Aurelian MARCU[1,2]

[1]*National Institute for Laser, Plasma and Radiation Physics, CETAL Department, Magurele 077125, Romania*
[3]*University" Politehnica" Bucharest, Bucharest 060042, Romania*
[3]*Department of Physics, University of Bucharest, Magurele 077125, Romania*
[4]*University of Kara, Kara, Togo*
Corresponding author: *aurelian.marcu@inflpr.ro*

Nanostructured materials have a wide range of applications from medical to industrial, and from sorption to particle acceleration processes. With the increase of the volume ratio, nanostructure dominant properties tend to be more related with the morphology and surface related properties rather than the bulk ones. A new cutting-edge surface morphology related application of nanowire layers is particle acceleration by high-power laser irradiation. In recent years, High-Power lasers acceleration, both from gas target or thin metallic targets, become a real competitor of the classic particle accelerators, while nanostructured targets have already proved their contribution in improving electron extraction efficiency. For now, nanoporous materials being easier and cheaper to be produced, have started to show their efficiency enhancement potential, while crystalline materials and aligned nanostructure layers are just starting to be tested.

In the present paper, we start exploring the possibility of using single-crystal nanowire on thick crystalline and non-metallic substrates as 'targets' for laser particles acceleration. We started by growing ZnO nanowire by PLD/VLS technique and performing morphology optimisation by controlling growing parameters In Fig.1 is an example on the temperature influence.

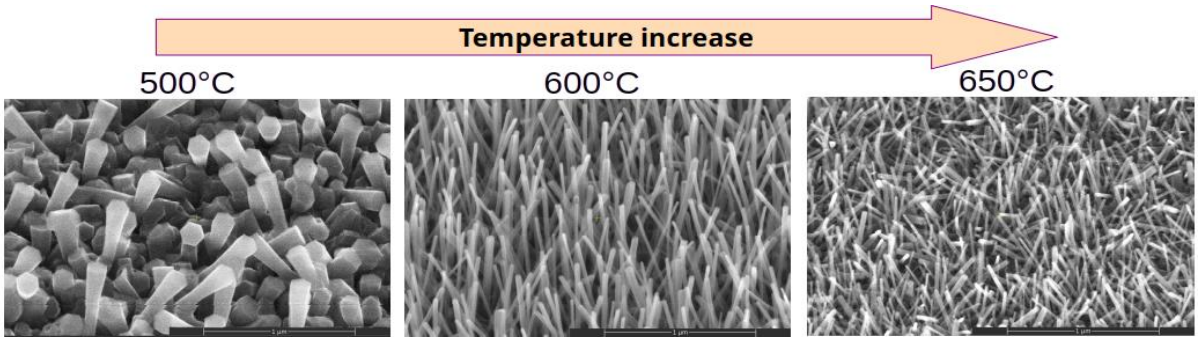

Fig. 1. SEM images of ZnO nanowires grown on quartz at different temperatures

We further performed simulation on light absorption and electron transport and scattering through such thick (and non-metallic) targets. Furthermore, experimental data were obtained from electron beams accelerators in order to understanding electron scattering and absorption by such 'thick' substrates. Presented results and discussed focussing focus on the laser extracted charge and generated electromagnetic fields, in correlation with the target properties.

Acknowledgements: We acknowledge funds from the Ministry of Education and Research, Romania / Institute of Atomic Physics, through ELI-RO 30/2024, ELI-RO 30/2025 support of the National Interest Infrastructure facility IOSIN - CETAL at INFLPR and Program contract No. 39/2024, Romanian National Core Program LAPLAS VII contract No. 30N/2023.

Development of Ultra-Low Density Foam Targets to Enhance fs-Laser-Plasma Coupling

Valentin CRACIUN[1,2], Alexandru MAGUREANU[2,3], Cristian MILOS[1], Alexei ZUBAREV[1,2], Gabriel P. BLEOTU[2], Gabriela DORCIOMAN[1], Petronela GAROI[1], Doina CRACIUN[1], Daniel URSESCU[2], Catalin M TICOS[2,3]

[1]*National Institute for Laser, Plasma and Radiation Physics, Măgurele 077125, Romania*
[2]*Extreme Light Infrastructure (ELI-NP), and Horia Hulubei National Institute for R&D in Physics and Nuclear Engineering (IFIN-HH), Bucharest-Magurele, Romania*
[3]*Engineering and Applications of Lasers and Accelerators Doctoral School (SDIALA), National University of Science and Technology POLITEHNICA Bucharest, Bucharest, Romania*
Corresponding author*:* *valentin.craciun@inflpr.ro*

The advancement of ultra-low-density targets manufacturing has emerged as a significant research direction, due to their proven potential to enhance the energy coupling in high-power laser experiments, particularly those focused on particle acceleration and radiation generation. In recent years, considerable attention has been devoted to optimizing laser–plasma coupling to achieve higher acceleration efficiencies. In this context, we report on the experimental development and characterization of structured ultra-low density carbon (ULD-C) targets fabricated via Pulsed Laser Deposition (PLD) on thin aluminum (Al) foil substrates. These targets exhibit densities on the order of a few tens of mg/cm^3, specifically tailored to improve laser energy absorption through volumetric interaction mechanisms.

A detailed experimental investigation of the laser-target interaction was carried out at the ELI-NP facility using a femtosecond pulsed laser system operating at millijoule energy levels and intensities around 10^{13} W/cm^2, in vacuum conditions. The plasma plume dynamics from ULD-C on Al foils was analyzed and compared to that obtained from bare Al foil targets. We performed a comparative analysis using an ultra-fast ICCD camera and Langmuir probe measurements to determine the time-of-flight of the emitted ions. The results showed a notably distinct behavior in plume expansion and kinetic energy profiles between the structured and simple Al foil targets.

Complementary radiative-hydrodynamic simulations were performed using the FLASH code to model the temporal evolution of the laser-induced plasma. The simulations revealed that, while bare aluminum foils exhibited surface-localized heating and limited plume expansion, the ULD-C targets facilitated volumetric energy absorption, resulting in a more uniform heating profile and explosion-like plasma dynamics. Preliminary tests performed at the 1 PW fs-laser level with an Al 1.5 μm+10 μm C foam target showed the detection of a proton beam of 27.8 MeV, significantly higher than the values obtained using bare Al foils. This work highlights the potential of engineered ULD-C targets to significantly enhance laser–plasma coupling and obtain high energy proton beams.

Acknowledgements: This research received funding from ELI-RO 15 (DELISM), ELI-RO 19 (HighProtonPLas), project PTE 41/2025, Nucleu contract PN 23 21 01 05, phase 5, and Nucleu-LAPLAS VII 30N/2023, Ministry of Education and Research, Romania.

Laser-Driven Gamma Irradiation for Industrial Imaging First-Stage Station: *Concept, Setup & Experimental Validation*

Liviu NEAGU[1,2], Ovidiu TESILEANU[1], Georgiana GIUBEGA[1,2], Yoshihide NAKAMIYA[1], Florin NEGOITA[1], Gabriel COJOCARU[1,2], Laura NALBARU (NITA)[3], M. MIREA[4], E. HERMANN[4], Marian NEAGU[4], Lucian TUDOR[1], Saibek NORBAEV[1], Alexandru LAZAR[1,3], Andrei BERCEANU[1], Madalin ROSU[1], Ioana FIDEL[1,5], Antonia TOMA[1], Lidia VASESCU[1], Mihai IOVEA[4]

[1]*Extreme Light Infrastructure - Nuclear Physics (ELI-NP), Horia Hulubei National R&D Institute forPhysics and Nuclear Engineering, 30 Reactorului Str., Magurele 0771255, Romania*
[2]*Center for Advanced Laser Technologies, National Institute for Lasers, Plasma and Radiation Physics (INFLPR), 409 Atomistilor Str., Magurele 077125, Romania*
[3]*National University of Science and Technology POLITEHNICA Bucharest, Splaiul Independentei no. 313, Bucharest 060042, Romania*
[4]*AccentPro2000 S.R.L (AP2K), Marasesti Str., Magurele 077125, Romania*
[5]*Interdisciplinary School of Doctoral Studies, ISDS, University of Bucharest, 36-46 Mihail Kogalniceanu Bd, Bucharest 050107, Romania*
Corresponding author: *liviu.neagu@eli-np.ro*

Laser-driven plasma accelerators (LPA) enable the generation of ultra-relativistic electron beams over centimeter-scale distances via the nonlinear laser Wakefield acceleration (LWFA) regime, providing a compact source of high-energy Bremsstrahlung gamma radiation. Such sources are of increasing interest for industrial radiography and non-destructive testing (NDT), particularly for dense and extended objects where multi-MeV photon energies are required.

We report on the design, implementation, and experimental validation of a first-stage laser-driven gamma irradiation station at the E4 interaction area where we use the 100 TW output beamline of HPLS at ELI-NP. Laser pulses with energies around 2 J and durations in the tens of femtoseconds were focused to a spot size of 21 μm × 24 μm, reaching peak intensities in the relativistic regime ($a_0 > 1$). The interaction with supersonic gas jets of Argon and Helium–Nitrogen mixtures at plasma densities of (3–6 × 10^{18} cm^{-3}) enabled stable electron acceleration via the LWFA mechanism, yielding broadband electron spectra with maximum energies up to 220 MeV and bunch charges of (311 ± 29) pC.

The accelerated electron beams were converted into gamma radiation through Bremsstrahlung emission in a 2 mm thick Aluminum target. The resulting photon beams exhibit sufficient flux and penetration capability for industrial imaging, achieving spatial resolutions on the order of 0.1 mm/px under current experimental conditions.

Furthermore, we present the first experimental evidence of the dependence of electron bunch charge density on laser pulse duration within this parameter regime, highlighting the role of pulse shaping in charge injection and beam loading processes. These results provide a quantitative basis for optimizing laser-driven gamma sources and represent a significant step toward scalable, high-repetition-rate systems for industrial inspection applications [1].

Acknowledgements: *This work was funded by the PN 23210105 contract funded by the Ministry of Education and Research, Romania, by the Extreme Light Infrastructure Nuclear Physics Phase II, a project co-financed by the Romanian Government and the European Union through the European Regional Development Fund and the Competitiveness Operational Programme (No. 1/07.07.2016, COP, ID 1334). We also acknowledge funds from Ministry of Education and Research, Romania / Institute of Atomic Physics (IFA), through ELI-RO-40/2024 project and support of National Interest Infrastructure Facility IOSIN-ELI.*

[1] G. Giubega et al. "High-Power laser-driven gamma irradiation station for industrial imaging: concept, setup and experimental benchmarking", Rom. Rep. Phys. **78**(1), 401 (2026).

PW-Class Laser: Compact Electron Accelerator and High-Peak Power THz Source

Alexei ZUBAREV[1], Marina CUZMINSCHI[1,2], Darius VESTEA[1], Constantin DIPLASU[1], Georgiana GIUBEGA[1,3], Gabriel COJOCARU[1,3], Razvan UNGUREANU[1], Mihai SERBANESCU[1], Sandel SIMION[1], Razvan STOIAN[4]

[1]*National Institute for Laser, Plasma and Radiation Physics, Magurele 077125, Romania*
[2]*Horia Hulubei National Institute for R&D in Physics and Nuclear Engineering, Magurele 077125, Romania*
[3]*Extreme Light Infrastructure (ELI-NP), Horia Hulubei National R&D Institute for Physics and Nuclear Engineering (IFIN-HH), Magurele 077125, Romania*
[4]*Laboratoire Hubert-Curien, UMR CNRS 5516, Université de Lyon, Université Jean Monnet, St. Etienne, F-42000, France*
Corresponding author: alexei.zubarev@inflpr.ro

Modern petawatt-class laser systems have demonstrated significant potential in the development of compact electron accelerators [1], with the energies up to GeV [2]. Recent experiments conducted at the CETAL-PW facility have revealed a strong dependence of electron energy on both laser intensity and target density [2]. Notably, relatively small variations in laser power (on the order of 20%) can induce changes of up to 50% in the mean energy of quasi-monoenergetic electron beams.

In addition, strong oscillations of electromagnetic fields in laser-produced plasmas lead to the emission of terahertz (THz) radiation, which can be utilized simultaneously with the accelerated electron beams [3]. Secondary THz radiation may be employed to enhance beam quality by reducing electron energy spread. Furthermore, the combined use of high-intensity THz radiation and relativistic electron beams enables novel radiation sources, such as third-order X-ray generation resulting from electron deceleration in THz-irradiated targets.

A comprehensive understanding of the physical mechanisms governing electron acceleration and THz emission in laser–plasma interactions require advanced numerical simulations. Such simulations provide insight into plasma dynamics, including current distributions (Fig. 1) and near-field effects, which are not directly accessible experimentally. In this work, we investigate laser interaction with a gas jet target using numerical simulations and compare the results with experimental data. The simulations were performed using the EPOCH PIC code [4], while the experiments were carried out at the CETAL-PW facility.

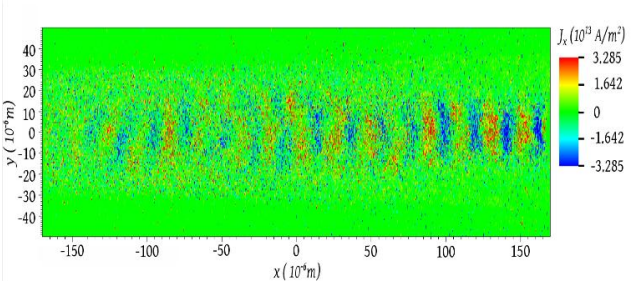

Fig. 1 Curent distribution in a gas jet plasma irradiated by high intensity laser pulse.

Acknowledgements: The authors acknowledge LAPLAS VII-contract No. 30N/2023 within PNCDI IV, A. C and M. C. ancknowledges CNCS-UEFISCDIPN-IV-P2-2.1-TE-2023-1102, PN-IV-P7-7.1-PED-2024-079; M.C. acknowledges PN-23-21-01 01/2023. The authors acknowledge the support of National Interest Infrastructure facility IOSIN–CETAL at INFLPR, IOSIN-ISS numerical facility and Olimpia Budriga, Aurelian Marcu and Alexandru Achim for their support in implementing numerical simulations and infrastructure support.

[1] B. Miao, *et al.*, "Multi-GeV electron bunches from an all-optical laser wakefield accelerator," Phys. Rev. X **12**(3), 031038 (2022).
[2] C. Diplasu, *et al.*, "Commissioning Experiment on Laser-Plasma Electron Acceleration at CETAL-PW Laser Facility," Rom. Rep. Phys. **73**(4), 401 (2021).
[3] A. Marcu, *et al.*, "Correlation of Laser-Accelerated Electron Energy with Electromagnetic Pulse Emission from Thin Metallic Targets," Appl. Sci. **15**(1), 29 (2025).
[4] T. D. Arber, *et al.*, "Contemporary particle-in-cell approach to laser-plasma modelling," Plasma Phys. Control. Fusion **57**(11), 113001 (2015).

Coherent Beam Combination of Two Terawatt Femtosecond Laser Pulses

Cecilia OANCA[1,2], Ana DINCA[1,3], Razvan UNGUREANU[1], Gabriel COJOCARU[1,4], Mihai SERBANESCU[1], Alexandru MIHALCEA[1,5], Razvan DABU[1], Sandel SIMION[1]

[1]*National Institute for Laser, Plasma and Radiation Physics, CETAL Department, 077125, Măgurele, Romania*
[2]*Doctoral School of Physics, University of Bucharest, 077125, Măgurele, Romania*
[3]*Faculty of Electronics, Telecommunications and Information Technology, National University of Science and Technology POLITEHNICA Bucharest, 061071, Bucharest, Romania*
[4]*National Institute for Nuclear Physics and Engineering – Horia Hulubei, Extreme-Light Infrastructure – Nuclear Physics, 077126, Măgurele, Romania*
[5]*Doctoral School of Electronics, Telecommunications and Information Technology, National University of Science and Technology POLITEHNICA Bucharest, 061071, Bucharest, Romania*
Corresponding authors: cecilia.oanca@inflpr.ro, sandel.simion@inflpr.ro

Coherent Beam Combination (CBC) offers a promising approach for increasing the output of ultrashort, high-power laser pulses, beyond the limits imposed by nonlinear effects, optical-damage thresholds and aperture constraints in single-channel CPA laser systems [1].

This work presents the development of a tiled-aperture CBC platform designed to coherently combine two TW-class fs pulses at TEWALAS Laser System, INFLPR. Chirped laser pulses of 1.5 mJ energy from the TEWALAS Front-End were amplified up to 18 mJ in two parallel 3-pass Ti:sapphire amplifiers and compressed to ~35 fs in a common compressor. Measured amplifier gain was consistent with the Frantz–Nodvik modelling and analysis [2].

Efficient CBC requires precise control of phase and temporal overlap, as even hundred-as timing jitter degrades the in-phase combination of femtosecond laser pulses. Phase stabilization was achieved using a quadrature-signal interferometric detector, which employs a CW laser diode whose beam propagates along the same optical path as laser pulses, but with a tiny tilt angle. The ABCD matrix formalism [3] was used to calculate the spatial separation between the CW and pulsed laser beams after propagation through the two beam expanders and the common compressor. Jones formalism [4] was used to describe the detector output electric signals. The quadrature sin/cos electrical signals are processed by an analog stage that generates the codes associated with the interference fringes [5]. These codes are then delivered to an FPGA-based (Field-Programmable Gate Array) digital stage for optical path correction. The tiled-aperture CBC configuration relies on overlapping the pulsed beams in the far-field plane of a focusing element. A CCD camera was placed in the focusing plane of a 1.5-m focal length lens, where the interference pattern of the two beams was actively stabilized using an electronic feedback that drives a piezoelectric actuator able to adjust the optical path with a 20-nm resolution. Preliminary measurements show a stability of far-field interference patterns corresponding to sub 100-nm RMS path variations and as much as 90% combining efficiency, approaching theoretical predictions for our CBC setup [1] (Fig.1).

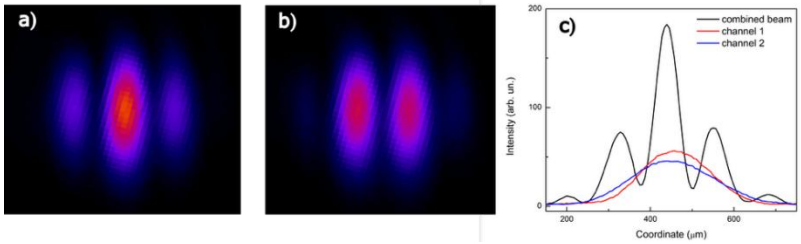

Fig. 1. Interference patterns corresponding to a) in-phase combination ($\Delta\varphi = 0$) and b) anti-phase combination ($\Delta\varphi = \pi$). c) Comparison of coherently combined fs-laser pulses intensity with the single channel laser pulse intensity.

Currently, our work is directed towards the improvement of phase control accuracy and development of a laser system for automatic in-phase combination of fs laser pulses.

Acknowledgements: For this research, we acknowledge funds from ELI-RO 20/2024 project and National Interest Infrastructure Facility IOSIN – CETAL, at INFLPR.

[1] V. E. Leshchenko, Opt. Express **23**(9), 12062-12076 (2015).
[2] L.M. Frantz, J.S. Nodvik, J. Appl. Phys. **34**(8), 2346-2349 (1963).
[3] A.E. Siegman, "Lasers," University science books (1986).
[4] R. C. Jones, J. Opt. Soc. Am. **38**, 671-685 (1948).
[5] S. Simion, *et al.*, Rom. Rep. Phys. **62**(3), 644-651 (2010)

Advanced Techniques for Coherent Beam Combination of High-Power Ultrashort Laser Pulses

Cecilia OANCA[1,2], Razvan UNGUREANU[1], Ana DINCA[1,3], Mihai SERBANESCU[1], Alexandru MIHALCEA[1,4], Razvan DABU[1], Sandel SIMION[1]

[1]*National Institute for Laser, Plasma and Radiation Physics, CETAL Department, 077125, Magurele, Romania*
[2]*Doctoral School of Physics, University of Bucharest, 077125, Magurele, Romania*
[3]*Faculty of Electronics, Telecommunications and Information Technology, National University of Science and Technology POLITEHNICA Bucharest, 061071, Bucharest, Romania*
[4]*Doctoral School of Electronics, Telecommunications and Information Technology, National University of Science and Technology POLITEHNICA Bucharest, 061071, Bucharest, Romania*

Corresponding authors: razvan.dabu@inflpr.ro, sandel.simion@inflpr.ro

Two general techniques are considered for the coherent beam combination (CBC) of ultrashort laser pulses: filled and tiled aperture combining. In the filled aperture combining laser beams are spatially overlapped in the near-field and focused, whereas in the tiled aperture (parallel) combining all beams are placed side by side and focused, generally by a parabolic mirror, to get high-intensity combined beams. The peak power limitations imposed by the current laser technologies, related to the size and damage threshold of critical optical laser components can be overcome by achieving CBC of high-power ultrashort laser pulses in a parallel configuration. The dependence of the combining efficiency on different instabilities and mismatches in a laser system based on CBC (especially optical path mismatch, phase difference, dispersion compensation accuracy, pointing instability, pulse front tilt) was analytically investigated [1]. The development of a laser system for fs pulses CBC should be based on some essential achievements: appropriate interferometric laser system configuration; high accuracy electronic control of the instabilities of the laser pulses phase difference and beam pointing; automatic setting of the working regime in the CBC mode of operation.

For an efficient CBC, femtosecond laser pulses must be synchronized with fs-accuracy and locked in phase with sub-hundred attosecond relative timing jitter. The relative jitter between the combined fs pulses, mainly determined by pump sources and environmental perturbations, is dominated by frequencies up to 100 Hz. A phase-error real-time correction with a sampling rate in the kHz range would be necessary to maintain the CBC state of high-power fs laser pulses. Because of the low repetition rate of TW-PW lasers, in the range of 0.1-10 Hz, an additional cw laser source, which propagates the same path as high-power laser pulses, would be necessary for the control of the optical path difference between fs laser pulses. Some experimental configurations of laser systems for CBC of fs laser pulses will be presented.

Experimentally proven active feedback methods for the control of optical path difference, based on interferometric techniques, will be discussed: near field interference fringe analysis using one-dimensional Fourier transform [2], electrical energy interferometry analogous to the Hansch-Couillaud detector [3], processing of the quadrature electric signals generated in an interferometer [4]. For the correction of optical path difference, the error signals are transmitted to a fast piezo-electric transducer (PZT). Non-linear optical processes, such as sum-frequency generation, can be used for the control of femtosecond pulses synchronization [5].

Machine learning methods can be employed to simultaneously measure the beam-pointing and phase errors in multi-beam tiled-aperture coherent-combination systems [6]. Neural networks are able to recognize the far-field interference patterns and to automatically generate the driving signals for the PZT to adjust the optical path in order to get the in-phase combination of the femtosecond pulses beams and to keep it during the laser system operation.

Prospects of the CBC of 2 × 10-PW femtosecond laser pulses at ELI-NP will be discussed.

Acknowledgements: For this research, we acknowledge funds from ELI-RO 20/2024 project and National Interest Infrastructure Facility IOSIN – CETAL, at INFLPR.

[1] V. E. Leshchenko, Opt. Express **23**(12), 15944-15970 (2015).
[2] C. Peng, *et al.*, Opt. Lett., **44**(17), 4379-4382 (2019).
[3] S. N. Bagayev, *et al.*, Opt. Lett. **39**(6), 1517-1520 (2014).
[4] S. Simion, *et al.*, Rom. Rep. Phys. **62**(3), 644-651 (2010).
[5] C. Peng, *et al.*, Opt. Lett. **42** (19), 3960-3963 (2017).
[6] R. Li, *et al.*, Chin. Opt. Let. **18**(4), 041402 (2020).

Engineering High-Entropy Alloy Thin Films by Pulsed Laser Deposition for Tunable Microwave Absorption

Stefan-Andrei IRIMICIUC[1,2], Petr HRUŠKA[1], Eva MAREŠOVÁ[1], Lenka VOLFOVA[1], Stanislav CICHOŇ[1], Sergii CHERTOPALOV[1], Valentin CRACIUN[2], Sergiu VATAVU[3], Jan LANCOK[1]

[(1)]*Institute of Physics of the Czech Academy of Sciences, Na Slovance 1999/2, Prague, Czech Republic*
[(2)]*National Institute for Laser, Plasma and Radiation Physics, Măgurele, 077125, Romania*
[(3)]*Moldova State University, Alexei Mateevici St 60, Chișinău, Moldova*
Corresponding author: *stefan.irimiciuc@inflpr.ro*

Complex high-entropy materials (HEMs)-including high-entropy alloys (HEAs), oxides (HEOs), and nitrides (HENs)-continue to deliver breakthrough performance across diverse applications. Their multi-principal-element chemistry enables access to wide compositional spaces and tunable functionalities within a single multielement system. Although high-quality HEA coatings are commonly produced by magnetron sputtering, pulsed laser deposition (PLD) offers distinct advantages: its inherently non-equilibrium, non-thermal nature facilitates the formation of unconventional high-entropy stoichiometries, and the exploration of new material families derived from established 5–6 elements.

In this work, we demonstrate the fabrication of HfNbTaTiZr high-entropy thin films with controllable stoichiometry using PLD across a broad processing window. Depositions were performed in inert (Ar) and reactive (O_2, N_2) atmospheres, at pressures up to 100 Pa, substrate temperatures up to 800 °C, and variable laser fluences. These parameters were systematically tuned to modulate the energy distribution and gas-phase chemistry of the expanding metallic plume. To capture the evolution of the plasma during growth, we employed complementary in situ diagnostics—space-resolved optical emission spectroscopy and angle-resolved electrical probing-which enabled the identification of a deposition geometry that minimizes gas-phase oxidation.

Comprehensive post-deposition characterization was carried out using AFM, SEM, XRD, XPS, and microwave absorption measurements. An optimization framework was then established to correlate processing conditions with resulting film properties. Our results show that precise control over ion dynamics enables deliberate tuning of microstructure, yielding amorphous, nanocrystalline, and mixed-phase architectures, as well as a wide range of compositional profiles and surface morphologies-from smooth, compact layers to rough, granular nanostructures. The microwave response of the coatings was strongly dependent on the deposition environment, producing metallic, reflective films in Ar; semi-transparent films in N_2; and fully transparent films in O_2. Overall, this study highlights the potential of architected multilayer metallic/ceramic high-entropy coatings with tunable structural and electromagnetic properties for advanced microwave absorption technologies.

Acknowledgements: This work was financed by project NATO SPS G6153, program NUCLEU-LAPLAS VII 30N/2023

POSTER PRESENTATIONS

Topic 1. Fundamentals, Diagnostics and Modelling in Laser, Plasma and Radiation Physics

Modeling the Growth of Tungsten Oxides Thin Films by Deposition of Aggregates Formed in Plasma

Cristina CRACIUN[1,2], Adrian BERCEA[1,2], Mihaela FILIPESCU[1], Marius DUMITRU-GRIVEI[1]

[1]*National Institute for Lasers, Plasma and Radiation Physics, Atomistilor 409, Magurele, Romania*
[2]*Doctoral School of Physics, Faculty of Physics, University of Bucharest, Atomistilor 405, Magurele, Romania*
Corresponding author: *cristina.craciun@inflpr.ro*

Tungsten oxides (WO_x) thin films with porous morphologies were produced by pulsed laser deposition (PLD) at room temperature and high gas pressure. Under these conditions, the material extracted from target agglomerates in plasma forming aggregates with dimensions ranging from a few thousand nm^2 to almost one μm^2. The thin films formed through deposition of these aggregates presents porous morphologies, as the low kinetic energy of the deposited particles and the low substrate temperature does not allow the reorganization of the deposited material.

The aggregation of material in plasma was modeled using a Diffusion Limited Aggregation (DLA) model. The morphological properties of the particles obtained on the samples produced with a low number of laser pulses were used to parametrize our model. The statistical and geometrical characteristics of the real particles and the modeled aggregates were studied, and the results were used to improve the model.

The growth of WO_x thin films was modeled through the successive deposition of aggregates constructed using DLA model. Modeled morphologies present similar features with experimental results and allow a better understanding of the growth mechanism of porous thin film.

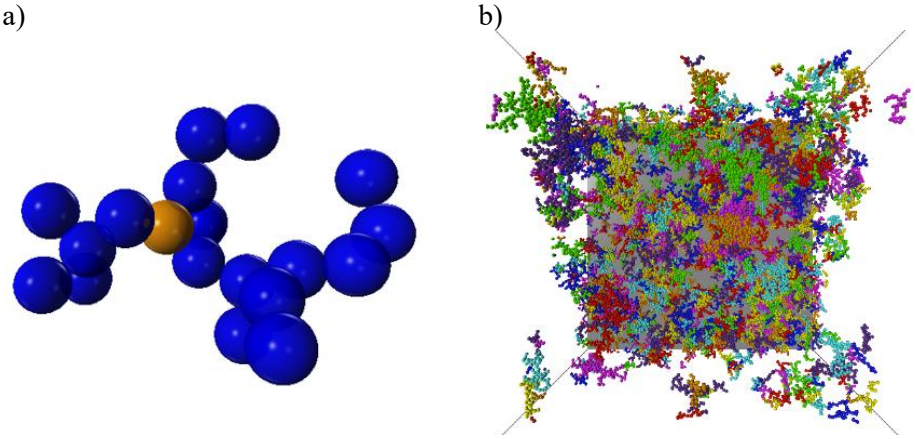

Figure 1. a) An aggregate modeled using DLA. b) The modeled films composed of 1250 aggregates with different dimensions.

Acknowledgements: This work was supported by a grant of the Ministry of Education and Research, Romania - UEFISCDI, project number PN-IV-P7-7.1-PED-2024-1292 (ELCHROM), within PNCDI IV.

P-02

Decoding Electron-CF_4 Interactions in Plasma Processing

Jonathan REID, Ryan BROOK, Dmitrii SHALASHILIN, Dimitrios KONTZIAMPASIS

University of Leeds, Leeds, United Kingdom
Corresponding authors: mwcl0950@leeds.ac.uk, r.brook@quantemol.com, D.Shalashilin@leeds.ac.uk, D.Kontziampasis@leeds.ac.uk

CF_4 is a widely used fluorocarbon in plasma processing, where electron-impact dissociation of the parent molecule governs the production of reactive fluorine-containing species. Despite extensive experimental study of electron-impact ionization and dissociation in CF_4, a predictive modelling framework for electron-driven fragmentation remains limited.

With an initial focus on the lowest electronically excited triplet states, which are expected to play a dominant role in electron-impact-induced dissociation, the first stage establishes a consistent set of electron CF_4 collision cross sections suitable for use in global plasma models. Electron-impact excitation cross sections are explored using established scattering frameworks, including the Quantemol platform. Where appropriate, semi-empirical calculations are used to benchmark total ionization behavior and ensure consistency across the dataset.

Building on this foundation, this work investigates excited-state dissociation dynamics in CF_4, beginning from the lowest triplet state. Nonadiabatic excited-state dynamics simulations are used to resolve fragmentation pathways, branching ratios, and characteristic dissociation timescales leading to neutral CF_x and F products. By combining state-specific excitation cross sections with triplet-state dissociation dynamics, this approach provides a route towards predicting channel-resolved dissociation cross sections from first principles.

The proposed framework bridges microscopic electron–molecule interaction physics and macroscopic plasma chemistry modelling. The resulting cross-section dataset and mechanistic insight improve the representation of CF_4 dissociation in global plasma models and contribute to a more grounded understanding of fluorocarbon plasma processing.

[1] M. Ziółkowski, A. Vikár, M. L. Mayes, Á. Bencsura, G. Lendvay, and G. C. Schatz, "Modeling the electron-impact dissociation of methane," J. Chem. Phys. **137**(22), 22A510 (2012).
[2] M. Dogan, W. Wolff, D. M. Mootheril, T. Pfeifer, and A. Dorn, "Electron impact single and double ionization and dissociation: revisiting CF_4 and CHF_3 with an improved experimental method," Phys. Chem. Chem. Phys. **27**(19), 10057-10072 (2025).
[3] D. V. Makhov, G. Armstrong, H.-H. Chuang, H. Ambalampitiya, K. Lemishko, S. Mohr, A. Nelson, J. Tennyson, and D. V. Shalashilin, "Dissociation of hydrofluorocarbon molecules after electron impact in plasma," J. Phys. Chem. Lett. **15**(12), 3404-3411 (2024).
[4] R. Brook, O. Bramley, D. V. Makhov, A. Nelson, G. Armstrong, J. Yong, E. Saunders, J. de Viggiani, J. Tennyson, and D. V. Shalashilin, "Rules of triplet state electron impact neutral dissociation in plasma from molecular dynamics simulations and an electrophore model," J. Vac. Sci. Technol. A. **43**(4), 043003 (2025).

Thermal and Chemical Choking in Pulsed Plasma CO_2 Dissociation: Mitigation Through Volumetric Expansion

Adrian SCURTU[1], Dorina TICOS[1], Maria Luiza MITU[1], Constantin DIPLASU[1], Nicoleta UDREA[1], Beatrice PARASCHIV[1], Catalin Mihai TICOS[1]

[1]*National Institute for Laser, Plasma and Radiation Physics, Magurele 077125, Romania*
Corresponding author: adrian.scurtu@inflpr.ro.

Non-thermal plasma dissociation of CO_2 can selectively channel electron energy into molecular excitation and dissociation, but the most efficient vibrational pathway is sensitive to gas heating, V–T relaxation, and reactant depletion. Under confined low-pressure operation, these effects promote thermal and chemical choking, limiting conversion and preventing scalable operation. We investigated CO_2 dissociation using a pulsed magnetoplasmadynamic (MPD) jet at Mars-relevant pressures (0.5–5 Torr) [1]. The discharge produces peak currents of ~12.5 kA and a Lorentz-force-accelerated supersonic jet sustaining two electron populations: a fast group ($T_e \approx 13$ eV) driving direct dissociation, and a slower group ($T_e \approx 4$–5 eV) feeding vibrational excitation [2,3]. Two reactor volumes were compared: a confined 4.56 L chamber and an expanded 110 L reservoir.

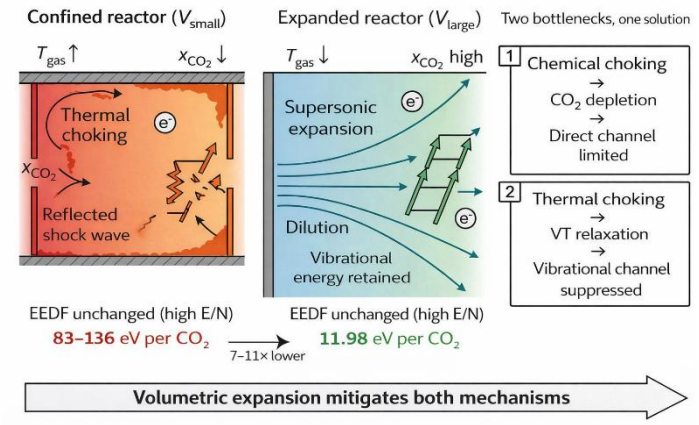

Fig. 1. Schematic representation of CO_2 dissociation in a supersonic MPD plasma jet under confined and expanded-volume conditions [1].

In the confined reactor, conversion saturated rapidly, consistent with shock-induced heating and progressive CO_2 depletion. These two pathways - thermal choking suppressing the vibrational channel and chemical choking limiting the direct channel - act on different molecular substrates [1]. The expanded volume mitigates both simultaneously: the jet develops freely, avoiding reflected-shock heating and maintaining high CO_2 availability. The result is a minimum energy cost of 11.98 ± 1.42 eV/CO_2 at 3 Torr - a 7-11× improvement over the confined case and ~2.7× more efficient than the MOXIE electrolyzer on Mars. Volumetric expansion thus provides a passive, catalyst-free scaling principle for CO_2 conversion under native Martian conditions.

Acknowledgements: This research was supported by the Ministry of Education and Research, Romania, under Romanian National Core Program, NUCLEU-LAPLAS VII-contract no. 30N/2023.

[1] A. Scurtu, "Scalable CO_2 dissociation via supersonic MPD plasma jets," Chem. Eng. J. **541**, 177676 (2026).
[2] A. Scurtu, *et al.*, "Harnessing high-density pulsed plasma for sustained oxygen supply on Mars," Energy Conv. Manag.: X **29**, 101495 (2025).
[3] A. Scurtu, *et al.*, "Ultra-rapid direct dissociation of CO_2 with dense pulsed plasma jets for Martian oxygen production," J. CO_2 Util. **104** 103326 (2026).

Multifractal Analysis for Fusion Plasma Disruption Prediction

Teddy CRACIUNESCU[1], Andrea MURARI[2,3] on behalf of JET Contributors*
and the EUROfusion Tokamak Exploitation Team**

[1]National Institute for Laser, Plasma and Radiation Physics, Magurele, 077125, Romania
[2]Consorzio RFX (CNR, ENEA, INFN, Università di Padova, Acciaierie Venete SpA), Corso Stati Uniti 4, 35127 Padova, Italy
[3]Istituto per la Scienza e la Tecnologia dei Plasmi, CNR, Padova, Italy
*See the author list of C.F. Maggi et al 2024 Nucl. Fusion 64 112012 https://doi.org/10.1088/1741-4326/ad3e16
**See the author list of N. Vianello et al 2026 submitted to Nuclear Fusion
Corresponding author: teddy.craciunescu@gmail. com

Disruptions are a potential showstopper on the route to developing a tomakak fusion reactor. Since their consequences can be more severe the larger the devices, in the next generation of machines they will have to be carefully managed from the beginning of operation. On the other hand, in new devices, the diagnostic coverage is typically limited and there will be no opportunity to collect many examples for the training of traditional machine learning classifiers. It is therefore important to develop predictors that can ideally operate satisfactorily without training and with minimal diagnostic information. During the last years several approaches based on the identification of dynamical changes in the time series corresponding to routinely available diagnostic signals (locked mode, plasma current) have been developed. Recently, robust evidence of strong variation in the multifractal spectrum of magnetic fluctuations in the discharge phases preceding disruptions has been obtained and used to develop a new disruption prediction method. Close to disruptions the structure of the multifractal spectra becomes characteristic of a cascade process. This specific signature allows a significant reduction of the false alarm rate. In addition to good statistical performances, the warning times are sufficient not only for mitigation but also for the prevention of most disruptive events. The method is compatible with a real-time implementation. It has been validated on a large dataset of discharges at JET including experiments belonging to the last DT campaigns.

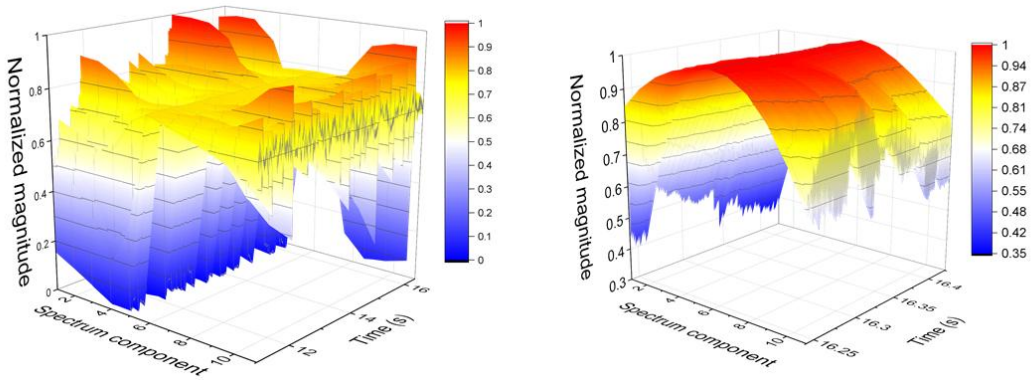

Figure 1- Typical multifractal spectrum of the locked mode signal during the normal behaviour of a discharge (left) and close to the disruption (right).

Acknowledgements: *This work has been carried out within the framework of the EUROfusion Consortium, funded by the European Union via the Euratom Research and Training Programme (Grant Agreement No 101052200 EUROfusion). Views and opinions expressed are however those of the author(s) only and do not necessarily reflect those of the European Union or the European Commission. Neither the European Union nor the European Commission can be held responsible for them. On of the authors (TC) acknowledges the support from program NUCLEU-LAPLAS VII 30N/2023, Ministry of Education and Research, Romania.*

Deuterium Desorption from Tungsten Layer by Laser-Based Methods

Sasa-Alexandra YEHIA-ALEXE[1], Andreea GROZA[1], Mihai SERBANESCU[2],
Bogdan BUTOI[1], Paul DINCA[1], Cornel STAICU[1], Flaviu BAIASU[3],
Maria Elena HURJUI[1], Corneliu POROSNICU[1]

[1]*National Institute for Laser, Plasma and Radiation Physics, Laboratory of Low Temperature Plasma, Magurele, 077125, Romania*
[2]*National Institute for Laser, Plasma and Radiation Physics, CETAL Department, Magurele 077125, Romania*
[3]*National Institute for Laser, Plasma and Radiation Physics, Laboratory of Plasma Physics and Nuclear Fusion, Magurele 077125, Romania*
Corresponding author: *sasa.yehia@inflpr.ro*

Part of the inner wall of the ITER project is designed to be built from tungsten-based materials due to its properties to handle high fluxes of charged particles, neutrons, and extreme temperatures. Even if the fusion plasma is magnetically confined, fuel isotopes such as deuterium and tritium are incorporated in the plasma-facing materials. The retention of hydrogen isotopes leads to high concern regarding safety and material's engineering. Thereby, in-situ methods for hydrogen isotopes release are required. Due to the extreme conditions in the divertor part of the fusion reactor, cooling gases such as Ne [1], Ar, N_2 are added. The study of the release of hydrogen isotopes from tungsten-based materials in the presence of cooling gases is of great interest.

Tungsten layers with deuterium inclusions were obtained during RF magnetron-sputtering discharge in Ar/D_2 and Ne/D_2 gaseous mixtures in order to investigate the release of hydrogen isotopes using a laser-based method [2,3]. Morphological and structural analyses were performed to evaluate the influence of the type of discharge gaseous mixtures on layer deposition. The synthesizing plasma was characterized by optical emission spectroscopy, Langmuir probe, and RFEA probe.

Deuterium was released from tungsten-deuterium layers by their ablation and desorption using a laser with pulse duration of 10 ns. The morphological changes induced by the laser impact on the samples were investigated by scanning electron microscopy. The released species during laser-sample interaction were monitored via quadrupole mass spectrometer. The amount of D released by laser induced ablation and desorption was compared with the total D inventory measured by thermal desorption spectroscopy to estimate the efficiency of the laser-based method for the release of hydrogen isotopes. The total amount of D released from the layers obtained in Ne/D_2 plasma was higher than in Ar/D_2 plasma. In the laser induced ablation regime the efficiency of D release decreases from 100 %, for the samples obtained in Ar/D_2 plasma, to 2 % for those obtained in Ne/D_2 plasma. In the laser desorption regime, the efficiency of D release decreases from 8 %, for the samples obtained in Ar/D_2 plasma, to 0.5 % for those obtained in Ne/D_2 plasma.

Acknowledgements: This work was financed by program NUCLEU-LAPLAS VII 30N/2023, Ministry of Education and Research, Romania.

[1] X. Bonnin, R.A. Pitts, V. Komarov, F. Escourbiac, M. Merola, L. Bo, L. Wei, L. Pan and A.S. Kukushkin, "ITER divertor plasma response to time-dependent impurity injection," Iscience **12**, 1100 (2017).
[2] S.A. Yehia-Alexe, M. Serbanescu, P. Dinca, B. Butoi, M.E. Zarif, C. Porosnicu and A. Groza, "Deuterium release from beryllium layers by laser induced plasma ablation and laser induced desorption coupled with quadrupole mass spectrometry," Spectroc. Acta Pt. B-Atom. Spectr. **229**, 107197 (2025).
[3] S.A. Yehia-Alexe, A. Groza, M. Serbanescu, M.E. Zarif, B. Bita, P. Dinca, B. Butoi, C. Staicu and C. Porosnicu, "Considerations on hydrogen isotopes release from thin films by laser induced ablation and laser induced desorption techniques," Spectroc. Acta Pt. B-Atom. Spectr. **208**, 106774 (2023).

Microscopic Insights into the Limitations of the Decorrelation Trajectory Method

Radu SAPUNARU[1,2], Dragos Iustin PALADE[2]

[1]*National Institute for Laser, Plasma and Radiation Physics, Lab 220, Plasma Theory Group, Magurele 077125, Romania*
[2]*Faculty of Physics, University of Bucharest, Magurele 077125, Romania*
Corresponding author: *radu.sapunaru@inflpr.ro*

Predicting turbulent transport in magnetically confined plasmas, particularly in tokamaks, remains a major challenge because no simple relationship exists between the statistical properties of turbulent fields and the resulting transport levels. The Decorrelation Trajectory Method (DTM), introduced two decades ago [1,2], provides an approximate statistical framework that has been widely used to estimate turbulent transport with qualitative success. However, the method relies on simplifying assumptions that limit its accuracy.

Here we investigate these limitations from a microscopic perspective by examining the behavior of DTM at the level of subensembles. This analysis reveals features of stochastic trajectories that are not captured by the standard formulation and clarifies the origin of discrepancies in its predictions. Based on these observations, we propose a heuristic refinement of the method and evaluate its accuracy.

Acknowledgements: *This work has been carried out within the framework of the EUROfusion Consortium, funded by the European Union via the Euratom Research and Training Programme (Grant Agreement No 101052200 - EUROfusion). Views and opinions expressed are however those of the author(s) only and do not necessarily reflect those of the European Union or the European Commission. Neither the European Union nor the European Commission can be held responsible for them.*
This work was also supported by a grant of the Ministry of Education and Research, Romania, CNCS - UEFISCDI, project number PN-IV-P2-2.1-TE-2023-1102, within PNCDI IV and by the Romanian National Core Program LAPLAS VII contract no. 30N/2023.

[1] M. Vlad, F. Spineanu, J. H. Misguich, R. Balescu, "Diffusion with intrinsic trapping in two-dimensional incompressible stochastic velocity fields," Phys. Rev. E **58**(6), 7359-7368 (1998).
[2] M. Vlad, F. Spineanu, J. H. Misguich, R. Balescu, "Diffusion in biased turbulence," Phys. Rev. E **63**(6), 066304 (2001).

Numerical Correlations of Temperature-Driven Modifications of Nanostructured Surfaces

Paul Wilhelm RAUECKER[1,2], Razvan MIHALCEA[1], Maria BALAN[1,3], Marius DUMITRU[1], Viorel CHIHAIA[4], Andreea NEACSU[4], Aurelian MARCU[1,3]

[1]*National Institute for Laser, Plasma and Radiation Physics, Magurele 077125, Romania*
[2]*University of Bucharest, Faculty of Physics, Magurele 077125, Romania*
[3]*National University of Science and Technology" Politehnica" Bucharest, Doctoral School of Applied Sciences, Bucharest 060042, Romania*
[4]*National Institute of Physical Chemistry "Ilie Murgulescu", Bucharest 060021, Romania*
Corresponding author: *aurelian.marcu@inflpr.ro*

Nanostructured surfaces have wide applications ranging from solar cells and sensors to particle accelerator targets, where understanding and controlling the nanostructure shape is crucial. In our paper ZnO nanowires were obtained by Pulsed Laser Deposition (PLD) in Vapor-Liquid-Solid (VLS) growth conditions, at 650°C. At low temperatures, the $\{10\bar{1}0\}$ side facets are energetically favored, and equilibrium geometry at higher temperatures leads to a rounding effect. Thus, in order to assess the rounding effect, samples were annealed at 600, 700 and 800°C and 1200°C for varying time durations (10 minutes and 3 hours). SEM investigations have shown melted nanowires at 1200°C, far below the bulk melting point of ZnO (1975°C). Quantitative analysis of this data was made possible by recent advances in computer vision techniques. We generated a synthetic dataset and trained a MaskFormer [1] style model with a custom regression head. We defined the main regression variable of interest as φ, an interpolation factor between ideally hexagonal and ideally cylindrical nanowire geometry. Using said model, we were able to approximate this factor for various SEM images captured of both unannealed and annealed samples of ZnO nanowires (Fig. 1).

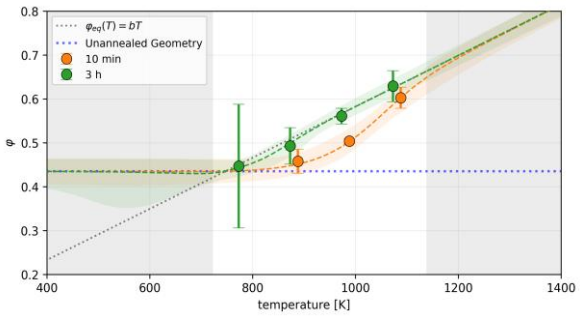

Figure 1: The theoretical fit of model to data with temperature-dependent τ

We furthermore hypothesized an equation describing the changes in morphology during annealing

$$\varphi\,(T,\,t) = \varphi_0 + [\varphi_{eq}\,(T) - \varphi_0]\,[1 - e^{-t/\tau\,(T)}] \qquad (1)$$

where φ_0 is the initial geometry of the unannealed sample, φ_{eq} is the temperature-dependent equilibrium geometry which gets fitted as 'bT' and τ is the *Arrhenius-style* characteristic timescale describing the kinetics of the rounding defined as $\tau_0 e^{Ea}/k_B T$. This allows the estimation of various physically meaningful parameters for the morphology change, like an activation energy of 0.95 ± 0.36 eV or a characteristic timescale of 6 minutes at 800°C but 38 minutes at 600°C.

Acknowledgements: We acknowledge funds from the Ministry of Education and Research, Romania / Institute of Atomic Physics, through ELI-RO 30/2024, ELI-RO 30/2025 support of the National Interest Infrastructure facility IOSIN – CETAL at INFLPR and Program contract No. 39/2024, Romanian National Core Program LAPLAS VII contract No. 30N/2023.

[1] B. Cheng, I. Misra, A. G. Schwing, A. Kirillov, and R. Girdhar, "Masked-attention Mask Transformer for Universal Image Segmentation," http://arxiv.org/abs/2112.01527

Quantitative Nanoscale Thermal Conductivity Measurements using DC Scanning Thermal Microscopy

Claudiu HAPENCIUC[1], Anita VISAN[1], Gianina POPESCU-PELIN[1], Irina NEGUT[1], Mihai OANE[1], A. ADAM[2], Theodorian BORCA-TASCIUC[3], Ion N. MIHAILESCU[1], Sinziana ANGHEL[1,4]

[1]*National Institute for Laser, Plasma and Radiation Physics, CETAL Department, Magurele 077125, Romania*
[2]*Physics Department, Faculty of Science, Sohag University, Sohag, 82524, Egypt*
[3]*Mechanical Aerospace and Nuclear Engineering Department, Rensselaer Polytechnic Institute, 110 8th St., Troy, New York 12180-3590, USA*
[4]*Faculty of Physics, University of Bucharest, Magurele, Ilfov, 077125, Romania*
Corresponding author: *sanziana.anghel@inflpr.ro*

This work presents a calibrated DC-based scanning thermal microscopy (SThM) method for quantitative thermal conductivity measurements at the nanoscale, with particular applicability to low-conductivity materials. The approach is based on a steady-state formulation derived as the zero-frequency limit of existing AC models, enabling a simplified experimental implementation without the need for lock-in detection or frequency-domain analysis. The method combines an analytical heat transfer model with an experimental calibration procedure based on reference substrates and the intersection method, allowing the determination of probe–sample contact parameters. A systematic sensitivity analysis is performed to evaluate the influence of key parameters, including probe resistivity, cantilever thermal conductivity, and heat losses to the environment. The results show that, despite parameter correlation, the extracted thermal conductivity remains stable within a few percent over a wide range of parameter values, demonstrating the robustness of the method. The approach is validated on multiple reference substrates and applied to thin films with thicknesses down to tens of nanometers. Measurement accuracy within 3–5% is obtained for materials with thermal conductivity in the range of 0.1–2 W m^{-1} K^{-1}. The analysis also highlights the intrinsic limitations of DC SThM at higher thermal conductivities, where the probe response becomes dominated by the thermal contact resistance.

Acknowledgements: I.N., C.H., A.V. acknowledge the support by grants of the Ministry of Education and Research, Romania, CCCDI-UEFISCDI, project number PN-IV-P7-7.1-PED-2024-0137 within PNCDI III. The INFLPR authors acknowledge with thanks the support of this work by the Romanian Ministry of Education and Research, under Romanian National NUCLEU Program LAPLAS VII-Contract No. 30N/2023.

Influence of Thermal Relaxation Time on the Improved Generalized Bioheat Equation: A Comparative Analytical-Numerical Study

Alexandra Maria Isabel TREFILOV[1], Mihai OANE[1], Liviu DUTA[1], Cristian Nicolae MIHAILESCU[1], Gerarldine Maria STANCIU[2], Natalia MIHAILESCU[1], Dorina TICOS[1], Anca NEDELCEA1[1], Cristina L. DOLIS[2], Liviu BADEA[3,4], Claudiu HAPENCIUC[1], Muhammad Arif MAHMOOD[5], Sinziana ANGHEL[1,4], Catalin Mihai TICOS[1,6], Georgian BALEA[7], Carmen RISTOSCU[1], Ion Nicolae MIHAILESCU[1]

[1]*National Institute for Laser, Plasma and Radiation Physics, LASERS Department, Magurelei 077125, Romania*
[2]*Prof. Dr. Alexandru Obregia Clinical Psychiatric Hospital, 10-12 Berceni Str., Bucharest, Romania.*
[3]*National Research & Development Institute for Non-ferrous and Rare Metals– IMNR, Bucharest, Romania.*
[4]*University of Bucharest, Faculty of Physics, Măgurele, Ilfov, 077125, Romania*
[5]*Hydro Extrusion North America, USA*
[6]*Extreme Light Infrastructure (ELI-NP), Magurele, 077125 Romania*
[7]*"Alexandru Marghiloman" High-School, Buzau, 120242 Romania*
Corresponding author: *alexandra.trefilov@inflpr.ro*

The Pennes bioheat equation remains the most widely used framework for modelling heat transfer in biological tissues during thermal exposure, originating from Fourier's classical law of heat conduction and incorporating energy exchange between blood vessels and surrounding tissue. Although numerous numerical approaches have been proposed and exact solutions exist for specific geometries and boundary conditions, analytical formulations of the bioheat equation are far less common. In this work, we develop a fully analytical three-dimensional model-implemented in MATHEMATICA and validated through COMSOL simulations-to characterize laser-induced heat transfer in biological tissues under a range of therapeutic conditions.

The study introduces three major advancements to the conventional bioheat framework: (a) a non Fourier extension of the Pennes equation that explicitly incorporates thermal relaxation time; (b) the integration of Dirac delta functions and the telegraph equation to represent localized point source heating of diseased tissue; and (c) the derivation of closed form analytical solutions for both the classical (Fourier based) and improved (non Fourier) formulations. Particular attention is given to the relationship between the relaxation time parameter in the telegraph equation and the thermal relaxation time used in bioheat modelling. Based on these considerations, an optimal thermal relaxation time of 1.16 s was identified for exposure durations ranging from 0.01 s to 120 s.

The generalized model developed here provides a more realistic description of heat exchange between tissue and blood flow by accounting for non-uniform temperature distributions and finite speed thermal propagation. The strong agreement between the analytical MATHEMATICA solutions and the numerical COMSOL simulations confirms the robustness of the proposed approach. Overall, this work advances the theoretical foundations of laser-based medical treatments and thermal therapies, offering a refined predictive tool for optimizing clinical protocols and improving therapeutic outcomes.

Acknowledgements: This work was partially financed by the Ministry of Education and Research, Romania, under ELI-RO/RDI/2024_039, ELI-RO/RDI/2024_015, ELI-RO/RDI/2024_019, PN-IV-P7-7.1-PED-2024-0796 Projects. and program NUCLEU-LAPLAS VII – Contract No. 30N/2023.

Humphreys α-line in H-I and the Solar Spectra Via Quantum Spectral-Model

Diana Rodica RADNEF-CONSTANTIN[1], Liliana PREDA[2], Mark RUSHTON[3], Agnetha MOCANU[4], Dumitru POPESCU[5], Valentin I. NICULESCU[6]

[1,3]*Institutul Astronomic al Academiei Romane, 5 Cutitul de Argint street, Bucuresti, Romania*
[2]*Universitatea Politehnica Bucuresti, 313 Splaiul Independentei street, Bucuresti, Romania*
[4]*Universitatea Hyperion, 169 Calarasilor street, Bucuresti, Romania*
[5]*ISMMA, 13 Calea 13 Septembrie street, Bucuresti, Romania*
[6]*National Institute for Lasers, Plasma and Radiation Physics, Magurele, Romania*
Corresponding author: *ghe12constantin@yahoo.com*

Starting from the quantum model of the hydrogen atom, we calculate and tabulate the peaks of α *Humphreys*-multiplet in fine-structure approximation (*fs*-approximation) [1,2]. We determine the spectral line peaks of this multiplet (Fig.1) using a new *MaximumLocalisation*-spectral-Model which is based on some several spectroscopic and statistical hypotheses [2-4]. By statistical analysis of the NIST and ACE data, we evaluate the parameters of the regression curves for the multiples from *Lyman to Pfund* and *Humphreys* spectral series. Furthermore, an algorithm for the quantum spectral reconstruction of multiplets in *fs*-approximation for any *Sn* spectral series of H-I is provided, *n* being the order of the spectral series. A plot representation is used to give a statistical global view of the first six series of H-I spectrum. The results confirm the measurements provided of the solar data from ACE mission [5].

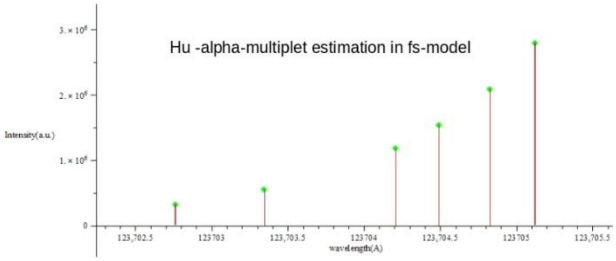

Fig 1. Plot of α Humphreys multiplet in fine-structure approximation in *(λ,I)* space.

Acknowledgements: We thank to our collaborator Valentin I. Niculescu which will pay the fee for our participation to the third edition of ICLPR-ST Conference, Brasov, June, 2026.

[1] A.E. Kramida, "A critical compilation of experimental data on spectral lines and energy levels of hydrogen, deuterium, and tritium," Atomic Data and Nuclear Data Tables (2010).
[2] D. R. Constantin, L. Preda, M. Rushton, U.P.B. Sci. Bull. Series A **85**-1, 167 (2023).
[3] D. R. Constantin, L. Preda, M. Rushton, U.P.B. Sci. Bull. Series A **85**-4, 201 (2023).
[4] Marius Iosifescu, *et al.*, "Mica enciclopedie de statistica," Ed. Stiintifica si Enciclopedica (1985).
[5] D. R. Constantin, L. Preda, "The Estimation of Humphreys A-Multiplet Spectral Composition for H-I Spectrum Using Maximumlocalisation-Spectral-Model," (2024). https://papers.ssrn.com/sol3/papers.cfm?abstract_id=4744616

Early-Time Dynamics in Polymer and Metal LIFT

Simona BRAJNICOV[1], Mihail Octavian CERNAIANU[2], Thomas LIPPERT[3,4], Maria DINESCU[1], Alexandra PALLA-PAPAVLU[1]

[1]*National Institute for Laser, Plasma and Radiation Physics, Laser Department, Magurele 077125, Romania*
[2]*Extreme Light Infrastructure - Nuclear Physics (ELI-NP) / Horia Hulubei National Institute of Physics and Nuclear Engineering, Reactorului Street 30, ZIP 077125, Magurele, Romania*
[3]*Laboratory for Multiscale Materials Experiments, Paul Scherrer Institute, Forschungsstrasse 111, Villigen PSI, 5232, Switzerland*
[4]*Department of Chemistry and Applied Biosciences, ETH Zürich, Zürich, 8093, Switzerland*
Corresponding author: *alexandra.papavlu@inflpr.ro*

Laser-induced forward transfer (LIFT) is a powerful technique for the precise deposition of thin-film materials, but the early-stage dynamics that govern flyer launch, shock-wave formation, and material preservation are still not fully understood, especially in the case of polymers. In this work, we combine time-resolved side-view shadowgraphy with hydrodynamic simulations to investigate the LIFT of aluminum (Al) and polyisobutylene (PIB) films propelled by triazene polymer (TP) sacrificial layers under nanosecond UV laser irradiation.

Al flyers are first used as a reference system to validate the hydrodynamic model against established experimental behavior, allowing a quantitative analysis of flyer position–time evolution and shock-wave propagation in both air and vacuum. We then extend the study to polymer transfer using donor stacks composed of 150 nm TP and 60 nm PIB, irradiated at laser fluences of 200, 350, and 600 mJ/cm².

The shadowgraphy experiments reveal a clear evolution of the transfer process with increasing fluence, from weak and barely detectable launch at low fluence, to efficient and coherent flyer ejection at intermediate fluence, and finally to overdriven conditions at high fluence where excessive heating leads to material loss and reduced flyer integrity. The simulations capture the main experimental trends, including the coupled ejection of the TP and PIB layers and the progressive degradation of flyer quality with increasing fluence. Comparison between metal and polymer systems further highlights the importance of sacrificial-layer thickness, energy deposition, and shock–flyer interaction in determining the outcome of the transfer process.

Overall, the combined experimental and modeling approach provides new insight into the transfer window required for intact polymer pixel deposition and demonstrates that hydrodynamic simulations are a valuable tool for interpreting time-resolved LIFT experiments. These findings are relevant for the optimization of laser-based patterning and polymer microfabrication technologies.

Acknowledgements: This work was supported by IFA (Institute of Atomic Physics) through the ELI-RO/RDI/2024_028 FLIGHT and ELI-RO/RDI/2024_016 DELPHI Projects, and by the Ministry of Education and Research, Romania, under the Romanian National Program-NUCLEU - LAPLAS VII – contract no. 30N/2023 and PN 23210105.

[1] M. O. Cernaianu, P. Ghenuche, T. Lippert, M. Dinescu, A. Palla-Papavlu, "Initial stages of laser-induced forward transfer using a release layer via hydrodynamic simulations," Appl. Surf. Sci. **742**, 167249 (2026).

Quantitative Imaging of Regolith Ejection Dynamics under Electron Beam Exposure

Nicoleta UDREA[1], Maria Luiza MITU[1], Beatrice PARASCHIV[1,2], Dorina TICOS[1], Adrian SCURTU[1], Catalin Mihai TICOS[1,2,3]

[1]*National Institute for Laser, Plasma and Radiation Physics 077125 Magurele, Romania*
[2] *Engineering and Applications of Lasers and Accelerators Doctoral School (SDIALA), National University of Science and Technology Politehnica of Bucharest, 313 Splaiul Independentei St., Bucharest RO-060042, Romania,*
[3]*Extreme Light Infrastructure-Nuclear Physics (ELI-NP), Horia Hulubei National Institute for R&D in Physics and Nuclear Engineering (IFIN-HH), Magurele 077125, Romania*
Corresponding author: *nicoleta.udrea@inflpr.ro*

Regolith contamination poses a major challenge for long-duration Lunar and Martian missions, significantly degrading the performance of optical, photovoltaic and thermal-control systems [1]. Conventional evaluation methods are generally limited to static pre- and post-exposure imaging, thereby overlooking the transient physical mechanisms governing particle detachment. In this work, a computer-vision-based methodology is presented for the quantitative analysis of regolith removal induced by a pulsed electron beam under vacuum conditions [2]. High-speed recordings acquired at 50 fps were processed using an automated image-analysis pipeline combining flat-field correction, adaptive thresholding, beam-artifact suppression and morphological filtering. More than 1,500 frames were analysed for three regolith simulants deposited on glass substrates: JSC-1A, JSC Mars-1A, and LHS-1D.

Frame-by-frame analysis [3] demonstrates that similar endpoint cleaning efficiencies can conceal fundamentally different removal dynamics. JSC-1A exhibits stochastic multi-burst behaviour associated with intense localized luminous structures, while the Martian simulant undergoes rapid and continuous removal with minimal optical emission. In contrast, LHS-1D produces fragmentation-driven ejection characterized by bright particle streaks and highly directional trajectories (Fig. 1).

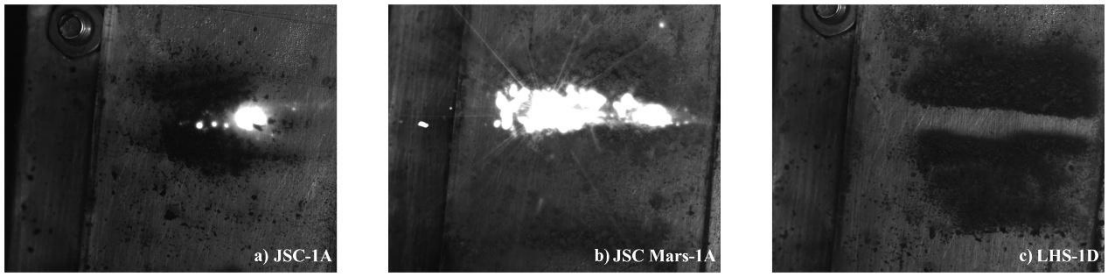

Fig.1. Regolith ejection dynamics under electron beam exposure

The proposed framework transforms qualitative visual observations into quantitative kinetic datasets suitable for statistical analysis and machine-learning-assisted diagnostics [4]. The results demonstrate that transient optical dynamics provide critical physical insights inaccessible through conventional endpoint measurements alone, offering a promising diagnostic approach for future autonomous dust-mitigation systems in space environments.

Acknowledgements: This work was supported by The European Space Agency and National Institute for Laser, Plasma and Radiation Physics, Contract number 4000144170, Programme Discovery and by the NUCLEU-LAPLAS VII 30N/2023, Ministry of Education and Research, Romania.

[1] M. Gaier, “The Effects of Lunar Dust on EVA Systems During the Apollo Missions,” NASA/TM-2005-213610 (2005).
[2] D. Ticoș, A. Scurtu, J. D. Williams, L. Scott, E. Thomas, D. Sanford, and C. M. Ticoș, “Rotation of a strongly coupled dust cluster in plasma by the torque of an electron beam,” Phys. Rev. E **103**(2), 023210 (2021).
[3] N. Udrea, M.L. Mitu, A. Scurtu, D. Ticos, C.M. Ticos, "Chaotic Oscillations of Vertically Aligned Microrods in a Plasma Sheath," IEEE Trans. Plasma Sci **51**(3), 835-846 (2023).
[4] M. L. Mitu, D. Ticoș, N. Udrea, A. Scurtu, and C. M. Ticoș, “Machine learning-based prediction of microparticle dynamics in externally driven strongly-coupled dusty plasmas,” Mach. Learn.: Sci. Technol. **6**(4), 045009 (2025).

High-Energy Pulsed Electron Beam-Induced Phase Transitions in a Plasma-Levitated Crystalline Dust Cluster

Beatrice PARASCHIV[1,2], Dorina TICOS[1], Nicoleta UDREA[1], Maria L. MITU[1], Adrian SCURTU[1], Catalin M. TICOS[1,3]

[1]*National Institute for Laser, Plasma and Radiation Physics, 077125, Magurele, Romania*
[2]*Engineering and Applications of Lasers and Accelerators Doctoral School (SDIALA), National Universityof Science and Technology Politehnica of Bucharest, 313 Splaiul Independenței St., Bucharest RO-060042,Romania*
[3]*Extreme Light Infrastructure-Nuclear Physics (ELI-NP), Horia Hulubei National Institute for Physics and Nuclear Engineering (IFIN-HH), Măgurele 077125, Romania*
Corresponding author*:* *beatrice.paraschiv@inflpr.ro*

Dust clusters with crystalline ordering in complex plasmas can undergo phase transitions under external perturbations [1,2]. In this study, we investigate the melting of a crystalline dust cluster composed of micrometer-sized plastic particles suspended in a radiofrequency argon plasma and irradiated with a pulsed electron beam in the 9–14 keV energy range. High-speed imaging combined with Voronoi analysis, pair correlation functions g(r), and particle tracking velocimetry (PTV) was used to characterize the structural and dynamical evolution of the system.

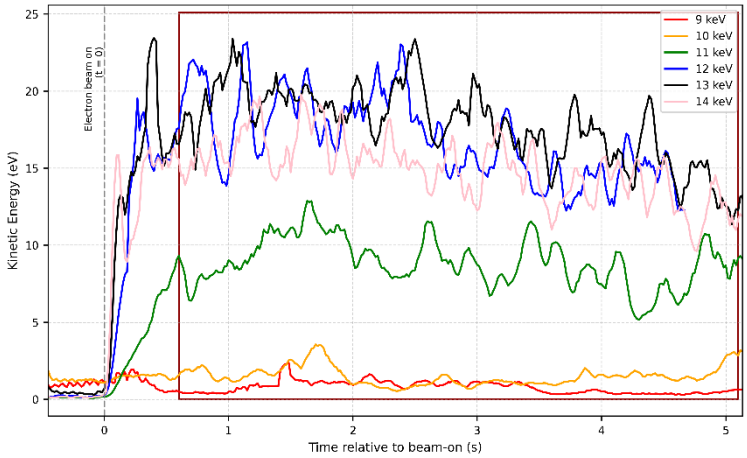

Fig. 1. Time evolution of the particles' kinetic energy for electron beam energies ranging from 9 to 14 keV. The electron beam is switched on at t = 0 [3].

The results show that the electron beam energy controls the melting dynamics. At 9–10 keV, the cluster undergoes gradual disordering accompanied by crystal rotation and hexatic-like behavior, indicating a continuous transition. At higher energies (11-14 keV), rapid destabilization, chaotic particle motion, and abrupt loss of crystalline order reveal a sharp transition, with melting times decreasing from 0.6 s to 0.1 s.

These findings demonstrate the ability of electron beam irradiation to control phase transitions in complex plasma crystals, with potential relevance for astrophysics, semiconductor processing, and fusion research.

Acknowledgements: This research was funded by the Ministry of Education and Research, Romania on project NUCLEU-LAPLACE VII, Contract No. PN 23 2101 05.

[1] G. E. Morfill and A. V. Ivlev, "Complex plasmas: An interdisciplinary research field," Rev. Mod. Phys. **81**(4), 1353-1404 (2009).
[2] V. E. Fortov, *et al.*, "Complex (dusty) plasmas: Current status, open issues, perspectives," Phys. Rep. **421**(1-2), 1-103 (2005).
[3] B. Paraschiv, D. Ticoș, N. Udrea, A. Scurtu, M. L. Mitu, and C. M. Ticoș, "High-energy pulsed electron-beam-induced phase transitions in a plasma-levitated crystalline dust cluster," Phys. Rev. E (accepted 2026), DOI: 10.1103/txxq-86mf.

Machine Learning-Based Prediction of Microparticle Dynamics in Externally Driven Strongly-Coupled Dusty Plasmas

Maria Luiza MITU[1], Dorina TICOS[1], Nicoleta UDREA[1], Adrian SCURTU[1], Beatrice PARASCHIV[1, 2], Catalin M. TICOS[1,3]

[1] *National Institute for Laser, Plasma and Radiation Physics, Magurele 077125, Romania*
[2] *Engineering and Applications of Lasers and Accelerators Doctoral School (SDIALA), National University of Science and Technology Politehnica of Bucharest, 313 Splaiul Independenței St., Bucharest RO-060042, Romania*
[3] *Extreme Light Infrastructure-Nuclear Physics (ELI-NP), Horia Hulubei National Institute for R&D in Physics and Nuclear Engineering, Magurele 077125, Romania*
Corresponding author: *maria.mitu@inflpr.ro*

We implemented unsupervised machine learning to study strongly coupled dusty plasmas with an emphasis on the dynamics of small plasma crystals rotated as a result of irradiation with a pulsed electron beam. By applying a combination of clustering algorithms such as K-means, DBSCAN, and Hierarchical clustering, along with statistical analysis, we classify the trajectories of microparticles in dust crystals levitated in the sheath of a radio-frequency plasma [1]. This approach enables the identification of dynamic patterns and facilitates predictions based on initial conditions and system parameters. We trained the clustering algorithms to predict dust trajectories, identifying the most likely ones based on the hierarchical relationships between them and the Silhouette and Davies–Bouldin scores. The integration of these algorithms and metrics enabled a robust and multidimensional analysis of microparticle trajectories, contributing to a deeper understanding of their dynamics in strongly-coupled plasmas and paving the way for future experimental and theoretical investigations. For each method, energy level and cluster configuration, we identified the top five best predictions based on their MSE scores, which quantify the precision of the predicted trajectories compared to the real trajectories. We performed a comparative evaluation of the clustering methods based on two performance metrics: MSE and Euclidean distance. Hierarchical clustering consistently surpassed both K-means and DBSCAN in trajectory prediction accuracy, achieving lower MSE and Euclidean Distance across both energy levels. Our study demonstrates the power of combining data science with experimental plasma physics to address challenges in manipulating levitated dust crystals [2]. The predictive model not only enhances our ability to control dust dynamics in strongly-coupled plasmas but also serves as a versatile tool for future research in dusty plasma systems.

Acknowledgements: This research was supported by program NUCLEU-LAPLAS VII 30N/2023, Ministry of Education and Research, Romania. We acknowledge the support of National Interest Infrastructure facility IOSIN – CETAL at INFLPR. C.M.T. acknowledges funding from IFA contract ELI-RO-19, Project "HighProtonPLas".

[1] D. Ticoş, A. Scurtu, J. D. Williams, L. Scott, E. Thomas, D. Sanford, and C. M. Ticoş, "Rotation of a strongly coupled dust cluster in plasma by the torque of an electron beam," Phys. Rev. E, **103** (2), 023210 (2021).
[2] M. L. Mitu, D. Ticoş, N. Udrea, A. Scurtu, and C. M. Ticoş, "Machine learning-based prediction of microparticle dynamics in externally driven strongly-coupled dusty plasmas," Mach. Learn.: Sci. Technol. **6**(4), 045009 (2025).

Towards ML-Stabilized Coherent Beam Combining using Single-Shot Complex Characterization of Ultrashort Laser Beam Pulses

Razvan UNGUREANU[1], Cecilia OANCA[1,2], Ana DINCA[1,4], Alexandru MIHALCEA[1,3], Mihai SERBANESCU[1], Gabriel COJOCARU[1,5], Constantin DIPLASU[1], Sandel SIMION[1], Razvan DABU[1]

[1]*National Institute for Laser, Plasma and Radiation Physics, CETAL Department, Magurele 077125, Romania*
[2]*Doctoral School of Physics, University of Bucharest, Faculty of Physics, Măgurele 077125, Romania*
[3]*Doctoral School of Electronics, Telecommunications and Information Technology, National University of Science and Technology POLITEHNICA Bucharest, Bucharest 061071, Romania*
[4]*Faculty of Electronics, Telecommunications and Information Technology, National University of Science and Technology POLITEHNICA Bucharest, Bucharest 061071, Romania*
[5]*Extreme Light Infrastructure (ELI-NP), Horia Hulubei National Institute for Physics and Nuclear Engineering (IFIN-HH), Magurele 077125, Romania*
Corresponding author: *razvan.ungureanu@inflpr.ro*

A promising technique for significantly scaling the peak power of ultra-intense laser facilities, while overcoming limiting factors such as the damage threshold or nonlinear phase accumulation in the chirped pulse amplification (CPA) technique [1], is to split the output beam of a femtosecond laser source (FRONT-END) and further amplify the pulses separately in identical multi-pass amplifiers and, after compression, temporally and spatially overlap them so that the resulting intensity scales with the number of channels. Subsequently, enabling independent multi-stage amplification chains [2].

Such is the case for the experimental setup implemented within the TEWALAS Laser Facility [3], where two parallel beams of amplified ultrashort IR pulses are overlapped spatially in the focal plane of a lens and also temporally by equalizing the optical paths with a mobile delay line. Accomplishing time delay control with precision down to a few percent of the laser wavelength, required for coherent beam combining (CBC) [4,5], the electric fields of the separately amplified pulses in each independent channel add coherently under a common envelope, producing an intensity peak higher than the sum of individual pulses [6]. However, the CBC efficiency may fall significantly below its theoretical maximum [6] due to fluctuations in each amplification channel, in addition to the strict requirements on delay time-control and spatial overlap.

We present experimental results correlating shot-to-shot fluctuations in pulse energy, spectral profile, beam-pointing, and wavefront with CBC efficiency. Efficiency is calculated from the spatial interference profile measured with a CCD camera at the lens focal plane, while the time delay between the two amplification channels is actively controlled within a closed loop, as shown in [7]. These statistical results are useful for the development of machine learning algorithms predicting the amount of control in laser parameters on each amplification channel that has to be accounted for in designing the hardware architecture of the CBC system control.

Acknowledgements *We acknowledge funds from the ELI-RO 20/2024 project, National Interest Infrastructure Facility IOSIN - CETAL, at INFLPR, and NUCLEU-LAPLAS project VII 30N/2023.*

[1] D. Strickland, G. Mourou, "Compression of amplified chirped optical pulses," Opt. Commun. **56**(3), 219-221 (1985).
[2] V. E. Leshchenko, "Coherent combining efficiency in tiled and filled aperture approaches," Opt. Express **23**(12), 15944-15970 (2015).
[3] R. Dabu, R. Banici, C. Blanaru, C. Fenic, L. Ionel, F. Jipa, L. Rusen, S. Simion, A. Stratan, M. Ulmeanu, D. Ursescu, M. Zamfirescu, "Tewalas 20-TW femtosecond laser facility," J. Optoelectron. Adv. Mater. **12**(1), 35-38 (2010).
[4] S. Simion, C. Blanaru, D. Ursescu, "Design considerations for an interferometer for coherent combination of ultrashort laser pulses," Rom. Rep. Phys. **62**(3), 644-651 (2010).
[5] S. Simion, Real-time synchronization of ultrashort pulse laser beams, based on interferometric methods. PhD Thesis, National University of Science and Technology POLITEHNICA Bucharest (2015).
[6] S. N. Bagayev, V. I. Trunov, E. V. Pestryakov, V. E. Leschenko, S. A. Frolov, V. A. Vasiliev, "High-intensity femtosecond laser systems based on coherent combining of optical fields," Opt. Spectrosc. **115**, 311-319 (2013).
[7] A Dinca, C. Oanca, R. Dabu, R Ungureanu, S. Simion, G. Cojocaru, A. Mihalcea, "Quadrature signal detection for phase stabilization in Coherent beam combination," 12th Markus Pessa International Summer School, 11 - 15 August, Tampere, Finland (2025).

Real-Time Beam Pointing Control System Design for CETAL-PW Front-End Laser

Alexandru MIHALCEA[1,2], Razvan UNGUREANU[1], Cecilia OANCA[1,3], Ana DINCA[1,4], Mihai SERBANESCU[1]

[1]*National Institute for Laser, Plasma and Radiation Physics, CETAL Department, Magurele 077125, Romania*
[2]*Doctoral School of Electronics, Telecommunications and Information Technology, National University of Science and Technology POLITEHNICA Bucharest, 061071, Bucharest, Romania*
[3]*Doctoral School of Physics, University of Bucharest, 077125, Magurele, Romania*
[4]*Faculty of Electronics, Telecommunications and Information Technology, National University of Science and Technology POLITEHNICA Bucharest, 061071, Bucharest, Romania*
Corresponding author: *alexandru.mihalcea@inflpr.ro*

The CETAL-PW Laser is a multi-stage double chirped pulse amplification (CPA) system [1,2] based on Ti: Sapphire, designed to amplify the output beam of a femtosecond oscillator with a gain of about 10^9. The complicated architecture of the CETAL-PW system can be divided into three main stages: first is the FRONT-END containing the oscillator, the pulse stretching, and several amplifiers that bring pulse power potentially up to terawatt level (E_{pulse} from nJ to 1.5J). The second stage is the final amplifier bringing the potential pulse power to petawatt level (E_{pulse} up to ~ 32 J), and finally the pulse temporal compressor that brings pulse duration close to the initial ultra-short duration, thus obtaining the PW peak power per pulse. One of the main difficulties in operating and maintaining laser systems with a complicated architecture and long optical length from the source (femtosecond oscillator) to target is maintaining a very strict alignment during daily usage and in-between beamtime sessions.

Small pointing deviations at early stages can propagate through the system and degrade the performance of downstream components, affecting both amplification efficiency and beam spatial profile. Therefore, reliable, real-time monitoring and highly reproducible correction of beam pointing is essential for any dedicated tool to assist the specialized personnel in system operation. To address these issues, our work presents the architecture implementation and the status of the integrated system, composed of hardware equipment such as optomechanics, optoelectronics, and networking, all integrated by a customized supervision software with a user-friendly graphical user interface (GUI).

The ongoing implementation includes not only the development of an automated system for laser beam pointing control but also a beam diagnostics component at the front-end stage of CETAL-PW petawatt-class laser system. The primary function of this system is to actively maintain the beam pointing at the input of critical amplifying stages, where spatial overlap between the pump and seed beams is essential for maximizing energy extraction and transfer efficiency. Besides the maintenance of the beam pointing aspect of the control system, additional features will be implemented, such as spatial profile homogeneity monitoring (hotspot and beam clipping detection) and approximate energy/power measurement, which will be valuable for benchmarking referential and traceability of the system operation.

Acknowledgements: We acknowledge funds from the ELI-RO 20/2024 project, National Interest Infrastructure Facility IOSIN – CETAL, at INFLPR and program NUCLEU-LAPLAS VII - project 30N/2023, Ministry of Education and Research, Romania.

[1] G. Matras, *et al.*, "First sub-25fs PetaWatt laser system," ASSL Congress OSA Technical Digest (online) (Optica Publishing Group, 2013), paper AF2A.3, Paris, France (2013).
[2] G. Matras, *et al.*, "First sub-25fs PetaWatt laser system," CLEO: Science and Innovations, San Jose, California, USA (2013).

High-Energy (Joule-Level) Pulse Post-Compression for Ultrafast Laser-Plasma Applications

Gabriel P. BLEOTU[1], Klaus M. SPOHR[1], Daniel URSESCU[1], Vojtech HORNY[1], Valentin CRACIUN[1], Alexia TANASEANU[1], Jon Imanol APIÑANIZ[2], Irene HERNÁNDEZ-PALMERO[2], Roberto LERA[2], Mauricio RICO[2], Carlos SALGADO-LÓPEZ[2], José Luis HENARES[2], Cruz MENDEZ[2], Gerard MOUROU[3]

[1] *Extreme Light Infrastructure: Nuclear Physics (ELI-NP), Magurele Romania.*
[2] *Centro de Láseres Pulsados (CLPU), Villamayor, Salamanca, Spain.*
[3] *Ecole Polytechnique, Palaiseau, France*
Corresponding author: gabriel.bleotu@eli-np.ro

The Thin Film Compression (TFC) technique [1-4] was implemented at 0.2 PW laser system (28 fs, 10 Hz, 800 nm) to induce spectral broadening of the initial pulse via self-phase modulation in 3 mm-thick fused silica plates. Dispersion was subsequently compensated using a pair of chirped mirrors prior to focusing and pulse characterization. Experiments were carried out at input pulse energies of 1 J, 3 J, and 5 J to assess both the performance and scalability of the post-compression scheme. A comprehensive diagnostic suite was employed, including spectral measurements, spectral phase retrieval via D-scan, focal spot intensity imaging, and spatial phase characterization using a wavefront sensor. Through optimization of the second-, third-, and fourth-order dispersion of the input pulse, an equivalent FWHM spectral bandwidth of 120 nm was achieved. Preliminary spectral phase reconstruction indicates pulse durations on the order of ~8 fs at the focal plane within the interaction chamber (see Fig. 1). In parallel, dedicated efforts focused on improving spatial phase control and focal intensity characterization following post-compression (f/4 OAP focusing), enabling stable and reliable operation for relativistic laser–plasma experiments. Efficient focusing of the ultrabroadband beam was demonstrated through the implementation of an additional deformable mirror.

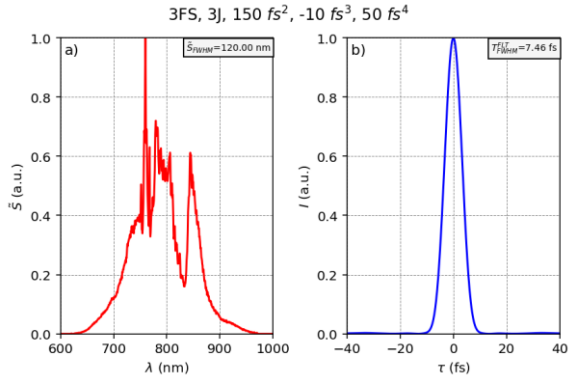

Figure 1. Experimental results retrieved inside the interaction chamber for 3 J input energy after dispersion compensation

In conclusion, this proof-of-concept study shows that precise control of the spectral broadening process, combined with the generation of ~8 fs pulses and optimized beam focusing, yields a 2.5-fold enhancement in peak intensity relative to the reference configuration. These results support further development of advanced laser systems [4, 5] and pave the way for novel particle acceleration schemes [6].

Acknowledgements: *This work was financed by project FALCON X 004/2025 financed by Ministry of Education and Research, Romania.*

[1] E.A. Khazanov, Quant. Electr. **52**, 208 (2022).
[2] J. A. Wheeler, G. Mourou, and T. Tajima, "Science of High Energy, Single-Cycled Lasers," Rev. Accel. Sci. Technol. **10**, 227(2019).
[3] P.G. Bleotu, J. Wheeler, S Y. Mironov, *et al.*, "Post-compression of high-energy, sub-picosecond laser pulses," High Power Laser Sci. Eng. **11**, e30 (2023).
[4] P.G. Bleotu, J. Wheeler, D. Papadopoulos, G. Mourou, "Spectral broadening for multi-Joule pulse compression in the APOLLON Long Focal Area facility," High Power Laser Sci. Eng. **10**, e9 (2022).
[5] Z. Li, Y. Leng, R. Li, "Further Development of the Short-Pulse Petawatt Laser: Trends, Technologies, and Bottlenecks," Laser Photon. Rev. **17**(1), 2100705.
[6] V. Horný, P.G. Bleotu, D. Ursescu, V. Malka, P. Tomassini, "Efficient laser wakefield accelerator in pump depletion dominated bubble regime," Phys. Rev. E **110**, 035202 (2024).

Study of Giant Electro-Magnetic Pulses in Laser-Thin Foil Interactions at Varying Laser Powers at PW Regime

Darius-Adrian VESTEA[1], Marina CUZMINSCHI[1,2], Razvan STOIAN[3], Alexei ZUBAREV[1]

[1]*National Institute for Laser, Plasma and Radiation Physics, Magurele 077125, Romania*
[2]*Horia Hulubei National Institute for R &D in Physics and Nuclear Engineering 077125 Măgurele, Romania*
[3]*Laboratoire Hubert-Curien, UMR CNRS 5516, Université de Lyon, Université Jean Monnet, St. Etienne, F-42000, France*
Corresponding author: *darius.vestea@inflpr.ro*

The generation of ultra-intense Terahertz radiation by laser-plasma interaction has emerged as a primary route towards achieving Giant Electro-Magnetic Pulses(GEMP) of TV/m level [1]. While the laser parameters are critical, angular distribution of emitted THz radiation in the PW-regime remains of high importance and insufficiently explored [2,3]. In this work, we present a study GEMP of generation from a thin foil target of Aluminum irradiated by a Petawatt-class laser. Our set-up consists of a petawatt laser with a power varying between (100TW-1PW) and a wavelength of 800 nm; a thin foil of thickness 1.5 µm with radius of focal spot of 10 µm (Fig. 1). The study was effectuated using Particle-in-cell (PIC) EPOCH code [4]. The intensity of GEMP was estimated by measuring alternative electro-magnetic field in far field area. The spectral distribution of the GEMP radiation was evaluated using fast Fourier transform. Were especially focused on the THz spectre range and effectuate a more detailed study of secondary THz radiation. We also estimated the energy distribution of the accelerated electrons and electron pulse duration. Our results indicate improvement in collimations of the Giant Electro-Magnetic pulse with increase in laser power.

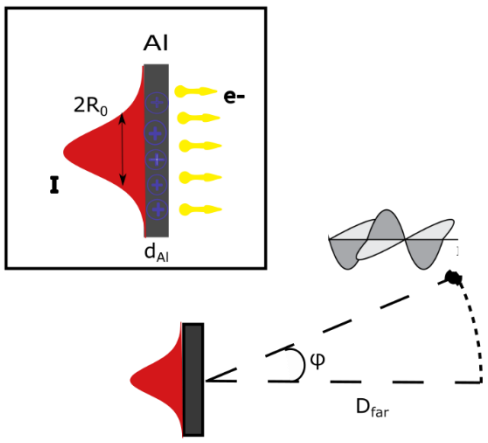

Fig. 1. Scheme of the numerical experiment.

Acknowledgements: D.V. acknowledges the project NUCLEU; A.Z. and M. C acknowledges LAPLAS VII-contract No. 30N/2023 within PNCDI IV, CNCS-UEFISCDIPN-IV-P2-2.1-TE-2023-1102, PN-IV-P7-7.1-PED-2024-079; M.C. acknowledges PN-23-21-01 01/2023. The authors acknowledge the support of National Interest Infrastructure facility IOSIN–CETAL at INFLPR, IOSIN-ISS numerical facility and Olimpia Budriga, Aurelian Marcu and Alexandru Achim for their support in implementing numerical simulations and infrastructure support.

[1] A. Marcu, M. Stafe, A. Groza, M. Serbanescu, R. Ungureanu, G. Cojocaru, C. Diplasu, B. Mihalcea, M. Ganciu, C. Negutu, *et al.*, "Correlation of Laser-Accelerated Electron Energy with Electromagnetic Pulse Emission from Thin Metallic Targets," Appl. Sci. **15**(1), 29 (2025).
[2] H. Y. Lei, *et al.*, "Highly efficient generation of GV/m-level terahertz pulses from intense femtosecond laser-foil interactions," Iscience **25** (5), 104336 (2022).
[3] G. Liao, *et. al.*, "Multimillijoule coherent terahertz bursts from picosecond laser-irradiated metal foils," Proc. Natl. Acad. Sci. U.S.A, **116** (10), 3994-3999 (2019).
[4] T. D. Arber, *et al.*, "Contemporary particle-in-cell approach to laser-plasma modelling," Plasma Phys. Control. Fusion **57**(11), 113001 (2015).

Topic 2. Advances in Optics, Laser and Photonics

Study of Laser Scanners with Rotational Refractive Polygons

Maria-Alexandra DUMA[1], Virgil-Florin DUMA[2]

[1]*Faculty of Science, Utrecht University, Princetonplein 5, 3584 CC Utrecht, The Netherlands*
[2]*3OM Optomechatronics Group, Department of Measurements and Electro-Optics, Faculty of Electronics, Telecommunications, and Information Technology, Polytechnic University of Timisoara, 2 Vasile Parvan Ave., 300223 Timisoara, Romania*

Corresponding author: *virgil.duma@upt.ro*

Laser scanners are employed in a wide range of applications [1,2], from commercial (in printing or barcode scanning) to industrial (in optical metrology or particle instantaneous velocity (PIV) measurements) and high-end (for example in optical coherence tomography (OCT) [3,4]), but also in remote sensing. The most common scanning systems are galvanometer-based [4,5], with rotational polygonal mirrors [3,6,7], and with Risley prisms [8,9]. Each one of them has certain advantages and disadvantages that makes them suitable for a certain application or another, as pointed out in the first part of this presentation. However, all these devices are characterized by a spread of the (reflected or refracted) laser beams over the field-of-view (FOV).

This study approaches a different, much less utilized type of scanning head, with rotational refractive polygons (RPs). Their advantage is that the refracted laser beam always emerges parallel to the incident one, in contrast to all other optomechanical laser scanners. Therefore, an RP-based scanner may not require (sometimes expensive) objective lens (including F-theta ones). To take advantage of this aspect, regular RPs with an even number of facets are considered, including square, hexagonal, and octagonal prisms. The aim of this work has been to perform experimentally multi-parameter analyses of the characteristics of RP-based scanners: scanning function and velocity, limit rotational angles, FOV, and duty cycle. A disadvantage of RPs is dispersion, due to the refractive element of the device, therefore this aspect must be considered, as well. Vignetting of the beam at the beginning and end of the scan of a facet is another issue. The study considers the constructive parameters of regular RPs: number of facets, apothem, refraction index, and eccentricity of the incident beam from the rotational pivot of the polygon. A validation of the theory we have developed is made using this experimental study. Finally, a comparison is made between RPs and the common galvanometer- and polygon mirror-based scanners.

Acknowledgements: *This work is supported by the European Union - NextGenerationEU, through the National Recovery and Resilience Plan (PNRR) of Romania, Component 9, Investment 4, under the Important Project of Common European Interest (IPCEI ME/CT), project ASSET-IxC - UPT (Contract No. 5.PI/I4/C9), implemented by the Polytechnic University of Timisoara in collaboration with Aumovio Technologies Romania (formerly Continental Automotive Romania). The content of this material does not necessarily represent the official position of the European Union or of the Government of Romania.*

[1] G.F. Marshall, G.E. Stutz, Eds., Handbook of Optical and Laser Scanning, CRC Press, (2011), London.
[2] M. Bass, Handbook of optics, third ed., Mc. Graw-Hill Inc., 30.1-30.68 (2009), New York.
[3] W. Y. Oh, S. H. Yun, G. J. Tearney, B. E. Bouma, "115 kHz tuning repetition rate ultrahigh-speed wavelength-swept semiconductor laser," Opt. Lett. **30**(23), 3159-3161 (2005).
[4] V.-F. Duma, "Laser scanners with oscillatory elements: Design and optimization of 1D and 2D scanning functions," Appl. Math. Model. **67**, 456-476 (2019).
[5] J. Montagu, "Scanners - Galvanometric and Resonant," Encyclopedia of Optical Engineering (2003), 2465-2487.
[6] Y. Li, "Single-mirror beam steering system: analysis and synthesis of high-order conic-section scan patterns," Appl. Opt. **47**(3), 386-398 (2008).
[7] V. F. Duma, M. A. Duma, "Optomechanical Analysis and Design of Polygon Mirror-Based Laser Scanners," Appl. Sci. (Basel) **12**(11), 5592 (2022).
[8] A. Li, X. Liu, J. Sun, Z. Lu, "Risley-prism-based multi-beam scanning LiDAR for high-resolution three-dimensional imaging," Opt. Lasers Eng. **150**, 106836 (2022).
[9] V. F. Duma, A. L. Dimb, "Exact Scan Patterns of Rotational Risley Prisms Obtained with a Graphical Method: Multi-Parameter Analysis and Design," Appl. Sci. (Basel) **11**(18), 8451 (2021).

Optical Path Control Using Quadrature Signal Detection

Ana DINCA[1,2], Cecilia OANCA[1,3], Razvan UNGUREANU[1], Gabriel COJOCARU[1,4], Mihai SERBANESCU[1], Alexandru MIHALCEA[1,5], Razvan DABU[1], Sandel SIMION[1]

[1]*National Institute for Laser, Plasma and Radiation Physics, CETAL Department, 077125, Măgurele, Romania*
[2]*Faculty of Electronics, Telecommunications and Information Technology, National University of Science and Technology POLITEHNICA, 061071, Bucharest, Romania*
[3]*Doctoral School of Physics, University of Bucharest, 077125, Măgurele, Romania*
[4]*National Institute for Nuclear Physics and Engineering, Horia Hulubei, Extreme-Light InfrastructureNuclear Physics, Măgurele, Romania*
[5]*Doctoral School of Electronics, Telecommunications and Information Technology, National University of Science and Technology POLITEHNICA Bucharest, 061071, Bucharest, Romania*
Corresponding authors: *ana.dinca@inflpr.ro*, *sandel.simion@inflpr.ro*

Coherent beam combination (CBC) in a parallel configuration is an important method to reach ultra-high intensity in low repetition rate PW-class femtosecond laser pulses, while overcoming constraints such as undesirable nonlinear effects, damage thresholds and restricted dimensions of optical components throughout a chirped pulse amplification [1] laser system.

The low repetition rate, 0.1-10 Hz, of high-power laser systems presents an additional difficulty, as it does not provide a sufficiently broad frequency bandwidth to enable effective optical path difference control for CBC. To overcome this, a continuous wave (CW) laser diode, operating in a feedback loop with a much broader frequency bandwidth, is aligned to propagate along the same optical path as the pulsed laser beams. It enables sub hundred-nm resolution path difference control, required for an efficient CBC of Ti:Sapphire CPA fs-laser pulses.

A purely interferometric detection and control method, based on a 808 nm CW laser diode is employed. It is based on the generation of quadrature electrical signals for phase error detection and correction through real-time monitoring of interference patterns [2]. This type of detector is very robust and capable of resolving nanometer-scale optical path differences, allowing sub femtosecond-level timing jitter control. The electronic control system consists of several analogue processing stages and one digital processing circuit, implemented in a field-programmable gate array (FPGA). A dedicated software has been developed to process the quadrature signals and analyze the phase measurements whose raw form is wrapped, making the apparent evolution of the optical path difference discontinuous, oscillating between ± λ/4, ± 202 nm (Fig. 1a). By applying a dedicated unwrapping routine, the script reconstructs the continuous phase trajectory and exposes the true drift and fluctuations (Fig. 1b). This processing step, which is essential for retrieving the real optical path difference and for accurately assessing interferometric stability, will be detailed in the poster presentation.

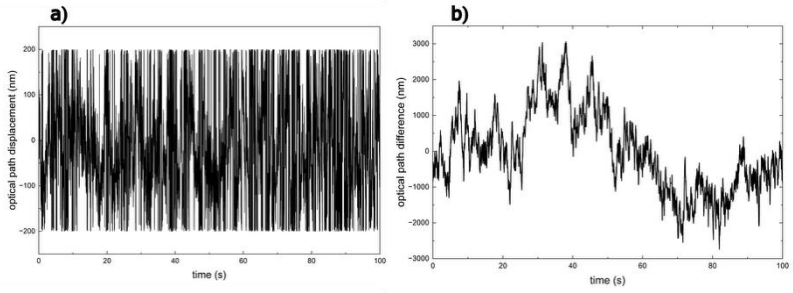

Fig. 1. Variation of optical path in time a) detected before implementing the software and b) after implementing the software

The experimental interferometric setup for the parallel coherent beam combination of two amplified femtosecond pulses of a Ti:Sapphire laser system in the focal plane of a lens, has been implemented and the automatic electronic control loop has been activated. The control system drives a translation stage with a piezoelectric actuator that actively compensates phase differences between the two parallel channels. Preliminary results indicate sub hundred-nm RMS optical path fluctuations and ongoing improvements aim to further increase the accuracy of phase detection and real-time feedback control.

Acknowledgements: For this research, we acknowledge funds from ELI-RO 20/2024 project and National Interest Infrastructure Facility IOSIN – CETAL, at INFLPR.

[1] D. Strickland, G. Mourou, Opt. Commun. **56** (3), 219-221 (1985).
[2] S. Simion, *et al.*, Rom. Rep. Phys. **62**(3), 644-651 (2010).

Error Analysis of a Metrology System for LISA

Diana I. COSAC, Gabriel CHIRITOI, Eugeniu M. POPESCU, Florin A. POPESCU

Institute of Space Science - INFLPR Subsidiary, 405 Atomistilor Street, Magurele 077125, Ilfov, Romania.
Corresponding author: gabriel.chiritoi@spacescience.ro

The metrology stage was developed to test the accuracy of the CAS system in centroiding measurements of stars and laser links on a SWIR CMOS sensor. The system consists of two stepper motor stages for coarse positioning and a fine positioning stage with nanometer-level precision, monitored using a 3-axis Zygo ZMI interferometer system [1].

An error budget analysis was performed for the interferometer system configuration, considering contributions from cosine error [2], laser wavelength stability, electronics, and environmental effects [3], cyclic interferometric errors [4].

The dominant sources of uncertainty arise from the refractive index variations due to pressure and temperature [3], while the remaining error sources contribute significantly less to the total uncertainty.

The interferometric error sources and their modeling are based on established methods in displacement interferometry [2], while cyclic error analysis and compensation follow established approaches in interferometer metrology [4-5].

The total measurement uncertainty is estimated to be approximately 55 nm (1σ), which is about two orders of magnitude less than the CAS system resolution (~5 μm). These results show that the metrology system meets the accuracy requirements, with environmental effects representing the main limitation.

Acknowledgements: This work was supported by ESA PRODEX PEA 4000136381.

[1] ZMI™ Optics Guide, Zygo Corporation Technical Guide OMP-0326AA (2020).
[2] V. Badami and P. de Groot, "Displacement measuring interferometry," Handbook of Optical Dimensional Metrology, CRC Press, Taylor & Francis Group (Boca Raton, London, New York), 157-238 (2013).
[3] B. Edlén, "The refractive index of air," Metrologia **2**(2), 71-80 (1966).
[4] J. Thijsse, A. K. Jamting, N. Brown, and H. Haitjema, "The Detection of Cyclic Nonlinearities in a ZMI2000 Heterodyne Interferometer," Proc. SPIE **5879**, Recent Developments in Traceable Dimensional Measurements III, 58790M (2005).
[5] M. J. Downs, K. P. Birch, "Cyclic error compensation interferometry systems," U.S. Patent 5,696,864 (1997).

Development of a Control System of a Laser Source for ns Emission Spectral Detection of Hydrogen and Deuterium Incorporated in Boron-Deuterium Layers

Mihai SERBANESCU, Andreea GROZA, Sasa Alexandra YEHIA-ALEXE, Oana POMPILIAN

[1]*National Institute for Laser, Plasma and Radiation Physics, CETAL Department, Magurele 077125, Romania*
Corresponding author: *mihai.serbanescu@inflpr.ro*

The study of the incorporation, retention, and release of hydrogen isotopes by optical emission spectroscopy is frequently used in the field of nuclear fusion materials research [1-3]. Laser induced ablation of a layer is produced by focusing a laser pulse on the sample and locally generation of a micro-plasma. The accuracy in the detection of the elements contained in the sample for the elucidation of the plasma dynamics could be improved by synchronizing the acquisition of the plasma optical emission spectra with the laser pulse ignition.

In this context, it was developed a command electronic system for the control of a Q-switched 10 ns laser source operating in standard conditions at 1 kHz repetition rate with 350 µJ pulse energy and 10 $\pm$ 3 ns pulse duration. The new system allows the variation of the laser repetition rate between 10 Hz to 10 kHz, implementation of a burst regime from 1 to 990 pulses and control the laser energy from 3.5 to 350 µJ. Supplementary, the Q-switched laser electronic system can command or can by synchronized with the starting of an Andor spectrometer for acquisition of optical emission spectra in ns to ms range.

The laser control system has been involved in the recording of the emission spectra provided by the plasma produced in the Boron-Deuterium layers. The optical emission spectra recorded after plasma ignition in Boron-Deuterium layers at various temporal intervals starting from 100 ns to 10 ms will be also presented.

Acknowledgements: *This research was financed by program NUCLEU-LAPLAS VII 30N/2023, Ministry of Education and Research, Romania, EUROfusion Consortium, funded by the European Union via the Euratom Research and Training Programme (Grant Agreement No 101052200 - EUROfusion) and the National Interest Infrastructure facility IOSIN – CETAL at INFLPR.*

[1] J. Indrek, *et al.*, "Laser-induced breakdown spectroscopy for helium detection in beryllium coatings," Nucl. Mater. Energy. **39**, 101677 (2024).

[2] S.A. Yehia-Alexe, M. Serbanescu, P. Dinca, B. Butoi, M. E. Zarif, C. Porosnicu, A. Groza, "Deuterium release from beryllium layers by laser induced plasma ablation and laser induced desorption coupled with quadrupole mass spectrometry," Spectroc. Acta Pt. B-Atom. Spectr. **229**, 107197 (2025).

[3] S.A Yehia-Alexe, A. Groza, M. Serbanescu, M. E. Zarif, B. Bita, P. Dinca, B. Butoi, C. Staicu, C. Porosnicu, "Considerations on hydrogen isotopes release from thin films by laser induced ablation and laser induced desorption techniques," Spectroc. Acta Pt. B-Atom. Spectr. **208**, 106774 (2023).

Ultrathin MoS_2 Layers for Applications in Sensing and Photonics

Petronela GHEORGHE, Gianina POPESCU-PELIN, Luiza-Izabela TODERAȘCU, Adrian PETRIS, Cristian ZAGĂR, Iulia ANTOHE, Gabriel SOCOL

National Institute for Laser, Plasma and Radiation Physics, Department of Lasers, Magurele 077125, Romania
Corresponding author: *petronela.gheorghe@inflpr.ro*

Molybdenum disulfide (MoS_2) is a highly promising two-dimensional (2D) nanomaterial widely used in photonics, particularly for the development of new sensors. Its unique electronic, optical, and mechanical properties, including a tunable bandgap, a high surface-to-volume ratio and excellent mechanical flexibility, render it superior to traditional silicon for many specialized sensing applications [1-4]. Consequently, MoS_2 is particularly valuable for producing a new class of detection devices characterized by high sensitivity, rapid response, and low manufacturing costs.

This study investigates MoS_2 thin films grown by pulsed laser deposition (PLD) on substrates with distinct structural and optical characteristics, including alumina with Au electrode, Z-cut quartz, and ultra-flat quartz-coated glass. Using compacted powder targets and adjusting the number of pulses allowed us to generate ultra-thin films with well-controlled features. The resulting samples were examined using UV-Vis spectroscopy, SEM, XRD, ellipsometry, nonlinear optical measurements, and gas-sensor-oriented tests to correlate morphology and structure with optical response and functional potential.

It should be noted that MoS_2 exhibits significant nonlinear optical properties, features that enable the development of advanced photonic devices. We report very recent preliminary results obtained in the investigation of the third-order optical nonlinearity of the MoS2 film using the Z-Scan method at a wavelength of 532 nm.

The obtained results suggest that the investigated MoS_2 material can be used in sensing and nonlinear photonics.

Acknowledgements: This work was financed by project 19PCE/2025, PN-IV-P1-PCE-2023-1902 and program NUCLEU-LAPLAS VII 30N/2023, Ministry of Education and Research, Romania.

[1] D. Mouloua, A. Kotbi, G. Deokar, K. Kaja, M. El Marssi, A. EL Khakani, M. Jouiad, "Recent Progress in the Synthesis of MoS_2 Thin Films for Sensing, Photovoltaic and Plasmonic Applications: A Review," Materials **14**(12), 3283 (2021).
[2] Neetika, A. Kumar, R. Chandra, V.K. Malik, "MoS_2 nanoworm thin films for NO_2 gas sensing application," Thin Solid Films **725**, 138625 (2021).
[3] R. Kumar, W. Zheng, X. Liu, J. Zhang, M. Kumar, "MoS_2-Based Nanomaterials for Room-Temperature Gas Sensors," Adv. Mater. Technol. **5**, 1901062 (2020).
[4] O. Samy, S. Zeng, M. D. Birowosuto, A. El Moutaouakil, "A Review on MoS_2 Properties, Synthesis, Sensing Applications and Challenges," Crystals **11**(4), 355 (2021).

In-Situ and Real Time Measurement of Laser Induced Damage Threshold of Metallic Thin Films Used for ns and fs-Laser Mirrors

C. MILOS[1], D. CRACIUN[1], R. UDREA[2], P. GAROI[2], S. A. IRIMICIUC[1], G. DORCIOMAN[1], G. BLEOTU[3], F. AL-ABEDJ[3], P. PANDELE[3], R. RADOI[3], E. MATACHE[3], S. DAS[3], D. SANDU[3], D. CRACANA[3], T. JITSUNO[3], A. TANASEANU[3], D. URSESCU[3], V. CRACIUN[1,3]

[1]*National Institute for Laser, Plasma and Radiation Physics, Magurele, Romania*
[2]*Apel Laser, Mogosoaia, Romania*
[3]*Extreme Light Infrastructure for Nuclear Physics, IFIN-HH, Magurele*
Corresponding author: *valentin.craciun@inflpr.ro*

It has been known from the early days of high-power laser-matter interaction studies that optical mirrors could be damaged when the laser fluence is above a certain value, usually known as the Laser induced damage threshold (LIDT). The first measurements of the LIDT values were based on optical observation of the surface damage induced during laser irradiation. One of the first observation was that the LIDT values decrease with the increased number of pulses on the same location, asymptotically reaching a value that was defined as the endurance limit. For the fluence corresponding to the endurance limit there will be no damage regardless of the number of pulses in the same location. The optical methods for the evaluation of this endurance limit are very time consuming, requiring extremely high number of laser pulses of the order of 10^{10}. Secondly, since the LIDT values have a statistic behaviour, there is no prior information that a particular mirror will exhibit a lower or a higher value, usually depending on its manufacturing.

We recently developed new ways to estimate the LIDT value of an optical coating based on electrical measurements. Langmuir probes (LP) have been long used to characterize the laser plasma for deposition processes such as Pulsed Laser Deposition (PLD) technique. An LP collects the charges emitted by the surface as an effect of laser irradiation. By recording the amount of charge emitted by a surface versus the laser fluence used for irradiation a plot having two regions was obtained. For low laser fluences, the amount of emitted charge increases very slowly up to a certain particular value. Once that value has been reached, for any other higher values the amount of the emitted charge greatly increases. Comparison with optical methods for LIDT determination showed that this fluence is very similar to the endurance limit one.

Once electrical charges are emitted from the surface as an effect of laser irradiation, that surface becomes charged. A compensating charge, equal to the amount of the emitted charge will be drawn from the environment to reach neutrality. If one measures the compensating charge then this will be equal to the emitted one. Now, if one plots instead of the emitted charge the compensated charge versus the laser fluence, the plot will look identical to that for the emitted charge described above and the inflection point between the two different regions will define the value of the LIDT fluence. The measurement of the compensating charge has several advantages versus the LP measurement. First, this measurement integrates all the charges that were emitted by the whole irradiated surface, whereas the LP measurement was limited to the charge emitted in a small solid angle that was defined by the area of the probe and the distance from the laser irradiated area. Secondly, the LP measurements should be performed in a high vacuum atmosphere, whereas the compensating charge measurement could be performed in much higher pressures. Examples of the LIDT measurements on thin Al and Ag thin films will be presented to illustrates the advantage of these electrical based methods in comparison with the optical based ones.

Acknowledgements: This research received funding from ELI-RO 15 (DELISM), ELI-RO 19 (HighProtonPLas), PTE_41/2025, Nucleu contract PN 23 21 01 05, phase 5, and Nucleu-LAPLAS VII 30N/2023 funded by the Ministry of Education and Research, Romania.

Investigation of Cleaning of Laser Carbonized Mirrors by Wet Washing Procedures

Veronica SATULU[1], Cristian STANCU[1], Catalin CONSTANTIN[1], Gabriel BLEOTU[2], Fattima Al-ABEDJ[2], Emilia MATACHE[2], Susobhan DAS[2], Takahisa JITSUNO[2], Daniel URSESCU[2], Valentin CRACIUN[1], Gheorghe DINESCU[1]

[1]*National Institute for Laser, Plasma and Radiation Physics, Laboratory of Low Temperature Plasma, Magurele 077125, Romania;*
[2]*Extreme Light Infrastructure - Nuclear Physics (ELI-NP), Horia Hulubei National Institute for Physics and Nuclear Engineering (IFIN-HH), Magurele 077125, Romania*
Corresponding author*:* *gheorghe.dinescu@inflpr.ro*

Carbonization of the optical mirrors in high-power laser systems is a critical problem that affects the long-term performance and stability of advanced photonic facilities. Carbonization occurs via deposition of residual hydrocarbon traces naturally present in the vacuum environment, followed by laser-induced modification of the carbon contaminated surface through photon exposure, ultimately resulting in costly mirror replacements [1, 2, 3].

In this study, we explore the effectiveness of wet washing procedures for removing these carbonized layers from laser-exposed mirror surfaces. Mirrors that had been exposed to laser-induced carbonization were cut into smaller samples that were subjected to various washing protocols. These included both short-term and long-term treatments using ethanol-based cleaning solutions along with ultrasonication. For the short-term washing procedure, samples were ultrasonicated for 15 minutes in a mild detergent solution, rinsed with distilled water, then ultrasonicated for 15 minutes each in acetone and ethanol. The process concluded with a final rinse in distilled water. For the long-term washing procedure, samples were ultrasonicated for 15 minutes in the same mild detergent solution, rinsed with distilled water, then ultrasonicated for 6 hours each in acetone and ethanol. A final rinse in distilled water completed the process. To assess the changes in surface chemistry before and after the washing, we utilized X-ray Photoelectron Spectroscopy (XPS), analyzing carbon distribution both on the surface and in-depth. We performed comparative analyses on non-washed samples affected by carbonization, carbonized samples subjected to short washing treatments, and carbonized samples that underwent longer washing treatments.

The findings revealed that untreated mirror samples were strong contaminated with carbon on both laser-exposed and non-exposed surfaces. While short washing procedures were effective in reducing superficial carbon content, they had limited success in addressing deeper carbonized layers. Conversely, the long washing treatments led to a further reduction in in-depth carbon content, although they did not achieve complete removal of the carbonization layer.

Overall, these results highlight that wet washing procedures can partially restore contaminated optical surfaces and offer valuable insights for maintaining and recovering large optical components used in high-power laser systems.

Acknowledgments: *This work was financed by project IFA-ELI 015 and program NUCLEU-LAPLAS VII 30N/2023, Ministry of Education and Research, Romania*

[1] P. Yadav, R. Gupta, A. Choubey, S. Ali, U. Goutam, M. Modi, "Carbon removal from a mirror-like gold surface by UV light, RF plasma, and IR laser exposure: a comparative study," Appl. Opt. **60**(1), 89-97 (2021).

[2] Z. Hubka, J. Novák, I. Majerová, J. T. Green, P. K. Velpula, R. Boge, R. Antipenkov, V. Šobr, D. Kramer, K. Majer, J. A. Naylon, P. Bakule, B. Rus, "Mitigation of laser-induced contamination in vacuum in high-repetition-rate high-peak-power laser systems," Appl. Opt. **60**(3), 533-538 (2021).

[3] M. Stehlik, J. Zideluns, C. Petite, V. Allard, M. Minissale, A. Moreau, A. Lereu, F. Lemarchand, F. Wagner, J. Lumeau, L. Gallais, "Investigation of laser-induced contamination on dielectric thin films in MHz sub-ps regime," Adv. Opt. Technol. **12**, 1261267 (2024).

Exploring Direct Diode Pumping Advantages - The Case of Nd:LGSB Laser Crystal

Catalina-Alice SUSALA, Lucian GHEORGHE, Nicolaie PAVEL

National Institute for Laser, Plasma and Radiation Physics, Laboratory of Solid-State Quantum Electronics, Magurele, 077125, Ilfov, Romania
Corresponding author: catalina.susala@inflpr.ro

The LGSB crystal was developed and reported in 2016 as a promising second order nonlinear crystal similar to YAB, envisaging efficient frequency doubling conversion and emission in green spectral region [1]. In 2019, the first 1.06 μm laser emission results were reported for the LGSB crystal doped with Nd^{3+}ions, with laser operation under continuous wave, quasi-CW, Q-switch or mode-locking regimes [2]. By now, highly efficient infrared lasing was demonstrated for Nd:LGSB crystal under indirect diode end pumping at conventional 807 nm wavelength [2-5]. In this work, the advantages of using direct or in-band CW or quasi-CW 880 nm pumping, are evaluated, for the Nd:LGSB crystal. The results achieved for the Nd:LGSB laser with similar resonator configuration and pumping geometry, however for different pumping wavelengths (for direct 880 nm- vs indirect 807 nm- pumping) are compared (Fig. 1). The enhancements in both optical-to-optical and slope efficiencies by using direct pumping, instead of indirect pumping, raised the interest for developing efficient green self-frequency doubling Nd:LGSB lasers operating under direct pumping condition [6].

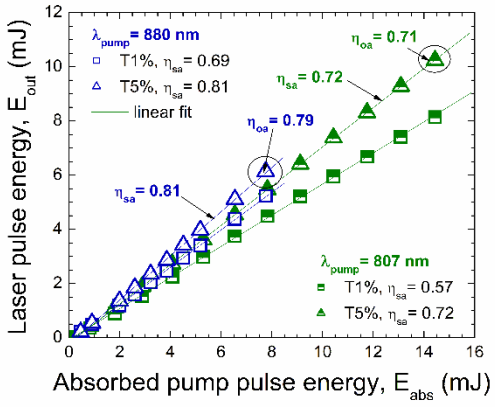

Fig. 1. Laser pulse energy vs absorbed pump pulse energy of Nd:LGSB laser under quasi-CW pumping at 880 nm vs 807 nm.

Figure 1 presents a comparison of the laser pulse energy delivered by the Nd:LGSB laser under direct vs indirect pumping for various output coupling conditions. At low OCM transmission of T= 1%, the direct pumping leads to 12% increase of the laser slope efficiency, while for optimum coupling condition (OCM with T= 5%) an increase of 9% of the laser slope efficiency is obtained with 880 nm pumping.

Acknowledgements: This work was financed by program NUCLEU-LAPLAS VII 30N/2023, Ministry of Education and Research, Romania.

[1] L. Gheorghe, F. Khaled, A. Achim, F. Voicu, P. Loiseau, and G. Aka, "Czochralski Growth and Characterization of Incongruent Melting $La_xGd_ySc_z(BO_3)_4$ (x + y + z = 4) Nonlinear Optical Crystal," Cryst. Growth Des. **16**(6), 3473-3479 (2016).
[2] C. A. Brandus, S. Hau, A. Broasca, M. Greculeasa, F. M. Voicu, C. Gheorghe, L. Gheorghe, T. Dascalu," Efficient 1 μm laser emission of Czochralski-grown Nd: LGSB single crystal," Materials **12**(12), 2005 (2019).
[3] M. Greculeasa, A. Broasca, F. Voicu, S. Hau, G. Croitoru, G. Stanciu, C. Gheorghe, N. Pavel, L. Gheorghe, "Bifunctional $La_xNd_yGd_zSc_{4-x-y-z}(BO_3)_4$ crystal: Czochralski growth, linear and nonlinear optical properties, and near-infrared laser emission performances," Opt. Laser Technol. **131**, 106433 (2020).
[4] C. A. Brandus, M. Greculeasa, A. Broasca, F. Voicu, L. Gheorghe, N. Pavel, "Diode- pumped bifunctional Nd:LGSB laser passively Q-switched by a Cr^{4+}:YAG saturable absorber," Opt. Mater. Express **11**(3), 685-694 (2021).
[5] A. Broasca, M. Greculeasa, F. Voicu, G. Stanciu, S. Hau, C. Gheorghe, C.A. Brandus, N. Pavel, M. Enculescu, L. Gheorghe, "Growth and characterization of 3.5 at.% Nd: LGSB bifunctional crystal," Opt. Mater. **123**, 111832 (2022).
[6] C. A. Susala, "Highly efficient Nd:LGSB laser under direct pumping," Measurement **276**, 121428 (2026).

Self Q-switched Mode-Locked Laser Operation of Nd:LGSB Crystal under Direct Pumping

Catalina-Alice SUSALA, Lucian GHEORGHE, Nicolaie PAVEL

National Institute for Laser, Plasma and Radiation Physics, Laboratory of Solid-State Quantum Electronics, Magurele, 077125, Ilfov, Romania
Corresponding author: catalina.susala@inflpr.ro

Mode-locking with a SESAM (Semiconductor Saturable Absorber Mirror) of Nd:LGSB laser, operating at 1.06 μm under the pump at 0.8 μm into the $^4F_{5/2}$ level, was previously reported [1]. In this paper, the subject of self mode-locking for a directly into the $^4F_{3/2}$ level pumped Nd:LGSB laser is addressed, for the first time to our knowledge. Q-switch-mode-locking operation is demonstrated for the Nd:LGSB crystal positioned in a specially designed long Z type cavity, without the insertion of additional intracavity loss modulators (Fig. 1). The laser tendency for continuous mode-locking operation and its stabilization is studied for several output coupling mirror (OC) conditions.

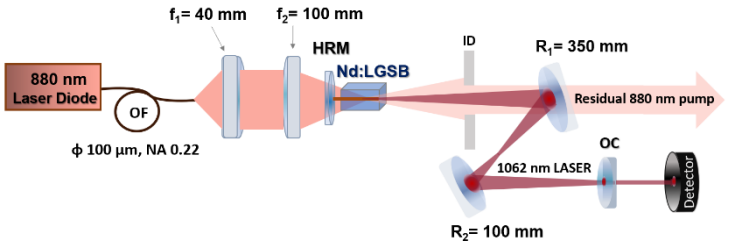

Fig. 1. The Nd:LGSB self-mode locked laser set-up. HRM: highly reflective mirror, ID: diaphragm, OC: output coupler.

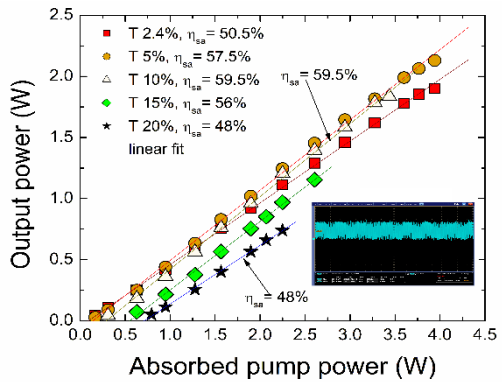

Fig. 2. The average power of the directly pumped Nd:LGSB laser vs absorbed pump power, for several OC conditions. Inset shows the oscilloscope frame containing the self-mode-locked train of pulses, at 20% transmission (T) of the OC and 2.25 W absorbed pump power level.

As shown in Fig. 2 the lasing threshold of Nd:LGSB laser starts below 100 mW for OC of low transmission, T= 2.4% and increases up to ~0.75 W for high T= 20%. A decrease from 2.13 W output power (at 3.94 W absorbed pump power, achieved for OC of T= 5%) down to 0.74 W output power (for 2.25 W absorbed pump power and OC of T= 20%) was observed. The increase of the lasing threshold could favour oscillation at fundamental mode instead at higher order modes, which is mandatory for mode-locking, however with the disadvantage of lowering the average power. Prospects for further average power up-scaling and clean mode-locking operation by solely exploiting the self-nonlinearities of Nd:LGSB laser are discussed.

Acknowledgements: This work was financed by program NUCLEU-LAPLAS VII 30N/2023, Ministry of Education and Research, Romania.

[1] C.A. Brandus, S. Hau, A. Broasca, M. Greculeasa, F.M. Voicu, C. Gheorghe, L. Gheorghe, T. Dascalu," Efficient 1 μm laser emission of Czochralski-grown Nd: LGSB single crystal," Materials **12**(12), 2005 (2019).

Fabrication and Laser Performance of Multilayered Yb^{3+}:Y_2O_3 Transparent Ceramics

George STANCIU[1], Flavius VOICU[1], Gabriela CROITORU[1], Alexandru CRACIUN[1], Cristina TIHON[1], Marius DUMITRU[2], Nicolaie PAVEL[1]

[1]*National Institute for Laser, Plasma and Radiation Physics, Laboratory of Solid-State Quantum Electronics, Magurele 077125, Ilfov, Romania*
[2]*National Institute for Laser, Plasma and Radiation Physics, Photonic Processing of Advanced Materials Group, Magurele 077125, Ilfov, Romania*

Corresponding author: *flavius.voicu@inflpr.ro*

Transparent ceramics have emerged as promising laser media, offering optical properties comparable to those of their single-crystal counterparts, with the added benefits of lower cost, faster production, and easier fabrication of large-scale multilayer structures. Furthermore, ceramic materials are superior to single crystals for creating composite structures because they allow for more flexible obtaining methods. This technology enables complex configurations, like multilayer structures, which improve thermal management and reduce heat gradients during laser operation [1-3]. In this work, two-layer x-at.% Y_2O_3/y-at.% Yb:Y_2O_3 (x=0, 3, 5; y= 3, 5, 8) transparent composite ceramics, as well as three-layer ceramics with a graded doping profile of Yb^{3+} ions, were obtained by solid-state reaction and multi-step sintering method. The phase structure, microstructure, optical properties, and laser performance of the resulting ceramic samples were investigated.

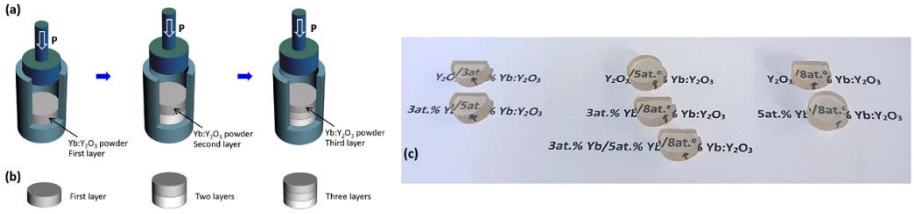

Fig. 1 (a) Schematic illustration of the sequential uniaxial dry pressing process of Yb: Y_2O_3 composite ceramic green bodies. **(b)** Representation of Yb: Y_2O_3 composite ceramic samples. **(c)** Photo of multilayer Yb: Y_2O_3 transparent composite ceramics.

Sequential uniaxial dry pressing method at the pressure P= 5 MPa [Fig. 1(a)] was used to produce two- and three-layer ceramic green bodies [Fig. 1(b)], followed by cold isostatic pressing at 410 MPa for 5 min. The photographs of the sintered Yb: Y_2O_3 composite ceramics are shown in Fig. 1(c). Phase identification by XRD showed that all sintered composite ceramics have the same cubic structure of Y_2O_3 without any impurities. The microstructure investigated by SEM shows good homogeneity for all composite ceramic samples, with an average grain size of about 20 µm. The EDS line scan analyses were performed to analyze the diffusion of Yb ions around the contact interfaces of the ceramic samples. Using fiber-coupled diode laser pumping at 971 nm operated in quasi-continuous mode, laser emission at 1.03 µm was obtained from all investigated ceramic samples. For example, the 3-at.% Yb:Y_2O_3/5-at.% Yb:Y_2O_3 ceramic sample efficiently emitted laser pulses with an energy E_p= 1.85 mJ for 11.6 mJ absorbed energy of the pumping pulse; the slope efficiency was 0.28. Obtaining composite laser media with well-defined doping of active ions, chosen such to ensure a specific profile of the absorbed pump radiation, is the objective of our future studies.

Acknowledgements: *This work was financed by project 30/2022, PN-III-P4-PCE-2021-0519, CCCDI - UEFISCDI, project number PN-IV-P6-6.1-CoEx-2024-0154, within PNCDI IV, and program NUCLEU-LAPLAS VII 30N/2023, Ministry of Education and Research, Romania.*

[1] A. Ikesue and Y. L. Aung, "Synthesis and performance of a, and dvanced ceramic lasers," JACS **89**(6), 1936-1944 (2006).
[2] L. Zheng, A. Kausas, T. Taira, ">30 MW peak power from distributed face cooling tiny integrated laser," Opt. Express **27**(21), 30217-30224 (2019).
[3] G. Stanciu, G. Croitoru, A. Craciun, F. Voicu, C. Tihon, M. Dumitru, M. Enculescu, N. Pavel, "Multilayered Yb^{3+}:Y_2O_3 transparent composite ceramics fabricated by direct dry pressing - Characterization and laser emission results," Ceram. Int. **51** (22) Part B, 37304-37311 (2025).

Photoluminescence Investigation and Up-Conversion Behavior under Different Excitation Wavelengths of (Er, Tm, Yb)-Doped CdF_2 Single Crystal

Cristina GHEORGHE[1], Hani BOUBEKRI[2,3], Stefania HAU[1],
Ana Maria VOICULESCU[1], Octavian TOMA[1], Madjid DIAF[3], Reda FARTAS[4]

[1]*National Institute for Lasers, Plasma and Radiation Physics, Laboratory of Solid-State Quantum Electronics, Magurele 077125, Ilfov, Romania*
[2]*Higher Normal School of Technological Education (ENSET), 21000, Azzaba, Skikda, Algeria*
[3]*Laser Physics, Optical Spectroscopy and Optoelectronics Laboratory, Badji Mokhtar Annaba University, POB 12, Annaba, Algeria*
[4]*08 May 1945 University, Guelma, Algeria*
Corresponding authors: *cristina.gheorghe@inflpr.ro*

A high-quality CdF_2 single crystal triply doped with Er^{3+} (4 mol%), Tm^{3+} (0.5 mol%), and Yb^{3+} (6 mol%) was successfully grown by the Bridgman technique (Fig. 1) and systematically investigated under 802, 973, and 1550 nm excitations. Judd–Ofelt analysis of Er^{3+} absorption spectra yielded intensity parameters ($\Omega_2 = 1.61\times 10^{-20}$ cm^2, $\Omega_4 = 0.74\times 10^{-20}$ cm^2, $\Omega_6 = 1.07 \times 10^{-20}$ cm^2) consistent with the highly symmetric fluorite structure and confirming the host's suitability for efficient luminescence. The intrinsically low phonon energy of CdF_2 (~384 cm^{-1}) effectively reduces multiphonon relaxation, favoring radiative transitions and enabling efficient upconversion (UC) (Fig. 2).

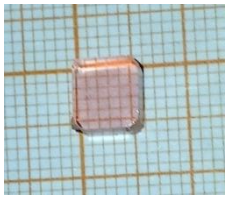

Fig. 1. Photo of the CdF_2: (Er, Tm, Yb) crystal sample

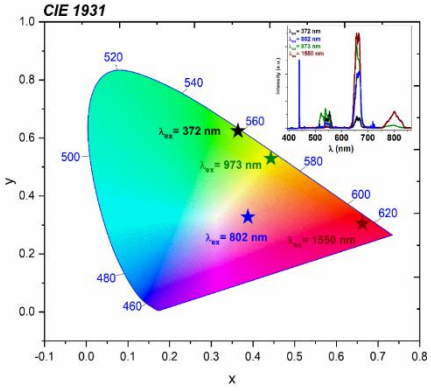

Fig. 2. Tuning of emission color of (Er, Tm, Yb) system in CdF_2 crystal as a function of excitation wavelength, together with the corresponding emission spectra as an inset image

Under 802 nm excitation, resonant pumping of Tm^{3+} ($^3H_4$) produces weak UC emission, while Er^{3+} green ($^2H_{11/2}$, $^4S_{3/2}$) and red ($^4F_{9/2}$) emissions exhibit prolonged decay times compared to 973 nm excitation, reflecting the reduced influence of Yb^{3+}-sensitized energy transfer. Excitation at 973 nm activates efficient $Yb^{3+} \rightarrow Er^{3+}/Tm^{3+}$ energy transfer, generating intense UC dominated by Er^{3+} red emission ($^4F_{9/2} \rightarrow {}^4I_{15/2}$) with fast rise times (2.5–7 μs), confirming rapid sensitization. Under 1550 nm excitation, resonant pumping of Er^{3+} ($^4I_{15/2} \rightarrow {}^4I_{13/2}$) produces deep-red emission via efficient Er–Er excited-state absorption and cooperative cross-relaxation. Power-dependent studies reveal photon orders consistent with two- and three-photon UC processes. CIE chromaticity analysis demonstrates pronounced wavelength- and power-dependent color tunability, spanning purplish-pink, yellowish-orange, yellowish-green, and deep red, with trajectories encircling the white point. These results highlight the exceptional excitation-tunable behavior of the CdF_2: Er, Tm, Yb system, positioning it as a highly promising candidate for infrared photonics, white-light generation, optical thermometry, displays, and anti-counterfeiting applications.

Acknowledgements: *This work was financed by CCCDI - UEFISCDI, project number PN-IV-P6-6.1-CoEx2024-0154, within PNCDI IV and Program LAPLAS VII - contract no. 30N/2023, Ministry of Education and Research, Romania.*

A Multimodal Temperature Sensing Based on Up-Conversion Luminescence of (Er, Y)-Co-Doped Fluorite Crystals

Stefania HAU[1], Hani BOUBEKRI[2,3], Madjid DIAF[3], Reda FARTAS[3,4], Cristina GHEORGHE[1]

[1]*National Institute for Lasers, Plasma and Radiation Physics, Laboratory of Solid-State Quantum Electronics, Magurele, 077125, Ilfov, Romania*
[2]*Higher Normal School of Technological Education (ENSET), 21000, Azzaba, Skikda, Algeria*
[3]*Laser Physics, Optical Spectroscopy and Optoelectronics Laboratory, Badji Mokhtar Annaba University, POB 12, Annaba, Algeria*
[4]*08 May 1945 University, Guelma, Algeria*
Corresponding author: *stefania.hau@inflpr.ro*

Single crystals of CdF_2 doped with 1% Er^{3+} ions and co-doped with 10% and 20% Y^{3+} ions, denoted as CdF_2: 1% Er, x% Y (x = 10, 20), with a partially disordered structure, were grown using the Bridgman technique in a vacuum furnace under a fluorine atmosphere [1]. Up-conversion emissions in both visible and infrared regions of Er^{3+} ions, excited at 973 nm and 1550 nm (Fig.1ac) were measured across a temperature range of 175–575 K. Multimodal optical temperature sensing studies based on the luminescence intensity ratio (LIR) employed thermally coupled levels (TCLs) ($^2H_{11/2}/^4S_{3/2}$) and $^4I_{13/2}$ ($Peak_1/Peak_2$), as well as non-thermally coupled levels (NTCLs) ($^2H_{11/2}/^4F_{9/2}$). The highest relative thermal sensitivity (Sr) values were observed from the ($^2H_{11/2}/^4S_{3/2}$) levels at 175 K, with Sr = 3.54% K^{-1} (Fig.1b) for the 1% Er, 10% Y crystal (λ_{ex} = 1550 nm) and Sr = 5.5% K^{-1} (Fig.1d) for the 1% Er, 20% Y crystal (λ_{ex} = 973 nm). From NTCLs ($^2H_{11/2}/^4F_{9/2}$), the maximum Sr was 2.7% K^{-1} at 150 K in the 1% Er, 20% Y crystal (λ_{ex} = 1550 nm). Thus, the degree of disorder in CdF_2: 1% Er, x% Y (x = 10, 20) single crystals, caused by Y^{3+} ion content, significantly impacts their temperature-sensing optical properties. Depending on the excitation wavelength, the exceptional sensing capabilities of multimodal optical temperature sensing based on CdF_2: Er, Y crystals underscore their strong potential for low-temperature sensing applications.

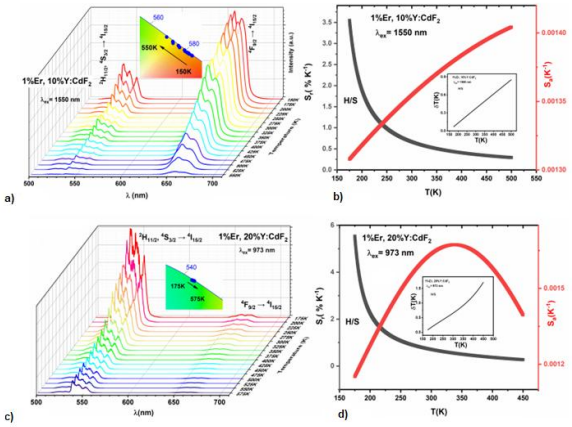

Fig. 1 Temperature dependence emission spectra of 1Er, 10Y under 1550 nm excitation (a) and 1Er, 20Y under 973 nm excitation (c) samples and their CIE chromaticity diagram as insets. The S_r and S_a curves, together with temperature uncertainty δT as insets (b, d).

Acknowledgements: *This work was financed by CCCDI - UEFISCDI, project number PN-IV-P6-6.1-CoEx2024-0154, within PNCDI IV project and program NUCLEU-LAPLAS VII 30N/2023, Ministry of Education and Research, Romania.*

[1] H. Boubekri, R. Fartas, M. Diaf, G. Cittadino, M. Tonelli, A. Bitam, O. Toma, "Luminescence properties of CdF_2 single crystals co-doped with Er^{3+} and Y^{3+} ions," Luminescence **39**(4), 4719 (2024).

Upconversion Properties and Optical Temperature-Sensing Performance in the Visible and Near-Infrared Region Based on Luminescence Intensity Ratio in a New Er^{3+}:$SrLaGaO_4$ Phosphor

Ana-Maria VOICULESCU, Stefania HAU, George STANCIU, Cristina GHEORGHE

National Institute for Laser, Plasma and Radiation Physics, Laboratory of Solid-State Quantum Electronics, Magurele, 077125, Romania
Corresponding author: *ana.voiculescu@inflpr.ro*

Novel green-emitting x at.% Er: $SrLaGaO_4$ (SLO) ceramic phosphors (x=1, 2, 3, 4, 5 at.%) have been successfully synthesized by the conventional solid-state reaction method using high-purity (≥99.99%) commercially available micropowders of $SrCO_3$, La_2O_3, Er_2O_3, and Ga_2O_3. The upconversion (UC) emission spectra of Er^{3+} ions were recorded under two excitation wavelengths (973 and 1550 nm). Two important parameters, correlated color temperature (CCT) and color purity (CRI), were calculated from the luminescence spectra, resulting in the highest values of CCT (between 5000 and 6000 K) and CRI (ranging from 90 to 97.4). The temperature dependence (in the range 75–623 K) of Er^{3+} emission in the visible and infrared domains was investigated using the luminescence thermometry (LIR) method for the thermally coupled levels $^2H_{11/2}$ and $^4S_{3/2}$ (TCLs) of Er^{3+} and non-thermally coupled levels $^2H_{11/2}$ and $^4F_{9/2}$ (NTCLs) of Er^{3+} ions under both excitation wavelengths. With increasing temperature, the energy gap between the barycenter of $^2H_{11/2}$ and $^4S_{3/2}$ levels decreases from $\Delta E = 661$ cm^{-1} for x=1 to $\Delta E = 555 cm^{-1}$ for x=5, suggesting that between the thermal coupling becomes stronger with the increase of Er concentration (Fig. 1a). The calculated LIR ($^2H_{11/2}$ /$^4S_{3/2}$) of all Er concentrations function of temperature is shown in Fig. 1b. The values of LIR, Sr, and δT decrease gradually both with temperature and with the concentration of Er ions.

The highest Sr values were achieved for the 1 % Er: SLO sample, with Sr = 1.38 % K^{-1} at 300 K from TCLs ($^2H_{11/2}$/$^4S_{3/2}$) under λ_{ex} = 973 nm (Fig.1 c). Under the 1550 nm excitation wavelength, the peak value of S_r = 1.09 % K^{-1} at 300 K was observed from TCLs for the 1 % Er: SLO sample, along with S_r = 0.98 % K^{-1} at 575 K from NTCLs for the 3Er: SLO sample. In the infrared domain, the maximum Sr value for 1 % Er: SLO was recorded at S_r = 0.88 % K^{-1} at 75 K.

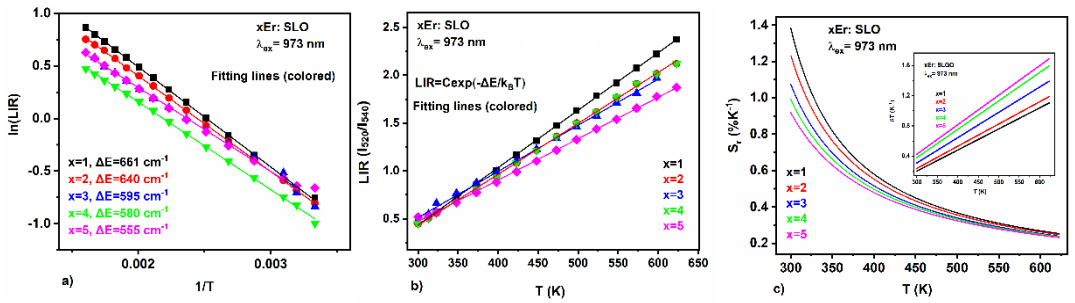

Fig. 1. The energy gap between the barycenter of $^2H_{11/2}$ and $^4S_{3/2}$ levels (a). Luminescence intensity ratio of TCLs ($^2H_{11/2}$/$^4S_{3/2}$) function of temperature with inset 14 cycling test between 300 K and 600 K (b) Plots of calculated values of Sr and δT (inset) as a function of temperature (c).

The results indicate that Er: $SrLaGaO_4$ phosphors possess the potential to function as optical temperature sensors and can be utilized in white light-emitting diode devices.

Acknowledgements: This work was financed by the program NUCLEU-LAPLAS VII 30N/2023, Ministry of Education and Research, Romania.

Excited-State Absorption in Low-Concentrated Er:$SrLaGaO_4$ Ceramic Phosphors

Ana-Maria VOICULESCU, Octavian TOMA, George STANCIU

National Institute for Laser, Plasma and Radiation Physics, Laboratory of Solid-State Quantum Electronics, Magurele, 077125, Romania
Corresponding author: *ana.voiculescu@inflpr.ro*

The $SrLaGaO_4$ (SLO) is one of the members of the olivine $ABCO_4$ family with a stable tetragonal structure, low phonon energy, and a bandgap of about 3.81 eV, which can provide a low symmetry coordination environment for RE ions, facilitating the enhancement of their characteristic luminescence [1]. The $ABCO_4$ family crystallizes in the K_2NiF_4 tetragonal structure with a space group of I_4/mmm. Having a complex and disordered lattice field, formed by the random distribution of Sr^{3+} and La^{3+} ions, which causes a large inhomogeneous broadening of the absorption and emission spectra, we might expect that the $SrLaGaO_4$ crystal may also be a potential laser material. However, research on rare-earth-doped SLO laser crystals is still limited [2,3]. The spectroscopic data on Er^{3+} doped SLO have not, to our knowledge, been presented in detail. In this work, we present the excited-state absorption (ESA) in visible (500 – 800 nm) from the $^4I_{13/2}$ level in the upconversion phosphor Er:SLO with low concentration (1% at. Er). The ceramic phosphors have been successfully synthesized by the conventional solid-state reaction method using high-purity (≥99.99%) commercially available micropowders of $SrCO_3$, La_2O_3, Er_2O_3, and Ga_2O_3 [4]. At this low concentration, excited state absorption is the dominant upconversion process. Two pump-probe experiments were performed: one of them used a laser at 973 nm to populate the two lowest excited levels ($^4I_{13/2}$ and $^4I_{11/2}$) of Er^{3+}; the other used a laser at 1550 nm to populate only $^4I_{13/2}$. The transitions corresponding to various spectral lines are identified and discussed. The luminescence lifetimes of Er excited levels are also measured and discussed. The data will be used to estimate the upconversion luminescence efficiency of erbium-doped materials as potential laser media.

Acknowledgements: This work was financed by the program NUCLEU-LAPLAS VII 30N/2023, Ministry of Education and Research, Romania.

[1] A. Dabkowski, H. A. Dabkowski, J. E. Greedan, "$SrLaGaO_4$-Czochralski crystal growth and basic properties," J. Cryst. Growth **132**(1-2), 205-208 (1993).
[2] M. Kaczkan, M. Malinowski, "Optical Transitions and Excited State Absorption Cross Sections of $SrLaGaO_4$ Doped with Ho^{3+} Ions," Materials **14**(14), 3831 (2021).
[3] S. Fang, L. Liang, W. Wang, Y. Lin, Y. Sun, G. Gong, C. Tu, H. Wen, "Growth, Structure, and Spectroscopic Properties of a Disordered Nd:$SrLaGaO_4$ Laser Crystal," Crystals **14**(2), 174 (2024).
[4] A. M. Voiculescu, S. Hau, G. Stanciu, C. Gheorghe, "A dual-mode temperature sensing based on UC luminescence of a new green Er^{3+}:$SrLaGaO_4$ phosphor," J. Alloys Compd. **1038**, 182727 (2025).

Dynamics of Excited States $^4I_{13/2}$ and $^4I_{11/2}$ of Er^{3+} in Ca:CdF_2

Octavian TOMA[1], Ana-Maria VOICULESCU[1], Hani BOUBEKRI[2], Madjid DIAF[3]

[1]*National Institute for Laser, Plasma and Radiation Physics, Laboratory of Solid-State Quantum Electronics, Magurele, 077125, Romania*
[2]*Higher Normal School of Technological Education (ENSET), 21000, Azzaba, Skikda, Algeria*
[3]*Laser Physics, Optical Spectroscopy and Optoelectronics Laboratory, Badji Mokhtar Annaba University, POB 12, Annaba, Algeria.*
Corresponding author: *octavian.toma@inflpr.ro*

A high-quality CdF_2 single crystal mixed with CaF_2 (30 mol.%) and doped with Er^{3+} (1%) was grown by the Bridgman technique. This material is very interesting for applications such as upconversion emission due to the intrinsically low phonon energy of CdF_2 (384 cm^{-1}), which effectively suppresses multiphonon relaxation, favoring radiative transitions and efficient upconversion. The lifetimes of the longest-lived excited levels ($^4I_{13/2}$ and $^4I_{11/2}$) of Er^{3+} are investigated in this material. These levels represent population reservoirs that feed the upconversion-emitting levels by excited-state absorption processes.

For the measurement of the lifetime of $^4I_{11/2}$, luminescence decay curves were recorded at 980 nm (transition $^4I_{11/2} \rightarrow {}^4I_{15/2}$) after pulsed laser excitation at 522 nm (transition $^4I_{15/2} \rightarrow {}^2H_{11/2}$).

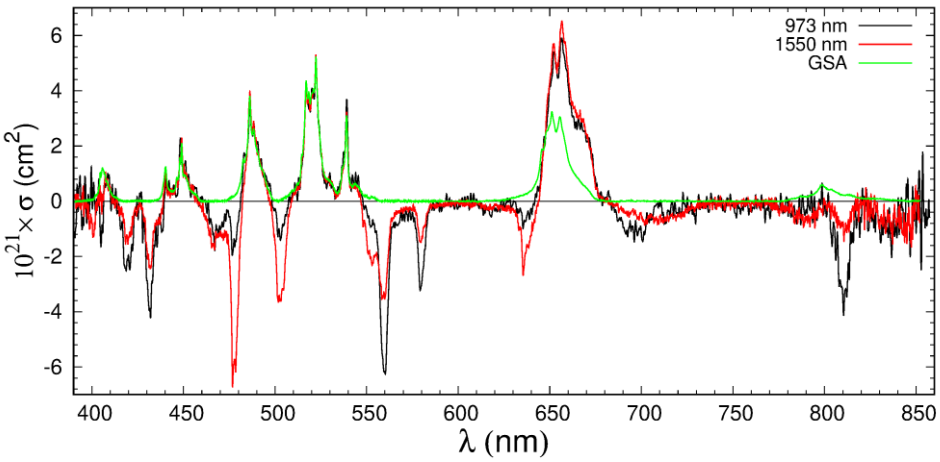

Fig. 1. Excited-state and ground-state absorption (GSA) spectra of Er:CaF_2:CdF_2. The pump wavelengths are indicated by plot legend.

Excited-state absorption spectra were then used for the estimation of the populations of the first two excited states of Er^{3+}. For pumping at 973 nm, the populations of $^4I_{13/2}$ and $^4I_{11/2}$ were a ratio of 17.9%, respectively 82.1% of the total population of the excited levels. For pumping at 1550 nm, the two ratios were 53.1% and, respectively, 46.9%. Using these values, a simple mathematical model enabled us to estimate the lifetime of $^4I_{13/2}$ and the branching ratio of transition $^4I_{11/2} \rightarrow {}^4I_{13/2}$. The cross sections of the main ground-state and excited-state absorption processes are found in the process.

The influence of the multiphonon processes on the luminescence lifetimes of Er^{3+} levels is also discussed.

The results highly recommend the crystalline material Er: Ca:CdF_2 for red upconversion emission and also as laser medium for the transition around 3 μm ($^4I_{11/2} \rightarrow {}^4I_{13/2}$).

Acknowledgements: This work was financed by the program NUCLEU-LAPLAS VII 30N/2023, Ministry of Education and Research, Romania.

Influence of Vacuum Sintering on the Microstructure and Spectroscopic Properties of Eu^{3+}-Doped $SrTiO_3$ Ceramics

Cristina TIHON, Catalina STANCIU, Stefania HAU

National Institute for Laser, Plasma and Radiation Physics, Laboratory of Solid-State Quantm Electronics, Magurele, 077125, Romania
Corresponding author: cristina.matei@inflpr.ro

In this work, we report on the optical properties of europium-doped $SrTiO_3$, synthesized in situ via the sol-gel method as nanopowders and sintered ceramic bulks by heat treatment in vacuum. The structure and morphology of the $Sr_{1-3x/2}Eu_xTiO_3$ (x = 0.01-0.07) nanopowders and ceramics, in relation to the europium concentration, were characterized by X-ray powder diffraction, field emission scanning electron microscopy, and transmission electron microscopy. The optical properties of as-prepared materials were also investigated. These analyses demonstrated that a temperature of 1425 °C in a vacuum of 10^{-4} Pa and a plateau of 4 hours are the optimal sintering conditions for $Sr_{1-3x/2}Eu_xTiO_3$ ceramics. Eu^{3+} doped $SrTiO_3$ ceramics exhibit visible red photoluminescence characteristics. The emission of $SrTiO_3$:Eu^{3+} phosphor with different amount of Eu^{3+}, excited by 395 nm and 465 nm light, was studied. The emission spectra exhibit characteristic luminescence from $^5D_0 \rightarrow {}^7F_j$ (j = 0, 1, 2, 3, 4) intra-4f shell Eu^{3+} ion transitions. The most intense transitions are $^5D_0 \rightarrow {}^7F_1$ (591 nm) for pumping at 395 nm and, $^5D_0 \rightarrow {}^7F_2$ (615 nm) at 465 nm. The corresponding coordinates CIE for the Eu-doped $SrTiO_3$ samples were calculated from the emission spectra obtained at 395 nm and 465 nm excitation wavelengths. This study demonstrates that the original protocol of materials engineering used is a simple and efficient method for manufacturing novel nanophosphors with enhanced reddish-orange emission. The as-obtained results indicated that the sol-gel synthesis combined with the sintering process in a vacuum at an appropriate temperature, plateau, could be a novel way to fabricate materials based on strontium titanate with reasonable optical properties.

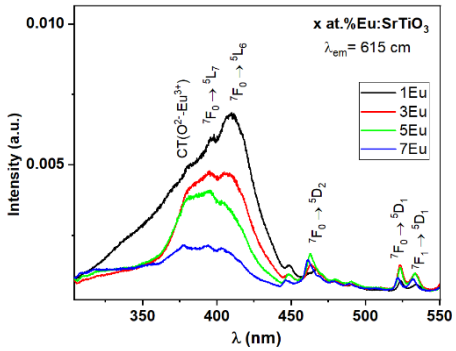

Fig. 1. Excitation spectra of $SrTiO_3$ samples doped with Eu^{3+}.

The spectra show three main peaks due to the transition of the activator ion (Eu^{3+}) from the ground state $^7F_0$ to the excited state; a broad excitation band is observed in the spectra. Peaks are observed at ~420 nm ($^7F_0 \rightarrow {}^5L_6$), 465 nm ($^7F_0 \rightarrow {}^5D_2$), 525 nm ($^7F_0 \rightarrow {}^5D_1$).

Acknowledgements: This work was financed by project PN-III-P1-1.1-TE-2021-1624 and program NUCLEU-LAPLAS VII 30N/2023, Ministry of Education and Research, Romania.

Controlled Synthesis and Spectroscopic Investigation of Eu-doped $SrTiO_3$ Ceramics

Catalina STANCIU, Cristina TIHON, George STANCIU, Stefania HAU

National Institute for Laser, Plasma and Radiation Physics Laboratory of Solid-State Quantum Electronics, Magurele, 077125, Romania
Corresponding author: catalina.vasilescu@inflpr.ro

In recent years, oxide materials doped with rare-earth (REs) have attracted significant attention because they can be excited with infrared and ultraviolet light to produce red, green, and blue emissions [1–3]. Luminescent oxides are phosphors that possess higher physical and chemical stability than traditional luminescent materials based on sulfur and phosphorus. They are also interesting because they can be synthesized with low-cost methods, and most of them are not toxic [4].

The present work focuses on the synthesis and spectroscopic characterization of Eu-doped $SrTiO_3$ ceramics, obtained by the sol-gel method, from stoichiometric quantities of high purity alkoxides. As a result of the thermal treatment, solid ceramic samples were obtained.

To establish the phase composition, the crystallinity of the precursors, and purity of the final powders and related ceramics, room temperature (RT) X-ray diffraction (XRD) measurements were performed. A HITACHI S2600N scanning electron microscope (SEM) coupled with energy-dispersive X-ray spectroscopy (EDX) analyzed the ceramic samples' microstructure and chemical composition. The grain size of the ceramics was determined as the mean intercept length by taking into account measurements on ~60 grains and was 80nm.

The narrow bands in the luminescent spectrum of Eu^{3+} are sensitive to the crystallographic site symmetry occupied by Eu^{3+} ions. The electric dipole transition, $^5D_0 \rightarrow {}^7F_2$, is allowed when Eu^{3+} is located at a non-centrosymmetric crystallographic site, while the $^5D_0 \rightarrow {}^7F_1$ magnetic dipole transition comes from Eu ions in sites with inversion symmetry. Usually, the luminescence intensity ratio of $^5D_0 \rightarrow {}^7F_2$ to $^5D_0 \rightarrow {}^7F_1$, also called the asymmetry ratio, is considered a probe to detect the inversion symmetry around Eu^{3+} ions in the host [29]. The luminescence properties of the perovskites are improved by increasing the europium concentration.

Acknowledgements: This work was supported by CNCS - UEFISCDI, project number PN-III-P1-1.1-TE-2021-1624 within PNCDI III and program NUCLEU-LAPLAS VII 30N/2023, by Ministry of Education and Research, Romania,

[1] Q. Liu, Y. Liu, Z. Yang, X. Li, and Y. Han, "UV-excited red-emitting phosphor Eu^{3+}-activated $Ca_9Y(PO_4)_7$," Spectrochim. Acta A Mol. Biomol. Spectros. **87**, 190-193 (2012).
[2] Z. Xia, J. Zhou, and Z. Mao, "Near UV-pumped green-emitting $Na_3(Y,Sc)Si_3O_9:Eu^{2+}$ phosphor for white-emitting diodes," J. Mater. Chem. C **1**(37), 5917-5924 (2013).
[3] X. Zhao, L. Fan, T. Yu, Z. Li, and Z. Zou, "High efficient blue emission of Ce^{3+} activated Ca_4P2O_9 phosphor for white LEDs," Opt. Express **21**(25), 31660-31667 (2013).
[4] V. Sivakumar and U. V. Varadaraju, "Intense red-emitting phosphors for white light emitting diodes," J. Electrochem. Soc. **152**(10), H168-H171 (2005).

Eu^{3+}-Doped $BiTa_7O_{19}$: A New Red Phosphor

Angela ENACHI, Octavian TOMA, Elena-Cristina TIHON, Ana-Maria VOICULESCU

National Institute for Laser, Plasma and Radiation Physics, Laboratory of Solid-State Quantum Electronics, Magurele, 077125, Romania
Corresponding author: angela.stefan@inflpr.ro

A novel red-emitting phosphor based on $BiTa_7O_{19}$ (BTO) doped with Eu^{3+} ions (x at.%, x = 0.1 - 10 %) concentrations was synthesized via a high-temperature solid-state method [1]. The structural and optical properties of Eu^{3+}-doped BTO were systematically investigated. X-ray diffraction confirmed the formation of a single-phase crystalline material. The luminescence measurements under blue excitation (λ_{ex}= 463 nm) showed intense red emission corresponding to the $^5D_0 \rightarrow {}^7F_2$ transitions of Eu^{3+} ions, indicating efficient energy transfer from the host lattice (Fig. 1). The optimal concentration of Eu^{3+}, beyond which concentration quenching occurs, has been determined.

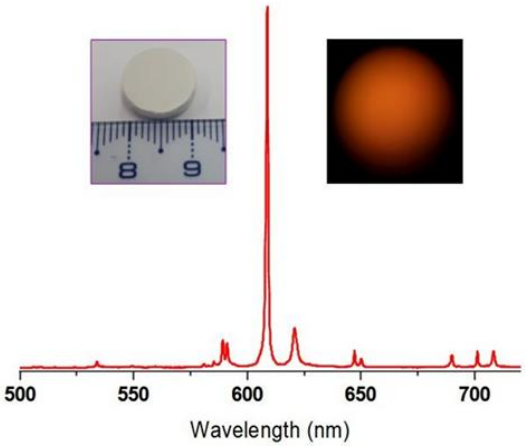

Fig. 1. Luminescence spectrum of BTO:Eu (10 at.%) excited at 463 nm. Insets: ceramic pellet under ambient light (left) and red luminescence under blue-light excitation (right).

The obtained materials exhibit strong emission intensity, good thermal stability, and tunable luminescence. Chromaticity analysis confirms their suitability for red-emitting components in white LED applications. In addition, the optimized phosphor shows potential for photonic and optical device applications.

Acknowledgements: This work was financed by program NUCLEU-LAPLAS VII 30N/2023, Ministry of Education and Research, Romania.

[1] H. Q. Cui, Y.Z. Cao; Y.H. Zhang, L. Cao, S. Y. Ran, X. Wang, D. Y. Wu, X. P. Li, X. Z. Zhang, B. J. Chen, "Extremely intense green up-conversion luminescent and ultra-high temperature sensitivity in Er^{3+}/Yb^{3+} co-doped $BiTa_7O_{19}$ phosphors," J. Lumin. **241**, 118484 (2022).

Inhomogeneous Line Broadening in Y_2O_3 Laser Ceramics

Octavian TOMA, Ana-Maria VOICULESCU, George STANCIU

National Institute for Laser, Plasma and Radiation Physics, Laboratory of Solid-State Quantum Electronics, Magurele, 077125, Romania
Corresponding author: octavian.toma@inflpr.ro

Inhomogeneous line broadening in rare-earth-doped sesquioxide transparent ceramics was observed and reported in the scientific literature. The phenomenon is attributed to the influence of the sintering additives (ions Sc^{3+} [1] or Zr^{4+} [2] ions) on the host crystalline matrix.

Fig. 1 illustrates the inhomogeneous line broadening in Er:La:Zr:Y_2O_3 for the luminescence spectrum of transition $^4F_{9/2} \rightarrow {}^4I_{15/2}$ recorded at room temperature. The narrow-band pumping at 489 nm and, respectively, 493 nm yields different profiles of the luminescence lines, thus putting into evidence the existence of various subpopulations of Er^{3+} ions that are differently excited by the two pump wavelengths. The spectral lines are also different from those obtained using broadband pumping at 973 nm that excites all Er^{3+} subpopulations almost evenly.

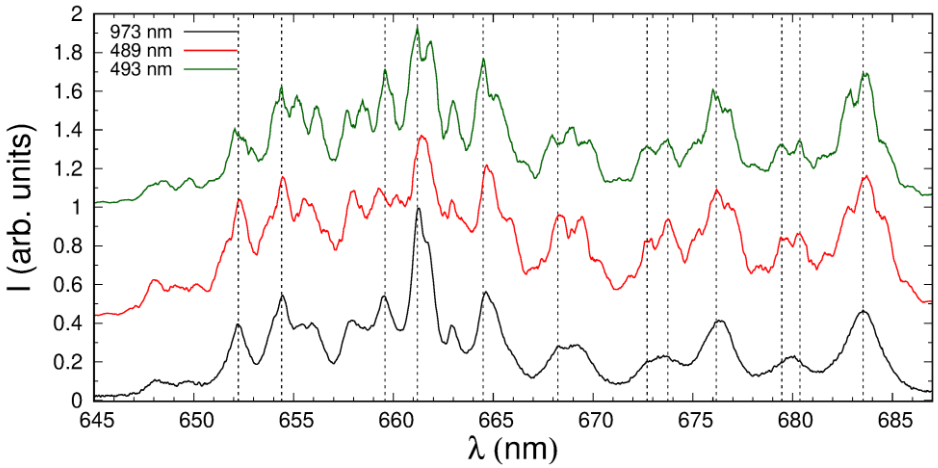

Fig. 1. Luminescence on Er^{3+} transition $^4F_{9/2} \rightarrow {}^4I_{15/2}$ obtained with three different pump wavelengths in Er:Y_2O_3 transparent ceramic at room temperature. The pump wavelength 973 nm comes from a wide-band laser source; the other two wavelengths are from a narrow-band laser source. The vertical dotted lines indicate wavelengths of superposing peaks.

In this work the influence of the sintering additives La^{3+} and Zr^{4+} on the spectral linewidths of laser ions Er^{3+} and Nd^{3+} doped in transparent Y_2O_3 ceramics is investigated.

Selective narrow-band pumping at low temperatures (10 K) is used for putting into evidence the inhomogeneous line broadening on various luminescence transitions of Nd^{3+} and Er^{3+} and for separating the spectral contributions of the various luminescent centers. Time-gated luminescence spectra are used for the investigation of the energy-transfer timescale in Er:Y_2O_3.

Acknowledgements: This work was financed by program NUCLEU-LAPLAS VII 30N/2023, Ministry of Education and Research, Romania.

[1] S. Normani, P. Loiko, R. Maksimov, L. Basyrova, V. Shitov, E. Dunina, A. Kornienko, L. Fomicheva, A. Braud, A. Hideur, B. Viana, P. Camy, "Solid-solution Er:$(Sc,Y)_2O_3$ transparent ceramics: Optical spectroscopy, inhomogeneous line broadening, C_{3i} sites and mid-infrared laser operation," Opt. Mater. **157**, 116288 (2024).

[2] N. Kunkel, J. Bartholomew, L. Binet, A. Ikesue, P. Goldner, "High-Resolution Optical Line Width Measurements as a Material Characterization Tool," J. Phys. Chem. C **120**, 13725-13731 (2016).

Influence of Cerium on Radiation-Induced Attenuation in LPG and FBG Optical Fiber Sensors

George Tony CONSTANTIN[1], Razvan MIHALCEA[1], Daniel NEGUT[2], Daniel IGHIGEANU[1], Anubhav SRIVASTAVA[3], Stefania CAMPOPIANO[3], Flavio ESPOSITO[3], Jan MRÁZEK[4], Ivo BARTOŇ[4], Agostino IADICICCO[3], Andrei STANCALIE[1]

[1]*Center for Advanced Laser Technologies (CETAL), National Institute for Laser, Plasma and Radiation Physics, Magurele 077125, Romania*
[2]*"Horia Hulubei" National Institute for R&D in Physics and Nuclear Engineering, Magurele 077125, Romania*
[3]*Department of Engineering, University of Naples "Parthenope", Naples 80143, Italy*
[4]*Institute of Photonics and Electronics, Czech Academy of Sciences, 18-200, Prague, Czech Republic*
Corresponding author: *george.constantin@inflpr.ro*

The effect of cerium on the radiation response of optical fiber sensors was studied using both long-period gratings (LPG) and fiber Bragg gratings (FBG) [1]. Two similar doped fibers were compared, one containing cerium and one without cerium [2]. The samples were irradiated using electron-beam and gamma sources [3], and their spectral response was monitored through changes in attenuation and resonance wavelength.

For both LPG and FBG sensors, the fibers containing cerium showed a larger radiation-induced attenuation than the Ce-free fibers. This suggests that cerium increases the loss-related response of the fiber under ionizing radiation. The wavelength shifts were generally comparable, indicating that the main influence of cerium is observed in attenuation rather than in a clearly enhanced spectral shift.

Ce-containing LPGs were also tested in a clinical X-ray accelerator. Detectable spectral changes were observed for accumulated doses between 0.5 Gy and 5 Gy. In a separate high-dose experiment, at accumulated doses around and above 100 Gy, the wavelength shift was found to depend on the accelerating potential. For the same dose reported in water, lower accelerating potential produced a larger wavelength shift.

The results indicate that cerium increases radiation-induced attenuation in doped optical fibers, while quantitative use of these sensors for dosimetry requires calibration with respect to radiation source, beam energy, and fiber composition.

Acknowledgements: *We acknowledge the support of the National Interest Infrastructure facility IOSIN–CETAL at INFLPR. This research was supported by Romanian Ministry of Education and Research under the Romanian National Nucleus Program LAPLAS VII under Contract No. 30N/2023 and Project TE119/2025 "LIFEFORMS". Romanian authors acknowledge the support of FAIR-RO-004 "SPARC-RO" funded by the Institute of Atomic Physics.*

[1] A. Stancalie, F. Esposito, R. Mihalcea, L. Mihai, D. Ighigeanu, A. Srivastava, S. Campopiano, A. Iadicicco, "Electron Radiation Impact on Long Period Gratings in Different Optical Fibers," IEEE Sensors J. **25**, 2806-2813 (2025).
[2] F. Esposito, A. Srivastava, R. Mihalcea, D. Negut, I. Florea, F. Orange, S. Campopiano, C. Marques, W. Blanc, A. Stancalie, A. Iadicicco, "Response to gamma radiation of long period gratings in nanoparticle-doped optical fibers," Sens. Actuators A: Phys. **407**, 117954 (2026).
[3] F. Esposito, A. Stancalie, A. Srivastava, R. Mihalcea, I. Bartoň, D. Negut, S. Campopiano, M. Śmietana, J. Mrázek, and A. Iadicicco, "Characterization of Gamma Radiation Sensitivity in Cerium, Lutetium and Aluminum Doped Optical Fiber with Long Period Gratings," J. Lightwave Technol. **44**, 2528-2534 (2026).

Thermal Management of High-Power Laser Diodes using Optimized Microchannel Cooling Plate

Oana GRIGORE, Alexandru CRACIUN

National Institute for Laser, Plasma and Radiation Physics, Laboratory of Solid-State Quantum Electronics, Magurele 077125, Romania
Corresponding author: oana.grigore@inflpr.ro

This work presents a coupled thermo-hydraulic analysis and optimization of a water-cooled plate designed for a high-power fiber laser diode. The system dissipates a total thermal load of 3.6 kW (24 diode lasers, 150 W per diode) and is intended for integration in a standard 19-inch rack configuration. The primary design objective is to minimize the temperature non-uniformity of the diodes, targeting a thermal spread below 1°C, while maintaining the total pressure drop under 1 bar. The cooling plate consists of two aluminum plates joined via friction stir welding, with internal channels machined in the thicker plate. Two main configurations were investigated: straight parallel channels (7 mm and 3 mm depth) and an optimized geometry incorporating distributed pin arrays. The simulations were performed in steady-state using COMSOL Multiphysics, coupling Laminar Flow and Heat Transfer in Solids and Fluids modules.

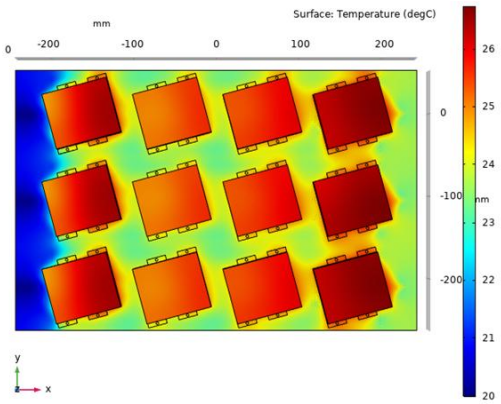

Fig. 1. Temperature distribution for optimized configuration showing ~1°C uniformity.

Results show that reducing channel depth from 7 mm to 3 mm increases flow velocity and improves convective heat transfer, reducing the maximum temperature from approximately 38°C to 36°C. Further enhancement is achieved by introducing non-uniform pin distributions along the flow direction, which locally disturb the boundary layer and increase the heat transfer coefficient. The optimized configuration achieves a maximum temperature of ~26.7°C and a thermal spread close to 1°C across all diodes.

Hydraulic analysis indicates a total pressure drop of approximately 0.39 bar, well below the imposed constraint, with a corresponding hydraulic power below 10 W. Thermal resistance analysis confirms that convective resistance dominates the heat transfer chain, while the influence of the indium interface layer remains secondary. The study demonstrates that a carefully tailored channel topology combined with localized pin-based enhancement provides an effective solution for high-uniformity cooling in high-power laser diode systems used for fiber lasers pumping.

Acknowledgements: *This work was funded from the project "Technological platform for the production of high-power lasers and laser processing equipment (LASER FO)," Contract no. 390058/16.09.2025, SMIS Code 329264, funded by the European Regional Development Fund under the Operational Program for Smart Growth, Digitization and Financial Instruments (POCIDIF), Priority 1 - Supporting and promoting an attractive and competitive CDI system in Romania, and by the Ministry of Education and Research, Romania, under Romanian National Nucleu Program LAPLAS VII - contract no. 30N/2023. The authors would like to thank the partner Rolix Impex Series SRL for their contribution to this work.*

Topic 3. Environmental Protection and Pollutants Monitoring

Hydrogen Gas Detection Using a Fiber-Optic-Based Plasmonic Sensor

Iulia ANTOHE[1], Luiza-Izabela TODERAȘCU[1], Cristian ZAGĂR[1,2], Andrei STOCHIOIU[1,2], Vlad-Andrei ANTOHE[2], Gabriel SOCOL[1]

[1]*National Institute for Laser, Plasma and Radiation Physics, Laser Department, Magurele 077125, Romania*
[2]*Faculty of Physics, University of Bucharest, Magurele 077125, Romania*
Corresponding author: *iulia.antohe@inflpr.ro;*

Hydrogen gas is increasingly used across various industrial and energy applications, including fuel cells, chemical production, and semiconductor manufacturing [1]. Despite its growing importance, hydrogen poses significant safety hazards due to its high flammability, low ignition energy, and colorless, odorless nature, which makes early and sensitive detection critical [2].

In this study, we report the development of a fiber-optic surface plasmon resonance (FO-SPR) sensor for real-time hydrogen monitoring. The sensor design integrates a palladium-based recognition layer onto the gold-coated fiber surface, exploiting palladium's strong affinity for hydrogen [3]. When hydrogen is absorbed by the palladium nanostructures, it alters the local refractive index at the metal–dielectric interface, resulting in detectable shifts in the SPR resonance wavelength. Experimental results demonstrate that the FO-SPR sensor exhibits rapid response times, selectivity for hydrogen, and very low detection limits, while its compact, FO-integrated design not only facilitates easy deployment but also enables continuous, real-time monitoring of hydrogen in remote or hard-to-access environments.

This FO-SPR sensor provides a promising tool for industrial safety, environmental monitoring, and process control, offering a sensitive, label-free, and real-time solution for hydrogen detection.

Acknowledgements: This research was supported by the National Authority for Research in the framework of the Nucleus Programme-LAPLAS VII (grant 30N/2023) and by the grants of the Ministry of Education and Research, Romania, CNCS/CCCDI-UEFISCDI, project no. 19 PCE/2025, PN-IV-P1-PCE-2023-1902 and project no. 72/2024, ERANET-M-3-Gas SensingMat-RT-1, within PNCDI IV and PoCIDIF nr. 390008/ 27.11.2024.

[1] S.M. Echim and S. Budea, "Use of Hydrogen Energy and Fuel Cells in Marine and Industrial Applications-Current Status," Hydrogen **6**(3), 50 (2025).
[2] L. Kumar and A.K. Sleiti, "A comprehensive review of hydrogen safety through a metadata analysis framework," Renew. Sustain. Energy Rev. **214**, 115509 (2025).
[3] M. M. Alkhabet, S. H. Girei, S. Paiman, N. Arsad, M. A. Mahdi, and M. H. Yaacob, "Highly Sensitive Hydrogen Sensor Based on Palladium-Coated Tapered Optical Fiber at Room Temperature," Eng. Proc. **2**(1), 8 (2020).

Pulsed Laser Deposited AZO and Al_2O_3/AZO Coatings for H_2 Selective Gas Sensor Structures

Gianina POPESCU-PELIN[1], Luiza-Izabela TODERASCU[1], Cristian ZAGAR[1], Cristian LUPAN[2], Nicoleta PREDA[3], Elisa-Gabriela BROASCA (DUMBRAVA)[1], Andrei STOCHIOIU[1], Gabriel SOCOL[1]

[1]*National Institute for Laser, Plasma and Radiation Physics, Lasers Department, Magurele 077125, Romania*
[2]*Center for Nanotechnology and Nanosensors, Department MIB Technical University of Moldova Chisinau, Moldova*
[3]*National Institute of Materials Physics, Laboratory of Functional Nanostructures, Magurele 077125, Romania*
Corresponding author: *gianina.popescu@inflpr.ro*

The development of gas sensors with high selectivity to hydrogen (H_2) is becoming a central research priority due to the growing use of H_2 as a clean energy carrier and the associated safety concerns (e.g. low ignition energy, high diffusivity), as reported in specialised literature calling for reliable detection at low concentrations and in complex gas environments [1-3]. Within this framework, aluminium doped zinc oxide (AZO) emerges as a relevant metal-oxide candidate, as its defect-mediated conductivity and the abundance of active adsorption sites sustain the surface-controlled interactions that govern the response to hydrogen [1,4].

In this work, AZO and Al_2O_3/AZO multilayer coatings were deposited by pulsed laser deposition (PLD) in order to obtain functional oxide architectures suitable for gas sensing applications. The thin films were grown onto alumina substrates with a pre-patterned Au electrode, as well as on Si and quartz, allowing the application of complementary physico-chemical and functional analyses on the resulting coatings. The samples were examined by scanning electron microscopy (SEM), X-ray diffraction (XRD) techniques and X-ray photoelectron spectroscopy (XPS) to assess their morphology, crystallinity and surface chemistry, including the oxidation states. Further, UV-VIS spectrometry provided insight into optical behavior and band-gap characteristics, while photoluminescence revealed the defect-related features of the coatings. Hydrogen sensing measurements complemented the evaluation and showed the architecture-dependent differences in response and stability, which become more evident under heated operation, when surface processes activated by temperature enhance the sensing response.

Together, these results outline how controlled layering of AZO and Al_2O_3/AZO coatings influence their interaction with H_2 and highlight the potential of PLD-fabricated metal-oxide heterostructures for selective gas sensing applications.

Acknowledgements: This research was supported by the National Authority for Research in the framework of the Nucleus Programme - LAPLAS VII (grant 30N/2023) and by the grants of the Ministry of Education and Research, Romania, CNCS/CCCDI - UEFISCDI, project no. 19PCE/2025, PN-IV-P1-PCE-2023-1902.

[1] A. Alaghmandfard, S. Fardindoost, A. L. Frencken, M. Hoorfar, "The next generation of hydrogen gas sensors based on transition metal dichalcogenide-metal oxide semiconductor hybrid structures", Ceram. Int. **50**(17) Part A, 29026-29043 (2024).
[2] B. Shen, Q. Zhang, X. Liu, J. Li, Y. Guan, D. Xiao, "Fast-Response Hydrogen Sensor Based on γ-Al_2O_3-Modified Graphene", Chemosensors **12**(12), 250 (2024).
[3] Z. Li, S. Yaseen, S. Jia, Z. Guo, L. Zhang, N. Cui, L. Gu, J. Liu, M. Ding, "High performance room-temperature hydrogen sensor using MOF-derived porous Pd@SnO2 composite", Sens. Actuators B Chem. **447**, Part 1, 138769 (2026).
[4] B.V. Goikhman, F.S. Fedorov, N.P. Simonenko, T.L. Simonenko, N.A. Fisenko, T.S. Dubinina, G. Ovchinnikov, A.V. Lantsberg, A. Lipatov, E.P. Simonenko and A.G. Nasibulin, "Quantum of selectivity testing: detection of isomers and close homologs using an AZO based e-nose without a prior training," J. Mater. Chem. A **10**, 8413-8423 (2022).

Reduced Graphene Oxide Based Chemiresistive Sensors for Hydrogen Detection

Cristian ZAGĂR[1,2], Iulia ANTOHE[1], Andrei STOCHIOIU[1,2], Vlad-Andrei ANTOHE[2], Gabriel SOCOL[1]

[1]*National Institute for Laser, Plasma and Radiation Physics (INFLPR), 077125 Magurele, Ilfov, Romania*
[2]*Faculty of Physics, Research and Development Center for Materials and Electronic & Optoelectronic Devices (MDEO), University of Bucharest, Atomiştilor 405, 077125 Magurele, Ilfov, Romania*
Corresponding authors: iulia.antohe@inflpr.ro; gabriel.socol@inflpr.ro

Chemiresistive sensors have attracted great interest in the area of gas sensing due to the versatility they display in comparison to, for instance, electrochemical sensors. Structural simplicity, cheap fabrication costs and fast response/relaxation time make this technology a great candidate for industrial-scale gas sensing [1].

The present work focuses on the manufacturing of such a sensor using PLD (Pulsed Laser Deposition) in order to obtain a reliable resistance, change at room temperature. Based on reduced graphene oxide (rGO) as its active substance, the sensor was tested for hydrogen and methane in a 1-100 ppm concentration range. The motivation for rGO arose from its excellent performance in previously built hybrid gas sensors with high selectivity for hydrogen [2,3]. Given the similarity in response profiles between the two gases, two other variants were also synthesized by PLD, in an attempt to increase hydrogen selectivity at room temperature. More specifically, a mixture of rGO and 50 nm metallic nanoparticles (Pd and Pt, respectively) was used as the PLD target, resulting in a film where a conducting rGO network is embedded with Pd/Pt nanoparticles, confirmed by SEM imaging. Catalytic contribution from Pd and Pt, based especially on their affinity towards hydrogen, was responsible for a larger but equally reliable resistance change.

Furthermore, hydrogen and methane sensorgrams in the 1-100 ppm range were performed in order to extract the sensitivity to both gases, for all the variants involved, namely rGO, rGO+Pd NPs and rGO+Pt NPs respectively, with the greatest sensitivity shown for the Pt NP variant.

Acknowledgments: *This research was supported by the National Authority for Research in the framework of the Nucleus Programme - LAPLAS VII (grant 30N/2023) and by the grants of the Ministry of Education and Research, Romania, CNCS/CCCDI- UEFISCDI, project no. 19PCE/2025, PN-IV-P1-PCE-2023-1902 and project no. 72/2024, ERANET-M-3-GasSensingMat-RT-1, within PNCDI IV and PoCIDIF nr. 390008/27.11.2024.*

[1] M. K. Hossain, *et al.*, "Chemiresistive Gas Sensing using Graphene-Metal Oxide Hybrids," Chem. Asian J. **19**, e202300529 (2024).
[2] P. Recum, T. Hirsch, "Graphene-based chemiresistive gas sensors," Nanoscale Adv. **6**, 11-31 (2023).
[3] A. Ilnicka, J. P. Lukaszewicz, "Graphene-Based Hydrogen Gas Sensors: A Review," Processes **8**(5), 633 (2020).

Influence of ZnO-Based Nanostructure Morphology on Gas Sensing Performance

Luiza Izabela TODERASCU[1], Cristian ZAGAR[1], Elisa Gabriela BROASCA (DUMBRAVA)[1], Nicoleta PREDA[2], Andrei STOCHIOIU[1], Gianina POPESCU-PELIN[1], Iulia ANTOHE[1], Gabriel SOCOL[1]

[1]*National Institute for Laser, Plasma and Radiation Physics, Laboratory of Lasers Magurele, 077125, Romania*
[2]*National Institute of Materials Physics Magurele 077125, Romania*
Corresponding author: *gabriel.socol@inflpr.ro*

Zinc oxide (ZnO) nanostructures have attracted considerable attention in gas sensing applications due to their wide band gap, high electron mobility, chemical stability, and strong surface reactivity. Among the various morphologies, ZnO nanoparticles, nanorods, and nanoflowers exhibit distinct structural and surface characteristics that significantly influence gas sensing performance. This study investigates the role of synthesis routes and the resulted morphology with respect to the gas response. ZnO-based nanostructures with different morphologies (nanoparticles, nanorods, and nanoflowers) were synthesized using a wet-chemical method followed by thermal treatment, enabling a comparative evaluation of how structural variations influence the gas sensing performance of the resulting materials [1,2].

The obtained materials were characterized through structural, compositional, and morphological analyses. XRD confirmed the crystalline structure and phase purity of ZnO, while SEM revealed a specific morphology and size distribution of the nanostructures which depends on synthesis route. Surface chemical composition and defect states were investigated by XPS, and photoluminescence spectroscopy provided information on optical properties and defect-related emissions.

Gas sensing measurements were performed to evaluate the influence of morphology on sensor performance, with particular focus on hydrogen (H_2) detection. The sensors were analyzed in terms of sensitivity, response time, and selectivity toward target gas. The results indicate that nanoflower structures exhibit enhanced sensitivity due to their porous architecture and increased active surface area, while nanorods provide improved charge transport properties [3]. Understanding the relationship between ZnO morphology and sensing behavior is essential for optimizing sensor design and improving H_2 gas detection performance.

This work highlights the importance of morphology-controlled ZnO-based nanostructures in advancing high-performance gas sensors and provides insights for the rational design of nanomaterials in environmental monitoring and industrial safety applications.

Acknowledgements: This work was financed by project, UEFISCDI no. 19PCE2025 and program NUCLEU-LAPLAS VII 30N/2023, Ministry of Education and Research, Romania.

[1] B. Ydir, A. Ajdour, M. Soumane, I. Antohe, G. Socol, L.I. Toderascu, D. Saadaoui, I. Choulli, R. Leghrib, H. Lahlou, "Optimized SILAR Growth of Vertically Aligned ZnO Nanorods for Low-Temperature Acetone Detection," Chemosensors **13**(8), 289 (2025).
[2] M. Bakry, W. Ismail, M. Abdelfatah, A. El-Shaer, "Low-cost fabrication methods of ZnO nanorods and their physical and photoelectrochemical properties for optoelectronic applications," Sci Rep. **14**(1), 23788 (2024).
[3] C. Prakash, R. Chaurasiya, A. J. Kale, A. Dixit, "Low-Temperature Highly Robust Hydrogen Sensor Using Pristine ZnO Nanorods with Enhanced Response and Selectivity," ACS Omega **7**(32), 28206-28216 (2022).

Chemoresistive Sensing Devices Based on Oxide Materials for Multipurpose Detection

Andrei-Silviu ZANCU, Maria-Luiza STÎNGESCU, Mihai-Adrian SOPRONYI, Mihai-Robert ZAMFIR, Nicu D. SCARISOREANU

National Institute for Laser, Plasma and Radiation Physics, C400 Department, Magurele 077125, Romania
Corresponding author: *andrei.zancu@inflpr.ro*

Given the variety of pollutants released into our surroundings, there's a growing demand for the development of advanced monitoring devices capable of multipurpose detection [1]. Thanks to their high sensitivity and scalability, metal oxide based chemoresistive sensors emerge as promising candidates for low-cost environmental monitoring [2-4]. In this study, Zinc Oxide (ZnO) was the material of choice to serve as the active sensing layer. Thus, ZnO thin films were synthesized using a large-area Pulsed Laser Deposition (PLD) system. The resulting films were structurally and morphologically characterized through X-ray diffraction (XRD), Ellipsometry, and Scanning Electron Microscopy (SEM). X-ray diffraction (XRD) analyses revealed the presence of characteristic zinc oxide peaks, indicating a hexagonal wurtzite crystal structure. A preferential growth was observed in the [100] and [101] crystalline directions, suggesting a columnar polycrystalline development of the film. Subsequently, gas sensing measurements were performed in presence of various compounds (NOx, CO_2, C_2H_5OH, and C_3H_6O) at operating temperatures ranging from 25°C to 200°C. It was revealed that the ZnO chemoresistive device presented a selective response (~23) towards ethanol at the operating temperature of 150°C, thus presenting an improved performance when compared to results in the literature of pristine ZnO thin films. Dynamic response curves were performed in the presence of NO_x and CO_x in order to analyse the sensors performance to repeated gas exposure. The ZnO based devices exhibited a stable baseline and rapid response/recovery times starting with the operating temperature of 150°C towards both gases. However, as it is usually encountered with many chemoresistive sensors, the samples exhibited poor selectivity, showing similar responses to the two analytes that underwent testing for the dynamic curves [5]. This study looks to reveal the selectivity that pristine ZnO presents and no limits of detection have been determined as of yet. Testing different concentrations of gas is part of next step in determining the efficacy of the obtained chemoresistive zinc oxide-based gas sensors.

Acknowledgements: This work was financed by project National Platform for Semiconductor Technologies (PNTS) SMIS 304244 and program NUCLEU-LAPLAS VII 30N/2023, Ministry of Education and Research, Romania, and was performed using the facilities of C400 - FOTOPLASMAT INFLPR.

[1] S. Dhall, B.R. Mehta, A.K. Tyagi, Kapil Sood, "A review on environmental gas sensors: Materials and technologies," Sens. Int. **2**, 100116 (2021).
[2] M. A. Franco, P. P. Conti, R. S. Andre, D. S. Correa, "A review on chemiresistive ZnO gas sensors," Sens. Actuators Rep. **4**, 100100 (2022).
[3] Y. Masuda, "Recent advances in SnO_2 nanostructure-based gas sensors," Sens. Actuators B: Chem. **364**, 131876 (2022).
[4] A. Pathania, N. Dhanda, R. Verma, A.-C.A. Sun, P. Thakur, A. Thakur, "Review - Metal Oxide Chemoresistive Gas Sensing Mechanism, Parameters, and Applications," ECS Sens. Plus **3**, 013401 (2024).
[5] P. M. Bulemo, D.-H. Kim, H. Shin, H.-J. Cho, W.-T. Koo, S.-J. Choi, C. Park, J. Ahn, A. T. Güntner, R. M. Penner, I.-D. Kim, "Selectivity in Chemiresistive Gas Sensors: Strategies and Challenges," Chem. Rev. **125**(8), 4111-4183 (2025).

MgPc: C Chemiresistive Sensor for Detection of Inflammatory Gases at Room Temperature

Elisa Gabriela BROASCA (DUMBRAVA)[1,2], Luiza Izabela TODERASCU[1], Iulia ANTOHE[1], Cristian ZAGAR[1], Gianina POPESCU-PELIN[1], Andrei STOCHIOIU[1], Gabriel SOCOL[1]

[1]*National Institute for Laser, Plasma and Radiation Physics, Magurele 077125, Romania*
[2]*Department of Analytical Chemistry and Environmental Engineering, Faculty of Chemical Engineering and Biotechnologies, Polizu Street No 1-7, Romania*
Corresponding author: elisa.broasca@inflpr.ro

Airborne pollutants have become a serious environmental and human health problem [1]. The increased frequency of accidental explosions caused by leakage has led to significant interest in the detection of explosive gas concentrations [2]. A wide variety of sensors are currently available for the detection of explosive hydrocarbon gases, offering high selectivity, sensitivity, and reproducibility, as well as the capacity for rapid monitoring at concentrations below the lower explosive limit. However, the requirement for integrated heaters remains a significant constraint. Eliminating these issues would substantially enhance the cost-effectiveness and power efficiency of chemiresistive sensors by enabling reliable room-temperature operation.

In this study, a chemiresistive gas sensor based on a magnesium phthalocyanine and carbon nanoparticles (MgPc:C) coating was deposited on an alumina substrate with a pre-patterned gold electrode. The coating was obtained by drop-casting a solution based of MgPc and C mixed in THF (tetrahydrofuran). The morphological and structural properties of the deposited film were investigated using Scanning Electron Microscopy (SEM) and X-ray Diffraction (XRD) techniques. X-ray Photoelectron Spectroscopy (XPS) and Energy-Dispersive X-ray Spectroscopy (EDXS) were further used to evaluate the elemental composition of the MgPc: C thin film. The resulting chemiresistive sensors were investigated for their ability to detect various inflammatory gases (H_2, butane, methane, propane, and GPL), which proved sensitive to concentrations as low as 10 ppm at room temperature. The main sensor parameters (i.e., sensitivity, Lower Limit of Detection (LOD), response, and recovery time) were determined according to the investigated gases. Fig. 1 shows the response of the sensor to a range of butane concentration between 10-1ppm in synthetic air, expressed as relative electrical resistance in percentage as a function of time.

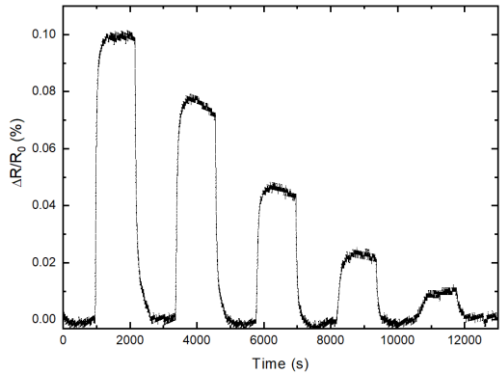

Fig. 1. *Sensorgram illustrating the dynamic response of the sensor to varying concentrations of C_4H_{10} within the 1-10 ppm range*

Acknowledgements: This work was financed by the project, UEFISCDI no. 19PCE2025, M-ERANET No. 72/2024 and program NUCLEU-LAPLAS VII 30N/2023, Ministry of Education and Research, Romania

[1] S. Dhall, B.R. Mehta, A.K. Tyagi, K. Sood, "A review of environmental gas sensors: Materials and technologies," Sens. Int. **2**, 100116 (2021).
[2] D. S. Lee, H. Y. Jung, J. W. Lim, M. Lee, S. W. Ban, J. S. Huh, D .D. Lee, "Explosive gas recognition system using thick film sensor array and neural network," Sens. Actuators B: Chem. **71**(1-2), 90-98 (2000).

Room-Temperature Chemiresistive Ammonia Sensor: Electron Beam Irradiation for Enhanced Performance

Andrei STOCHIOIU[1,2], Ana-Maria POPA[1,2], Luiza-Izabela TODERAȘCU[1,3], Oana GHERASIM[1], Vlad-Andrei ANTOHE[2,4], Elena MĂNĂILĂ[1], Gabriela CRĂCIUN[1], Cătălin LUCULESCU[1], Gabriel SOCOL[1], Iulia ANTOHE[1,5]

[1]*National Institute for Laser, Plasma and Radiation Physics (INFLPR), Magurele, 077125, Ilfov, Romania*
[2]*Faculty of Physics, Research and Development Center for Materials and Electronic & Optoelectronic Devices (MDEO), University of Bucharest, Atomiștilor Street 405, Măgurele, 077125, Ilfov, Romania*
[3]*Faculty of Chemistry, University of Bucharest, Splaiul Independenței 91-95, Bucharest, 0500951, Romania*
[4]*Institute of Condensed Matter and Nanosciences (IMCN), Université Catholique de Louvain (UCLouvain), Place Croix du Sud 1, Louvain-la-Neuve, B-1348, Belgium*
[5]*Academy of Romanian Scientists (AOSR), Ilfov 3, Bucharest, 050044, Romania*
Corresponding author: *andrei.stochioiu@inflpr.ro*

Ammonia (NH3) is a gas that, at high levels, threatens human health, making its detection essential. In this context, conductive polymers used as sensing material have proven advantageous for gas detection due to their generally high sensitivity and ability to operate at room temperature. This study presents the fabrication and characterization of a chemiresistive NH3 sensor based on polyaniline (PANi) coatings. PANi thin films were synthesized on alumina substrates with interdigitated gold electrodes using the chemical oxidation method and further exposed to electron beam irradiation (EBI) with doses ranging between 50 and 150 kGy. Structural and chemical modifications induced by EBI were analyzed using SEM, FTIR-ATR, XPS and Raman Spectroscopy techniques. The dose of 150 kGy was identified as an irradiation threshold that induced a significant modification of the chemical structure of PANi, with influence on the sensor performances in terms of selectivity and sensitivity to NH3. Gas testing measurements conducted in a controlled gas chamber showed that EBI-treated sensors exhibited enhanced sensitivity and selectivity toward NH3, achieving a limit of detection as low as 2.82 ppm across a range of 1–100 ppm.

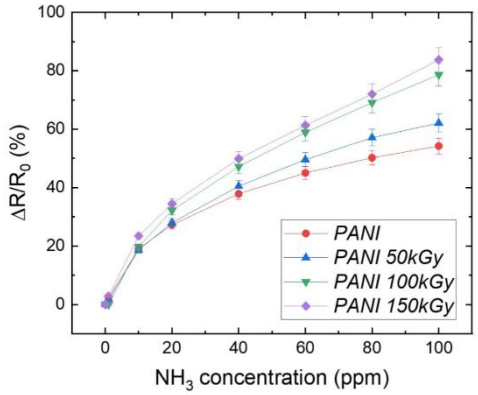

Fig. 1. Ammonia sensitivity of PANI-based gas sensors after irradiation with different doses.

These findings highlight the potential of electron beam-modified conducting polymers in developing next-generation gas sensors for critical environmental, health, and safety monitoring.

Acknowledgements: This work was supported by the National Authority for Research in the framework of the Nucleus Programme - LAPLAS VII (grant 30N/2023), and by the Ministry of Education and Research, Romania, CNCS/CCCDI-UEFISCDI, project no. 19PCE/2025 (PN-IV-P1-PCE2023-1902) and project no. 72/2024 (ERANET-M-3-GasSensingMat-RT-1), within PNCDI IV and PoCIDIF (nr. 390008/27.11.2024). We also acknowledge the support of the National Interest Infrastructure facility IOSIN – CETAL at INFLPR and the doctoral scholarship provided by University of Bucharest, Faculty of Physics.

Development of Laser-Reduced Graphene Oxide (rGO) Sensors for Gas Detection

Khadija BOUCHANE[1,2], Islem MESKINI[1,3], Luiza-Izabela TODERAȘCU[1], Cristian ZAGĂR[1,3], Elisa Gabriela BROASCĂ (DUMBRAVĂ)[1,4], Andrei STOCHIOIU[1,3], Gianina POPESCU-PELIN[1], Gabriel SOCOL[1], Iulia ANTOHE[1]

[1]*National Institute for Laser, Plasma and Radiation Physics, Laser Department, Magurele 077125, Romania*
[2]*Faculty of Sciences, IBN ZOHR University, 80000 Agadir, Morocco*
[3]*Faculty of Sciences, University of Monastir, Monastir 5019, Tunisia*
[4]*Faculty of Physics, University of Bucharest, Magurele 077125, Romania*
[5]*National University of Science and Technology POLITECHNICA Bucharest, Faculty of Chemical Engineering and Biotechnology, 011061 Bucharest, Romania*
Corresponding authors: *iulia.antohe@inflpr.ro; gabriel.socol@inflpr.ro*

Reduced graphene oxide (rGO) has emerged as a highly promising material for gas sensing applications due to its high surface area, tunable electrical conductivity, and abundant defect sites that facilitate gas adsorption [1]. Among various synthesis methods, laser reduction of graphene oxide (GO) offers a rapid, mask-free, and chemical-free approach to fabricate rGO with controlled morphology and electrical properties [2].

In this work, we review and discuss recent advances in the development of laser-reduced graphene oxide (LrGO) gas sensors. Moreover, LrGO sensors were fabricated and evaluated for gas-sensing performance toward ammonia (NH_3) at room temperature. The structural and chemical changes induced by laser irradiation were characterized using scanning electron microscopy (SEM) and X-ray photoelectron spectroscopy (XPS). Electrical measurements showed that LrGO sensors exhibited enhanced conductivity compared to pristine GO. Gas sensing tests demonstrated a strong response to NH_3, with rapid response and recovery times.

Overall, laser reduction represents a versatile and scalable technique for engineering high-performance graphene-based gas sensors [3]. Future work should focus on improving selectivity through functionalization, enhancing environmental stability, and integrating LrGO sensors into portable and smart sensing systems.

Acknowledgments: *This research was supported by the National Authority for Research in the framework of the Nucleus Programme-LAPLAS VII (grant 30N/2023) and by the grants of the Ministry of Education and Research, Romania, CNCS/CCCDI-UEFISCDI, project no. 19 PCE/2025, PN-IV-P1-PCE-2023-1902 and project no. 72/2024, ERANET-M-3-Gas SensingMat-RT-1, within PNCDI IV and PoCIDIF nr. 390008/ 27.11.2024.*
K.B. and I.M. acknowledge the Romanian Ministry of Foreign Affairs and the Agence Universitaire de la Francophonie (AUF) for the Eugen Ionescu research and mobility grant at the National Institute for Laser, Plasma and Radiation Physics (INFLPR).

[1] P. Recum and T. Hirsch, "Graphene-based chemiresistive gas sensors," Nanoscale Adv.**6**, 11-31 (2024).
[2] K.Y. Lau and J. Qiu, "Broad applications of sensors based on laser-scribed graphene," Light Sci Appl **12**, 168 (2023).
[3] C. Tharwat, Y. Badr, S.M. Ahmed, *et al.*, "CW laser beam-based reduction of graphene oxide films for gas sensing applications," Opt. Quant. Electron. **57**, 69 (2025).

ABO_3 Thin Films for SAW Sensors

Mihai-Adrian SOPRONYI[1], Adela TANASE[1,2], Mihai-Robert ZAMFIR[1], Valentin ION[1], Cristian VIESPE[1], Nicu D. SCARISOREANU[1]

[1]*National Institute for Laser, Plasma and Radiation Physics, PHOTOPLASMAT Department, Magurele 077125, Romania*
[2]*University of Bucharest, Faculty of Physics, 405, Atomistilor, 077125, Magurele – Ilfov, P.O. Box MG-11*
Corresponding author: *mihai.sopronyi@inflpr.ro*

The growing demand for eco-friendly, multifunctional sensor technologies has driven extensive research into lead-free ABO_3 perovskites, such as Barium Strontium Titanate (BST), Barium Calcium Zirconate Titanate (BCTZ), and Bismuth Ferrite ($BiFeO_3$). This study focuses on the development of highly sensitive Surface Acoustic Wave (SAW) sensors based on epitaxial $BiFeO_3$ (BFO) thin films. The BFO layers were grown on $SrTiO_3$ (111) substrates utilizing Pulsed Laser Deposition (PLD). The research evaluates the material's cross-sensitivity capabilities for detecting Volatile Organic Compounds (VOCs), ethanol, noxious gases (COx, NOx), humidity, and temperature variations under strictly controlled mass flow conditions. To optimize the device response, a systematic thickness-dependent study was conducted. The structural epitaxy and phase purity were confirmed via X-ray Diffraction (XRD), while Scanning Electron Microscopy (SEM) and Energy-Dispersive X-ray Spectroscopy (EDX) validated the surface morphology and target-to-film stoichiometry. Spectroscopic ellipsometry was employed to accurately extract the optical constants specifically the refractive index *n* and extinction coefficient *k* alongside film thickness. For functional device characterization, Gold (Au) Interdigital Transducers (IDTs) incorporating a Chromium (Cr) adhesion layer were patterned onto the BFO surface via successive thermal evaporation. The electromechanical coupling and gas-induced resonance frequency shifts were accurately recorded utilizing a wideband signal amplifier coupled with a high-resolution pendulum frequency counter. The results demonstrate the viability of optimized epitaxial BFO architectures for advanced environmental monitoring systems [1], [2].

Acknowledgements: This work was financed by project "Platformă Națională pentru Tehnologiile Semiconductorilor" (PNTS) SMIS 304244, and program NUCLEU-LAPLAS VII 30N/2023, Ministry of Education and Research, Romania. This work was performed using the facilities of C400 – FOTOPLASMAT INFLPR.

[1] N. Enea, *et al.*, "Lead-Free Perovskite Thin Films for Gas Sensing through Surface Acoustic Wave Device Detection," Nanomaterials **14**(1), 39 (2023).
[2] N. Enea, *et al.*, "Laser Processed Hybrid Lead-Free Thin Films for SAW Sensors," Materials **15**(23), 8452 (2022).

Influence of Gas-Phase Parameters on the Properties of TiO_2 Nanopowders Synthesized by Laser Pyrolysis

Evghenii GONCEARENCO[1,2], Elena DUTU[1], Iuliana MORJAN[1], Claudiu FLEACA[1], Iulia-Ioana LUNGU[1], Valentin ION[1], Andrei ZANCU[1], Monica SCARISOREANU[1]

[1]*National Institute for Laser, Plasma and Radiation Physics, LASERS Department, Magurele 077125, Romania*
[2]*Faculty of Physics, University of Bucharest, Magurele, 077125, Romania*
Corresponding author: *monica.scarisoreanu@inflpr.ro*

In this study, TiO_2 nanoparticles were synthesized via laser pyrolysis using titanium tetrachloride ($TiCl_4$) vapors and synthetic air as precursors, with ethylene (C_2H_4) employed as sensitizer gas. The synthesis parameters, including gas composition, gas flow rates, and reaction pressure, were systematically varied in order to investigate their influence on particle formation mechanisms, morphology, and surface properties. The morpho-structural properties of the obtained nanopowders were investigated using energy-dispersive X-ray spectroscopy (EDX), X-ray diffraction (XRD), transmission electron microscopy (TEM), X-ray photoelectron spectroscopy (XPS), and Brunauer–Emmett–Teller (BET) surface area analysis. The results reveal that, while only minor phase variations from anatase (crystallite size: 11–22.2 nm) toward rutile (crystallite size: 17–24.3 nm) are observed, the synthesis parameters have a strong impact on nanoparticle morphology and surface characteristics. In particular, the specific surface area shows a significant variation, increasing from 61 m^2/g to 129 m^2/g depending on the synthesis conditions, indicating substantial changes in particle size and aggregation behavior. The maximum surface area (129 m^2/g) approaches the upper range for gas-phase TiO_2, highlighting laser pyrolysis as a scalable method for high-purity nanopowders. The present study demonstrates that careful control of synthesis parameters in laser pyrolysis provides an effective route for tailoring the morphology and surface properties of TiO_2 nanopowders. The optimized materials exhibit promising potential for applications in chemiresistive gas sensors, where high surface area and enhanced surface reactivity are essential for improved sensing performance.

Acknowledgements: This work was supported by a grand of the Ministry of Education and Research, Romania, CCCDI-UEFISCDI, project number PN-IV-P6-6.1-CoEx-2024-0154, within PNCDI IV and by a project of Romanian Ministry of Research, Innovation and Digitalization under Romanian National Nucleu Program LAPLAS VII – contract no. 30N/2023.

Polyoxometalate-Functionalized Optical Fiber SPR Sensors for Detection of Organic Pollutants in Aqueous Media

Islem MESKINI[1,2], Khadija BOUCHANE[1,3], Luiza-Izabela TODERASCU[1], Cristian ZAGAR[1,4], Elisa Gabriela BROASCA (DUMBRAVA)[1,5], Andrei STOCHIOIU[1,4], Gianina POPESCU-PELIN[1], Gabriel SOCOL[1], Iulia ANTOHE[1]

[1]*National Institute for Laser, Plasma and Radiation Physics, Laser Department, Magurele 077125, Romania*
[2]*Faculty of Sciences, University of Monastir, Monastir 5019, Tunisia*
[3]*Faculty of Sciences, IBN ZOHR University, Agadir 80000, Morocco*
[4]*Faculty of Physics, University of Bucharest, Magurele 077125, Romania*
[5]*National University of Science and Technology POLITECHNICA Bucharest, Faculty of Chemical Engineering and Biotechnology, Bucharest 011061, Romania*
Corresponding authors: *iulia.antohe@inflpr.ro; gabriel.socol@inflpr.ro*

Polyoxometalates (POMs) are a versatile class of metal–oxygen clusters with tunable redox properties, high charge density, and strong affinity for organic species, making them promising materials for chemical sensing in liquid environments [1]. In this work, we report the synthesis, structural characterization, and application of novel POM-functionalized optical fiber surface plasmon resonance (FO-SPR) sensors for the detection of organic pollutants, with a focus on phenolic compounds and cationic dyes in aqueous media.

Three POM compounds were successfully synthesized: $(C_6H_{13}N_4)_2[V_{2.29}W_{3.71}O_{19}]$, $(C_6H_8N)_4(C_{6.20}H_{8.60}N)[VW_{12.48}O_{40}]$, and $Na_{3.4}[V_1W_5O_{19}]\cdot H_2O$ [2]. These structures consist of vanadium-substituted tungsten oxide clusters with varying sizes and charge distributions, enabling diverse interaction mechanisms with target analytes. Complementary physicochemical characterization using SEM, XPS, and XRD is underway to elucidate morphology, surface chemistry, and structural stability.

For sensing applications, thin films of the synthesized POMs were immobilized onto gold-coated optical fibers (FO) to fabricate surface plasmon resonance-based sensors. The sensing mechanism is based on changes in the local refractive index induced by adsorption and charge-transfer interactions between the POM layer and organic pollutants. Experimental results demonstrate that the sensors exhibit clear and reversible SPR responses upon exposure to model phenolic compounds and cationic dyes (e.g., methylene blue), with sensitivity dependent on POM composition and structure.

The developed POM-functionalized FO-SPR sensors exhibit good repeatability and potential selectivity toward organic pollutants in water, highlighting their applicability for environmental monitoring. These findings demonstrate that integrating structurally tailored POMs with FO-SPR sensors provides a promising strategy for developing sensitive, label-free sensors for real-time detection of hazardous organic contaminants in aqueous systems.

Acknowledgments: *This research was supported by the National Authority for Research in the framework of the Nucleus Programme-LAPLAS VII (grant 30N/2023) and by the grants of the Ministry of Education and Research, Romania, CNCS/CCCDI-UEFISCDI, project no. 19 PCE/2025, PN-IV-P1-PCE-2023-1902 and project no. 72/2024, ERANET-M-3-Gas SensingMat-RT-1, within PNCDI IV and PoCIDIF nr. 390008/ 27.11.2024.*
I.M. and K.B. acknowledge the Romanian Ministry of Foreign Affairs and the Agence Universitaire de la Francophonie (AUF) for the Eugen Ionescu research and mobility grant at the National Institute for Laser, Plasma and Radiation Physics (INFLPR).

[1] I. Gregorovic, L. Lotfian, R. Khajavian, *et. al.*, "Polyoxometalates in environmental remediation and energy storage," Environ. Sci.: Nano **13**, 1295-1346 (2026).
[2] I. Meskini, F. Capet, G. Fraqueza, *et. al.*, "Dawson- and Lindqvist-Type Hybrid Polyoxometalates: Synthesis, Characterization and Ca^{2+}-ATPase Inhibition Potential," Molecules **30**(22), 4334 (2025).

Engineered Laser Photodegradation: A Promising Strategy for Mitigating Micro- and Nanoplastic Pollution in Aquatic Environments

Adriana SMARANDACHE, Ionut-Relu ANDREI, Andra DINACHE, Iuliana URZICA, Angela STAICU

National Institute for Laser, Plasma and Radiation Physics, Lasers Department, Magurele 077125, Romania
Corresponding author: adriana.smarandache@inflpr.ro

In the larger context of global plastic pollution, the widespread contamination of environment by micro-/nanoplastics (MNPs) has become a major concern. It is acknowledged as one of the three major challenges facing humanity, along with biodiversity loss and global climate change [1]. Therefore, effective removal or accelerated degradation solutions for MNPs are critical for minimizing their long-term environmental impact.

This study investigates the potential of engineered photodegradation using a pulsed Nd:YAG laser (λ = 266 nm, 10 Hz, 9 ns pulse duration) to mitigate MNPs pollution. Three distinct irradiation configurations were evaluated using polystyrene (PS) and poly(methyl methacrylate) (PMMA) particles (0.1–100 μm) suspended in water, under constant stirring (600 rpm). Results revealed that the third configuration, achieving energy densities of 13.34–20 J/cm², significantly accelerated photodegradation compared to the lower-density setups (0.024–0.036 J/cm²). SEM and DLS confirmed substantial morphological transformations. Spectroscopic analyses (LIF, UV-VIS and FTIR) further validated the formation of photoproducts and irradiation-dependent molecular modifications in both polymer types. These findings show that customized laser-driven setups may effectively induce the structural collapse and chemical breakdown of MNPs, providing a scalable solution for remediating contaminated aquatic environments.

Acknowledgements: This work was supported by project 43TE/2025, PN-IV-P2-2.1-TE-2023-1686, and Nucleu Program LAPLAS VII-contract no. 30N/2023, Ministry of Education and Research, Romania.

[1] Y. Wu, R. Yi, Y. Wang, C. Zhang, J. Zheng, P. Ning, D. Shan, and B. Wang, "Light-driven degradation of microplastics: Mechanisms, technologies, and future directions," J. Hazard. Mater. Adv. **17**, 100628 (2025).

Heavy Metals Detection in Soil by Terahertz–Time Domain Spectroscopy Method

Cristian UDREA, Mihaela BOJAN

National Institute for Lasers Plasma and Radiation Physics, Măgurele 077125, Ilfov, Romania
Corresponding author: *cristian.udrea@inflpr.ro*

Heavy metal pollution in soil endangers food safety and human health [1]. This study presents a nondestructive detection method for different heavy metals like $CuSO_4$ (copper sulfate) and Zn (zinc) and in soil, studied by THz spectroscopy. THz spectrum it is located between the microwave and infrared region of the electromagnetic spectrum. We have tried to establish the content of the heavy metal by the absorption coefficients at the selected frequency point. The samples were prepared at different concentrations in ppm (parts per millions).

The samples spectra were acquired with the THz-TDS spectroscopy kit (from Ekspla) which emits in the frequency range of 0.1 – 4 THz. They are obtained by the ratio of the reference and samples spectra. In the experiment, The THz spectrum of soil was collected by transmission mode of THz spectrometer. Also, knowing the transmission, we have calculated the absorbance rate. The transmission spectra of the samples were acquired many times to mediate them.

The results proved that THz spectroscopy has good qualitative and quantitative detection ability for soils contaminated with heavy metals which could bring new opportunities for detection of pollutants in soil.

Acknowledgements: This work was financed by project NUCLEU-LAPLAS VII 30N/2023, Ministry of Education and Research, Romania.

[1] W. Lu, H. Luo, L. He, W. Duan, Y. Tao, X. Wang, S. Li, "Detection of heavy metals in vegetable soil based on THz spectroscopy," Comput. Electron. Agric. **197**, 106923 (2022).

Topic 4. Devices Based on Photonic and Plasma Technologies

Real-Time Spatio-Temporal Measurement of Electromagnetic Field Using Magneto-Optical Crystals

Ana-Maria TIULEANU[1,2], Răzvan UNGUREANU[1], Bogdan BUTOI[1], Dorin MOLOVATA[1,3], Aurelian MARCU[1,3]

[1]*National Institute for Laser, Plasma and Radiation Physics, CETAL Department, Magurele 077125, Romania*
[2]*Department of Physics, University of Bucharest, Magurele 077125, Romania*
[3]*University" Politehnica" Bucharest, Bucharest 060042, Romania*
Corresponding author: *aurelian.marcu@inflpr.ro*

Characterizing non-uniform, transient electromagnetic phenomena require sensing capabilities that offer high temporal precision alongside spatial data. Unlike traditional scanning probe techniques which are limited by their sequential data acquisition, this study utilizes the magneto-optical effect in a $Tb_3Ga_5O_{12}$ (TGG) crystal to achieve real-time, high- resolution mapping of dynamic magnetic flux density.

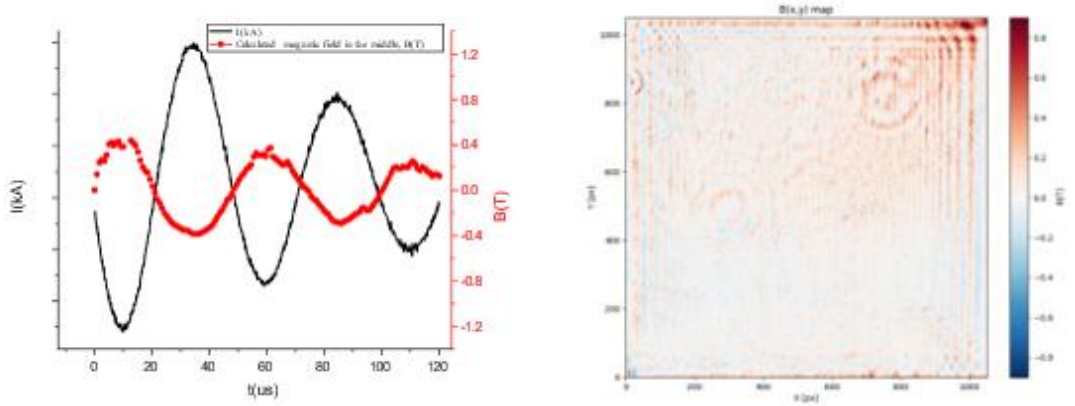

Fig. 1. a) Temporal measurements of magnetic fields, and b) spatial measurements of magnetic fields

The magnetic environment used to test the functionality of this method was created using a pulsed high-current source that unloads onto a 'custom shaped' copper inductor, placed in the vicinity of the magneto-optical crystal, to obtain a temporarily transient and anisotropic magnetic field distribution. In order to simultaneously capture both the spatial and temporal aspects of the magnetic field, without relying on an expensive equipment like an ultra-high frame rate camera, we used two ordinary detectors: a CCD camera and a photodiode to capture the change in the laser beam. Open-source Python libraries were used to develop camera communication protocols, as well as image acquisition and manipulation routines. Developed software performs automated image processing, including region of interest detection and exposure optimization, as well as computes the magneto-optical response pixel-by-pixel to obtain the spatial magnetic field distribution. The results are visualized using 2D and 3D representations, by combining the photodiode signal (Fig.1a) with the camera signal (Fig.1b) in order to obtain a complete spatio-temporal deconvolution of the magnetic field. Presented method has been tested and calibrated in the range of ±0.9 T, giving a spatial resolution of about 6 μm^2 and a temporal resolution of about 6 ns.

Acknowledgements: *This work was financed by projects ELI-RO 30/2024, ELI-RO 30/2025, support of the National Interest Infrastructure facility IOSIN - CETAL at INFLPR and Program contract No. 39/2024, and program NUCLEU-LAPLAS VII 30N/2023, Institute of Atomic Physics/ Ministry of Education and Research, Romania.*

Versatile Pixelated Scintillators: Advancing Medical and Industrial Performance

Nicoleta ENEA, George STANCIU, Luiza-Maria STINGESCU, Alexandru DAN, Nicu SCARISOREANU

National Institute for Laser, Plasma and Radiation Physics, Photonics and Plasma Innovation Center - PHOTOPLASMAT, Magurele 077125, Ilfov, Romania
Corresponding author: nicoleta.enea@inflpr.ro

In the field of modern radiation detection, modern X-ray imaging demands a continuous balance between maximizing spatial resolution and minimizing radiation exposure. Scintillator screens play a pivotal role in this domain by converting incident ionizing radiation into visible light, which is subsequently captured by digital photodetector arrays. Among various luminescent materials, Cesium Iodide (*CsI*) has emerged as an attractive choice due to its high light yield, favorable atomic number (*Z*) and excellent matching with the spectral sensitivity of conventional silicon-based sensors. However, traditional thin-film or columnar *CsI* screens suffer from intrinsic lateral light scattering, which significantly degrades the spatial resolution. To overcome this limitation and advance both low-dose medical diagnostics and high-energy industrial non-destructive testing, structuring the scintillator into isolated, micro-scale pixels is essential [**Fig.1**]. This work presents the development, microfabrication and performance optimization of an innovative, low-cost pixelated *CsI* scintillator integrated into a micro-structured silicon matrix.

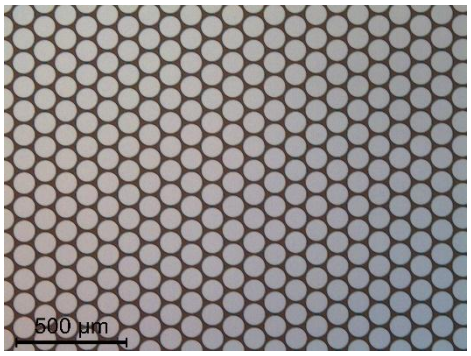

Fig. 1. SEM micrographs of Si micropores.

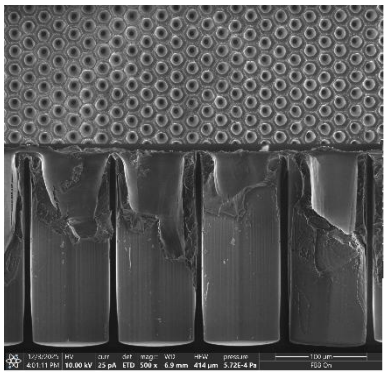

Fig. 2. SEM micrographs of Si micropores filled by the drop-casting method.

Silicon (*Si*) substrates were micro-structured to define pixel arrays with nominal lateral dimensions of 100 × 100 µm² separated by ultra-thin isolating walls of 8 µm, uniformly distributed over an active area of 5 × 5 cm². Due to the highly hygroscopic nature of *CsI*, the commercial raw powder was subjected to a thermal dehydration process at 100°C to eliminate absorbed environmental moisture. To ensure proper filling, the dried material was wet-milled in an acetone medium using a planetary ball mill. Filling the micro-cavities was done through two distinct methods: a repetitive drop-casting technique utilizing a supersaturated solution of the *CsI* powder dissolved in an ethanol-distilled water solvent mixture [**Fig. 2**] and an alternative partial thermal melting technique performed directly inside the micro-cavities.

The structured samples were exposed to a high-energy X-ray flux generated at a tube voltage of 130 kV, a beam current of 3 mA and a signal integration time of 500 ms. Under ionizing radiation, the samples successfully demonstrated distinct visible scintillation emissions, validating the functional mechanics of the matrix, which establishes a clear path toward manufacturing large-scale, homogeneous flat-panel screens for low-dose medical radiography and high-performance industrial inspection.

Acknowledgements: This work was founded through the „Platforma Națională pentru Tehnologiile Semiconductorilor (PNTS)" project, SMIS Code: 351364 (fost 304244); Contract number: G2024-85828/390008/27.11.2024. Part of this work was performed using C400 PHOTOPLASMAT facilities acquired within the POC153/2016 IN2-FOTOPLASMAT project

Organic Light Emitting Transistors based on Organic Semiconductors and Nanostructured Dielectric Interface

Carmen BREAZU[1], Marcela SOCOL[1], Oana RASOGA[1], Nicoleta PREDA[1], Cristina BESLEAGA[1], Andreea COSTAS[1], Gabriel SOCOL[2], Geanina POPESCU-PELIN[2]

[1]*National Institute of Materials Physics Laser, 405A Atomistilor Street, Magurele 077125, Romania*
[2]*National Institute for Laser, Plasma and Radiation Physics, 409 Atomistilor Street, Magurele 077125, Romania*
Corresponding author: *carmen.breazu@infim.ro*

Organic light-emitting transistors (OLETs) represent a promising class of optoelectronic devices that merge light generation with transistor functionality in a single architecture. In this work, we report on OLETs based on organic semiconductors integrated with nanostructured substrates to enhance charge transport and light outcoupling. The active organic layers and the gate electrode are deposited by Matrix-Assisted Pulsed Laser Evaporation (MAPLE), enabling gentle processing. The dielectric layers is fabricated by spin-coating, offering a smooth, conformal film compatible with the nanostructures and suitable for low-voltage operation. The dielectric interface is modified by forming a two-dimensional periodic network of nanostructures in a UV-curable polymer resist, deposited on different substrates, whose structural parameters can be tuned through the processing conditions. The nanostructured substrates are realized by Nanoimprint Lithography, providing well-defined periodic relief patterns that are preserved throughout the subsequent dielectric and MAPLE deposition steps. Nanoimprint lithography (NIL) technique is a nonconventional nanopatterning method used to produce structures from micro-to nanoscale assuring higher resolution beyond the limits of light diffraction [1,2]. A large variety of substrates, including the flexible ones can be patterned using NIL.

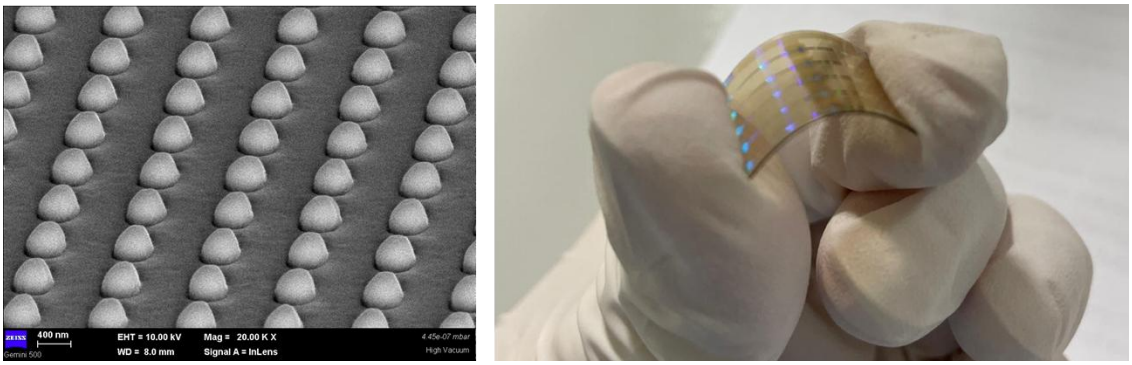

Fig. 1. (a) ITO/PES substrate-Pillar nanostructures. (b) Flexible nanostructured OLET structure.

We investigate the influence of substrate nanostructuring and layer fabrication conditions on the optical, morphological and electrical characteristics of the resulting OLETs. The obtained results demonstrate that combining MAPLE-deposited organic semiconductors, spin-coated dielectrics and nanoimprinted substrates can be obtained solution-compatible OLETs, highlighting a versatile route toward advanced organic optoelectronic devices.

Acknowledgements: This work was financed by project PN−IV-P2-2.1-TE-2023-1626, Ministry of Education and Research, Romania.

[1] P. H. Wang, C. M. Wang, "Review of nanoimprinted photonics," Nanotechnology **36**, 442002 (2025).
[2] N. Song, X. Guo, H. Zha, B. Li, N. Liang, T. Zhai, "Nanoimprint Lithography Enabling High-Performance Organic Optoelectronics: Advances and Perspectives," Nanomicro Lett. **4**(18), 236 (2026).

Indium Tin Oxide Films Prepared on Patterned Flexible Substrates by Pulsed Laser Deposition

Marcela SOCOL[1], Nicoleta PREDA[1], Carmen BREAZU[1], Gabriela PETRE[1], Ionel STAVARACHE[1], Gianina POPESCU-PELIN[2], Anca STANCULESCU[1], Gabriel SOCOL[2]

[1]*National Institute of Materials Physics, 405A Atomistilor Street, Magurele 077125, Romania*
[2]*National Institute for Lasers, Plasma and Radiation Physics, 409 Atomistilor Street, Magurele 077125, Romania*
Corresponding author: marcela.socol@infim.ro

Today, flexible electronics are designed into a wide range of commercial products [1]. The development of such foldable and stretchable devices requires flexible plastic substrates and compatible materials. Lightweight in thin film form, organic semiconductors emerge as promising candidates for flexible electronic area. Hence, flexible organic photovoltaic (OPV) cells have been widely studied in order to be integrated as power supply into wearable electronics. Therefore, tremendous efforts were made to improve the OPV performances by the optimization of the active layer, transparent conductive electrode (TCE) and device architecture [2]. The effective light manipulation using patterned surface is an interesting strategy in OPV, which can lead to an enhancement of the light harvesting in the organic photoactive layer [3]. Thus, in the present study, patterned polyethylene terephthalate (PET) substrates with two different structures: (i) pillars (~300 nm height, ~400 nm diameter and ~1100 periodicity) and (ii) pyramids (~940 nm height, ~2 μm diameter and ~2.5 μm pitch) were covered with indium tin oxide (ITO) films by pulsed laser deposition (PLD). The laser deposition was also carried out on flat PET and glass substrates in order to highlight the influence of the periodic patterns on the properties of the obtained ITO films. The laser fluence (1.2 J/cm^2 or 1.3 J/cm^2) was varied for obtaining electrodes with adequate optical and electrical properties. The ITO films deposited on rigid, flexible flat and flexible patterned substrates were investigated from morphological, optical, and electrical point of view. The morphological analysis proves that the ITO films retain the pattern of the PET substrate after PLD deposition. The electrical investigations show that ITO films deposited on patterned PET reveal a low electrical resistivity (5.5×10^{-4} Ωcm). Also, an improvement in the Hall mobility (23.8 cm^2/Vs) is acquired in the case of the patterned (pyramids) ITO layers. The outcome of this work emphasizes the potential of the patterned ITO films in the field of the flexible optoelectronic devices.

Acknowledgements: *This work was supported by a grant of the Ministry of Education and Research, Romania, CCCDI-UEFISCDI, project number PN-IV-P7-7.1-PED-2024-0884 and project number PN−IV P2-2.1-TE-2023-1626, within PNCDI IV.*

[1] D. Corzo, G. Tostado-Blázquez and D. Baran, "Flexible Electronics: Status, Challenges and Opportunities," Front. Electron. **1**, 594003 (2020).
[2] Y. Sun, Y. Kan, K. Gao, B. Tang, Y. Li, "Flexible Organic Solar Cells: Progress and Challenges," Small Sci. **1**(5), 2100001 (2021).
[3] W. Wang, L. Qi, "Light management with patterned micro-and nanostructure arrays for photocatalysis, photovoltaics, and optoelectronic and optical devices," Adv. Funct. Mater. **29**(25), 1807275 (2019).

Development of Broadband Dielectric Mirrors Based on HfO_2 and ZrO_2 Coatings

Stefan-Andrei IRIMICIUC[1,2], Jiri BULIR[2], Gabriel BLEOTU[1,3], Doina CRACIUN[1], Petronela GAROI[1], Sergii CHERTOPALOV[2], Sasa YEHIA - ALEXE[3], Daniel URSESCU[3], Jan LANCOK[2], Valentin CRACIUN[1,3]

[1]*National Institute for Laser, Plasma and Radiation Physics, Magurele 077125, Romania*
[2]*Institute of Physics of the Czech Academy of Sciences, Na Slovance 1999/2, Prague, Czech Republic*
[3]*Extreme Light Infrastructure-Nuclear Physics (ELI-NP), 30 Reactorului Street, Magurele 077125, Romania*
Corresponding author: *stefan.irimiciuc@inflpr.ro*

Ultra-intense laser systems have become indispensable instruments for frontier science, enabling breakthroughs in nuclear physics, particle acceleration, and high-field quantum electrodynamics. The Extreme Light Infrastructure – Nuclear Physics (ELI-NP) hosts the world's most powerful lasers, operating at up to 10 PW, yet their performance is still fundamentally constrained by the reliability of optical components exposed to ultrashort, high-intensity pulses. The durability of mirrors and dielectric coatings under femtosecond irradiation is a critical bottleneck for advancing extreme-light experiments.

In this work, we demonstrate the fabrication of broadband dielectric coatings based on HfO_2 and ZrO_2 with tunable stoichiometry, produced using pulsed laser deposition and magnetron sputtering. Depositions were conducted in pure O_2 atmospheres for PLD and in mixed Ar/O_2 atmospheres for sputtering, across a wide parameter space to achieve precise stoichiometric control via oxygen partial pressure. Additional deposition parameters were systematically adjusted to modulate the energy distribution and gas-phase chemistry of the expanding oxide or metallic plasmas. To understand plasma evolution during growth, we employed in situ diagnostics, including space-resolved optical emission spectroscopy and ICCD fast-camera imaging.

Comprehensive post-deposition characterization was performed using AFM, SEM, XRD, XPS, and LIDT measurements. An optimization strategy was established to correlate processing conditions with the resulting film properties. Our results show that fine control over deposition conditions enables tuning of microstructure and optical performance. We further propose paths to enhance LIDT by introducing selected metallic interlayers that promote high-quality interfaces. Overall, this study outlines effective approaches for engineering broadband dielectric mirrors with controllable and improved laser-induced damage thresholds.

Acknowledgements: This work was financed by project ELI004/2025, program NUCLEU-LAPLAS VII 30N/2023, Ministry of Education and Research, Romania.

Vanadium Dioxide Thin Films for Adaptive Infrared Stealth

Adrian BERCEA[1,2], Mihaela FILIPESCU[1], Antoniu MOLDOVAN, Alexandra PALLA-PAPAVLU[1]

[1]*National Institute for Laser, Plasma and Radiation Physics, Laser Department, Magurele 077125, Ilfov, Romania*
[2]*Faculty of Physics, University of Bucharest, Atomiștilor Street 405, Magurele 077125, Ilfov, Romania*
Corresponding author: *bercea.adrian@inflpr.ro*

This study focuses on the fabrication of vanadium dioxide (VO_2) thin films by pulsed laser deposition (PLD) on c-sapphire (c-Al_2O_3) and metal substrates. VO_2 thin films have the potential for targeting infrared (IR) stealth applications. VO_2 is a material known for its reversible metal-insulator transition (MIT) near 68 °C. The MIT enables a substantial change in IR emissivity.

Here, the VO_2 deposition by PLD is performed under controlled conditions: an oxygen pressure of 2.2×10^{-2} mbar, a substrate temperature of 500 °C, and with an ArF excimer laser (193 nm wavelength), working at a fluence of 3 J/cm². The MIT-related emissivity modulation is assessed via spectroscopic ellipsometry and IR thermography, while the ABCD matrix method was employed to optimize film thickness for enhanced stealth performance.

Structural and morphological characterization demonstrates that the pulsed laser deposition parameters are crucial for obtaining phase-pure VO_2. At room temperature, X-ray diffraction (XRD) confirms the monoclinic (M1) phase. The XRD results are also confirmed by and Raman spectroscopy. Atomic force microscopy (AFM) and scanning electron microscopy (SEM) reveal uniform grain morphology with a root-mean-square (RMS) roughness below 10 nm, which helps minimize optical losses. The resulting films show a sharp MIT (hysteresis width < 8 °C) and a tunable emissivity variation ($\Delta\varepsilon > 0.6$ in the 8–14 μm range), consistent with an abrupt resistivity drop of three orders of magnitude.

Our findings show the potential of VO_2 for dynamic thermal camouflage. Future efforts will focus on integrating VO_2 layers into active devices for encrypted communication.

Acknowledgements: These results are funded by the Ministry of Education and Research, Romania, UEFISCDI, project number PN-IV-P7-7.1-PED-2024-1371 (TWIST), within PNCDI IV and program NUCLEU-LAPLAS VII 30N/2023, Ministry of Education and Research, Romania.

A Comparative Study of Vanadium Oxides Deposited by PLD for Infrared Stealth

Adrian BERCEA[1,2], Mihaela FILIPESCU[1], Cristina CRACIUN[1], Maria DINESCU[1]

[1]*National Institute for Laser, Plasma and Radiation Physics, Laser Department, Magurele 077125, Ilfov, Romania*
[2] *Faculty of Physics, University of Bucharest, Atomiştilor Street 405, Măgurele 077125, Ilfov, Romania*
Corresponding author: *bercea.adrian@inflpr.ro*

Vanadium dioxide (VO_2) and vanadium pentoxide (V_2O_5) are two functional oxides with distinct properties. VO_2 is known for its temperature induced metal to insulator transition (MIT) near 68 °C, while V_2O_5 exhibits semiconducting and electrochromic behavior. Here, VO_2 and V_2O_5 are obtained as thin films by pulsed laser deposition (PLD) and radio-frequency (RF) assisted PLD, using a metallic vanadium target (ArF excimer laser, target–substrate distance 4.5 cm). Our work shows that by adjusting the PLD parameters (e.g.: oxygen pressure, substrate temperature, laser fluence, and RF power), we can selectively obtain either pure VO_2 or pure V_2O_5 thin films. The VO_2 and V_2O_5 thin films are deposited onto Platinum coated Silicon substrate and c-axis sapphire substrates. As an example, pure VO_2 films are obtained at an oxygen pressure of 2.2×10^{-2} mbar, substrate temperature of 500 °C, laser fluence of 3 J/cm², and RF power of 25 W. Whereas V_2O_5 formation occurred, substrate temperature of 500 °C, at an oxygen pressure of 2.2×10^{-2} mbar and under higher RF power (100 W) promoting over-oxidation.

Morphological analyses by atomic force microscopy (AFM) and scanning electron microscopy (SEM) reveal distinct differences between the two functional oxides. VO_2 films exhibit uniform and compact granular morphology with root-mean-square roughness as low as 1.0 nm on sapphire and approximately 3 nm on Pt/Si substrate. In contrast, V_2O_5 films show slightly higher roughness of 3.3 nm and a different surface texture, consistent with its layered orthorhombic structure. Structural characterization by X-ray diffraction (XRD) confirms the monoclinic M1 phase for VO_2, with clear (020) reflections, while V_2O_5 exhibits additional orthorhombic peaks. Raman spectroscopy further differentiates the phases: VO_2 displays characteristic modes at ~194, 223, and 614 cm^{-1}, whereas V_2O_5 shows distinct V=O stretching vibrations.

Spectroscopic ellipsometry is used to extract the complex dielectric functions of both functional oxides. VO_2 exhibits a strong optical contrast upon heating through its semiconductor to metal transition proven by significant changes of the ellipsometric angles (Ψ and Δ), while V_2O_5 shows no phase transition. For infrared stealth applications, this pronounced optical contrast in VO_2 enables tunable emissivity, which is particularly valuable for thermal management. In contrast, V_2O_5 is more readily formed by PLD under higher RF power and can serve as a low-loss spacer layer in Fabry–Perot cavity structures for infrared stealth. The complementary use of AFM, SEM, XRD, Raman, and ellipsometry proves essential for validating phase purity in functional oxide thin films.

Acknowledgements: These results are funded by the Ministry of Education and Research, Romania, UEFISCDI, project number PN-IV-P7-7.1-PED-2024-1371, within PNCDI IV and program NUCLEU-LAPLAS VII 30N/2023, Ministry of Education and Research, Romania.

The Influence of Angular Anisotropy in Pulsed Electron Beam Deposition on Oxide Thin Films Growth

Daniela DOBRIN[1], Ion BURDUCEA[2], Decebal IANCU[2], Cristina BURDUCEA[2], Florin GHERENDI [1], Magdalena NISTOR[1]

[1]*National Institute for Lasers, Plasma and Radiation Physics, Magurele 077125, Romania*
[2]*"Horia Hulubei" National Institute for Research & Development in Physics and Nuclear Engineering, Magurele 077125, Romania*
Corresponding author: *daniela.dobrin@inflpr.ro*

Angular anisotropy in plumes produced by lasers and pulsed electrons plays a decisive role in the transfer of the material from the target to the substrate during film growth, but its impact on film composition remains insufficiently quantified, particularly in the case of pulsed electron beam deposition (PED). Barium strontium titanate (BST) thin films are widely used as tunable dielectric, electrical, and ferroelectric properties depending on the barium/strontium ratio, which requires the control of the thin film composition [1]. In this work, BST thin films were grown at 0.01 mbar pressure in argon background gas by PED at room temperature [2], based on the model used for PLD and presented in reference [3]. A "semi-sphere" holder with a fixed distance of 40 mm from the target to the substrate at all angles was employed. The angular thickness and composition profiles of these films were determined from Rutherford backscattering spectrometry (RBS) measurements at different substrate angular positions as a function of applied fluence. These film profiles have forward-shaped peaks with measurable thicknesses of up to 80-90° for the major axis and similar shapes for all fluences. The cation angular distributions lead to systematic deviations from target stoichiometry at large angles, with heavier elements of the film exhibiting narrower emission profiles. These findings demonstrate that plume anisotropy is a key factor in the non-uniform composition of PED-grown complex oxide thin films and highlight the need to control the plume dynamics when designing materials for oxide electronics applications.

Acknowledgements: Ion beam experiments have been performed at 3 MV Tandetron accelerator from "Horia Hulubei" National Institute for Research & Development in Physics and Nuclear Engineering (IFIN-HH) and were supported by the Romanian Governmental Programme through the National Programme "Instalații și Obiective Speciale de Interes Național" (IOSIN). D.I., I.B, C.B. acknowledge the project PN 23210201. MN, DD, FG acknowledge the program NUCLEU-LAPLAS VII 30N/2023, Ministry of Education and Research, Romania.

[1] J.P. Goud, A. Kumar, K. Sandeep, S. Ramakanth, P. Ghoshal, K.C.J. Raju, "Tunable Microwave Device Fabrication on Low Temperature Crystallized $Ba_{0.5}Sr_{0.5}TiO_3$ Thin Films by an Alternating Deposition and Laser Annealing Process," Adv. Elect. Mater. **7**(3), 2000905 (2021).

[2] D. Dobrin, I. Burducea, D. Iancu, C. Burducea, F. Gherendi, M. Nistor, "Angular distribution of species in pulsed electron beam deposition of $Ba_xSr_{1-x}TiO_3$," Appl. Surf. Sci. **657**, 159757 (2024).

[3] A. Ojeda-G-P, C.W. Schneider, M. Dobeli, T. Lippert, A. Wokaun, "Angular distribution of species in pulsed laser deposition of $La_xCa_{1-x}MnO_3$," Appl. Surf. Sci. **336**, 150-156 (2015).

Functional Oxide Heterostructures: Structure-Property Correlations and Interface-Driven Phenomena

Ioan M. GHITIU[1,2], Elena I. BANCU[1,2], Mihai ZAMFIR[2], Alexandru DAN[2], Floriana CRACIUN[3], Nicu D. SCARISOREANU[2]

[1]*Faculty of Physics, University of Bucharest, Magurele 077125, Romania*
[2]*National Institute for Laser, Plasma and Radiation Physics, C400 Photoplasmat, Magurele 077125, Romania*
[3]*CNR-ISM, Istituto di Struttura Della Materia, Area Della Ricerca di Tor Vergata, Via del Fosso del Cavaliere, 100 Rome, Italy*
Corresponding author: ioan.ghitiu@inflpr.ro

The investigation of functional oxide heterostructures has revealed a wide range of emergent phenomena driven by interface structure, strain, and defect chemistry. Among these, the formation of conductive states at buried interfaces in nominally insulating oxides remains of particular interest, both fundamentally and for device-oriented applications. However, accessing such deeply buried functionalities and correlating them with structural features remains experimentally challenging.

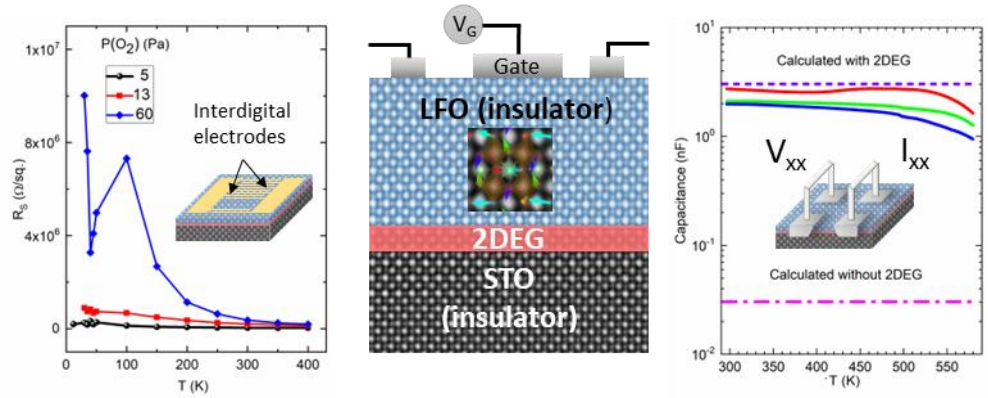

Fig. 1. Electrical measurements and device structure diagrams for the investigation of the metallic interface.

In this work, we explore structure–property correlations in epitaxial oxide heterostructures through a combination of electrical probing and advanced electron microscopy. Focusing on $LaFeO_3/SrTiO_3$ systems, we demonstrate that a conductive interface can be identified indirectly via in-plane capacitance measurements using surface interdigital electrodes. The observed response is consistent with the modelling results for the presence of a buried conductive layer and is further supported by direct transport measurements. Importantly, this behavior is obtained for films grown on untreated $SrTiO_3$ substrates, highlighting the emergence of interfacial conductivity without conventional surface preparation.

By systematically varying growth conditions, particularly the oxygen pressure, we show that the interfacial electronic properties are strongly influenced by defect formation and interface structure. The results suggest a combined role of oxygen vacancies, interface quality, and local atomic rearrangements in enabling the formation of the conductive state. Complementary scanning transmission electron microscopy analyses provide insight into the structural and chemical characteristics governing these effects. Beyond this case study, the same experimental framework can be extended to other oxide heterostructures, where strain engineering and multilayer architectures are used to tailor functional responses such as polarization and interfacial coupling. This approach enables a unified perspective on how structural distortions, defects, and interfaces govern emergent properties in complex oxide systems.

Acknowledgements: This work was financed by UEFISCDI, through the PN-III-P4-PCE-2021-1906 PCE97/2022 project, Ministry of Education and Research, Romania and performed using C400 Photoplasmat facility equipment.

Effect of Nitrogen Content on Physical and Mechanical Properties of Tantalum Nitride Films

Marius MOCANU[1,2], Flaviu BAIASU[1], Mihaela GHERENDI[1], Claudia Paraschiva DRAGOMIR[3], Diana Maria VRANCEANU[3], Alina VLADESCU(DRAGOMIR)[4], Eduard GRIGORE[1]

[1]*National Institute for Laser, Plasma and Radiation Physics, Magurele 077125, Romania*
[2]*Doctoral School of Industrial Engineering and Robotics, UNSTPB, Bucharest 060042, Romania*
[3]*DRUGON INTERNATIONAL SRL, Tractorului str., no. 2, Cumpana 907105, Romania*
[4]*National Institute for Optoelectronics, Magurele 077125, Romania*
Corresponding author: *mocanu.marius@inflpr.ro*

Transition metal compounds in general and nitrides in particular have attracted great interest from the scientific community over the years due to their remarkable properties in terms of mechanical properties, chemical stability and high melting point, to name just a few. By far, Ti compounds have received the most attention due to a combination of ease of production, low cost and versatility of their properties, while the other transition elements have received limited attention. Tantalum is one of these elements that received limited attention. Most studies related to tantalum are connected to application of tantalum nitride (TaN) in the field of semiconductor industry due to its outstanding properties such as low temperature [1] and voltage coefficient of resistivity [2], high thermal stability and barrier capabilities in electronic interconnection [3]. On the other hand, its high melting point and high microhardness values recommend TaN as a possible candidate for tribological application.

In this paper TaN films with various nitrogen contents, intended for use as hard coatings, were deposited by Magnetron Sputtering (DCMS) method and High-Power Impulse Magnetron Sputtering (HiPIMS). The study was performed to assess the correlations between relevant deposition parameters (in particular nitrogen flow rate) and physical and mechanical properties of the films.

Structural and chemical characterizations were performed by X-ray diffraction (XRD) and Glow Discharge Optical Emission Spectrometry (GDOES), respectively. The morphology of the films was characterized by Scanning Electron Microscopy (SEM), while mechanical properties were evaluated by microhardness measurements and wear resistance investigations using a pin-on-disc tribometer. The thickness of the deposited layers was in the range of 3-5 μm. XRD measurements indicated a mixture of Ta and Ta_2N phases for the coatings with high microhardness values. It was found that the hardness of the films increases with nitrogen content, with a highest value corresponding to a nitrogen content of ~20 at.% while the size of the crystalline grains decreases significantly. As far it concerns the microhardness, a value of 2500 HV0.025 was measured for the film with 20 at.% nitrogen content.

Acknowledgements: This work was financed by project 95PED (PN-IV-P7-7.1-PED-2024-1580), Ministry of Education and Research, Romania.

[1] N. Arshi, J. Lu, Y.K. Joo, J.H. Yoon, B.H. Koo, "Effects of nitrogen composition on the resistivity of reactively sputtered TaN thin films," Surf. Interface Anal. **47**(1), 154-160 (2015).
[2] Y. J. Lee, B. S. Suh, S. K. Rha, C. O. Park, "Structural and chemical stability of Ta-Si-N thin film between Si and Cu," Thin Solid Film **320**(1), 141-146 (1998).
[3] K. H. Min, K. C. Chun, K. B. Kim, "Comparative study of tantalum and tantalum nitrides (Ta_2N and TaN) as a diffusion barrier for Cu metallization," J. Vac. Sci. Technol. B **14**(5), 3263-3269 (1996).

Carbon-Metal Composite Coatings Obtained by DC Sputtering

Emilia VISAN[1], Arcadie SOBETKII[1], Valentina CAPATINA[1], Cristian Petrica LUNGU[2], Bianca-Georgiana SOLOMONEA[2,3], Alexandru ANGHEL[2], Cornel STAICU[2], Bogdan BUTOI[2], Corneliu POROSNICU[2], Paul DINCA[2], Oana POMPILIAN[2], Anca Constantina PARAU[4], Mihaela DINU[4], Lidia Ruxandra CONSTANTIN[4], Alina VLADESCU (DRAGOMIR)[4], Catalin VITELARU[4]

[1]*MGM Star – Bucharest, Romania*
[2]*National Institute for Laser, Plasma and Radiation Physics, Low Temp. Plasma Laboratory, Magurele 077125, Romania*
[3]*Doctoral School of Physics, Faculty of Physics, University of Bucharest, Magurele 077125, Romania*
[4]*National Institute for Research and Development in Optoelectronics INOE 2000, Magurele, 077125, Romania*
Corresponding author*:* *cristian.lungu@inflpr.ro*

Carbon-metal composite coatings were synthesized via direct current (DC) magnetron sputtering using an Inconel 600 target (25 cm diameter) operated at 500 V and 1 kW. Simultaneously, a high-density graphite target was sputtered using High-Power Impulse Magnetron Sputtering (HiPIMS), with a pulse repetition frequency of 900 Hz, a pulse width of 65 µs (5.9% duty cycle), and an average power of 6 kW. Substrate biasing was achieved using a separate DC power supply delivering 1 kW [1].

The deposited films were systematically characterized in terms of morphology, composition, microstructure, surface chemistry, thickness, microhardness, and tribological behavior. Comparative analysis reveals that carbon incorporation is essential for the formation of a mechanically stable tribological layer. Furthermore, the controlled addition of oxygen significantly enhances coating performance by promoting the development of a mixed metallic–oxide microstructure.

This structural evolution leads to a marked increase in hardness, from 0.84 GPa to 1.59 GPa, improved adhesion, and a substantial reduction in friction and wear. The enhanced tribological response is attributed to the formation of chromium- and nickel-based oxide phases, which act as solid lubricants and protective barriers during sliding contact.

These results demonstrate that the tribological properties of NiCrFe-based coatings can be effectively tailored through oxygen incorporation. Fig 1 presents the coefficient of friction behavior.

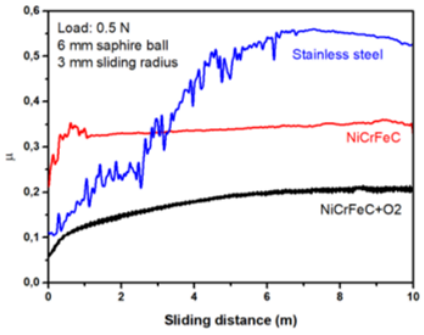

Fig. 1. Coefficient of friction behavior of the prepared layers: 0.5N load, 6 m sapphire ball, 15 mm/s sliding speed.

In particular, the NiCrFeC+O_2 system exhibits a stable friction coefficient of approximately 0.20 and minimal wear, defining a promising parameter window for low-friction, dry-sliding applications. Such coatings are especially suitable for environments where conventional lubrication is impractical, including high-temperature systems, vacuum conditions, and components requiring extended service life with minimal maintenance.

Acknowledgements: This work was supported by the Ministry of Education and Research, Romania, UEFISCDI, Grants No. 13PTE/2025and Grant No.37 PTE/2025

[1] B. G. Solomonea, A. Anghel, C. P. Lungu, C. Staicu, B. Butoi, C. Porosnicu, P. Dincă, O. Pompilian, A. Sobetkii, A. C. Parau, M. D. L. R. Constantin, A. Vladescu (Dragomir), and C. Vitelaru, "Oxygen Addition Influence on NiCrFe Mixed Layers," Coatings **16**(1), 96-106 (2026).

Morphological Transfer of Superhydrophobic Features from Laser-Ablated Metallic Molds to Flexible Polymer Replicas

Iuliana URZICA, Mihaela BOJAN, Petronela GHEORGHE, Cristian UDREA

National Institute for Lasers Plasma and Radiation Physics, Măgurele 077125, Romania
Corresponding author: *cristian.udrea@inflpr.ro*

The rapid evolution of nanotechnology has necessitated the development of advanced surfaces with precise wetting properties for applications in nanobiotechnology, electronics, and microfluidics [1].

This study presents an innovative, flexible, and cost-effective method for the fabrication of superhydrophobic metallic molds using nanosecond laser ablation. A nanosecond pulsed Nd:YAG laser (λ=355 nm, τ=6 ns, f=10 Hz, laser beam energy E=0.6÷130 mJ) was employed was employed to functionalize aluminum alloy surfaces. Inspired by biomimetic structures such as lotus leaf, the proposed system generates hierarchical surface morphologies capable of sustaining stable Cassie-Baxter states with water contact angles exceeding 150°.

These laser-patterned metallic surfaces function as high-fidelity "fingerprints" for the replication of micro- and nanostructures onto flexible polymeric substrates, including polydimethylsiloxane (PDMS) and polyethylene terephthalate (PET). The resulting polymeric substrates retain the essential functional attributes of the metallic molds, offering extreme water repellency, self-cleaning capabilities, and enhanced resistance to bio-fouling and corrosion.

By integrating nanoscale characterization techniques - such as Scanning Electron Microscopy (SEM), X-ray Photoelectron Spectroscopy (XPS), and profilometry - the study demonstrates that the resulting polymeric substrates fully retain the essential functional attributes of the metallic molds.

This method represents a reliable and efficient alternative to conventional lithographic techniques, offering a practical solution to current industrial challenges, such as high production costs and limited scalability in the fabrication of functionalized polymer surfaces.

Acknowledgements: This work was financed by project 43TE/2025, PN-IV-P2-2.1-TE-2023-1686 and program NUCLEU-LAPLAS VII 30N/2023, Ministry of Education and Research, Romania.

[1] C.V. Ngo, D. M. Chun, “Fast wettability transition from hydrophilic to superhydrophobic laser-textured stainless-steel surfaces under low-temperature annealing,” Appl. Surf. Sci. **409**, 232-240 (2017).

Microwave Plasma-Synchronized Co-Vaporization Enables Plasmon-Free, Interface-Dominated Optical Response at Sub-Percent Metal Loadings

Natalia MIHAILESCU[1], Marian MOGILDEA[2], Oana BRINCOVEANU[3], Cosmin ROMANITAN[3], Bogdan S. VASILE[4,5], Nikolay DJOURELOV[6], Andreea Bianca SERBAN[6], George MOGILDEA[2]

[1]*National Institute for Laser, Plasma and Radiation Physics, Magurele 077125, Romania*
[2]*Institute of Space Science - INFLPR, Magurele 077125, Romania*
[3]*National Institute for Research and Development in Microtechnologies, Voluntari 077190, Romania*
[4]*National Research Center for Micro and Nanomaterials, Bucharest National Polytechnic University of Science and Technology, Bucharest 060042, Romania*
[5]*Research Center for Advanced Materials, Products and Processes, Bucharest National Polytechnic University of Science and Technology, Bucharest 060042, Romania*
[6]*Extreme Light Infrastructure - Nuclear Physics, "Horia Hulubei" National R&D Institute for Physics and Nuclear Engineering (IFIN-HH), 30 Reactorului Street, Magurele 077125, Romania*
Corresponding author: natalia.serban@inflpr.ro

In conventional plasmonic systems, strong optical behavior is typically associated with significant metal loadings required to sustain collective electron oscillations. Here, we demonstrate that comparable optical effects can emerge in the complete absence of plasmonic excitation at sub-percent metal loadings. This is achieved through a microwave plasma-synchronized co-vaporization process that enforces synchronized vaporization of core–shell metallic wire precursors (Pb sheath with Au cores), ensuring simultaneous vaporization of all components. The process operates via a field-emission-driven plasma–material feedback mechanism under strongly non-equilibrium conditions, enabling atomic-level mixing, in situ oxidation, and rapid quenching. As a result, ultrafine (~3-5 nm) PbO and PbO–Au nanocomposites are formed, consisting of a crystalline β-PbO matrix embedding metal clusters encapsulated by a thin amorphous Pb^{4+}-rich (PbO_2-like) surface layer.

Despite sub-percent metal content, the nanocomposites exhibit pronounced, metal-dependent optical behavior, including band gap shifts and distinct color changes, in the absence of localized surface plasmon resonance features, placing the system in a sub-plasmonic regime.

These findings demonstrate that strong optical responses can originate from interface-driven electronic interactions rather than plasmonic excitation. Microwave plasma-synchronized co-vaporization thus establishes a scalable route to plasmon-free, ligand-free, and interface-dominated optical behavior in metal–oxide nanocomposites.

Acknowledgements: This work was financed by program NUCLEU-LAPLAS VII 30N/2023, Ministry of Education and Research, Romania.

Evaluation of a DBD Linear Plasma Source for Pest Control

Bogdana MITU[1], Cristian STANCU[1], Catalin I. CONSTANTIN[1,2], Andrei TEODORU[3], Constantina CHIRECEANU[4]

[1]*National Institute for Lasers, Plasma and Radiation Physics, Magurele 077125, Romania*
[2]*Faculty of Physics, University of Bucharest, 405 Atomistilor Str., Magurele 077125, Romania*
[3]*Institute for Research and Development in Plant Protection,8 Ion Ionescu de la Brad 8 Blv., Bucharest 013813, Romania*
Corresponding author: *mitu.bogdana@inflpr.ro*

Common bean (*Phaseolus vulgaris* L.) and related legume crops such as such as chickpea, lentil, pea and cowpea, are essential sources of plant protein, carbohydrates, minerals, and dietary fibre, but their production and storage are frequently affected by insect pests. In the field, pest attacks can impair plant growth, reduce seed yield, and compromise seed quality, while during storage, insects such as bruchids and other seed-feeding pests may cause substantial postharvest losses by consuming the cotyledons, reducing seed weight, lowering germination capacity, and contaminating the stored product with frass and insect residues [1]. In this context, plasma treatment of infested seeds or stored products may represent an environmentally friendly and residue-free alternative to conventional chemical pest-control methods, contributing to safer storage, improved seed quality preservation, and reduced postharvest losses [2,3].

The present study examines the effectiveness of atmospheric-pressure plasma treatment applied to common bean seeds infested with the bean weevil *Acanthoscelides obtectus* (Order Coleoptera, Family Chrysomelidae). The experiments have been performed by using a linear DBD plasma jet of 10 cm width and 2 mm length generated at 13.56 MHz using an RF power of 50 W in flowing Argon as the main gas (3000 – 5000 sccm), and injected in several cases with a small amount of oxygen (1%). The treatment involved the exposure of 50 g of bean seeds infested with 30 bean weevils to the plasma in a semi-enclosed configuration that keeps the insects, while exposing them to the plasma environment during a scanning procedure. Thus, direct plasma exposure occurred only when the DBD source passed over the seed–insect mixture, corresponding to 14.25% of the total treatment time, whereas exposure to plasma-generated reactive species occurred continuously throughout the experiment. Total treatment time was chosen in the range 3 – 15 min. The insect mortality results showed complete extinction of weevils in all experiments after 10 days of evaluation. However, the rate of mortality depended on the treatment duration: the 3 min treatment reached 90% mortality after 9 days, whereas the 15 min treatment achieved the same mortality level after only 4 days. The addition of oxygen during treatment is also increasing significantly the mortality rate.

Acknowledgements: The study was performed under the project ADER 2.1.7, Ministry of Agriculture and Rural Development, Romania. The INFLPR authors acknowledge the program NUCLEU-LAPLAS VII 30N/2023, Ministry of Education and Research, Romania.

[1] T. Mesele, K. Dibaba, C.A. Garbaba, E. Mendesil, "Effectiveness of different storage structures for the management of Mexican bean weevil, Zabrotes subfasciatus (Boheman) (Coleoptera: Bruchidae) on stored common bean, Phaseolus vulgaris L. (Fabaceae)," J Stored Prod Res. **96**, 101928 (2022).
[2] M. Martami, M.S. Nikouei Fard, M. Abouheydari, et al., "Cold plasma as a dual strategy for insect control and seed quality enhancement in chickpea, lentil, and cereal by-products," Sci. Rep. **16**, 18221 (2026).
[3] M. Magureanu, C. Chireceanu, B. Mitu, "Non-thermal plasma as a tool for pest control in agriculture-a review," J. Phys. D Appl. Phys. **59**(13), 133002 (2026).

Topic 5. Energy Production and Storage

Tailored WO_x-Based Heterostructures for Electrochromic Applications

Mihaela FILIPESCU[1], Adrian Ionut BERCEA[1,2], Marius DUMITRU-GRIVEI[1], Alina RADU[1], Cristina CRACIUN[1], Alexandra PALLA-PAPAVLU[1], Maria DINESCU[1]

[1]*National Institute for Laser, Plasma and Radiation Physics, 409 Atomistilor Street, Magurele 077125, Romania*
[2]*University of Bucharest, Magurele 077125, Romania*
Corresponding author: *mihaela.filipescu@inflpr.ro*

This work reports on the fabrication and characterization of complex oxide heterostructures (AZO/$TaWO_x$/Ta_2O_5/MoS_2/WO_x/AZO) designed for integration into solid-state electrochromic devices, using pulsed laser deposition (PLD). Two distinct heterostructure configurations were developed, differing in the morphology of the active WO_x layer: nanostructured compact and mesoporous architectures.

The heterostructure containing nanostructured WO_x, deposited at an optimized substrate temperature of 500 °C, exhibited dense, uniform, and well-adhered multilayers (fig. 1a). Cross-sectional SEM analysis revealed sharp and continuous interfaces without cracks or delamination, indicating excellent structural integrity. X-ray diffraction confirmed the presence of crystalline WO_3 (tetragonal) and TaO (cubic) phases, with average crystallite sizes of ~15–18 nm and low lattice strain (<2%), suggesting good crystallinity and controlled growth.

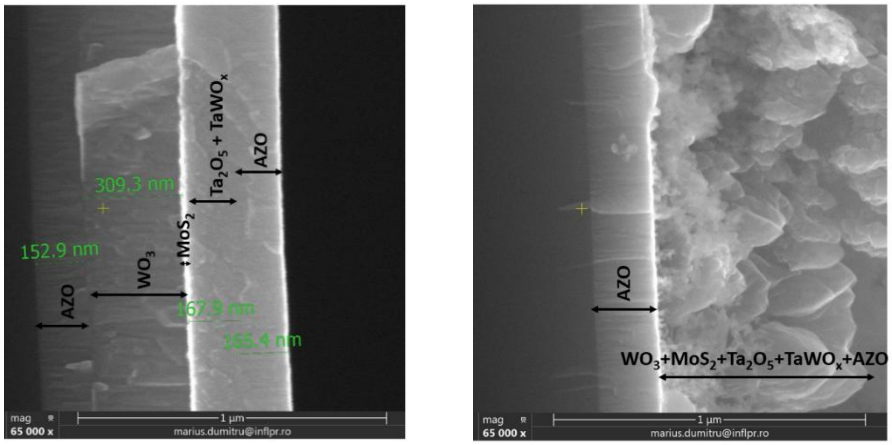

a) **b)**

Fig. 1. SEM cross-sectional images of the heterostructures incorporating **(a)** nanostructured-dense WO_x layer and **(b)** mesoporous WO_x layer

The second heterostructure (fig. 1b), incorporating mesoporous WO_x, exhibited a highly developed 3D morphology with columnar, micro-stalagmite-like features and significantly increased surface roughness (~1 µm). Although the clear stratification of the upper layers was reduced due to the highly porous morphology, the structure remained mechanically stable and free of cracks. Structural analysis revealed smaller WO_3 crystallite sizes (~5 nm) and increased lattice strain (~3.1%), indicating that porosity strongly influences crystallinity. This mesoporous architecture is particularly promising for electrochromic applications due to its enhanced surface area and potential for improved ion transport.

These results demonstrate that precise control of PLD parameters enables tuning of heterostructure morphology and properties, with dense nanostructured films ensuring mechanical robustness, while mesoporous structures provide functional advantages for electrochromic performance.

Acknowledgements: This work was supported by a grant of the Ministry of Education and Research, Romania - UEFISCDI, project number PN-IV-P7-7.1-PED-2024-1292 (ELCHROM), within PNCDI IV.

Tailoring Nanostructured WO_3 Thin Films for Transparent Electrode Applications

Maria DINESCU[1], Adrian Ionut BERCEA[1,2], Marius DUMITRU-GRIVEI[1], Alina RADU[1], Mihaela FILIPESCU[1]

[1]*National Institute for Laser, Plasma and Radiation Physics, 409 Atomistilor Street, Magurele 077125, Romania*
[2]*University of Bucharest, Faculty of Physics, Magurele 077125, Romania*
Corresponding author: *mihaela.filipescu@inflpr.ro*

This study investigates the influence of nanostructured tungsten trioxide (WO_3) films on the surface properties of transparent electrodes used in organic photovoltaics, specifically indium tin oxide (ITO) and fluorine-doped tin oxide (FTO). The aim is to improve their compatibility with the conductive polymer PEDOT:PSS used as a hole-transport layer (HTL).

We show that pulsed laser deposition (PLD) parameters, particularly the number of laser pulses, influence surface architecture, wettability, and optical behavior of WO_3.

The X-ray diffraction investigation reveals that thicker layers adopt a monoclinic structure. The integration of PEDOT:PSS with nanostructured WO_3 layers could help mitigate degradation caused by PEDOT:PSS acidity, creating interfacial conditions that have been associated in the literature with improved device stability and performance.

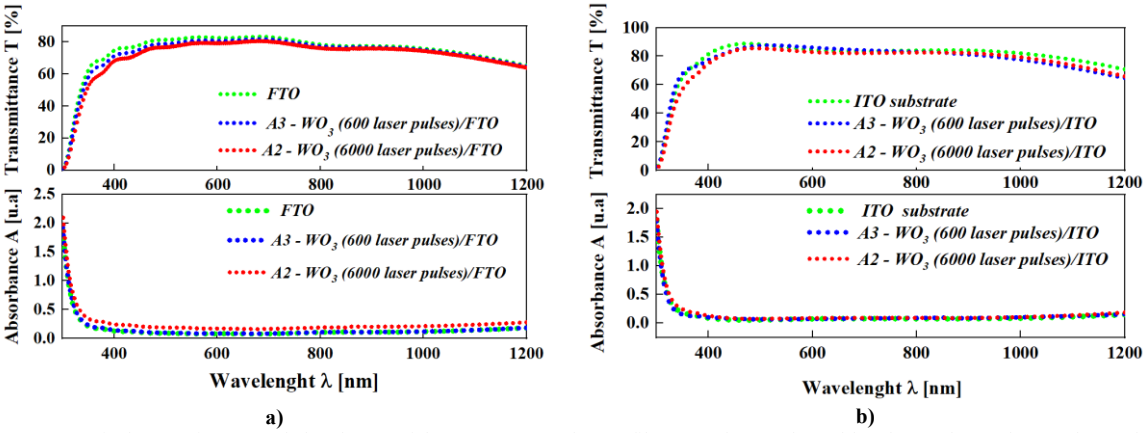

Fig. 1. Optical transmittance and absorbance of the nanostructured WO_3 films (600 laser pulses - blue dots and 6000 laser pulses red dots) on **(a)** FTO/Glass substrate (green dots); **(b)** ITO/Glass substrate (green dots)

Optical measurements show that thicker WO_3 films enhance absorption in the ultraviolet and near-infrared regions while maintaining high transmittance in the visible range (fig.1).

Additionally, the surface morphology of the WO_3 layer significantly improves electrode hydrophilicity, reducing the water contact angle and enabling uniform PEDOT:PSS deposition without changing HTL thickness.

The nanostructured WO_3 film acts as an interfacial modifier that preserves HTL thickness, an important parameter for organic photovoltaic cells and other optoelectronic devices requiring stable interfaces and efficient charge transport. These insights contribute to the optimization of transparent electrodes for enhanced efficiency in organic photovoltaic applications.

Acknowledgements: This work was supported by a grant of the Ministry of Education and Research, Romania - UEFISCDI, project number PN-IV-P7-7.1-PED-2024-1292 (ELCHROM), within PNCDI IV.

Hybrid Proton-Exchange Membrane Architecture Combining Perfluorosulfonated Polymers with a Resorcinol-Formaldehyde Hydrogel Network for Energy-Efficient PEM Fuel Cell Applications

Alexandra Maria Isabel TREFILOV[1], Adriana Elena BALAN[2]

[1]*National Institute for Laser, Plasma and Radiation Physics, LASERS Department, Magurele 077125, Romania*
[2]*University of Bucharest, Faculty of Physics, 3NanoSAE Research Center, Magurele 077125, Romania*
Corresponding author: *alexandra.trefilov@inflpr.ro*

Proton-exchange membranes remain central to the advancement of high-efficiency fuel cells, driving ongoing efforts to design materials with improved hydration, stability, and ionic transport. The limitations of pristine PFSA Membranes particularly its reduced conductivity and structural relaxation at elevated temperatures have motivated the incorporation of secondary materials to reinforce the polymer network and stabilize proton-transport pathways. In this context, hybrid proton-exchange membranes were developed by integrating organic resorcinol–formaldehyde (RF) hydrogels into a perfluoro-sulfonated acid (PFSA) matrix to enhance water uptake, thermal stability, and proton transport. The study investigates how uniformly distributed RF clusters influence the structural and functional characteristics of the host polymer. The composite membranes were obtained via an in-situ sol-gel process within the membrane pores. The resin concentration was controlled by the time taken for resorcinol and formaldehyde to be impregnated using water or ethanol as solvents. The RF content was controlled by adjusting the impregnation time of resorcinol and formaldehyde precursors in either water- or ethanol-based solutions. Morphological and chemical modifications were examined using atomic force microscopy, UV–Vis spectroscopy, and Fourier-transform infrared spectroscopy. Thermal stability and degradation behaviour were assessed through thermogravimetric analysis, while proton conductivity at 80 °C under controlled relative humidity was measured using an in-plane four-point probe method.

The hybrid PFSA–RF membranes demonstrated significantly improved thermal resistance up to 46 °C higher than the pristine polymer and enhanced proton conductivity at low RF loadings, particularly under low-humidity conditions when ethanol was used as the impregnation solvent. Fuel cell testing of membrane–electrode assemblies incorporating RF-modified membranes revealed excellent gas-crossover suppression and strong electrochemical performance at 80 °C and 40% relative humidity, achieving a 76% increase in power density compared to a reference assembly containing the unmodified PFSA membrane.

Acknowledgements: This work was partially financed by the Ministry of Education and Research, Romania, under ELI-RO/RDI/2024_039, ELI-RO/RDI/2024_015, ELI-RO/RDI/2024_019, PN-IV-P7-7.1-PED-2024-0796 Projects. and program NUCLEU-LAPLAS VII – Contract No. 30N/2023.

Deposition of Boron Layers by PECVD at Low and High Deposition Rates Using Diborane as Precursor

Sorin VIZIREANU, Daniel STOICA, Tomy ACSENTE, Veronica SATULU, Marius DUMITRU, Evghenii GONCEARENCO, Florian DUMITRACHE, Gheorghe DINESCU

National Institute for Laser, Plasma and Radiation Physics, Magurele 077125, Romania
Corresponding author: sorin.vizireanu@inflpr.ro

Boron and boron-based materials are utilized in multiple industries/application fields (dopant in electronics, coatings with good mechanical properties and thermal stability, in nuclear fission for their high neutron absorption cross-section and also in fusion [1]. The boron coatings protect the tokamak walls, reduce the impurity flux and improves plasma performance. For next-generation tokamaks requiring improved life time of the W tiles, it is very important to develop and test new methods for cover tungsten with boron coatings.

In this work, we present the deposition of boron films by using two PECVD set-ups in vacuum: i) a plasma jet (J) and ii) parallel-plate electrode glow discharge (GD). For both plasma sources we used RF power supply, Argon as main gas for discharge and diborane (B_2H_6) as precursor gas. The boron films were deposited on silicon and polished tungsten as substrate, for various deposition time.

We found smooth boron film at low Ar flow and very rough films with cracks films at high Ar flows rate. For the GD case the growth rate was 4-8 nm/min, while in the jet (J) case we have high deposition rates (more than 40 times higher), by using the same flow of diborane (5 sccm). In the samples deposited in the J configuration, we found in their composition metallic boron and oxide bonds type, while in the GD samples we found mostly boron nitride bonds type. After increasing the temperatures in the jet configuration (400-700 C), we observed the formation nano-structures sponge-like cauliflower with many oxidized boron bonds in the film composition.

This work demonstrates our possibilities to obtain boron films by PECVD with high deposition rates, exceeding conventional boronization by more than one order of magnitude. These findings (high deposition rate and sponge structure) could be relevant for the optimization of boron-based deposition techniques for tokamaks. The transition from conventional nanometre-scale boronization layers to significantly thicker coatings is important for studies focused on erosion behaviour, impurity retention, and walls lifetime.

Acknowledgements: This work was financed by project 39/2024, ELI-RO Program, ELI-RO/RDI/2024_039 and program NUCLEU-LAPLAS VII 30N/2023, Ministry of Education and Research, Romania.

[1] B. Schurink, W. T. E. van den Beld, R. M. Tiggelaar, R. W. E. van de Kruijs, and F. Bijkerk, "Synthesis and Characterization of Boron Thin Films Using Chemical and Physical Vapor Depositions," Coatings **12**(5), 685 (2022).

Synthesis of Nanostructured Materials (Iron Oxide/Silica) for Nanofluids as Heat Transfer Agents

Florian DUMITRACHE[1], Iulia LUNGU[1], Anca CRIVEANU[1], Evghenii GONCEARENCO[1], Ana-Maria BANICI[1], Claudiu Teodor FLEACA[1], Lavinia GAVRILA-FLORESCU[1], Gabriela HUMINIC[2], Eugenia TANASE[3]

[1]*National Institute for Laser, Plasma and Radiation Physics, LASERS Department, Magurele 077125, Romania*
[2] *Transilvania University of Brasov, Mechanical Engineering Department, 29, Bulevardul Eroilor, Brasov 500036, Romania*
[3]*National Centre of Micro and Nanomaterials, National University of Science and Technology Politehnica, Bucharest, Romania*
Corresponding author: *florian.dumitrache@inflpr.ro*

Nanoparticles have been extensively used in advanced heat transfer systems due to their high specific surface area and tunable physicochemical properties. Particularly, transition metal oxide nanoparticles exhibit enhanced chemical stability and thermal performance when dispersed in liquids, making them promising candidates for next-generation nanofluids. These systems are of interest for energy-related applications, where improved thermal conductivity and heat exchange efficiency are critical.

This study focuses on the synthesis, by laser pyrolysis, of hybrid oxide nanoparticle aggregates based on iron oxide combined with silica, with emphasis on systems containing structurally distinct Fe-based and Si(O,C) phases. The Fe and Si precursors used in the CO_2 laser pyrolysis experiments were iron pentacarbonyl ($Fe(CO)_5$) and hexamethyldisiloxane (HDMSO), respectively. Three morpho-structural configurations were investigated: physically mixed aggregates, homogeneous mixed oxides, and core-shell architectures. The most promising results were obtained for hybrid aggregates with distinct oxide phases.

These nanomaterials were obtained using laser pyrolysis, a highly versatile and controllable technique capable of producing nanoparticles with narrow size distribution (from a few to tens of nanometers) and high production rates, favourable conditions for obtaining nanofluids. The morpho-structural characterizations include TEM, SEM-SAED, EDX, XRD. The resulting materials consist of loosely packed NPs aggregates that have been stabilized with carboxymethyl cellulose (CMC-Na) in aqueous based suspensions and analysed for their stability (DLS) and thermal conductivity. These findings highlight the potential of laser pyrolysis-derived hybrid nanomaterials used for obtaining efficient nanofluid components for heat transfer applications.

Acknowledgements: *This work was financed by CCCDI - UEFISCDI, project number PN-IV-P6-6.1-CoEx2024-0154, within PNCDI IV and Program LAPLAS VII - contract no. 30N/2023, Ministry of Education and Research, Romania*

New Complex Nanofluids Based on Laser Pyrolysis Synthesized Si-SiC Nanoparticles and Natural Aluminosilicate Short Nanotubes

Claudiu Teodor FLEACA[1], Florian DUMITRACHE[1], Anca BADOI[1], Ana-Maria NICULESCU[1], Lavinia GAVRILA-FLORESCU[1], Iuliana MORJAN[1], Nicu D. SCARISOREANU[2], Ioan Mihail GHITIU[2], Razvan DUMITRACHE[3], Gabriela HUMINIC[4]

[1]*National Institute for Laser, Plasma and Radiation Physics, LASERS Department, Magurele 077125, Romania*
[2]*National Institute for Laser, Plasma and Radiation Physics, FOTOPLASMAT Department, Magurele 077125, Romania*
[3]*Faculty of Physics, University of Bucharest, Magurele 077125, Romania*
[4]*Transilvania University of Brasov, Mechanical Engineering Department, 29, Bulevardul Eroilor, Brasov 500036, Romania*
Corresponding author: claudiu.fleaca@inflpr.ro

Benefiting from laser pyrolysis technique versatility we obtained first the composite nanopowders that show the signature of both elemental silicon and silicon carbide phases with mean crystalline sizes (from XRD) of 17.7 and 5.97 nm, respectively. The resulted mixt stoichiometry was possible by using an excess of silane over acetylene gas precursor, first gas playing also the laser energy transfer agent role [1]. For the nanofluids preparation we first dissolved 4 g/l hydrophylizing anionic polyelectrolyte sodium carboxymethylcellulose (CMCNa, low viscosity type) in water using a rotation-vibration device and an ultrasonic bath. Then a mixture of composite silicon-based nanopowder and natural aluminosilicate clay short nanotubes ($Al_2Si_2O_5(OH)_4 \cdot 2H_2O$ halloysite type, noted HNTs) [2] with 50-70 nm mean diameters and few micrometers/submicronic lengths were added to the polymer solution and preliminary dispersed using domestic rotational twin blade mixer. The light grey-brown suspension was then transferred into a tronconical stainless steel recipient and further processed using a powerful ultasonication horn (1000 W) during one hour with the elimination of the generated heat via an external cool water bath. The suspensions up to 8 g/l total particle concentrations (containing equal masses of the two types of solids) were investigated by Dynamic Light Scattering (DLS) showing polydisperse populations of hundreds of nanometers and few microns mean hydrodynamic sizes for lower concentration, whereas for highest one monodispersity accompanied by diminished mean diameter appears probably due to abrasive role of Si/SiC NPs on HNTs in crowded environment under strong ultrasonication. Also, considerable negative Zeta potential values were identified for all nanofluids due to the presence of polyanionic CMCNa. They and also presented limited viscosity increase (under 20%) versus pure water accompanied with a notable enhancing of thermal conductivity. Also, TEM images from dry suspension deposit revealed a homogeneous mixture of the silicon-based different nanoparticles with rounded shapes and also short tubules and their fragments, with polymer coatings. Moreover, EDS mapping identified the main elements in suspensions: Si, C, Al, O and also Na from ionic polymer.

Acknowledgements: *This work was financed by CCCDI - UEFISCDI, project number PN-IV-P6-6.1-CoEx2024-0154, within PNCDI IV and Program LAPLAS VII - contract no. 30N/2023, Ministry of Education and Research, Romania*

[1] G. Huminic, A. Huminic, C. Fleaca, F. Dumitrache, I. Morjan, "Thermo-physical properties of water based SiC nanofluids for heat transfer applications," Int. Commun. Heat Mass Transfer **84**, 94-101 (2017).
[2] J. A. Alberola, R. Mondragón, J. E. Juliá, L. Hernández, L. Cabedo, "Characterization of halloysite-water nanofluid for heat transfer applications," Appl. Clay Sci. **99**, 54-61 (2014).

Topic 6. Life Sciences Applications

Ceramic-Composites Surfaces for Pareodontal Applications

Laurentiu RUSEN, Anca BONCIU, Luminita Nicoleta DUMITRESCU, Valentina DINCA

National Institute for Laser, Plasma and Radiation Physics, Magurele 077125, Ilfov, Romania
Corresponding author: *laurentiu.rusen@inflpr.ro*

Bioinstructive micro- and nanotextured composite ceramic interfaces are redefining the role of implant surfaces from passive boundaries to active regulators of tissue response. By combining the mechanical robustness and chemical stability of ceramics with hierarchical micro/nanotopographies and multifunctional hybrid compositions, these interfaces can direct the earliest biological events at the biomaterial–tissue interface.

In this study, zirconia-polymer composites were developed into microstructured membranes for periodontal applications. The membranes were characterized by contact angle and surface energy measurements, as well as SEM, EDAX, and AFM analyses, to assess their wettability, morphology, composition, and surface topography. Preliminary in vitro results showed no cytotoxic effects, although the degradation profile varied depending on membrane composition.

Acknowledgements: *This work was financed by project 97PED/2025 and program NUCLEU-LAPLAS VII 30N/2023, Ministry of Education and Research, Romania.*

Physicochemical Properties of Calcium Phosphate-Poly (methyl methacrylate) Composite Layers Produced by Radio Frequency Magnetron Sputtering Technique

Andreea GROZA, Maria Elena HURJUI, Sasa-Alexandra YEHIA-ALEXE, Bogdan BUTOI

National Institute for Laser, Plasma and Radiation Physics, CETAL Department, Magurele 077125, Romania
Corresponding author: andreea.groza@inflpr.ro

Magnetron sputtering discharges represent powerful techniques for synthesis of ceramic and ceramic-polymer composite layers for biomedical applications [1, 2]. Among these materials, of large interest are calcium phosphates and poly(methyl-methacrylate). As layers, such compounds are used in orthopedical prothesis for improvement of their mechanical properties.

In this work, the incorporation of poly(methyl-methacrylate) in layers containing calcium phosphate has been performed by radio-frequency (rf) magnetron sputtering technique. This process is developed at two working powers of 50 and 150 W.

The spectral analysis of the plasma obtained in Ar gas reveals the excitation and ionization processes encountered during the deposition processes. The intensities of the Ca I, P I, H_α atomic lines and CaO, PO, POH, CO, CH, C_2 molecular bands varies as function of the applied rf power. These findings, in correlation with dissociation, excitation, and ionization energies of the atoms and molecules from the plasma allow the establishment of the dissociation pattern of poly(methyl-methacrylate).

The depositions at highest rf power modify substantially the chemical structure of the polymer, polymer type and the layer morphologies. At 50 W the polymer molecular structure revealed by Fourier Transform Infrared Spectroscopy remain unaltered for a Ca/P ratio of 1.72. At 150 W the IR spectral characteristic bands of the polymer are reduced and revealed only by peak fitting analysis, while the Ca/P ratio increases up to 1.9 due to the formation of tetra-calcium phosphate compounds. As the working power increases, the surface morphologies evolve from grain-like to worm-like structures. The surface of the CaP-PMMA composite layer produced at 150 W is dominated by C-C/C-H, C-OH/C-O-C polymeric bonds due to plasma polymers formation as XPS studies show.

The relationship between the rf power, the plasma processes and the composite layer properties will be presented and discussed.

Acknowledgements: This research was supported by Ministry of Education and Research, Romania, National Core Program NUCLEU-LAPLAS VII - contract no. 30N/2023.

[1] A. Groza, M. E. Hurjui, S. A. Yehia-Alexe, B. Butoi, S.D. Stoica, "Calcium Phosphate-Poly(methyl-methacrylate) Composite Layers Synthetized in Radio-Frequency Magnetron Sputtering Discharge," Polymers (Basel) **18**, 547 (2026).

[2] M. E. Zarif, S. A. Yehia-Alexe, B. Bita, I. Negut, C. Locovei, A. Groza, "Calcium Phosphates-Chitosan Composite Layers Obtained by Combining Radio-Frequency Magnetron Sputtering and Matrix-Assisted Pulsed Laser Evaporation Techniques," Polymers (Basel) **14**, 5241 (2022).

Influence of Selenium Doping on the Mechanical Properties, Wettability, Dissolution Resistance, and *In Vitro* Apatite-Forming Ability of Pulsed Laser Deposited Biogenic Calcium Phosphate Thin Films

Gabriela DORCIOMAN[1], Daniel CRISTEA[2], Sohail Muhammad ASGHAR[3], Gianina POPESCU-PELIN[1], Valentina GRUMEZESCU[1], Irina ZGURA[4], Ali Oguz ER[5], Oguzhan GUNDUZ[6], Liviu DUTA[1]

[1]*Lasers Department, National Institute for Laser, Plasma and Radiation Physics, Magurele 077125, Romania*
[2]*Transilvania University of Brasov, Brasov, Romania*
[3]*Ministry of Education Key Laboratory of Green Preparation and Application for Functional Materials, Scool of Materials Science and Engineering, Hubei University, 430062 Wuhan, China*
[4]*National Institute of Materials Physics, Magurele 077125, Romania*
[5]*Department of Physics and Astronomy, Western Kentucky University, Bowling Green, 42101 KY, USA*
[6]*Center for Nanotechnology and Biomaterials Application and Research (NBUAM), Marmara University, 34722 Istanbul, Turkey*
Corresponding author: liviu.duta@inflpr.ro

We report here the synthesis, by Pulsed Laser Deposition, of undoped and selenium-doped (0.5 and 1 wt.%) calcium-phosphate thin films obtained from abundant, renewable, and low-cost bovine bone resources. The investigated structures, namely BioCaP, BioCaP:Se0.5, and BioCaP:Se1, were comparatively assessed from the mechanical, structural, morphological, compositional, wetting, dissolution-resistance, and in vitro apatite-forming perspectives.

Adhesion tests showed a clear mechanical benefit associated with Se, with the bonding strength values of the Se-doped BioCaP films being approximately 1.5 times higher than those of BioCaP and more than three times above the minimum threshold set by international standards. Selenium also lowered the coefficient of friction and improved scratch resistance, underscoring a consistent strengthening effect.

X-ray Diffraction revealed thin, crystalline BioCaP layers dominated by hydroxyapatite (HA) reflections. Fourier Transformed InfraRed (FTIR) spectroscopy displayed the characteristic phosphate vibrations and indicated that Se acts as a structural modifier within the HA lattice. Surface imaging showed rough, irregular films, build from spherical to ovoid aggregates with a broad size distribution. Se increased particle size and density, pointing to a dopant-mediated change in growth during deposition.

Wetting measurements captured a pronounced shift from the hydrophobic Ti controls (contact angle, CA ~ 121°) to super superhydrophilic behaviour (CA < 5°) for the Se-doped films.

In aqueous media, all BioCaP films followed the expected sequence of initial dissolution followed by biomimetic CaP reprecipitation. Selenium accelerated apatite nucleation and growth, with BioCaP:Se0.5 transforming most rapidly toward dense spherulitic layers. After 30 days in simulated body fluid, BioCaP:Se0.5 developed a compact acicular network of well-interconnected particles, consistent with advanced biomimetic mineralization. FTIR band narrowing further supported the Se-driven acceleration of CaP nucleation and improved phase ordering, highlighting the beneficial role of Se in promoting biomineralization.

Beyond the performance imparted by Se doping, the use of bovine-derived feedstock emphasizes sustainability and cost effectiveness, positioning BioCaP:Se thin films as attractive, renewable alternatives to synthetic HA for bone-implant applications.

Acknowledgements: GD, GPP, VG, and LD acknowledge support from the Ministry of Education and Research, Romania, under Romanian National NUCLEU Program LAPLAS VII – Contract No. 30N/2023. All authors would like to thank G.E. Stan for his helpful discussions regarding XRD results.

Biofunctional Oxide Coatings for the Surface Modification of Alloy-Based Implants

Oana GHERASIM[1], Stefan IRIMICIUC[1], Gabriela DORCIOMAN[1], Valentina GRUMEZESCU[1], Liviu DUTA[1], Bianca GALATEANU[2], Ariana HUDITA[2]

[1]*National Institute for Laser, Plasma and Radiation Physics, Magurele 077125, Romania*
[2]*University of Bucharest, Department of Biochemistry and Molecular Biology, Bucharest 050095, Romania*
Corresponding author: valentina.grumezescu@inflpr.ro

Surface modification of metallic implants using laser-processed coatings has attracted significant attention for orthopaedic and orthodontic applications due to its potential to enhance implant functionality, including biomechanical performance, bioactivity, and long-term clinical stability. In this context, composite coatings represent a promising strategy, as they combine improved corrosion resistance with superior biocompatibility, while fulfilling the stringent biological requirements for implantable medical devices. Alloy-based bone implants are designed to provide mechanical support during the initial implant process. Following bone regeneration, their controlled degradation enables them to effectively serve as temporary therapeutic replacements. Consequently, a thorough understanding of interfacial bonding within composite coatings, as well as their degradation behaviour under physiological conditions, is essential for the development of reliable biofunctional implant surfaces. The interfacial bonding between different layers within the composite coating and the degradation behavior need to be thoroughly studied when developing biofunctional coatings for alloy-based implants.

In the present study, metallic surfaces (Ti-6Al-4V, Co-Cr, or Mg-alloys) were modified with nanostructured oxide-based coatings (e.g. ZnO) fabricated by laser processing. Detailed compositional and microstructural analyses provided critical insight into the coatings' functional behaviour under biosimulated conditions. The biological performance was evaluated using the human pre-osteoblastic hFOB 1.19 cell line, a well-established *in vitro* model for osteoprogenitor response at the bone–implant interface. The nanostructured coatings exhibited a significantly enhanced ability to support osteoblast-related cellular responses, as evidenced by improved cell adhesion, cytoskeletal organization and spreading, as well as increased viability and proliferation. The combined cellular and hemocompatibility findings highlight the beneficial interaction between nanostructured oxide surfaces and bone-forming cells, a key prerequisite for successful osseointegration. Overall, the superior biocompatibility of the proposed laser-processed nanostructured oxide coatings supports their potential to enhance the bioactivity of metallic implant surfaces and to contribute to the development of next-generation implantable devices for bone-related applications.

Acknowledgements: This work was financed by project number PN-IV-P2-2.1-TE-2023-1950 within PNCDI IV, Ministry of Education and Research, Romania.

Picosecond Laser-Induced Periodic Surface Structures on $TiAl_6V_4$: Dual-Functionalization for Metallic Implants

Emanuel AXENTE[1], Florin JIPA[1], Paula FLORIAN[1,2], Madalina ICRIVERZI[1,2], Gianina POPESCU-PELIN[1], Adrian CERNESCU[3], Roxana Eliss BUDEI[4], Dragos BUDEI[5], Koji SUGIOKA[6], Felix SIMA[1,6]

[1]*National Institute for Laser, Plasma and Radiation Physics (INFLPR), Magurele 077125, Romania*
[2]*Institute of Biochemistry of the Romanian Academy, 296 Splaiul Independentei, Bucharest 060031, Romania*
[3]*Nanoscale Analytics @ attocube systems GmbH, Eglfinger Weg 2, 85540 Haar, Germany*
[4]*University of Medicine and Pharmacy "Carol Davila" Bucharest, Endodontics Department, Romania*
[5]*Dentix Millennium SRL, Giurgiu 087153, Romania*
[6]*RIKEN Center for Advanced Photonics, 2-1 Hirosawa, Wako, Saitama, 351-0198, Japan*
Corresponding authors: emanuel.axente@inflpr.ro, felix.sima@inflpr.ro

Materials processing with picosecond laser pulses is an efficient tool for the fabrication of various kinds of micro- and nanostructures, and thus the creation of new functionalities [1]. In particular, laser-induced periodic surface structures (LIPSSs) has proved the possibility of surface improvement for metallic implants [2]. Surface functionalization of Titanium is often necessary to *improve osseointegration* in case of implants and *minimize bacterial invasion* for dental abutments. Here we present the fabrication of LIPSSs on large scale TiAl6V4 surfaces, by laser-texturing (τ_{las}<10 ps, λ=532 nm, f=500 kHz), in a fast but contamination-free approach, followed by morpho-chemical analyses by SEM and s-SNOM. To prove dual-functionalization of the surfaces, the behavior of human mesenchymal stem cells, primary human gingival epithelial cells, and gingival fibroblast cells, in response to laser-textured samples is investigated. We show that LIPSSs are beneficial for improving cells adhesion while minimizing the risk of bacterial infection. By inducing favorable cellular responses in the hard and gingival tissues, LIPSS may contribute to faster biological sealing of the prosthetic abutment area, following dental procedures.

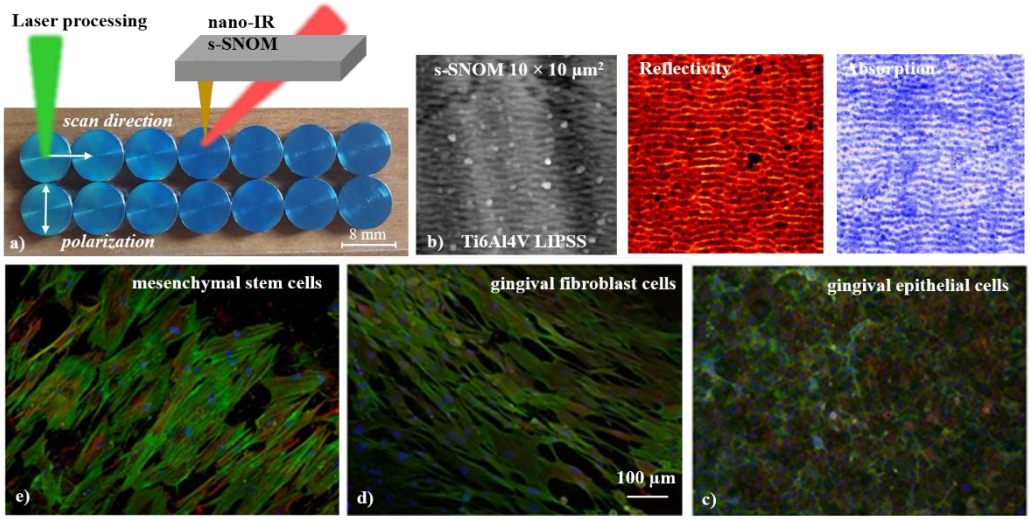

Fig. 1. (a) Large-scale laser-texturing of TiAl6V4 surfaces. **(b)** s-SNOM images of LIPSSs (height, amplitude, phase). **(c)** Immunofluorescence images of hGEpiCs, **(d)** hGFCs and **(e)** hMSCs in contact with laser processed TiAl6V4. Proteins visualization: actin (green), vinculin (red), nucleus (Hoechst-blue).

Acknowledgements: *This work was supported by POC 361 project (SMIS 122040), by the Ministry of Education and Research, Romania, under Romanian National Programme NUCLEU-LAPLAS VII 30N/2023, and PCE89 projects. We acknowledge the support of the National Interest Infrastructure facility IOSIN – CETAL at INFLPR.*

[1] R. Stoian and J. Bonse, "Ultrafast Laser Nanostructuring - The Pursuit of Extreme Scales (Springer Nature)," Cham (2023).
[2] P. Florian M. Icriverzi, F. Jipa, A. Cernescu, G. Popescu-Pelin, R. Eliss Budei, D. Budei, E. Axente, K. Sugioka, F. Sima, "Fabrication, s-SNOM Characterization and in vitro Testing of Laser-Induced Periodic Surface Structures for Dental Abutment Applications," IEEE Photonics J. **18**(2), 3700113 (2026).

Influence of the Sensitizer in the Synthesis Process of Iron Oxide Nanoparticles Obtained by Laser Pyrolysis

Anca CRIVEANU[1], Iulia LUNGU[1], Claudiu Teodor FLEACA[1], Florian DUMITRACHE[1], Iuliana MORJAN[1], Lavinia GAVRILA[1], Ana BANICI[1], Vlad SOCOLIUC[2,3]

[1]*National Institute for Laser, Plasma and Radiation Physics, Laser Department, Laboratory of Laser-Induced Photochemistry, Magurele 077125, Romania*
[2]*Romanian Academy-Timisoara Branch, Center for Fundamental and Advanced Technical Research, Laboratory of Magnetic Fluids, 24 Mihai Viteazu Ave., 300223 Timisoara, Romania*
[3]*Politehnica University of Timisoara, Research Center for Complex Fluids Systems Engineering,1 Mihai Viteazu Ave., 300222 Timisoara, Romania*
Corresponding author: anca.criveanu@inflpr.ro

Magnetic iron oxide nanopowders were synthesized via laser pyrolysis, utilizing ethylene, isopropyl alcohol, and ethanol as sensitizers. In this process, energy from a continuous-wave (CW) CO_2 laser—operating at a wavelength of 9.25 μm is transferred to the precursors through excited sensitizer molecules, inducing rapid thermal decomposition of the $Fe(CO)_5$ vapor in an oxygen atmosphere.

The primary distinction between ethylene and alcohol-based sensitizers lies in the chemical purity and dispersibility of the resulting nanopowders. XRD analysis revealed that switching to alcohols reduced the crystallite size from 10–15 nm to 3–10 nm. Furthermore, alcohol vapors yield more hydrophilic nanoparticles, enhancing their dispersibility in aqueous media for biomedical applications. This was confirmed by DLS measurements in distilled water, which showed significantly smaller aggregate sizes for alcohol-sensitized samples (43 nm for isopropanol and 88 nm for ethanol) compared to ethylene (138 nm).

This improved dispersion is attributed to a drastic reduction in carbon content, which drops from 4% to 0.5% when alcohols are used. The lower carbon concentration allows the iron oxide surface to interact more effectively with water molecules via -OH groups. Consequently, these nanoparticles are easier to functionalize with biomolecules, such as L-DOPA, making them ideal candidates for nanomedicine. Despite these structural differences, all three samples exhibited superparamagnetic behavior with a saturation magnetization exceeding 60 emu/g.

Acknowledgements: The work of A. Criveanu, I. Lungu, I. Morjan, L. Gavrila and F. Dumitrache was financed by program NUCLEU-LAPLAS VII 30N/2023, Ministry of Education and Research, Romania. The work of V. M. Socoliuc was supported by ECO NEXUS project (PCIDIF/159/PCIDIF_P1/OP1/RSO1.1/PCIDIF_A1).

Multifunctional Ultra-Small Nanoparticles: Antimicrobial Action and Photocatalytic Performance

Alexandru-Mihai IAMANDI[1,2], Liviu - Daniel GHICULESCU[2], Alexandru DAN[1], Florina ZORILA[3], Mioara ALEXANDRU[3], Cezar NET [1], Ioan GHITIU [1], Nicu D. SCARISOREANU[1]

[1]*National Institute for Laser, Plasma and Radiation Physics, FOTOPLASMAT Department, Magurele 077125, Romania*
[2]*National University of Science and Technology POLITEHNICA Bucharest, Splaiul Independenței 313, Bucharest 060042, Romania*
[3]*National Research and Development Institute for Nuclear Physics and Engineering "Horia Hulubei", Magurele 077125, Romania*
Corresponding author: alexandru.iamandi@inflpr.ro

Ultra-small nanoparticles are promising materials with multiple useful applications, including antimicrobial activity, and photocatalysis. In this work, we study the properties of silver (Ag) and nickel (Ni) nanoparticles in different experimental systems. The nanoparticles were obtained by pulsed laser ablation in liquid (PLAL) technique, using a Nd-YAG laser working at 355nm, 532 nm and 1064 nm wavelengths. Ultrapure water was used as liquid and different laser pulse numbers were fired onto pure metallic targets (Ni, Ag) for achieving solutions with different concentrations of nanoparticles. The obtained nanoparticles were analyzed by scanning electron and high-resolution transmission electron microscopy (SEM, HR-TEM) as well as Dynamic Light Scattering (DLS) techniques with polydispersity index of less than 0.7, indicating a narrow size distribution with cationic and anionic character.

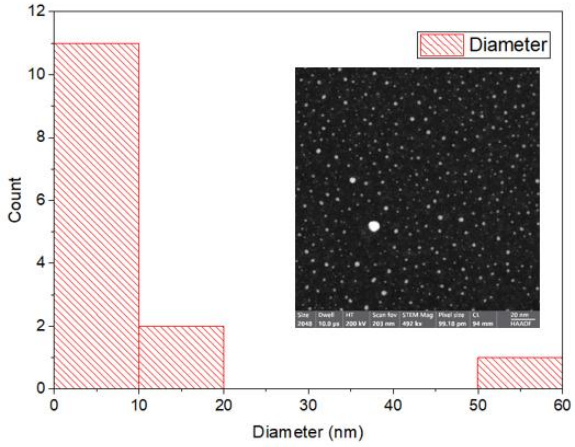

Fig. 1. Particle distribution and TEM characterization

Silver nanoparticles were tested for their ability to inhibit bacterial growth and biofilm formation. Experiments were performed on Staphylococcus aureus and Escherichia coli. The results show that Ag nanoparticles significantly reduce bacterial viability and prevent biofilm development, in agreement with previous studies. Scanning electron microscopy (SEM) images revealed clear structural damage to bacterial cells after treatment, while fluorescence microscopy confirmed metabolic inactivity of bacteria. In addition, Ni nanoparticles showed electro photocatalytic activity under light exposure, indicating possible applications in environmental remediation and energy production processes. Overall, this study demonstrates that ultra-small metallic nanoparticles can serve as multifunctional materials, combining antimicrobial effects and photocatalytic properties, making them useful for a wide range of applications.

Acknowledgements: *This work was performed using C400 PHOTOPLASMAT facilities.*

In Vitro Optimization of Bioactive Concentrations of Standardized *Aloe Vera* Extract for Wound Healing Applications

Ion Cosmin CALINA[1], Anca SCARISOREANU[1], Maria DEMETER[1], Andreea Mariana NEGRESCU[1,2]

[1]*National Institute for Laser, Plasma and Radiation Physics, Laboratory of Accelerators, Magurele 077125, Romania*
[2]*Department of Biochemistry and Molecular Biology, Faculty of Biology, University of Bucharest, 91-95 Spl. Independentei, Bucharest 050095, Romania*
Corresponding author: *calina.cosmin@inflpr.ro*

Wound healing is a complex biological process involving the coordinated action of keratinocytes and fibroblasts, key cell types responsible for re-epithelialization and extracellular matrix remodeling. Chronic wounds represent a persistent clinical challenge, driving the development of biomimetic hydrogel dressings based on natural polymers that replicate extracellular matrix properties. Aloe vera extract has attracted considerable scientific interest for its pro-proliferative, anti-inflammatory, and cytoprotective effects on skin cells, including stimulation of fibroblast and keratinocyte proliferation and modulation of wound-healing growth factors. However, standardized quantitative data defining the optimal bioactive concentration range in dermal-relevant cell models remain scarce, limiting its rational incorporation into advanced wound-dressing formulations. This study aimed to determine the non-cytotoxic concentration range of a standardized Aloe vera extract exerting pro-regenerative activity on human epidermal keratinocytes (HaCaT) and murine fibroblasts (L929), seeded at 10,000 and 6,000 cells/cm², respectively. Cells were treated 24 h post-adhesion with extract concentrations ranging from 5 to 2000 µg/ml in serum-supplemented DMEM (HaCaT) or MEM (L929) for 24 and 72 h. Cell viability and proliferation were assessed by MTT reduction assay, cytomorphological changes by phase-contrast microscopy, and membrane integrity by lactate dehydrogenase (LDH) release quantification. MTT results revealed a concentration-dependent increase in metabolic activity, with peak values recorded for both cell lines at 80–250 µg/ml, most prominently at 72 h. Concentrations ≥500 µg/ml were associated with a moderate reduction in cell viability. Phase-contrast microscopy confirmed preservation of characteristic morphology across all conditions, with notably higher cell densities within the 80–250 µg/ml range. LDH release remained low and comparable to untreated controls for 5–250 µg/ml (HaCaT) and 5–175 µg/ml (L929), indicating absence of significant membrane damage. These results demonstrate that standardized Aloe vera extract exerts a dose- and time-dependent pro-regenerative effect on dermal cell types, with an optimal bioactive window of 80–250 µg/ml, supporting its rational incorporation into biomimetic wound-dressing formulations at biologically relevant doses.

Acknowledgements: This work was financed by a grant from the Ministry of Education and Research, Romania, CNCS-UEFISCDI, project number PN-IV-P2-2.1-TE-2023-0453, within PNCDI IV, as well as from the Ministry of Education and Research, Romania, under the Romanian National Core Program LAPLAS VII–Contract no. 30N/2023.

Electron-Beam Crosslinked Gelatin-Dextran Hydrogels Incorporating Standardized *Aloe Vera* Extract for Biomimetic Wound Healing Applications

Anca SCARISOREANU, Ion Cosmin CALINA, Maria DEMETER

[1]*National Institute for Laser, Plasma and Radiation Physics, Laboratory of Accelerators, Magurele 077125, Romania*
Corresponding author: anca.scarisoreanu@inflpr.ro

In the context of increasing antimicrobial resistance and the need for advanced dressings capable of modulating the wound microenvironment, biomimetic materials based on natural biopolymers and plant extracts represent a promising strategy for the management of acute and chronic wounds [1,2]. This study reports the development of biomimetic gelatin–dextran hydrogels loaded with standardized Aloe vera extract and crosslinked by electron-beam irradiation, designed for topical wound-healing applications. The formulations were prepared from gelatin, dextran, glycerol, and tannic acid as a natural crosslinking agent, and processed using a linear electron accelerator at doses ranging from 12 to 28 kGy, to simultaneously achieve three-dimensional network formation and sterilization. Initially, systems without chemical crosslinkers, with and without Aloe vera, were investigated; gel fraction and equilibrium swelling degree indicated adequate network formation, yielding transparent, flexible hydrogels with favorable handling properties. Based on these findings, the synthesis strategy was optimized by introducing tannic acid and glycerol, adjusting pH (6.4–7.4), and defining irradiation dose windows, resulting in homogeneous hydrogel films exhibiting gel fractions exceeding 70% and equilibrium swelling degrees above 3000%, with high mechanical integrity suitable for clinical manipulation. Physico-chemical analysis highlighted the synergistic influence of polymer composition, Aloe vera extract, and irradiation dose on crosslink density, confirming the suitability of the optimized formulations as biomimetic wound dressings capable of maintaining a moist, oxygen-permeable environment conducive to tissue regeneration

Acknowledgements: This work was financed by a grant from the Ministry of Education and Research, Romania, CNCS-UEFISCDI, project number PN-IV-P2-2.1-TE-2023-0453, within PNCDI IV, as well as from the Romanian Ministry of Education and Research under the Romanian National Core Program NUCLEU-LAPLAS VII–Contract no. 30N/2023.

[1] S. Vitale, S. Colanero, M. Placidi, G. Di Emidio, *et al.*, "Phytochemistry and Biological Activity of Medicinal Plants in Wound Healing: An Overview of Current Research," Molecules **27**(11), 3566 (2022).

[2] A. Revete, A. Aparicio, B.A. Cisterna, J. Revete, *et al.*, "Advancements in the Use of Hydrogels for Regenerative Medicine: Properties and Biomedical Applications," Int. J. Biomater. **2022**, 3606765 (2022).

Laser-Functionalized Nanofibrous Scaffolds for Wound Healing Applications

Claudiu HAPENCIUC[1], Irina NEGUT[1], Anita Ioana VISAN[1], Carmen RISTOSCU[1], Gratiela GRADISTEANU- PIRCALABIORU[2,3], Anca-Constantina PARAU[4], Mihaela DINU[4], Andrei MATEI[5], Oana CRAMARIUC[5]

[1]*National Institute for Laser, Plasma and Radiation Physics, Lasers Department, Magurele 077125, Ilfov, Romania*
[2]*eBio-Hub Research Center, University Politehnica of Bucharest—CAMPUS, 6 Iuliu Maniu Boulevard, Bucharest 061344, Romania*
[3]*Faculty of Biology and the Research Institute of the University of Bucharest (ICUB), University of Bucharest, Bucharest 050657, Romania*
[4]*National Institute for Research and Development in Optoelectronics INOE 2000, Magurele 077125, Ilfov, Romania*
[5]*IT Ctr Sci & Technol, 25 Av Radu Beller Str, Bucharest 011702, Romania*
Corresponding author: claudiu.hapenciuc@inflpr.ro

The development of advanced wound dressings requires precise control over the deposition of bioactive agents onto sensitive polymer templates. In this study, we investigate the functionalization of electrospun cellulose acetate (CA) nanofibrous scaffolds using Matrix-Assisted Pulsed Laser Evaporation (MAPLE). To achieve a controlled coating of bioactive glass (BG) and ciprofloxacin (Cip), we employed a KrF* excimer laser operating at 248 nm.

The laser processing was conducted at a fluence of 300 mJ/cm², utilizing a total of 100,000 pulses to ensure a robust and homogeneous functional layer. This specific energy density was chosen to facilitate the "soft" ablation of the frozen target, allowing the bioactive components to be transferred to the substrate while maintaining their molecular integrity and the structural stability of the underlying CA nanofibers. Morphological characterization by SEM of the uncoated scaffolds revealed a uniform nanofibrous network with fiber diameters ranging between 1.5 and 3.0 μm.

Post-processing analysis confirmed the retention of this architecture, demonstrating that the cumulative energy did not induce thermal degradation or melting of the micro-scale fibers. FTIR spectroscopy verified the stoichiometric transfer of ciprofloxacin, with no detectable photodegradation of the drug's functional groups. Surface wettability measurements showed a significant increase in hydrophilicity, which is essential for wound exudate management. In vitro results demonstrated that the laser-functionalized scaffolds exhibit low cytotoxicity and support cell viability, while the presence of ciprofloxacin provides necessary antibacterial functionality. These findings highlight how the optimization of laser-matter interaction parameters in MAPLE can precisely engineer multifunctional surfaces for next-generation wound dressings.

Acknowledgements: *The authors acknowledge the support of the Ministry of Education and Research, Romania, CCCDI - UEFISCDI, project number PN-IV-P7-7.1-PED-2024-0137 within PNCDI III. The INFLPR authors acknowledge with thanks the support of this work by the Ministry of Education and Research, Romania, under Romanian National Program NUCLEU-LAPLAS VII-Contract No. 30N/2023*

Laser-Driven X-Ray Photodynamic Therapy

Angela STAICU[1], Mihaela BALAS[2], Viorel NASTASA[3], Andra DINACHE[1], Diana DRAGHICI[1], Tatiana TOZAR[1], Ana-Maria UDREA[1], George STANCIU[1], Mihai BONI[1], Ionut Petrisor UNGUREANU[14], Daniel AVRAM[1], Marius DUMITRU[1], Cosmin DOBREA[1], Ionut Relu ANDREI[1], Adriana SMARANDACHE[1], Cristian UDREA[1], Madalina Andreea BADEA[2], Sorina Nicoleta VOICU[2], Anamaria Cristina BUNEA[2], Teodora BORCAN[2], Diana NAUM[3], Liviu NEAGU[3], Andi CUCOANES[3], Mihaela BACALUM[3], Petru GHENUCHE[3], Domenico DORIA[3]

[1]*National Institute for Lasers, Plasma and Radiation Physics, Magurele 077125, Ilfov, Romania*
[2]*Department of Biochemistry and Molecular Biology, Faculty of Biology, University of Bucharest, Bucharest, Romania*
[3]*Extreme Light Infrastructure-Nuclear Physics ELI-NP, "Horia Hulubei" National Institute for Physics and Nuclear Engineering IFIN-HH, Magurele 077125, Ilfov, Romania*
[4]*Faculty of Physics, University of Bucharest, Magurele 077125, Ilfov, Romania*
Corresponding author: *angela.staicu@inflpr.ro*

Cancer continues to be the second leading cause of death worldwide, highlighting the urgent need for more effective and precisely targeted therapies. Limitations of conventional treatments such us - systemic toxicity, drug resistance, and limited efficacy have driven interest in alternatives like photodynamic therapy (PDT), which offers a more targeted and promising approach [1].

PDT is minimally invasive and has low toxicity but suffers from poor tissue penetration. To overcome this, scintillating nanoparticles (NPs) were utilized to convert ionizing radiation, such as X-rays, into visible light, activating nearby photosensitizers. NPs were synthesized by sol-gel method and conjugated with a porphyrin-based photosensitizer. To assess the X-PDT capabilities of our complexes, we have examined the use of high-power laser-induced Bremsstrahlung radiation. The study employed a 10 PW laser (~250 J energy before compressor, 25 fs pulse) with a gas jet target (98% helium and 2% nitrogen) to produce relativistic electron beams [2], which were directed at a lead converter to generate photon beams with an energy cutoff of several GeV. To assess the effects of laser-driven radiation on biological samples we used various cell lines, including both tumor and normal breast cells. These samples were exposed to several radiation shots to achieve a relevant accumulated dose.

To evaluate the therapeutic potential of the PS-NP complexes, cell viability, oxidative stress, and genotoxicity were assessed 24 hours post-activation via X-Ray-PDT using a 3 Gy dose. A significant increase in reactive oxygen species generation was detected selectively in cancer cells, indicating their heightened susceptibility to oxidative stress compared to normal breast cells. Moreover, X-Ray-PDT treatment resulted in a strong inhibition of colony formation in breast cancer cells, while normal cells were significantly less affected, confirming the selective anti-tumor activity of nanocomplexes.

The results highlight the potential of high-power laser systems for radiobiology and oncology. These methodologies provide a foundation for investigating radiobiological phenomena at ultra-high dose rates, with promising applications in understanding and leveraging FLASH effects.

Acknowledgements: *This research was funded by the Institute of Atomic Physics through the project ELI-RO/RDI/2024_022, ELI-RO/RDI/DEZ/DFG/2025_2025_024; the Ministry of Education and Research, Romania by NUCLEU Program LAPLAS VII contract no. 30 N/2023, Nucleu PN 23 21 01 05, and Ministry of Investments and European Projects, within, Dr. Laser Project.*

[1] M. Balas, S. Nistorescu, M. A. Badea, A. Dinischiotu, M. Boni, A. Dinache, A. Smarandache, A. M. Udrea, P. Prepelita, and A. Staicu, "Photodynamic Activity of TMPyP4/TiO_2 Complex under Blue Light in Human Melanoma Cells: Potential for Cancer-Selective Therapy," Pharmaceutics **15**(4), 1194 (2023).

[2] V. Năstasă, R. Moisă, C. I. Drăghici, D. Naum, A. S. Cucoaneş, A. Staicu, M. Balas, I. Mitu, M. G. Popovici, M. Boni, L. Tudor, C. Ticoş, I. Ungureanu, I. R. Andrei, A. Lupu, L. Neagu, R. Anghel, D. Catana, P. Ghenuche, M. Radu, M. Bacalum, and D. Doria, "Exploring High-Dose-Rate Electron Irradiation for Radiobiology Using a 10 PW Laser Source," Rom. Rep. Phys., in press (2026).

Nanocomplexes for X-Ray-Activated Photodynamic Therapy

Diana-Elena DRAGHICI[1,2], Ionut-Petrisor UNGUREANU[1,3], Andra DINACHE[1], Tatiana TOZAR[1], Ana-Maria UDREA[1], Mihai BONI[1], George STANCIU[1], Mihaela BALAS[4], Madalina-Andreea BADEA[4], Sorina-Nicoleta VOICU[4], Anamaria Cristina BUNEA[4], Teodora BORCAN[4], Viorel NASTASA[5], Liviu NEAGU[5], Daniel AVRAM[1], Marius DUMITRU[1], Cosmin DOBREA[1], Angela STAICU[1]

[1]*National Institute for Laser, Plasma and Radiation Physics, Magurele 077125, Romania*
[2]*Biophysics and Cellular Biotechnology Dept., "Carol Davila" University of Medicine and Pharmacy, Bucharest 050474, Romania*
[3]*Faculty of Physics, University of Bucharest, 409 Atomistilor Street, Magurele 077125, Ilfov, Romania*
[4]*Faculty of Biology, University of Bucharest, 050095, Romania*
[5]*Extreme Light Infrastructure-Nuclear Physics ELI-NP, "Horia Hulubei" National Institute for Physics and Nuclear Engineering IFIN-HH, Magurele 077125, Romania*
Corresponding author: diana.draghici@inflpr.ro

Photodynamic therapy (PDT) is a clinically approved treatment, which employs a photosensitizer (PS) exposed at a certain light wavelength to generate reactive oxygen species (ROS) in order to kill cancer cells. Although PDT is minimally invasive and has low toxicity, it still has some drawbacks, like shallow tissue penetration. As a solution for this problem, X-ray induced PDT (X-PDT) was developed as a new therapy approach which uses ionizing radiation instead of visible light [1].

In this study, we report the synthesis and characterization of several lanthanide X-ray-excited luminescent nanoparticles (NPs). NPs have been successfully synthesized by doping several lanthanides into TiO_2 host matrices and were effectively employed in combination with several PSs. Ce and Eu doped TiO_2 NPs were synthesized by sol-gel method. Their physicochemical properties were investigated using dynamic light scattering (DLS), UV-VIS absorption, Fourier-transform infrared (FTIR) and fluorescence spectroscopy. Subsequently, the nanoparticles were loaded with the porphyrin-based PS and further characterized using the same analytical techniques. DLS was used to determine mean hydrodynamic diameter for NPs and PS-nanocomplexes. UV-VIS and FTIR spectroscopy confirmed the loading of PS on NPs and UV-VIS absorption spectroscopy enabled to determine the concentration of both PS and NPs in the suspensions to be used in biological assays. Fluorescence spectroscopy confirmed the compatibility between NPs and porphyrin by analyzing their excitation and emission properties. To assess the X-PDT potential of our complexes, a conventional X-ray source operating at 45 kV and 800 μA was employed. Radiation doses of 1, 2 and 4 Gy were applied for the biological evaluation of PS-nanocomplexes in both normal and tumoral cell models, specifically using MCF-12A normal cells and MDA-MB-231 triple-negative breast cancer cells. Biological investigations performed to confirm the maintenance of cell viability included clonogenic and MTT assays [2,3].

Our research contributes to laying the foundation for a new generation of anticancer therapies, integrating these fields to enable a more effective fight against cancer.

Acknowledgements: This research was funded by the Institute of Atomic Physics through the project ELI-RO/RDI/2024_022; the Ministry of Education and Research, Romania by NUCLEU Program LAPLAS VII contract no. 30 N/2023.

[1] P. Agostinis, K. Berg, K. A. Cengel, T. H. Foster, A. W. Girotti, S. O. Gollnick, S. M. Hahn, M. R. Hamblin, A. Juzeniene, D. Kessel, et al., "Photodynamic therapy of cancer: an update," CA Cancer J Clin. **61**(4), 250-281 (2011).
[2] A. M. Udrea, A. Smarandache, A. Dinache, C. Mares, S. Nistorescu, S. Avram, and A. Staicu, "Photosensitizers-loaded nanocarriers for enhancement of photodynamic therapy in melanoma treatment," Pharmaceutics, **15**(8), 2124 (2023).
[3] L. He, X. Yu, and W. Li, "Recent progress and trends in x-ray-induced photodynamic therapy with low radiation doses," ACS nano, **16**(12), 19691-19721 (2022).

Oncobreast - Molecular Similarity Search for Breast Cancer Drug Research

Ana UDREA, Ionut Petrisor UNGUREANU, Mihai BONI, Angela STAICU

[1]*National Institute for Laser, Plasma and Radiation Physics, Laser Department, Magurele 077125, Romania*
Corresponding author: *ana.udrea@inflpr.ro*

Breast cancer remains one of the most prevalent malignancies affecting women worldwide, underscoring the urgent need for more efficient therapeutic discovery strategies [1]. *In silico* approaches have emerged as powerful tools to accelerate both drug discovery and drug repurposing, enabling rapid analysis of large-scale chemical datasets. To address this need, we developed OncoBreast, a platform that integrates open resources on drug response across breast cancer cell lines with molecular descriptors and chemical similarity methods. The key idea behind OncoBreast is that structurally similar compounds tend to exhibit similar biological response patterns, making similarity-based prioritization a valuable strategy for early-stage screening.

In this work, we present an *in silico* workflow that combines DepMap PRISM breast cancer drug-response data with chemical structure information retrieved from ChEMBL [2–4]. Molecules were standardized and converted into optimized 3D conformations, after which RDKit was employed to compute a comprehensive molecular descriptor set encompassing 2D and 3D descriptors, fingerprint-based representations (ECFP4 and MACCS), and shape-based descriptors (USR/USRCAT) [5,6]. Similarity-based analysis was then used to compare query compounds against the curated reference library, enabling the estimation of drug-response trends across a panel of breast cancer cell lines (Fig. 1).

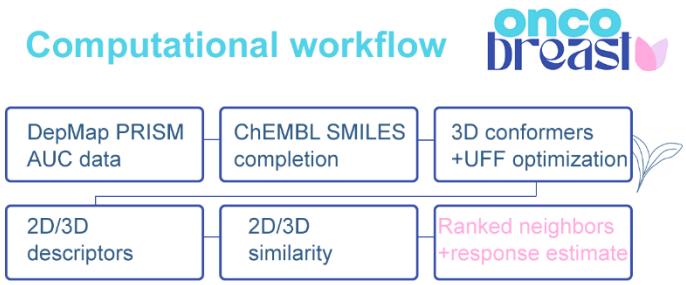

Fig. 1. The computational workflow of OncoBreast platform

This framework provides an interpretable approach for compound prioritization and supports early-stage drug repurposing studies in breast cancer.

Acknowledgements: This research was funded by the Institute of Atomic Physics through the projects number ELI-RO/RDI/2024_022 and ELIRO/RDI/DEZ/DFG/ 2025_024 and the Ministry of Education and Research, Romania by Program NUCLEU-LAPLAS VII- contract No. 30 N/2023.

[1] Breast Cancer Available online: https://www.who.int/news-room/fact-sheets/detail/breast-cancer
[2] DepMap - Broad Institute Available online: https://depmap.org/repurposing
[3] S. M Corsello, R. T. Nagari, R. D. Spangler, J. Rossen, M. Kocak, J. G. Bryan, *et al.*, "Discovering the Anticancer Potential of Non-Oncology Drugs by Systematic Viability Profiling," Nat. Cancer **1**, 235-248 (2020).
[4] M. Davies, M. Nowotka, G. Papadatos, N. Dedman, A. Gaulton, F. Atkinson, L. Bellis, J. P. Overington, "ChEMBL Web Services: Streamlining Access to Drug Discovery Data and Utilities," Nucleic Acids Res. **43**, 612-620 (2015).
[5] A. M. Schreyer and T. Blundell, "USRCAT: Real-Time Ultrafast Shape Recognition with Pharmacophoric Constraints," J Cheminform. **4**, 27 (2012).
[6] RDKit Available online: https://www.rdkit.org

In Silico Evaluation of Radium-223 Energy Deposition and DNA Double-Strand Break Induction in Human Cells

Tatiana TOZAR[1,2], Cristina MARIN[1], Violeta IANCU[1]

[1]*"Horia Hulubei" National Institute for R&D in Physics and Nuclear Engineering, Extreme Light Infrastructure - Nuclear Physics, Magurele 077125, Romania*
[2]*National Institute for Laser, Plasma and Radiation Physics, Lasers Department, Magurele 077125, Romania*
Corresponding author: *tatiana.tozar@eli-np.ro*

Radium-223 is an alpha-emitting radiopharmaceutical utilized in targeted alpha therapy for metastatic castration-resistant prostate cancer. Its high-linear energy transfer alpha particles deposit energy over short ranges (<100 μm), inducing highly cytotoxic clustered DNA double-strand breaks (DSBs). Because it is difficult to directly measure such complex, nanometer-scale DNA damage experimentally, advanced Monte Carlo track-structure simulations serve as a tool for quantifying DSB yields and understanding alpha-particle radiobiology.

The purpose of this work was to model the full 223Ra decay chain, which involves the emission of four primary alpha particles with energies ranging from 5.78 to 7.53 MeV. Macroscopic energy deposition and particle range profiles as a function of depth were evaluated across relevant media, such as water, compact bone, and hydroxyapatite. At the microscopic level, DNA damage was simulated within a cellular target using Geant4-DNA. To quantify lesions, a Density-Based Spatial Clustering of Applications with Noise (DBSCAN) algorithm was implemented to spatially group breaks into complex DSBs based on interaction distances and energy thresholds.

The Geant4 simulations captured the multi-peak energy deposition profiles corresponding to the distinct alpha emissions of the 223Ra cascade, with maximum penetration depths reaching approximately 70 μm in water. At the microscopic DNA level, the DBSCAN-coupled Geant4-DNA model predicted a highly complex damage topology. These in silico predictions demonstrated excellent agreement with experimental benchmark data, tightly mirroring the linear density and frequency of γ-H2AX and 53BP1 radiation-induced damage tracks (foci) measured in *ex vivo* irradiated blood samples.

Geant4-DNA provided a computational framework for simulating the physical track structure of 223Ra and its resulting microscopic DNA damage. By predicting the induction of clustered DSBs across clinically relevant environments, this computational model offers insights into the underlying radiobiological mechanisms of targeted alpha therapies, providing improved dosimetry planning and therapeutic optimization.

Acknowledgement: *This work was carried out under the contract PN 23.21.01.06 sponsored by the Ministry of Education and Research, Romania.*

Laser-Engineered Porosity in Transparent CuI-PDMS Composite Films

Simona BRAJNICOV, Valentina DINCA, Antoniu MOLDOVAN, Alexandra PALLA-PAPAVLU

National Institute for Laser, Plasma and Radiation Physics, Laser Department, Magurele 077125, Romania
Corresponding author: alexandra.papavlu@inflpr.ro

Transparent, mechanically compliant sensors integrated onto architectural glass are key components for smart buildings, enabling *in situ* strain monitoring and early detection of structural degradation without affecting daylight transmission.

In this work, we report the development of transparent piezoresistive coatings based on copper(I) iodide (CuI) incorporated into an elastomeric polymer matrix, together with UV-laser-induced porosification as a strategy to tune both the optical and electromechanical properties of the films.

CuI–polymer composite coatings were first prepared using polydimethylsiloxane (PDMS) and deposited on glass substrates by spin coating. Microstructural investigations reveal the formation of an interconnected CuI network across micro- and submicrometric length scales, providing a conductive framework suitable for piezoresistive sensing.

To induce controlled porosity, a 355 nm Nd:YAG laser system delivering 6–8 ns pulses was employed. As expected from the weak linear absorption of pristine PDMS in the UV–visible spectral range, PDMS-only films show no measurable morphological modification at laser fluences of 0.1–0.3 J/cm². By contrast, PDMS–CuI composites exhibit localized optical scattering and whitening, indicative of the onset of closed-cell microcavity formation. This porosification mechanism relies on CuI nanoparticles acting as nanoscale heat sources: their strong absorption at 355 nm generates rapid photothermal heating, which leads to the formation of transient polymer-vapor microbubbles. These microbubbles expand into closed-cell pores and become stabilized as the surrounding PDMS resolidifies.

Beyond applications in smart-glass structural monitoring, this laser-assisted porosification approach can be extended to a broad range of functional composites, opening perspectives for transparent and stretchable pressure or strain sensor arrays for human–machine interfaces and wearable health-monitoring technologies.

Acknowledgements: This work was supported by a grant of the Ministry of Education and Research, Romania, CNCS/CCCDI - UEFISCDI, project number ERANET-ClearSensTech, within PNCDI IV.

Biointerfaces Designed for Modulating Cellular Response

Valentina DINCA[1], Andreea M. NEGRESCU[2], Anca BONCIU[1], Simona NISTORESCU[1], Laurentiu RUSEN[1], Anisoara CIMPEAN[2]

[1]*National Institute for Laser, Plasma and Radiation Physics, Magurele 077125, Romania*
[1]*Faculty of Biology, University of Bucharest, Splaiul Independenţei 91-95, Bucharest 050095, Romania*
Corresponding author: *valentina.dinca@inflpr.ro*

Fibrotic tissue encapsulation of implants remains one of the most critical and frequent causes for device failure. New honeycomb-like microstructures were design to address multiple aspects of fibrotic encapsulation (i.e. disruption in the fibroblasts' adhesion, reduction in the macrophages' activation) by providing geometric control of microstructures at specific scales. In this regard, microtextured Polydimethylsiloxane (PDMS) - hexagonal matrices with lateral dimensions of 51 µm unit, 5 µm depth, 25 µm internal length per unit, were obtained by replication using moulds obtained by a process of excimer laser texturing assisted by a grayscale mask [1].

Scanning electron microscopy (SEM), as well as atomic force microscopy (AFM), contact angle and surface free energy measurements were used for analysing the morphological features, respectively the wettability of the PDMS substrates. *In vitro* analysis using CCD-1070Sk fibroblasts and RAW 264.7 macrophages validated that silicone surface topography can be rationally engineered to modulate the foreign body response and support the development of implant surfaces with reduced capsular contracture risk.

This study demonstrates that surface topography can be rationally tailored to modulate macrophage and fibroblast behaviour, inducing physiologically relevant cellular responses.

Acknowledgements: This work was financed by project 97PED/2025 and program NUCLEU-LAPLAS VII 30N/2023, Ministry of Education and Research, Romania.

[1] A.M. Negrescu, S. Nistorescu, A. Bonciu, L. Rusen, N. Dumitrescu, I. Urzica, A. Moldovan, P. Hoffmann, G. Gradisteanu Pircalaboiu, A. Cimpean, V. Dinca, "PDMS biointerfaces featuring honeycomb-like well microtextures designed for a pro-healing environment," RSC Adv. **15**(13), 9952-9967 (2025).

Kinetic Modelling of Chemotherapeutic Drug Release from Radiation-Crosslinked Hydrogels for Wound Dressing Applications

Maria DEMETER, Anca SCARISOREANU, Ion Cosmin CALINA

National Institute for Laser, Plasma and Radiation Physics, Laboratory of Accelerators, Magurele 077125, Romania
Corresponding author: maria.demeter@inflpr.ro

The systemic administration of chemotherapeutics is a clinical challenge that frequently requires specialized delivery systems capable of maintaining a moist microenvironment and allowing the controlled release of therapeutic compounds. Due to their adjustable physicochemical characteristics and the ability to deliver drugs over an extended period, polymer-based hydrogels have become extremely promising options in this regard. Using biocompatible polymers such as poly(vinylpyrrolidone), sodium carboxymethylcellulose, and poly(ethylene glycol), two hydrogel formulations were developed through electron beam cross-linking. This led to the formation of highly swollen networks, which were well-suited for the loading and controlled release of two distinct chemotherapeutic drugs, doxorubicin and 5-fluorouracil (5-FU). The in vitro loading and release of both drugs were investigated under various experimental conditions, and the release profiles were analyzed using several kinetic models commonly applied in polymer-based delivery systems, including the first-order model, Korsmeyer–Peppas, Peppas–Sahlin 1, Makoid–Banakar, and Weibull. Model selection criteria (MSC), Akaike information criterion (AIC), and the coefficient of determination (R^2) were used to evaluate the model's performance. First-order kinetics proved to be less relevant than the Korsmeyer–Peppas, Peppas–Sahlin 1, and Makoid–Banakar models, as it provided only a secondary description of the data, with consistently higher AIC values and lower MSC. Release exponents were typical for Fickian diffusion with only a minor contribution from polymer relaxation and erosion, showing favorable information criteria and excellent correlations ($R^2 = 0.99$). A biphasic release profile with an initial burst phase and a diffusion-controlled stage was further validated by Weibull analysis with $\alpha > 1$ and $\beta < 1$. Wound dressings require a high local dose followed by sustained drug release; kinetic models generally show that the drug release from the investigated hydrogels is primarily controlled by diffusion. Ongoing research extends this mathematical framework to the drug loading process, in an attempt to provide an integrated description of drug transport in these systems.

Acknowledgements: This work was financed by a grant from the Ministry of Education and Research, Romania, CNCS-UEFISCDI, project number PN-IV-P2-2.1-TE-2023-0453, within PNCDI IV, as well as from the Romanian Ministry of Education and Research under the Romanian National Core Program LAPLAS VII-Contract no. 30N/2023.

Graphene/Metal Composite Sensor for Cortisol Detection: DFT Simulation and Experimental Implementation

Marina CUZMINSCHI[1,2], Alexandra TREFILOV[1], Ana-Maria IORDACHE[3], Stefan-Marian IORDACHE[3], Arcadie SOBETKII[4], Alexei ZUBAREV[1]

[1]*National Institute for Laser, Plasma and Radiation Physics, Magurele 077125, Romania*
[2]*Horia Hulubei National Institute for R&D in Physics and Nuclear Engineering Magurele 077125, Romania*
[3]*National Institute of Research and Development for Optoelectronics - INOE 2000, Magurele 077125, Romania*
[4]*SC MGM STAR CONSTRUCT SRL, 7 Pancota Street, Bucharest 022773, Romania*
Corresponding author: marina.cuzminschi@inflpr.ro

Cortisol is an important biomarker for stress detection, as it plays a key role in regulating the circadian rhythm and the morning wake-up response [1]. Cortisol levels fluctuate throughout the day and can rise sharply in stressful situations. Real-time monitoring of cortisol can enhance stress management and reduce the risk of stress-related diseases. Electrochemical sensors are well-suited for measuring cortisol in biological fluids such as saliva [2] and sweat, enabling non-invasive and convenient monitoring.

In this work, we present a novel electrochemical sensor for cortisol detection in sweat, based on graphene doped with metal oxide nanoparticles. The efficiency of the sensor design was validated using density functional theory (DFT) simulations performed with the SIESTA software. We analyzed the interaction of multilayer graphene (up to three layers) with induced metallic defects and cortisol molecules, comparing binding energies and charge density distributions for different molecular orientations (Fig. 1). The simulations indicate that the surface graphene layer undergoes geometrical changes upon cortisol adsorption, which in turn reduces graphene conductivity.

Experimentally, the sensor prototype was fabricated via liquid-liquid deposition on a titanium substrate, with metal oxide nanoparticles (CuO and Fe_2O_3) deposited through chemical reduction. The quality of deposition was verified using SEM, EDS, and Raman microscopy, with an average nanoparticle size of approximately 3 nm. Sensor performance was evaluated using cyclic voltammetry, demonstrating a sensitivity of approximately 0.4 ng/L.

Fig. 1. The electron distribution in Cu doped graphene with captured cortisol molecule.

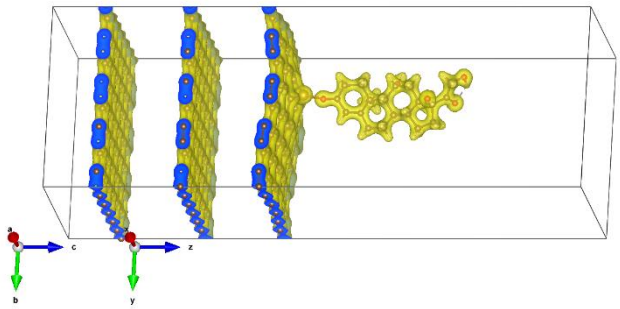

Acknowledgements: Authors acknowledges NUCLEU-LAPLAS VII-contract No. 30N/2023 within PNCDI IV, CNCS—UEFISCDIPN-IV-P2-2.1-TE-2023-1102, PN-IV-P7-7.1-PED-2024-079;
Maria Cuzminschi acknowledges PN-23-21-01 01/2023. The authors acknowledge the support of National Interest Infrastructure facility IOSIN–CETAL at INFLPR, IOSIN-ISS numerical facility and Olimpia Budriga, Aurelian Marcu and Alexandru Achim for their support in implementing numerical simulations and infrastructure support.

[1] C. J. Weber, *et al.*, "Advances in electrochemical biosensor design for the detection of the stress biomarker cortisol," Anal. Bioanal. Chem. **416**(1), 87-106 (2024).
[2] A. Zubarev, *et al.*, "Graphene-based sensor for the detection of cortisol for stress level monitoring and diagnostics," Diagnostics **12**(11), 2593 (2022).
[3] A. García, *et al.*, "Siesta: Recent developments and applications," J. Chem. Phys. **152**(20), 204108 (2020).

An Estimation of Lifetime for the Pulsatory Liposome

Diana Rodica RADNEF-CONSTANTIN[1], Dumitru POPESCU[2], Agnetha MOCANU[3], Valentin I. NICULESCU[4]

[1]*Institutul Astronomic al Academiei Romane, 5 Cutitul de Argint Street, Bucuresti, Romania*
[2]*ISMMA, 13 Calea 13 Septembrie Street, Bucuresti, Romania*
[3]*Universitatea Hyperion, 169 Calarasilor Street, Bucuresti, Romania*
[4]*National Institute for Lasers, Plasma and Radiation Physics, Magurele 077125, Romania*
Corresponding author: *ghe12constantin@yahoo.com*

We consider a unilamellar liposome filled with an aqueous solution of an osmotic solute. Due to the osmosis process the lipid vesicle swells up to a maximum size, when a transbilayer pore suddenly appears. The liposome deflates and returns to its initial size. The swelling begins again and the liposome begins a cyclical evolution. All the processes which contribute to the liposome relaxing and its coming back to the initial size are described by three differential equations which can be integrated using analytical or numerical methods [1-4]. After performing a number of cycles, the pulsatory liposome stops. It can be assimilated to a biophysical engine. We will calculate the activity time of the pulsatory liposome.

[1] D. Popescu, A. G. Popescu, J. Theor. Biol. **254**, 515-519 (2008).
[2] D. Popescu, A. G. Popescu, "Pulsatory Liposome: A possible biotechnological device. In Liposomes - Recent Advances," New Perspectives and Applications, IntechOpen Ed. Rajeev K. Tyagi. **6**, 85 (2023).
[3] D. R. Constantin, D. Popescu, Rom. J. Phys. **69,** 1-2 (2024).
[4] D. Popescu, D. R. Radnef-Constantin, Rom. Rep. Phys. **77**, 602 (2025).

Long-Range Interaction and Oscillation Control in Hanging Droplets

Ionut-Petrisor UNGUREANU[1,2], Mihai BONI[1], Ionut Relu ANDREI[1], Angela STAICU[1]

[1]*National Institute for Laser, Plasma and Radiation Physics, Laser Department, Magurele 077125, Ilfov Romania*
[2]*Faculty of Physics, University of Bucharest, 409 Atomistilor Street, Magurele 077125, Ilfov, Romania*
Corresponding author: *ionut.ungureanu@inflpr.ro*

The interaction between two hanging droplets as they approach each other, without direct contact, is a complex phenomenon that is not yet fully understood. Evaporation, thermal gradients, and surface tension variations in the gas phase between the neighboring liquid interfaces drive long-range interactions, which are characterized by attractive and repulsive forces acting between the droplets separated by a thin air layer [1,2]. Mass transfer and natural convection also play a role in sustaining these interactions, leading to the onset of interface instabilities [3].

This study investigates how these long-range interactions can be used to generate and control surface oscillations. Using an experimental setup with vertically aligned needles, the inter-droplet distance is precisely adjusted via a stepper motor. This approach allows for the observation of droplet behavior during approach and retraction cycles, ensuring that no physical contact occurs. The experimental analysis is based on digital image processing using a custom algorithm developed in Python, which enables subpixel tracking of the interface.

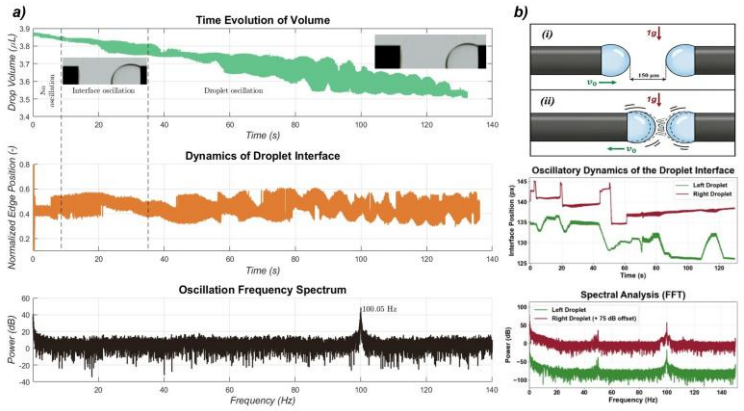

Fig. 1. Oscillation analysis: **a)** a single droplet evaporating and reaching the critical volume; **b)** distance-dependent oscillations during the approach and retraction of two droplets.

The results show that interface oscillations depend on both inter-droplet distance and volume. A critical volume (V_{crit}=3.8 µL) is identified as a necessary condition for the onset of instability. At this volume, droplets begin to oscillate at their resonance frequency (Fig. 1a). It is shown that two droplets near this critical volume start to oscillate as they approach each other, driven by vapor-mediated coupling. By varying the distance, these oscillations can be effectively controlled: the interaction strengthens and the amplitude increases during approach, while retraction causes the oscillation to stop (Fig. 1b). This work provides a new perspective on non-contact droplet coupling, contributing to a better understanding of the long-range interaction mechanism.

Acknowledgements: This work was supported by a grant from the Ministry of Education and Research, Romania, National Research Authority, and UEFISCDI, project number PN-IV-P7-7.1-PED-2024-1995, within PNCDI IV, and Romanian National NUCLEU-LAPLAS VII, project number 30N/2023.

[1] L. Shen, J. Ren, F. Duan, "Surface temperature transition of a controllable evaporating droplet," Soft Matter **16**(41), 9568-9577 (2020).
[2] H. Zhao, D. Orejon, K. Sefiane, M.E.R. Shanahan, "Long-Range Vapor-Mediated Interactions between Adjacent Droplets," Langmuir **41**, 3986-3994 (2025).
[3] A. Okhotsimskii, M. Hozawa, "Schlieren visualization of natural convection in binary gas-liquid systems," Chem. Eng. Sci. **53**(14), 2547–2573 (1998).

Two Drops, Zero Gravity: Capillary Bridge Dynamics on the International Space Station

Mihai BONI[1], Mihail L. PASCU[1], Ionut R. ANDREI[1], Ionut P. UNGUREANU[1], Ilia V. ROISMAN[3], Mugurel BALAN[2], Brice SAINT-MICHEL[4]

[1]*National Institute for Laser, Plasma and Radiation Physics, Magurele 077125, Romania*
[2]*Institute for Fluid Mechanics and Aerodynamics, TU Darmstadt, Germany*
[3]*Romanian InSpace Engineering SRL, Bucharest, Romania*
[4]*European Space Research and Technology Centre, European Space Agency, Netherlands*
Corresponding author: *mihai.boni@inflpr.ro*

The Droplet Coalescence (DropCoal) device on the ISS [1] provides a unique platform to study capillary bridge dynamics and wave propagation in the absence of buoyancy. Theory predicts that in the inertial-capillary regime the bridge neck radius grows as $r/R_{eff} = C(\tau/\tau_{eff})^{1/2}$ [2,3], where $R_{eff} = 2R_1R_2/(R_1 + R_2)$ is the harmonic-mean effective radius ($R_{eff} = R$ for equal-size pairs) and $\tau_{eff} = \left(\rho R_{eff}^3/\sigma\right)^{1/2}$ for millimetric droplets, gravity-free conditions are essential to obtain undeformed spherical drops and clean capillary-driven dynamics [4]. Eight configurations were studied, four equal-size pairs (D = 2-5 mm) and four asymmetric pairs (size ratios up to 2.5:1). Power-law fits yield a universal exponent n = 0.49 ± 0.03, in excellent agreement with the theoretical value of 1/2, and prefactor C = 1.08-1.22. Normalising by R_{eff} collapses all data onto the same universal curve regardless of size ratio.

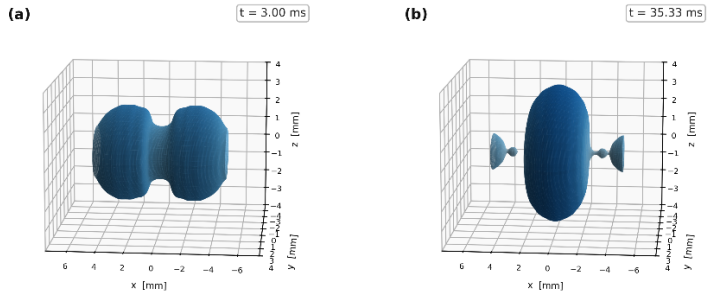

Fig. 1. 3D OpenFOAM simulation (interIsoFoam isoAdvector VOF, 5+5 mm water droplets, conical needle, 50 µm mesh). **(a)** Bridge growth phase at t = 3.00 ms, characteristic hourglass shape of the merging droplets. **(b)** Lamb shape oscillation after detachment from needles at t = 35.33 ms, small liquid caps remain pinned at the conical needle rims.

Numerical simulations were carried out using the geometric Volume-of-Fluid (isoAdvector) solver within OpenFOAM (interIsoFoam), with PIMPLE pressure-velocity coupling and adaptive time-stepping (Co $\leqslant$ 0.5) on a structured hexahedral mesh with the real trumpet-cone needle geometry ($r_{rim} = 0.943$mm). A grid independence study shows 100 µm over-predicts bridge radius by 10 – 35% at $\tau < 3$ ms; 25 µm recovers agreement within 0.2% at τ = 3-5 ms. Simulations are initialised from the experimentally measured pre-coalescence contour rather than an ideal sphere. Full 3D simulations (Fig. 1) validate the axisymmetric approximation and reproduce Gibbs contact-line pinning at the needle rim.

Acknowledgements: This work was financed by project PN-IV-P7-7.1-PED-2024-1995 within PNCDI IV and program NUCLEU-LAPLAS VII 30N/2023, Ministry of Education and Research, Romania. The authors gratefully acknowledge the ESA for funding the DropCoal mission, supporting the development and deployment of the payload on the International Space Station.

[1] M. Boni, M. Balan, J. B. Schmidt, *et al*., "DropCoal: An instrument to study the drop coalescence in microgravity," Results Eng. **29**, 109855 (2026).
[2] X. Xia, X. Chi, and P. Zhang, "Scaling law in the inviscid coalescence of unequal-size droplets," J. Fluid Mech. **1010**, R2 (2025).
[3] J. Eggers, J. R. Lister, and H. A. Stone, "Coalescence of liquid drops," J. Fluid Mech. **401**, 293-310 (1999).
[4] J. Eggers, J. E. Sprittles, and J. H. Snoeijer, "Coalescence dynamics," Annu. Rev. Fluid Mech. **57**, 61-87 (2025).

AUTHOR INDEX

A

B

C

D

E

F

G

H

I

J

K

L

M

N

O

P

R

S

T

U

V

W

Y

Z

ICLPR - ST

iclpr-st.inflpr.ro

Number of Pages: 194
ISSN: 2821-7101
ISSN-L: 2821-7101